Chapter 2: Land-Climate Interactions

Coordinating Lead Authors: Gensuo Jia (China), Elena Shevliakova (United States of America)

Lead Authors: Paulo Artaxo (Brazil), Nathalie De Noblet-Ducoudré (France), Richard Houghton (United States of America), Joanna House (United Kingdom), Kaoru Kitajima (Japan), Christopher Lennard (South Africa), Alexander Popp (Germany), Andrey Sirin (Russian Federation), Raman Sukumar (India), Louis Verchot (Colombia)

Contributing Authors: William Anderegg (United States of America), Edward Armstrong (United Kingdom), Francesco Cherubini (Italy), Edouard Davin (Switzerland), Cecile De Klein (New Zealand), Giacomo Grassi (Italy), Rafiq Hamdi (Belgium), David Kanter (United States of America), Gerhard Krinner (France), Sonali McDermid (India/United States of America), Josep Peñuelas (Spain), Stephanie Roe (United States of America), Martijn Slot (Panama), Rolf Sommer (Germany), Benjamin Sulman (United States of America), Phil Williamson (United Kingdom), Yuyu Zhou (China/United States of America)

Review Editors: Pierre Bernier (Canada), Jhan Carlo Espinoza (Peru), Sergey Semenov (Russian Federation)

Chapter Scientist: Xiyan Xu (China)

Date of First-Order Draft: May 27, 2018

Table of Contents

Executive Summary

This chapter assesses the literature on two-way interactions between climate and land, with focus on findings since AR5. It examines scientific advances in our understanding of interactive climate and land changes, including climate change and variability that influence land surface processes and characteristics, and feedbacks from terrestrial biosphere to climate system. As some aspects of the land-climate interactions were not reported or discussed in depth in AR5 reports, studies prior to AR5 reports have been included into this chapter assessment.

Land use/cover and climate change interact and couple across spatial and temporal scales. There is range of coherence levels in understanding response of terrestrial ecosystems to climate change and terrestrial biosphere feedback across AR5 working groups. Overall, major uncertainties remain about the magnitude of biosphere feedback and climate change impacts on land, but some uncertainty about the sign and magnitude of changes in land-climate interactions is gradually reducing through IPCC cycles (2.1).

The new understanding emerged about plants, soils and hydrological processes shaping exchanges of water, energy, greenhouse gases (GHGs) and short-lived species between land and atmosphere, which have potential to amplify both negative and positive land feedbacks on climate. However, these processes (phenological mechanisms, acclimation of photosynthesis and respiration, soil microbial dynamics) are not included in most climate and Earth system models (ESMs).

CO_2 fertilisation and its nutrient down-regulation remain the key uncertainty in the prediction of future carbon sinks and sources *(robust evidence, high agreement*). The nutrients availability would eventually determine the upper limit of plant growth responses and ecosystem carbon sequestration to increasing CO_2 (*robust evidence, high agreement*). However, new observational and modelling evidence suggest that plant adaptation, particularly through plant-microbe symbioses, could alleviate some nitrogen limitation to plant growth under CO_2 fertilisation (*medium evidence, high agreement*) (2.2.2 -2.2.4).

In recent decades drought and heat stress have been linked to widespread tree mortality, which are often exacerbated by insect outbreak and fire (*robust evidence, high agreement*). Tree mortality will also alter land albedo, roughness, and other biophysical properties of forests. Most terrestrial biogeochemistry dynamic vegetation and Earth system models use empirical climate stress envelopes or plant carbon balance estimations to predict climate-driven mortality and loss of forests, which are unlikely to provide robust projections of biome shifts and impacts of disturbance from extreme climate vents on vegetation transient climate responses and losses of vegetation carbon (2.2.5).

The key processes affecting soil organic carbon stocks (SOC) are warming, which is expected to accelerate SOC losses through microbial respiration, and enhanced of plant growth, which increases inputs of C to soils (*robust evidence, high agreement*). Changes of soil moisture and high-latitude/altitude permafrost are key drivers as well. However, complex mechanisms underlying SOC responses to both warming and carbon addition drive considerable uncertainty in projections of future changes in SOC stocks. Warming experiments have shown significant variability in temperature responses across biomes and climates. While it's well established that the biological processes, which drive decomposition, will accelerate at warmer temperatures, it proved remarkably difficult to constrain uncertainty in the temperature sensitivity of soil decomposition and nutrient mineralisation and thus future projections of soil carbon stocks and emissions (2.2.6).

There is a growing understanding of the biogeophysical climate feedbacks of various agricultural land management strategies and the response of managed vegetation (*medium confidence, medium evidence*). Improvements in observational datasets are now elucidating important trends and processes by which agricultural land management is impacting regional and global climate systems (2.2.7, 2.6).

An increasing body of evidence demonstrates that intensive irrigation potentially exerts a strong climate forcing (*high confidence, robust evidence*). Nearly 70% of global freshwater withdrawals, about 3300 km^3yr^{-1} in 2010, are currently used for agricultural irrigation with groundwater accounting for about 30%-40% of this total. Addition of such vast amounts of water to the land surface can substantially modify regional energy and moisture balances, particularly in conjunction with highly productive agricultural crops with high rates of evapotranspiration. Most of CMIP5 models did not include water management (2.2.7, 2.6).

Climate is a primary determinant of regional land characteristics and functioning, so climate change due to natural or anthropogenic causes can alter these. Observations suggest that ongoing climate change has impacted regional land functioning such as drought, forest dieback and desertification, however, in many instances it is currently difficult to distinguish between the pure climate impacts and other human activities. It is *very likely* that land-based systems will be exposed to disturbances beyond the range of current natural variability as warming-induced novel climates emerge that are beyond the envelope of current natural variability in terms of means and extremes. This is *very likely* to alter the structure, composition and functioning of many land-based systems (2.3.1).

The percentage of global arid land area is *very likely* to increase as a result of anthropogenic warming. The extent of global drylands has increased over the last 60 years and is projected to accelerate in the 21st century such that it is *likely* 56% and 50% of total land surface will be covered by drylands by 2100 under RCP8.5 and RCP4.5 respectively. Dryland expansion will *likely* lead to reduced carbon sequestration, enhanced regional warming, result in decreased agricultural yields and runoff and increased drought frequency and persistence (2.3.2).

Mean climate change, even under aggressive mitigation, is *likely* to have regionally-distributed impacts on agricultural production, which may impact food security globally (*medium confidence, medium evidence*)**.** In the sub-tropics, tropics, and water-limited environments, changes in rainfall variability, drought, growing season temperature increases and climate extremes are expected to negatively impact agricultural production both in magnitude and variability. At middle and higher latitudes, the lengthening of growing seasons, reduced frost damage, CO_2 fertilisation effects, potential for increased rainfall and expansion of the crop climate envelope through warmer temperatures may serve to improve crop productivity and/or mitigate climate-induced losses (2.3.4).

Temperature extremes (very hot days, hot nights, heat waves) have a greater negative impact on terrestrial land functioning than rainfall extremes. Hot temperature extremes are *very likely* to increase in a warming climate with deleterious impacts on land functioning. In a warming climate heat waves will *more likely than not* become longer and more frequent in many African regions and unusual heat wave conditions today will occur regularly by 2040 under the RCP8.5 scenario (2.3.5).

It is therefore *more likely* that extreme ENSO events will become more frequent in the future with implications for twenty-first century land type and functioning (*medium evidence*). Although there is *low confidence* in any specific projected change in ENSO and related regional phenomena for the 21st century, the occurrence of extreme El Niño and La Niña events is expected to double from one in every 20 years to one in every 10 years for El Niño and one in every 23 years to one in every 13 years for La Niña (2.3.6).

Fire regimes are influenced by a complex interaction of various climatic factors, vegetation structure and human activities. Although the total land area burned has not increased in recent decades, and in fact may even have decreased slightly, there is emerging evidence that fire weather seasons have lengthened by 18.7% between 1979 and 2013 globally. Further, there are clear indications that fire regimes are being increasingly driven by changes in temperature (as opposed to precipitation and human activity), a factor that has important implications for future fires in a warming world (Box 2.1).

Land use and land cover change (LULCC) and changes in natural terrestrial systems impact the atmospheric GHGs concentration in major ways and have consequences for global climate change *(robust evidence, high agreement*) Land is both source and sink for CO_2, N_2O, and CH_4 from both natural and anthropogenic drivers. The net effect of anthropogenic activity on the land accounts for 29% of all anthropogenic greenhouse gas emissions over the past decade *(medium confidence*). The spatial and temporal variations of these exchanges, the influences of land-climate feedbacks, and the difficulties in attributing change to natural versus anthropogenic drivers continue to be major sources of uncertainty in quantifying anthropogenic impacts on the climate system (2.4, 2.6).

According to models' estimate, during 2007-2016 the response of natural lands to changing climate and rising atmospheric CO_2 concentrations produced a land sink of -11.0 +/- 2.9 $GtCO_2e$ yr^{-1} **(28% of all anthropogenic emissions)** *(low confidence).* Combined effect of land use and land management and enhanced carbon uptake from changing climate and increasing atmospheric CO_2 concentration is the net land sink of - 6.3 $GtCO_2e$ yr^{-1} for 2007-2016. The models-based estimate of the net land carbon sink is consistent with the 5.1- 8.4 $GtCO_2e$ yr^{-1} estimate from the inversion studies, relying on atmospheric observations of CO_2 concentration (2.4).

Land overall is a net source of CH4 (426-438 $TgCH_4$ yr^{-1}**). The major sources are natural wetlands (172-187 $TgCH_4$ yr^{-1}), and anthropogenic emissions from agriculture (137-140 $TgCH_4$** yr^{-1}**), landfills (60 $TgCH_4$** yr^{-1}**), and biomass burning (17 $TgCH_4$** yr^{-1}**).** Land related emissions account for about 62% of anthropogenic CH_4 emissions. Atmospheric CH_4 concentrations increased through the 1990s, paused between 2000 and 2006, and then started increasing again but at a slower rather than in the 1990s. AR5 attributed inter-annual variations in CH_4 accumulation rate to variability in natural wetland emissions, but new evidence points to the importance of atmospheric loss (*high certainty)*(2.4).

Agriculture is the main anthropogenic source of N_2O due to application of fertiliser and manure management (4.1 Tg N_2O-N yr^{-1}**).** Emissions are largely from North America, Europe, East Asia, and South Asia, but emissions are growing across the tropics. Natural sources of N_2O are estimated to be around 11 Tg yr^{-1} and these sources have decreased by approximately 0.9 Tg yr^{-1} due to tropical deforestation (2.4).

While there was a progress in quantifying regional emissions of anthropogenic and natural land aerosols (e.g. mineral dust; black, brown and organic carbon; biogenic volatile organic compounds) considerable uncertainty still remains about their historical trends, their inter-annual and decadal variability and about any changes in the future (*robust evidence, high agreement*). There are no direct observations of natural aerosols on global or regional scales.

Emissions are derived either from remotely sensed observations of atmospheric concentrations of constituents (e.g. mineral dust), from top –down or bottom-up inventories (e.g. carbonaceous aerosols), or models (e.g. BVOCs). There have been attempts to incorporate process- based approaches for simulation of dust and carbonaceous aerosols in the ESMS. CMIP5-class ESMs have difficulties in properly model BVOCs emissions, chemistry and secondary aerosols production (2.5).

Land cover and uses (e.g. urban expansion, deforestation / afforestation, irrigation – ploughing, conversion to croplands) exert significant influence on atmospheric states (e.g. temperature, rainfall, wind intensity) and phenomena (e.g. monsoons), at various spatial and temporal scales, through their biophysical impacts on climate *(robust evidence, high agreement*). As land continuously exchanges heat, energy, water, greenhouse gases, non-greenhouse gases and aerosols with the atmosphere, it affects its temperature, humidity, and composition. Horizontal gradients of land cover or states (e.g. greenness, moisture) provoke horizontal and vertical gradients in the atmosphere and affects atmospheric circulation (e.g. horizontal winds, convection) (2.2, 2.4, 2.5, 2.6).

Historical land use induced land cover changes (HLULCC) have resulted in significant ambient air cooling (as large as about -0.5°C) in large continental areas in the northern hemisphere, for at least one of the four seasons, through their biophysical impacts on climate *(robust evidence, high agreement*). HLULCC in the northern lands are largely dominated by deforestation, forests being converted into croplands. Increased albedo following such conversion is especially large during winter-time and early spring and leads to cooling *(robust evidence, high agreement*). Changes in evapotranspiration dominate the temperature change in late spring, summer and early fall and often leads to warming *(medium agreement*). The net annual temperature change is very uncertain although most models show a resulting cooling(2.6.1.)

There is no agreement on the net impact of historical land use induced land cover changes (HLULCC) on ambient air temperature. Global annual warming results from net emissions of CO_2 following HLULCC *(robust evidence, high agreement*). Global annual warming results from the Earth greening and the northward and upward migration of treelines *(low evidence, low agreement*). HLULCC alone result in a small annual global cooling *(medium agreement*) (2.6.1).

Future land use induced land cover change (FLULCC) will contribute to enhance globally and annually the GHG-induced warming through an additional contribution to atmospheric CO_2 content, whatever the socio-economic scenario *(medium evidence, medium agreement*). However FLULCC holds a potential for climate mitigation (with respect to reducing ambient air temperature) in some areas where the biophysical effects of FLULCC are the largest and can decrease by -11% to -23% the GHG-induced warming (2.6.1, 2.6.5).

Whatever the land change (e.g. afforestation, urbanisation), its location on Earth determines the sign and magnitude of its impacts on climate *(robust evidence, high agreement)*. The so-called background climate (e.g. cold and wet versus warm and semi-arid) significantly influences how land/atmosphere exchanges respond to the imposed change. Deforestation for example cools boreal climate, warms up the tropics and has little annual impact in the temperate regions. The same mechanisms at the land/atmosphere interface are triggered by the loss of trees, but the magnitude of the flux changes depends on e.g. the amount and extent of snow, the amount of incident radiation, soil moisture. In boreal and temperate regions in winter the snow-albedo feedbacks exert the largest influence on the changes in the energy budget, while in the tropics the hydrological cycle has the dominant effect (2.6.1, 2.6.2, 2.6.4, 2.6.5).

The impacts of land changes on the atmospheric GHG content have consequences on global

climate change, while their impacts on the physical exchanges between land and atmosphere, and on the atmospheric content of non-GHG and aerosols have consequences on local/regional climate, and often limited to the areas where the land changes occur *(robust evidence, high agreement*). The impacts of deforestation / afforestation on local/regional climate evolve and may change through time as a) biophysical and biogeochemical effects do not play roles at the same time and spatial scales, and b) background climate may evolve through time for example long term drying or wetting (*high confidence* although not enough literature yet).

Changes in Land Cover, Uses or Management (LCUM) affect local temperature extremes more than mean climate conditions *(medium confidence*). Absolute temperature changes due to LCUM tend to be larger for extreme temperatures and for daily minimum / maximum temperatures compared to mean daily-monthly temperatures. This is because LCUM-induced changes in surface albedo have an asymmetric effect on temperature owing to the stronger radiative forcing exerted during clear-sky conditions. LUCM-induced changes in extreme temperatures, such as those induced by irrigation, are also likely to have an asymmetric effect on temperature because of the strong relationship between moisture limitation and hot extremes. Historical deforestation increased the local magnitude of hot extremes in temperature regions (*low confidence*). In addition, changes in management also had a crucial impact. Irrigation in particular may have contributed to a decrease in extreme temperature in strongly irrigated areas (*medium confidence)* (2.6.3).

Urbanisation increases the risks associated with extreme events (*high confidence*). Urbanisation suppresses evaporative cooling and amplifies heatwave intensity (*high confidence*). Urban areas stimulate storm occurrence and heavy precipitations in part due to the presence of aerosols. Urbanisation also increases the risk of flooding during heavy rain events (2.6.2.4, 2.6.3).

Land surface processes modulate the likelihood, intensity and duration of many extreme events including heatwaves, droughts and heavy precipitations (*high confidence*). There is *robust evidence* that dry soil moisture anomalies favour summer heat waves. Part of the projected increase in heat waves and droughts can be attributed to soil moisture feedbacks in regions where evapotranspiration is limited by moisture availability (*medium confidence*). Vegetation changes can also amplify or dampen extreme events through changes in albedo and evapotranspiration, which will influence future trends in extreme events (*medium confidence)* (2.6.3).

Urbanisation amplifies the GHG-induced warming (ambient air temperature) in different climatic regions with a strong impact on minimum temperatures *(very likely, high confidence*). In Western Europe, future urbanisation in Flanders has a strong impact on minimum temperatures that is comparable to the climate change signal only for the near future (horizon 2035, +0.6 °C). In the USA-Arizona's Sun Corridor region, Seoul, Tokyo, and Sydney, it is found that the combined effect of global warming and urbanisation produces an increase in minimum temperature that is substantially larger than the increase due to global warming alone. The increase of minimum temperature may be attributed to: (i) the higher thermal inertia, which, in combination with lower albedo of urban surfaces, delays the cooling of the cities at nights compared to rural areas, (ii) to the limited evapotranspiration which prevents evaporative cooling of urban areas, and (iii) during night hours, the contribution of anthropogenic heat can also influence long-term trend of near-surface air temperature. Urbanisation modifies precipitation patterns, frequency, and intensity(2.2.8, 2.6.2.4).

There are many different options available for implementing land-based mitigation both in terms of reducing and avoiding emissions, and enhancing sinks. Estimates of potential of individual mitigation options from the literature include: 1.1 to 6.9 $GtCO_2e\ yr^{-1}$ from reduced land use change emissions (reduced deforestation, degradation, conversion, draining and burning peatlands, etc.); 3.2 to 17.1 $GtCO_2e\ yr^{-1}$ from carbon sink enhancement (afforestation, reforestation, forest management, agroforestry, restoration of peatlands and coastal wetlands, soil carbon sequestration); 2.0 to 12.0 $GtCO_2e\ yr^{-1}$ from bioenergy with carbon capture and storage (BECCS); 0.3 to 0.5 $GtCO_2e\ yr^{-1}$ from substituting construction materials with long-loved wood products; and 1.5 to 2.0 from agricultural measures (cropland and pasture management, rice, enteric fermentation, manure management and synthetic fertiliser production). Reducing food and agricultural waste could reduce emission by 0.38 to 0.45 $GtCO_2e\ yr^{-1}$; while shifting to healthy diets could save 2.2-6.4 $GtCO_2e\ yr^{-1}$ (2.7).

Unregulated land-based mitigation can have high consequences for the land system, but alternative pathways do exist. Climate change mitigation pathways can shape the land system dramatically as global forest area can change from about -500 Mha up to +-1000 Mha in 2100 compared to 2010, and demand for 2nd generation bioenergy crops can range from less than 5000 up to about 20,000 million ton per year by 2100 in RCP2.6 scenarios, sourced from about 200-1500 million ha of land (*robust evidence; high agreement*). Other, less land demanding, alternative integrated pathways of achieving climate change targets do exist with less need for terrestrial carbon dioxide removal (CDR). Those rely on lifestyle changes and agriculture intensification in which reduced cattle stocks play an important role, rapid and early reduction of GHG emissions in other sectors and extension of CDR portfolio beyond land-demanding options such as afforestation and BECCS (*robust evidence; high agreement*) (2.7).

About a quarter of the mitigation pledged by 2030 by countries under the Paris Agreement is expected to come from land-based mitigation measures. Full implementation of country pledges (Nationally Determined Contributions, NDCs) is expected to result in sinks of 0.4 to 1.3 $GtCO_2e\ yr^{-1}$ in 2030 compared to the net flux 2010 (range represents low to high mitigation ambition in countries, not uncertainty in estimates). Most of the NDCs submitted by countries include land-based mitigation, but focused on reduced deforestation and forest sinks. Few included soil carbon sequestration, agricultural management or bioenergy. Overall, the full sector NDCs fall short of the ambition necessary to reach the 2 degree target with current commitments more compatible with 2.5°C to 3°C of warming by 2100 (2.7).

2.1 Introduction: Land – climate interactions (scene setting)

2.1.1 Climate determines land covers & land processes affect climate

This chapter assesses the literature on two-way interactions between climate and land surface changes, with focus on literature published since AR5. Since some land-climate interaction issues were not assessed by previous IPCC reports, we extend on literature prior to AR5. It examines science advances in our understanding on interactive changes of climate and land, including climate change and variability that influence land surface processes, and feedbacks of land surface changes to climate system. **Key issues are highlighted below**:

- Important processes and mechanisms behind land and climate interactions, including advanced understanding of well recognised processes and some emerging issues documented recently.

- Climate change and extremes that influence soil conditions, growing season vegetation conditions and distribution, emissions of GHG and non GHG components. They therefore affect desertification, land degradation, food security (that are discussed respectively in chapters 3-4-5), sustainable land management (discussed in chapter 6).

- Terrestrial GHG and non-GHG fluxes in natural and managed ecosystems and related stocks.

- Biophysical and non-GHG feedbacks on climate.

- Consequences for the climate system of land-based adaptation and mitigation options.

The chapter starts with a brief assessment of key processes and mechanisms in land-climate interactions and emerging constraint (Section 2.2), followed by synthesis on the historical and projected responses of land patterns and functioning to climate change and extremes are assessed in (Section 2.3). We then assess the historical and future changes in terrestrial GHG (Section 2.4) and non-GHG (Section 2.5) fluxes from unmanaged and managed land. Section 2.6 focuses on how historical and future land use induced changes on land surface processes affect climate and climate change through biophysical effects, and how climate-induced land changes feedback on climate itself. Finally, we conclude with an assessment of the consequences for the climate system of land-based adaptation and mitigation options through changes in land cover, GHG and non-GHG flux and biophysical and effects.

Particularly, in sections 2.4 and 2.7 we deal with implications of the Paris Agreement for land-climate interactions, and the scientific evidence base for ongoing negotiations around operalisationing the Paris rulebook, the global stock take, and transparency and credibility in monitoring reporting and verification of the climate impacts of anthropogenic activities on land. It also examines how land mitigation strategies may act on climate change through biophysical feedbacks and radiative forcing of land use changes on climate change and extremes (Sections 2.6), and concludes with policy relevant future changes in land use and so-called sustainable land management for mitigation and adaptation (Section 2.7).

Since this is an integrated assessment of land and climate interactions, the chapter also includes several boxes in order to integrate information across chapter sections. In this regard, boxes focus on processes, regions/biomes, and themes that are relevant to the climate-land interaction focus. These include boxes that focus on conceptual framework of key processes (Box 2.1), role of fire (Box 2.2), biophysical mechanisms of climate effects (Box 2.3).

The chapter is organised with key storylines as:

First, land and climate interact through a series of feedback loops. Variability in terrestrial vegetation growth and phenology can modulate fluxes of water, heat, energy and momentum to the atmosphere, and thus affects the climatic conditions that in turn regulate vegetation dynamics. Biosphere–atmosphere feedbacks are considered as globally widespread, and explain up to 30% of precipitation and surface radiation variance in regions where feedbacks occur. Substantial biosphere–precipitation feedbacks are often found in regions that are transitional between energy and water limitation, such as semi-arid or monsoonal regions. Substantial biosphere–radiation feedbacks are often present in several moderately wet regions and in the Mediterranean (Green et al. 2017a).

Second, the dynamics of terrestrial ecosystems and land use are largely determined by changing climate. Global terrestrial ecosystems are sensitive to climate variability and change (Seddon et al. 2016). Climate change is expected to alter the distribution patterns of land cover (Schlaepfer et al. 2017), alter species composition and diversity, vegetation structure and productivity (Zhu et al. 2016), and nutrient and water cycles. The impacts of climate change on vegetation are reflected in a series of physiological processes, including changes in net plant carbon uptake, plant water use, plant growth and biomass allocation, competitive interactions, and responses to disturbances. However, data availability and science understanding on impacts of climate change on ecosystem and land use are highly heterogeneous across regions and biomes over the globe and geographical areas (Pugh et al. 2016). Climate change is also reported to alter the seasonality of ecosystems at large scale (Gonsamo et al. 2017). Meanwhile, climate extremes are increasing recognised as a driver behind interrupted changes of land surface through catastrophic disaster events (Lesk et al. 2016).

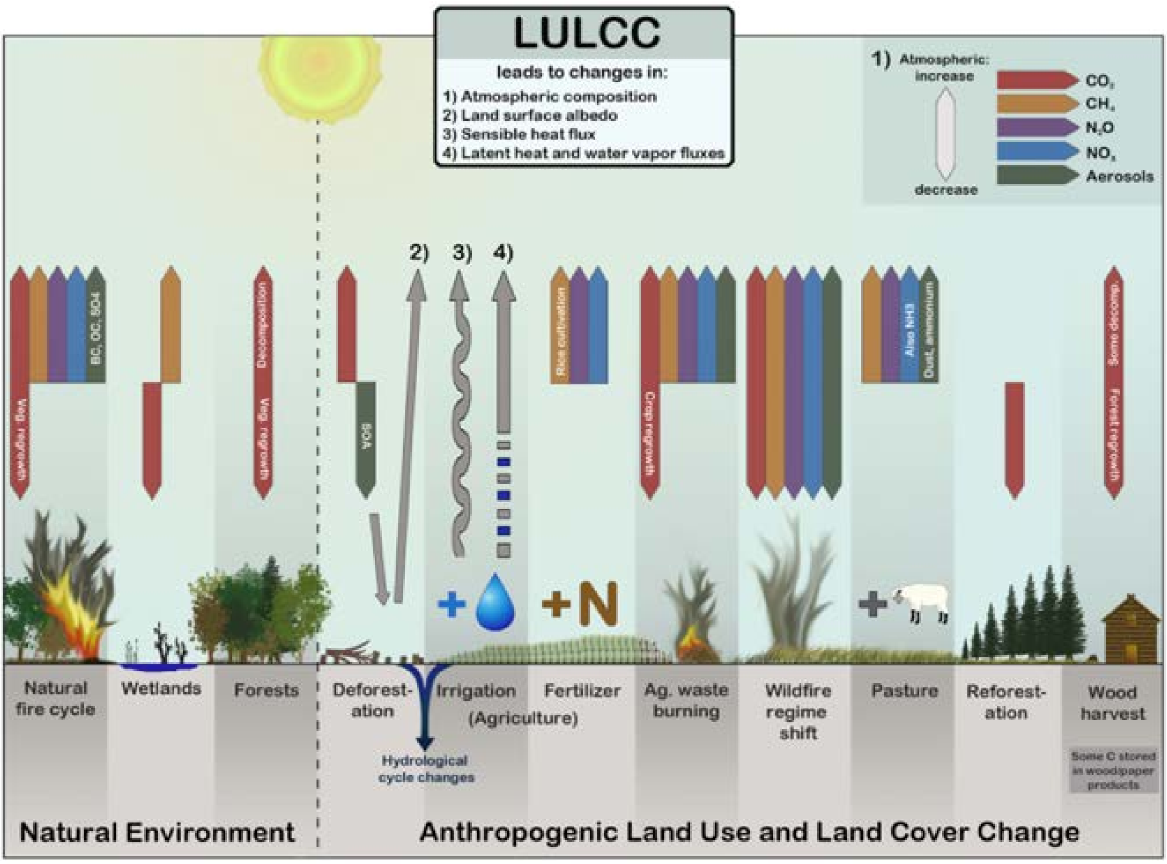

Figure 2.1.1 A schematic Illustration of the climate impacts of Agriculture Forestry and Other Land Use (AFOLU) (from (Ward et al. 2014)). (To be further adapted to the needs of the chapter)

Third, land use and cover changes play an important and complex role in the climate system (Pielke et al. 2016; (Alkama and Cescatti 2016). It affects the climate via both biogeochemical and biophysical processes (Figure 2.1.1). Biogeochemically it is a source and a sink for several greenhouse gasses (2.4) and aerosols and other non-GHG atmospheric constituents (2.6). Plus the nature of the land surface affects several biophysical properties and processes such as albedo, evapotranspiration, surface energy flux and alteration of energy partitioning of sensible and latent heat, surface roughness, and albedo (Burakowski et al. 2018), which in turn affecting temperature, precipitation, humidity, cloud cover, and the planetary boundary layer at local, regional and global scales. Land surface processes also modulate the severity of heat waves (Wim et al. 2017), droughts, and other extreme events (Findell et al. 2017). The most notable land cover conversions are identified as deforestation and afforestation, agriculture to grassland, desertification, and urbanisation. There is an overall consensus that the average global biophysical climate response to complete global deforestation is atmospheric cooling and continental drying. Observed estimates of temperature change following deforestation indicate a smaller effect than model-based regional estimates in boreal regions, comparable results in the tropics, and contrasting results in temperate regions (Perugini et al. 2017). Recent satellite observation and model simulation suggest that Amazonian deforestation in past three decades (Tyukavina et al. 2017a) led to a shift towards a net carbon source (Baccini et al. 2017a) and a dynamically driven hydroclimate (Pitman and Lorenz 2016; Zemp et al. 2017), with enhanced rainfall seen downwind of deforested areas (Lorenz et al. 2016a; Khanna et al. 2017). Similar impacts of deforestation is also found in west Africa rainforests (Klein et al. 2017). Satellite observation also reveal that the recent dynamics in global vegetation (Zhao et al. 2018a) have had contrasting biophysical impacts on the local climates, showing that the increasing trend in LAI contributed to the warming of boreal zones through a reduction of surface albedo and to an evaporation-driven cooling in arid regions (Forzieri et al. 2017a).

This chapter also pays special attention to advanced understanding in scales, emerging issues, heterogeneity, and teleconnections.

The biophysical impacts of land use change on climate are considered to be locally significant only (AR5), however, increasing evidence suggest that these impacts may go well beyond local level. Changes of land use and land cover are reported at larger scales and extents than previously recorded, with recent advances in Earth observation and field network. Land cover change can significantly affect surface energy and water balance through modification of albedo, evapotranspiration, surface roughness, and leaf area, and therefore, alter local and regional climate (De Vrese et al. 2016).

Meanwhile, **increasing evidence demonstrated the potential of sustainable land management in mitigating regional climate change** (Hirsch et al. 2017; Grassi et al. 2017), and that natural climate solutions can provide 37% of cost-effective CO_2 mitigation needed through 2030 for a greater than 66% chance of holding warming to below 2°C (Griscom et al. 2017). In the context of the Paris Climate Agreement, assuming full implementation of NDCs (Forsell et al. 2016), land use, and forests in particular, could turn globally from a net anthropogenic source during 1990–2010 (1.3±1.1 $GtCO_2e\ yr^{-1}$) to a net sink of carbon by 2030 (up to-1.1-±-0.5 $GtCO_2e\ yr^{-1}$), and providing a quarter of emission reductions planned by countries (Grassi et al. 2017). However, negative emissions may be limited by biophysical and economic factors (Smith et al. 2016b).

Major spatial heterogeneity exists, e.g. multiple satellite-based analysis and modeling reveal complex climate effects of temperate forests and related energy budget (Ma et al. 2017b). Nevertheless, **major uncertainty still remains in our understanding of land-climate feedback**

(Berg et al. 2017). The LUCID and CMIP5 models agree on the albedo-induced reduction of mean winter temperatures over mid-latitudes. In contrast, there is less agreement concerning the response of the latent heat flux and, subsequently, mean temperature during summer, when evaporative cooling plays a more important role (Lejeune et al. 2017).

2.1.2 Recap of previous IPCC and other relevant reports as baselines

Issues related to interactions between climate change and land surface processes in previous IPCC reports were covered separately by three working groups. AR5 WGI report assessed the role of land use change in radiative forcing, land-based GHGs source and sink, and water cycle changes that focused on changes of evapotranspiration, snow and ice, runoff, and humidity. AR5 WGII examined impacts of climate change on various land use and cover, including terrestrial and freshwater ecosystems, managed ecosystems, and cities and settlements. AR5 WGIII assessed land-based climate change mitigation goals and pathways in the AFOLU chapter 11. **Here, this chapter brings together land-related issues that cut across all three working groups, it also builds in previous special reports such as the Special Report on 1.5, the Special Report on Renewable Energy and touches on the IPCC Good Practice Guidance methodologies for greenhouse gas inventories in the land sector. Meanwhile, this chapter goes further beyond that, as we bring here knowledge that has never been reported in none of those previous reports.**

Here we briefly recapture key issues and findings from previous IPCC reports:

<u>**GHGs and forcing**</u>: AR5 reported that atmospheric CO_2 and CH_4 increased by 40% from 278 ppm to 390.5 ppm and 150% from 722 ppb to 1803 ppb during 1750-2011, respectively. The CO_2 radiative forcing in AR5 (2011) is 1.82±0.19 Wm^{-2}, an increase of 0.165Wm^{-2} in relative to AR4 (2005) due to 12ppm increases in atmospheric CO_2 mixing ratio. The CH_4 radiative forcing in AR5 is 0.48±0.5Wm^{-2}, an increase of 0.01Wm^{-2} in relative to AR4 due to 29 ppb increases in atmospheric CH_4 mixing ratio. **Annual net CO_2 emissions from anthropogenic land use change were 0.9 (0.1-1.7) GtC yr^{-1} on average during 2002 to 2011 (medium confidence).** From 1750 to 2011, CO_2 emissions from fossil fuel combustion have released 375 (345-405) GtC to the atmosphere, while deforestation and other land use change are estimated to have released 180 (100-260) GtC. Of these cumulative anthropogenic CO_2 emissions, 240 (230-250) GtC have accumulated in the atmosphere, 155 (125-185) GtC have been taken up by the ocean and 160 (70-250) GtC have accumulated in natural terrestrial ecosystems (i.e., the cumulative residual land sink)(Ciais et al. 2013).

<u>**Terrestrial carbon source/sink**</u>**: Carbon uptake in vegetation biomass and soils not affected by land use change (160±90 PgC) almost offset the carbon emission due to land use change.** Land carbon uptake projected among Climate Modelling Intercomparison Project Phase 5 (CMIP5) Earth System Models is very uncertain due to the combined effects of climate change and land use change. There is high confidence that tropical ecosystems will uptake less carbon and there is medium confidence that at high latitudes, land carbon storage will increase in a warmer climate. Thawing permafrost in the high latitudes is potentially a large carbon sources at warmer climate, but the magnitude of CO_2 and CH_4 emissions due to permafrost thawing is still uncertain. In addition, Low nitrogen availability may limit carbon storage on land according to RCPs projections.

<u>**Land use change altered albedo**</u>: **AR5 provided robust evidence that anthropogenic land use change has increased the land surface albedo, which leads to an RF of –0.15 ± 0.10 W m^{-2}**, however, it also indicated a large spread of estimates owing to different assumptions for the albedo of natural and managed surfaces and the fraction of land use changes before 1750. Generally, our

understanding on albedo change due to land use alteration has enhanced from AR4 to AR5, with narrower range of estimates and higher confidence level. The radiative forcing of land use induced albedo change was estimated at -0.15 W m^{-2} (-0.25 to about -0.05), with moderate confidence in AR5 (Myhre et al. 2013). While in AR4, the estimated radiative forcing was -0.2 W m^{-2} (-0.4 to about 0), with *moderate-low confidence* (Sagayama et al. 2008).

<u>Hydrologic feedback to climate</u>: Land use change causes additional modifications that are not radiative, but impact the surface temperature, in particular through the hydrologic cycle. These are more uncertain and they are difficult to quantify, but tend to offset the impact of albedo changes. As a consequence, there is low agreement on the sign of the net change in global mean temperature as a result of land use change (Hartmann et al. 2013).

In terms of land-based water cycle changes, AR5 reported increased global evapotranspiration from the early 1980s to 2000s, however, the further increase is constrained due to lack of soil moisture availability. The increasing aerosols level, declining surface wind speed and solar radiation are regionally dependent explanation to the decreasing evapotranspiration. In vegetated regions, rising CO_2 concentration can limit stomatal opening and thus transpiration as a main contribution to evapotranspiration. AR5 concluded increased global near surface air specific humidity since 1970. However, the moistening trend on land has abated since 2000, resulted in decreased near-surface relative humidity.

<u>Climate-related extremes on land</u>: AR5 reported with *very high confidence* that impacts from recent climate-related extremes, such as heat waves, droughts, floods, cyclones, and wildfires, **reveal significant vulnerability and exposure of some ecosystems and many human systems to current climate variability**. Impacts of such climate-related extremes include alteration of ecosystems, disruption of food production and water supply, damage to infrastructure and settlements, morbidity and mortality, and consequences for mental health and human well-being. For countries at all levels of development, these impacts are consistent with a significant lack of preparedness for current climate variability in some sectors (Burkett et al. 2014).

<u>Land-based climate change mitigation</u>: AR5 reported that Adaptation and mitigation choices in the near-term will affect the risks of climate change throughout the 21st century(Burkett et al. 2014)**.** Agriculture, forestry and other land use (AFOLU) are responsible for about 10-12 $GtCO_2eq$ yr^{-1} anthropogenic greenhouse gas emission mainly from deforestation and agricultural production. CO_2 emission from global forestry and other land use has been declined since AR4, largely due to decreasing deforestation rates and increased afforestation. With idealised implementation transformation scenarios, land-related mitigation, including bioenergy, could contribute 20% to 60% of total cumulative abatement to 2030, and 15% to 40 % to 2100. Policy coordination and implementation challenges make the real costs and net emission reduction potential of mitigation uncertain (Conway 2012a).

Meanwhile, UNEP Global Environment Outlook (GEO-6) recently synthesised large-scale land surface changes, and concluded that the harvested crop area increased by 23% and global crop production rose by 87% between 1984 and 2015. In the 1990s, about 10.6 million ha yr^{-1} of natural forests were lost. For the period 2010-2015, this rate had dropped to 6.5 million ha/yr. From 1975-2015, urban settlements have expanded approximately 2.5 times, accounting for 7.6% of the global land area. Assessment based on satellite data shows that land degradation hotpots cover about 29 % of global land area (GEO-6 2017).

Asia and the Pacific region experience the world's fastest urbanisation, accounting for 48% of

global urban population in 2014. This is projected to increase to 63% by 2050. Natural forest areas in Southeast Asia is deforested annually by more than 10,000 km^2, resulting in hundreds of millions of tonnes of carbon dioxide emissions per year between 2005 and 2015. 60% of the original mangroves in Southeast Asia has been cleared for coastal development (GEO-6 2017). From 2001 to 2013, cropland increased by 17% and pasture increased by 57% converted from forest in Latin America and the Caribbean. Deforestation to cropland from 1993 to 2013 is 405,000 ha in Canada, a much reduced deforestation rate compared to 1,286,000ha from 1970 to 1990 (GEO-6 2017). In Africa, about 500,000 km^2 of land is degraded every year. The key drivers of land degradation are urbanisation, deforestation, over-cultivation and overgrazing. Forest cover in Africa is continually shrinking. The projected forest area is less than 6 million km^2 by 2050 due to the increasing conversion of forests to agricultural and housing need to support continuously increasing population (GEO-6 2017).

2.2 Progress in understanding of processes underlying land-climate interactions

2.2.1 Biogeophysical and biogeochemical interactions

Terrestrial ecosystems affect climate through biogeophysical and biogeochemical interactions. **'Biogeophysical interactions'** (Figure 2.2.1) are formed by the physical processes that depend on land surface characteristics such as albedo and roughness, amount of green vegetation (e.g. leaf area index, LAI) and biological processes (e.g. leaf stomatal opening). The biophysical interactions influence exchanges of shortwave and long-wave radiation, turbulent fluxes (i.e. evapotranspiration and sensible heat flux) and momentum (Alkama and Cescatti 2016; Forzieri et al. 2017a; Mahmood et al. 2014; Burakowski et al. 2018). Ecosystems, particularly forests, are also prime regulators of the water cycle and heat transfer; forest covers and their functions at regional scales strongly influence both biogeochemical and biophysical phenomena at local and regional scales (Ellison et al. 2017) *(robust evidence, high agreement).*

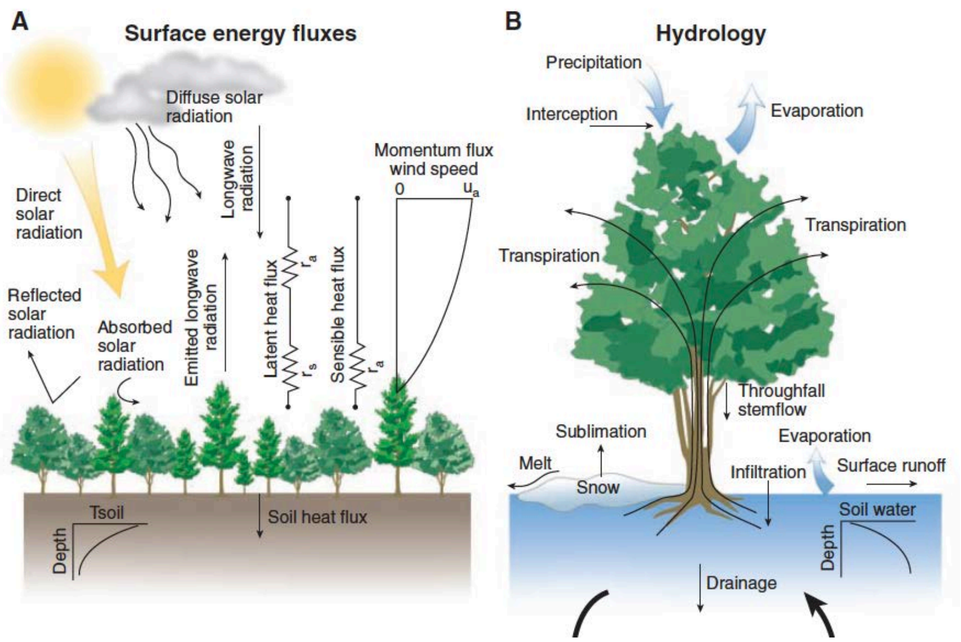

Figure 2.2.1: Schematic of the biophysical exchanges that occur at the land (soil-vegetation) / atmosphere from (Bonan 2008). On the left components of the energy budget (radiation, turbulent and diffusive heat

fluxes), on the right components of the water budget.

''Biogeochemical interactions' (Figure 2.1.1, section 2.1) encompass exchanges of greenhouse gases and aerosols between land and the atmosphere, which are determined by the state of the terrestrial ecosystems, their structure and functioning (section 2.5). Future uptake and release of carbon and other greenhouse gases (e.g. CH_4 and N_2O) are among the greatest uncertainties in our efforts to model the Earth's climate system (Ciais et al. 2013). It is widely believed that since 1960s land carbon sink has been increasing (Ballantyne et al. 2012) and reaching 3.1 ± 0.9 PgC net removal of CO_2 from the atmosphere during 10 years, that is 25-30% of total anthropogenic emissions of carbon (2.1, 2.4). However, the mechanisms responsible are still not well understood. Potential causes include enhanced vegetation growth under elevated atmospheric CO_2 and nitrogen (N) deposition (i.e. "fertilisation"), re-growth of secondary forests recovering from prior harvesting and agricultural abandonment, lengthening of the growing season in the high latitudes.

Land use and land cover changes (LULCC) not only affect the atmospheric physical state and chemical composition locally, where such changes occur, but also remotely through atmospheric teleconnections (section 2.6) and globally through their contribution to levels of greenhouse gases (section 2.4). LULCC modulate flux of fresh water, nutrients, and particular matters from land to ocean, and influences productivity and circulation patterns of ocean. Conversion of forests to agriculture, urbanisation and hydrological engineering (e.g., dam construction flow alteration, waste water treatment, wetland management) influence such phenomena. (AR5, WII). In tropics such conversion resulted in large positive carbon emissions, particularly from conversion of peatland forests (Van Der Werf et al. 2010a) (section 2.4). Deforestation leads to soil erosion (Borrelli et al. 2017) and carbon loss (Jackson et al. 2017). Afforestation and reforestation reverse the flow of carbon and remove carbon from the atmosphere as forests grow, but as tree plantations go through harvest cycles, the long-term result of conversion from natural forests to man-made forests is a long-term net reduction in the size of terrestrial carbon storage (needs reference). Furthermore, fire suppression may lead to increased fuel load and wild fire in man-made forests, but such wildfires are difficult to incorporate into models (see chapter Box 2.1).

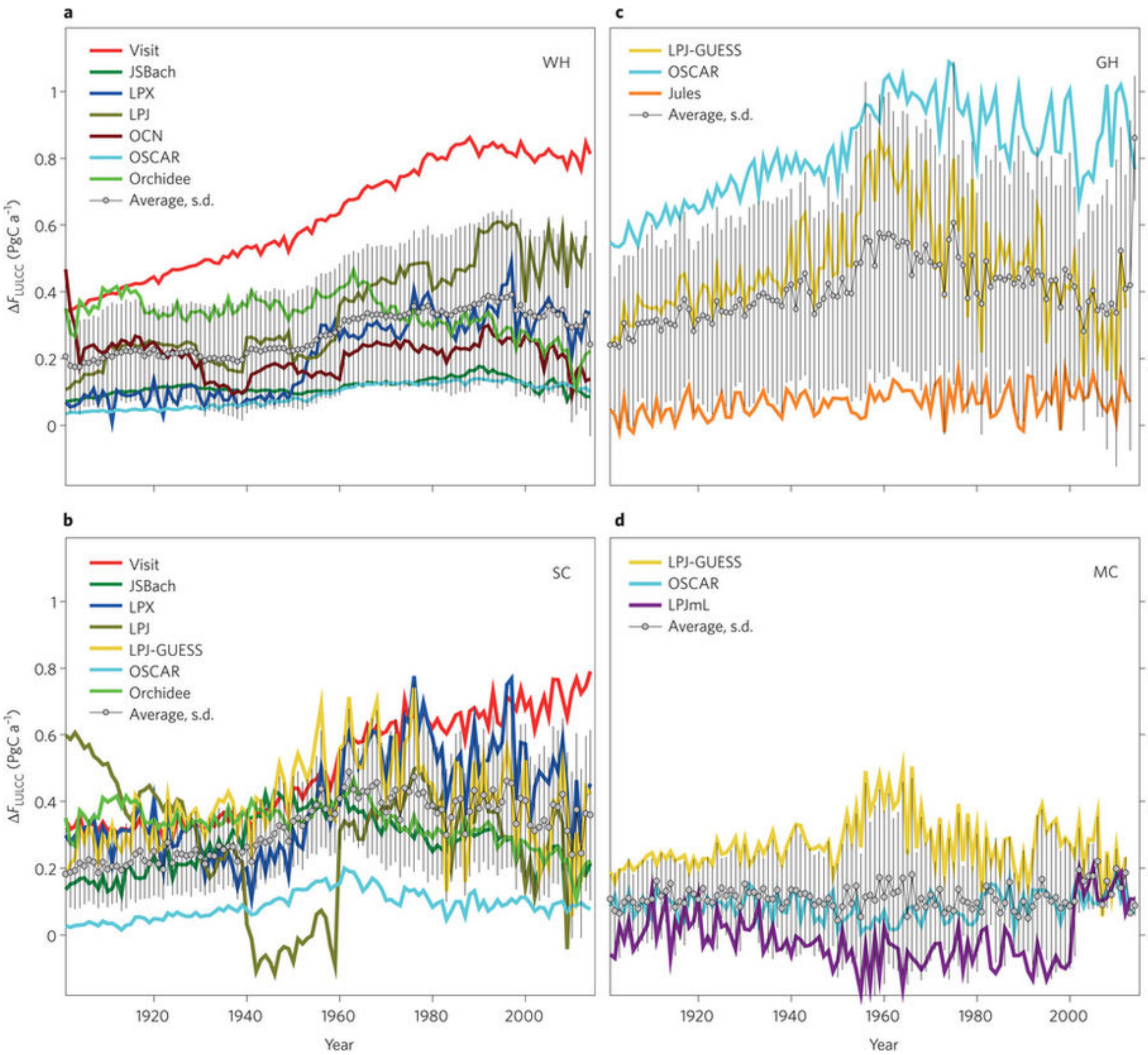

Figure 2.2.2 Difference in LULCC emission flux (ΔF_{LULCC}) due to individual processes. a, Wood harvesting. b, Shifting cultivation. c, Grazing and crop harvesting (using the grass functional type). d, Full crop representation. Coloured lines represent different models, grey symbols and hairlines are average ±1 standard deviation (Arneth et al. 2017a).

The magnitude and sign of LULCC depends on the region. In tropical latitudes, deforestation causes decreases of evapotranspiration and latent heat transfer at local scales, and smoother land surface without trees reduces local convective rainfall (Khanna et al. 2017). In the temperate zones, the two processes are expected to be offsetting each other (Findell et al. 2017). These complex interactions require improved understanding of the multiple factors involved in climate-land interactions across temporal and spatial scales.

Some changes in the land characteristics or GHG emissions, such as changes in the albedo or GHG emissions from the LULCC, are considered to be ‘forcing’ on the climate systems. Other changes, such as changes in the strength of land carbon sinks or sources, are considered to be ‘feedbacks’ to the climate system – processes that modulate climate change response to ‘forcings’ (e.g. anthropogenic GHGs). An example of a negative biogeochemical feedback is enhanced uptake of atmospheric CO_2 by terrestrial biosphere (Ballantyne et al. 2012). An example of a positive biogeochemical feedback is a potential release of CO_2 and CH_4 from melting permafrost. In southernmost permafrost regions forest trees substantially delays thawing of permafrost and thus slow down impacts of climate warming (Baltzer et al. 2014). The coupled climate-biogeochemical cycle models (hereafter referred to as, Earth System Models, ESMs) are used to evaluate these multiple feedbacks between changing climate, vegetation and soils, and LULCC (Green et al. 2017b). ESMs studies evaluate how different types of vegetation and soil processes such as photosynthesis, respiration, evapotranspiration, plant mortality or fires respond to changes in temperature, precipitation, short-wave radiation, etc. Variations among ESM results, such as prediction of atmospheric CO_2 are likely due structural uncertainty of the land models (Hoffman et al. 2014).

AR5 concluded that ESMs were still at early stages in capturing processes shaping biogeochemical and biophysical interactions necessary for simulating the effects of land use, land use change and forestry (AR5, WG1, Section 6.3). More specifically, it listed six types of terrestrial biosphere processes that were yet to be adequately incorporated in models: (1) disturbances that influence strength and resilience of forest carbon sinks, such as fire, logging harvesting, insect outbreaks and resulting variations in forest age structures, (2) decomposition processes in ecosystems with high organic carbon contents, including permafrost and wetlands (especially peatlands), (3) soil nutrient dynamics and their influence on vegetation functions, (4) impacts of tropospheric ozone and other pollutants, (5) coupling of water and heat transfer in soil-plant-atmosphere continuum, (6) surface transport of water and soil (via erosion). These processes interact with each other, and often their responses to climate factors are non-linear.

Since AR5, a number of observational and modelling studies have refined understanding of how these processes could affect regional and global climate. A growing number of studies suggest that diversity of plants, animals and microbes, ecosystem complexity and their biological responses, including adaptive migration and acclimation of organisms, play an important role and were missing in the AR5-class ESMs. Furthermore, more studies have examined how human modifications of environment in rural and urban ecosystems affect land-climate interactions. This section provides an overview of the terrestrial processes that are receiving increasing attention or continue to be under intense scientific studies since AR5.

2.2.2 Plant physiological responses and acclimations to increases in CO_2 and temperature

The process of CO_2 exchange by all plant leaves share a common physiological mechanism of photosynthesis inside chloroplasts, optimisation of CO_2 uptake and water loss through stomata, and thermal acclimation of respiration by plant leaves (autotrophic respiration). The first two processes are adequately modelled by the biochemical model of photosynthesis (Farquhar, Caemmerer, & Berry, 1980; Farquhar, 1989), which allows modeling of atmospheric CO_2 concentration, effects of water availability via stomatal adjustment (more in 2.2.5), and nutrient availability (more in 2.2.3). This model has been incorporated in many climate-vegetation interaction models, and has allowed quantitative prediction of CO_2 fertilisation effects of increased photosynthetic production by terrestrial plants. Gross photosynthesis has less acute (but still significant) responses to temperature, compared to exponential increase of metabolic rate and respiration. At the time of AR5, short- and long-term responses of autotrophic respiration to warmer temperature regimes represented the largest source of uncertainty in estimation of vegetation Net Primary Production (NPP) in vegetation dynamic models (Malhi et al. 2011). However, recent empirical work allows improved model prediction of photosynthesis-carbon balance in the warmer and CO_2 rich future.

CO_2 fertilisation

Increasing atmospheric CO_2 could potentially enhance photosynthesis and water use efficiency of individual leaves, resulting in increased rates of plant growth and carbon sequestration (Field et al. 1995). This is empirically supported by long term measurements of CO_2 and water vapour that show increases in net ecosystem carbon uptake and increases of photosynthetic water use efficiency in temperate and boreal forests (Keenan et al. 2013). A modelling study suggests that it may be possible for CO_2 fertilisation effects to ameliorates the impacts of future droughts and heat stresses in grassland net carbon uptake (Roy et al. 2016) .

The realised CO_2 effect on growth observed FACE experiments is highly variable (Paschalis et al. 2017), due to nutrient limitations and other constraints on plant growth (Körner 2015). While elevated CO_2 does indeed result in increased short-term CO_2 uptake per unit leaf area, it is not certain whether this translates to increased growth rates of the whole plant, vegetation communities, ecosystems and biomes at decadal or longer time scales. Apparent inconsistencies among studies stem from multiple factors that constrain plant growth, such as whole-plant resource allocation constraints, nutrient limitation (especially N, P and possibly K), plant and soil water balance, light limitation, soil organic matter decomposition, and changes in plant community composition, mortality rates and biomass turnover (Körner 2006). Still, some studies show CO_2 fertilisation even when soil N supply is limited, but generally this may be restricted to species capable of overcoming N limitation by mutualistic association between roots and microbes (Terrer et al. 2017). Plant root-soil-microbe interaction plays an important role in mediating the nature of nutrient acquisition for supporting enhanced productivity under increasing CO_2 levels (section 2.2.3).

The most consistent consequence of elevated CO_2 is increased water-use efficiency by plants by stomatal regulation, resulting in enhanced tolerance of droughts by crop and plants in semi-arid areas (Berry et al. 2010; Ainsworth and Rogers 2007). There is strong evidence from long-term CO_2 and water vapour flux measurements that water-use efficiency in temperate and boreal forests of the Northern Hemisphere has increased much more over the past two decades than predicted by theory and several terrestrial biosphere models (Keenan et al. 2013). Further, this increase has been accompanied by enhanced photosynthesis and decreased evapotranspiration at the ecosystem level, suggesting benefits to NPP from CO_2. Several studies have used tree ring records to pick up possible signals of the CO_2 fertilisation effect over time scales of several decades to a century or more. Increased water-use efficiency (of 30-35% over the past 150 years) is observed in three tropical wet forests across the globe through inferences of stable carbon isotope ratios in tree rings, but there was no evidence for any acceleration of tree growth rates in support of the CO_2 fertilisation effects (van der Sleen et al. 2014). Experimental work at three FACE sites in the temperate region, in which tree ring and a combination of stable carbon and oxygen isotopes of wood were analysed, confirms increased water use efficiency over time (Battipaglia et al. 2013). There is, however, considerable uncertainty whether such increase in leaf-level water use efficiency actually translates into plant growth and benefits in NPP across ecosystems and biomes. At the levels of whole plant and vegetation, growth is constrained by availability of soil nutrients, in particular nitrogen and phosphorus (Reich and Hobbie 2013; Norby et al. 2010) (section 2.2.3).

Regional differences should be considered in order to evaluate the total effects of warming, anthropogenic CO_2 fertilisation, precipitation change, and nitrogen deposition. Newer statistical treatment of tree ring and isotope data from 37 published studies representing all the major biomes concluded that intrinsic water use efficiency (iWUE) was consistently positive (in the range of 10%-60% during 1960-2010) but this did not necessarily translate into enhanced tree growth rates (Silva and Anand 2013). Only in boreal, alpine and Mediterranean trees about an increase of 20% in iWUE resulted in increased growth; indeed, in other major biomes including temperate, subtropical and tropical forests, there was actually a negative relationship between iWUE and tree growth rate. Analyses of records from the International Tree Ring Data Bank (ITRDB) indicated that only about

20% of the global sites showed increasing trends in tree growth that cannot be explained by climate variability, N deposition, elevation or latitude; thus this is taken as evidence for direct CO_2 fertilisation of forests on a limited scale during the 20th century (Gedalof and Berg 2010). Local site conditions and individual species' responses would determine future forest dynamics and the nature of the CO_2 effect.

Approaches using top-down analyses from satellite data of changes in global vegetation greenness and global mass balance model argue for significant increase in NPP that can be attributed to CO_2 fertilisation. Using a "reconstructed vegetation index" (RVI) for the period 1901-2006 from MODIS satellite-derived NDVI (Normalized Vegetation Difference Index), and precipitation and temperature data for a more recent period, a global analysis concluded that CO_2 fertilisation conservatively contributed 0.7 PgC yr^{-1} or 40% of the recently observed land carbon sink (Los 2013). Another framework for reconciling the various estimates of terrestrial carbon feedbacks within the global mass balance context, using the process model intercomparison TRENDY and two atmospheric models (TransCom and RECAP), also concludes that 60% of the recent terrestrial carbon sink can be directly attributed to increasing atmospheric CO_2 (Schimel et al. 2015). Problems in reconciling bottom-up estimates from ground-based measurements of vegetation productivity versus top-down approaches of using satellite and atmospheric data on vegetation and CO_2 fluxes may be reduced by improved detection and attribution methods (Saeki and Patra 2017) (section 2.4).

2.2.2.1 Acclimation and other physiological responses

Acclimation is broadly defined as the biochemical, physiological, morphological or developmental adjustments within the lifetime of organisms that result in improved performance at the new condition. Acclimation often operates over a time span of days to weeks, and can mitigate negative effects of climate change on plant growth and ecosystem functions (Tjoelker 2018). Plants can acclimate to changing CO_2 levels, temperature, and other environmental conditions through adjustment of gene expressions and physiological mechanisms. Optimal temperature for forest NPP (Tan et al. 2017) is not just a matter of optimal temperature for gross photosynthesis, because temperature response of respiratory processes, which are generally negligible at the leaf level, play an important role as determinant of the optimal temperature for net carbon balance at the stand level *(robust evidence, high agreement).* Bayesian statistical estimates of global photosynthesis and total ecosystem respirations suggest that they exhibit different responses to thermal anomaly during the last 35 years (Li et al. 2018b).

Yet, thermal responses of respiration in short and long term have not been appropriately incorporated in most dynamic vegetation models. Assumptions associated with respiration have been a major source of uncertainty. In most existing models, a simplistic assumption that respiration doubles with each 10°C increases of temperature (i.e., $Q_{10} = 2$) is adopted, ignoring acclimation. Such assumption on thermal responses of respiration can strongly influence estimated net carbon balance at large spatial scales of ecosystems and biomes, as well as over the time period of multiple decades (Smith and Dukes 2013; Smith et al. 2016a). For example, experimental data from a tropical forest canopy show that temperature acclimation ameliorate the negative effects of rising temperature to leaf and plant carbon balance (Slot et al. 2014). However, at the time of AR5, model parameterisation was difficult due to data paucity, particularly from tropical forests.

To amend this situation, global database (GlobResp) has been compiled to amend such data deficiency, leading to meta-analysis of 899 plant species, spanning a range of plant functional types and biomes from sea level to 3450m above sea level (Atkin et al. 2015), and another of 231 plants species across seven biomes (Heskel et al. 2016). The empirical data generated during the last decade on thermal responses of respiration demonstrate a globally convergent empirical pattern; acclimation results in reduced sensitivity of respiration with rising temperature, i.e., down regulation of warming-related increase in respiratory carbon emission in all biomes (Slot and Kitajima 2015; Tjoelker 2018). Empirical functions on thermal responses of plant respiration allow more realistic parameterisation of the land surface flux components of earth system models.

above sea level

Comparisons of models with and without thermal acclimation of respiration show that that acclimation can halve the increases of plant respiration with predicted temperature increase by the end of 21st century (Vanderwel et al. 2015). According to a sensitivity analysis, a newly derived function of instantaneous responses of plant respiration to temperature (instead of a traditional exponential function of $Q_{10} = 2$) makes a significant reduction of autotrophic respiration especially in cold biomes (Heskel et al. 2016). Parameterisation of a gridded earth system model (JULES) with this newly derived empirical function of temperature response of leaf respiration, as well as consideration of plant functional types for non-leaf respiration, results in significant shifts in estimated autotrophic respiration in most biomes at pre-industrial and projected future time, with an overall conclusions that whole plant respiration may be about 30% higher than previous estimates (Huntingford et al. 2017).

Acclimation of photosynthesis is not well implemented in the models either. During acclimation to warming, the optimum temperature for photosynthesis shifts towards the acclimation temperature, but across species and functional groups TOpt generally does not increase as much as growth temperature (Slot and Winter 2017; Yamori et al. 2014). The shift in Topt is underpinned by a complex interaction of biochemical, respiratory, and stomatal regulation. Typically, however, the ratio of maximum electron transport rate (J_{max}) to maximum RuBP carboxylation (V_{cmax}) decreases with increasing growth temperature (e.g., Kattge and Knorr 2007) , providing a simple algorithm that has been employed to address acclimation in several recent modelling studies. Mercado *et al.* (2018), using this approach, found that inclusion of biogeographical variation in photosynthetic temperature response was critical for estimating future land surface carbon uptake. This stresses the need for empirical data on acclimation of photosynthesis from across the globe, but especially from tropical forests, which are currently lacking. Acclimation to simultaneous changes of temperature and CO_2 are even less well understood and represented in the models.

2.2.3 Nutrient limitation of plant growth

The stoichiometry of C:N:P would eventually determines the upper limit of growth responses of individual plants and ecosystem carbon sequestration to increasing CO_2 (Sardans et al. 2012). In other words, increased atmospheric CO_2 concentrations, without concomitant increases in availability of N and P, would not lead to the long-term growth enhancement expected from CO_2 fertilisation.

Nitrogen as a limiting factor for plant growth, either in N-poor soils or progressive N depletion in systems with accelerated plant growth from CO_2 fertilisation, has been well-recognised (Terrer et al. 2017) (*robust evidence, high agreement*). Experimental evidence for N as the primary constraint to enhanced productivity has been shown in both forest (Norby et al. 2010) and grassland (Reich and Hobbie 2013) ecosystems. Enhanced growth of plants in tundra and boreal forests under longer growing seasons and warmer climate (partially *via* enhanced nitrogen availability) may result in significant compensation of carbon loss from thawing permafrost (Schuur et al. 2015).

Yet, there is considerable uncertainty in long-term responses of various ecosystems to interactive effects of elevated CO_2 (eCO_2) and nutrient availability. At the Oak Ridge FACE experiment site in a temperate deciduous forest, NPP significantly increased under exposure to 550 ppm as compared to ambient CO_2 by 24% during 2001-2003 but then declined to only 9% by 2008; this could explained by declining N availability (Norby et al. 2010). Similarly, lowered soil N availability in a long-term temperate grassland experiment reduced productivity by half during 2001-2010 compared to the previous decade under eCO_2 (Reich and Hobbie 2013). When both N and moisture (summer rainfall) became limiting at this temperate grassland site, there was no stimulation of plant biomass (Reich et al. 2014), contrary to expectations from semi-arid habitats where plant water-efficiency induced by eCO_2 would enhance soil moisture and productivity (including C4 grasses that are not expected to benefit much from eCO_2)(Donohue et al. 2013; Morgan et al. 2011; Derner et al. 2003). After more than 12 years of eCO_2 growth of C4 grasses unexpectedly started to be stimulated, while growth of C3 grasses was the same as at ambient CO_2, because N mineralisation increased C4 grass plots but not in C3 grass (Reich et al. 2018).

New evidence suggest that plant adaptation, particularly through plant-microbe symbioses, could alleviate some nitrogen limitation to plant growth under CO_2 fertilisation (Terrer et al. 2017)*(medium evidence, high agreement).* In the Duke FACE experiment, accelerated soil N cycling supported increased N uptake, supporting growth enhancement (Drake et al. 2011). Similar results were observed in an aspen forest (Talhelm et al. 2014; Zak et al. 2011) and in an oak woodland (Hungate et al. 2013). Explanations of the apparent contradiction (with some sites becoming nitrogen limited after a few years and others sustaining growth through accelerated N uptake) have focused on the role of rhizosphere priming effects and mycorrhizal associations. (Terrer et al. 2016) found that ectomycorrhizal-associated ecosystems sustained enhancement of plant growth under elevated CO_2 and low-nitrogen conditions while arbuscular mycorrhizal-associated ecosystems became nitrogen limited. Measurements of root exudation have supported the possibility that enhanced root exudation under elevated CO_2 can accelerate soil N cycling (Phillips et al. 2011).

Model assessments that included rhizosphere priming effects and ectomycorrhizal symbioses have also suggested that acceleration of SOM cycling through these microbial symbioses could explain enhanced N availability and plant growth (Sulman et al. 2017; Orwin et al. 2011; Baskaran et al. 2017). However, the ability of ectomycorrhizal fungi to decompose SOM varies among species (Pellitier and Zak 2018) and the capacity of ecosystems to sustain long-term growth through these symbioses is still under debate (Ridge 2017). A recent study by (Houlton et al. 2018) suggests that bedrock weathering is a significant source of nitrogen to plants, accounting for 19 to 31 Tg yr^{-1} of nitrogen mobilisation.

Anthropogenic alteration of global and regional N and P cycles has major implications for future C storage by natural and managed ecosystems (Peñuelas et al. 2013) *(robust evidence, high agreement).* Both CO_2 and N fertilisation have had positive effects on carbon sequestration by vegetation, but other nutrients may become the limiting factor (Peñuelas et al. 2017). During 1997-2013, the contribution of N deposition to the global C sink has been estimated at 0.27 (+/- 0.13) Pg C yr^{-1}, and the contribution of P deposition as 0.054 (+/- 0.10) Pg C/ yr^{-1}; these constitute about 9% and 2% of the total land C sink, respectively (Wang et al. 2017c). Thus, anthropogenic nitrogen depositions may enhance carbon sequestration by vegetation (Liu and Greaver 2009; Reich et al. 2014; Schulte-Uebbing and de Vries 2018), but it may lead to imbalance of nitrogen *vs.* phosphorus availability (Peñuelas et al. 2013) and reduced ecosystem stability (Chen et al. 2016c).

Phosphorus is also an essential nutrient that can limit plant productivity and the carbon cycle (Reed et al. 2015) (*medium evidence, medium agreement*). In contrast to N, which is biologically cycled, P inputs to soil come largely from bedrock weathering, and thus, P cycles can respond quite differently to environmental change. Broadly, boreal and temperate ecosystems are more likely to be limited by N while tropical ecosystems are limited by P availability, although supporting evidence from P-fertilisation experiments is missing lacking (Schulte-Uebbing and de Vries 2018), likely as a result of the strongly species-specific-rather than community-specific-nature of P limitation of tropical tree growth (Turner et al. 2018a). Still, it is important to incorporate parameters and processes relating to the P cycle into global land C sink models in the tropics (Reed et al. 2015). New study with an Earth System Model (Zhang et al. 2013c) capturing both N and P limitations, indicate that the simulated future C-uptake on land was reduced significantly when both N and P are limited as compared to only C-stimulation, by 63% (of 197 Pg C) under RCP2.6 and by 67% (of 425 Pg C) under RCP8.5.

Phosphorus availability afforded by mycorrhizal fungi can explain variable results associated with the growth-enhancing effects CO_2 fertilisation in interaction with soil nitrogen availability (Terrer et al. 2017). A synthesis of data from several studies show that species that establish symbiotic associations with ectomycorrhizal fungi show significant 30% (+/- 3%) biomass increase as compared to plants that do not have such association, irrespective of N limitation. A strong case has also been recently made for potassium (K) as a possible limiting factor for plant productivity in terrestrial ecosystems especially in water-limited systems; N deposition has inhibitory effects on K availability, and thus interactive effects of N, P, K and water need to be incorporated into ESMs (Sardans and Peñuelas 2015).

2.2.4 Seasonality of ecosystem processes relevant for land-atmosphere interactions

It is well documented that phenology, i.e., seasonal activities of organisms, respond to cues such as temporal patterns of temperature, day length, and moisture. Shifts in phenological timing have been documented in various organisms in the past half century in response to on-going climate change (Gordo and Sanz 2010; Shen et al., 2015). The IPCC AR5 reported that Spring Greenup (SG), the time at which plants begin to grow leaves in northern mid- and high-latitude ecosystems, has advanced at a rate of between 1.1 and 5.2 days per decade over different periods and regions, as inferred from multiple studies. Newer evidence indicates greater advances of SG especially over northern hemisphere high latitudes (Goetz et al. 2015; Xu et al. 2016a). Pulliainen et al. (2017) determined the annual timing of spring recovery from space-borne microwave radiometer observations across northern hemisphere boreal evergreen forests for 1979-2014, reporting a trend of advanced spring recovery of carbon uptake for this period, with an average shift of 8.1-d (2.3 days per decade). They use this trend to estimate the corresponding changes in gross primary production (GPP) by applying *in situ* carbon flux observations. Micrometeorological CO_2 measurements at four sites in northern Europe and North America indicate that such advance in SG has increased the January-June GPP sum by 29 gCm^{-2} (8.4 gCm^{-2} (3.7%)/decade) (Pulliainen et al. 2017).

There is good consensus that the enhanced GPP in recent decades is the result of both longer growing season and greater greening during the growing season. Three satellite based leaf area index (GIMMS3g, GLASS and GLOMAP) records imply increased growing season LAI (greening) over 25-50% and browning over less than 4% of the global vegetated area, resulting in greening trend of $0.068\pm\ 0.045\,m^2\,m^{-2}\,yr^{-1}$ over 1982-2009 (Saunois et al. 2016; Zhu et al. 2016). For example, GIMMS3g NDVI infers 42.0% greening and 2.5% browning of the northern vegetation from 1982 to 2014, and the greening explains 20.9% increases in the growing season productivity since 1982 (Park et al. 2016).

The seasonal cycle of atmospheric CO_2 is largely driven by phenology of plant photosynthesis and ecosystem respiration. In northern ecosystems under various climate warming scenarios, it is likely that additional carbon uptake attributable to enhanced photosynthetic production in summer months is greater than increased respiratory carbon emission in dormant months (Pulliainen et al. 2017). The seasonal phase of atmospheric CO_2 level may not be easily inferred by the observed phenological shift because both photosynthesis and respiration increase during SG (Gonsamo et al. 2017).

Seasonal leaf area cycle affects both biogeochemical and biophysical interactions between vegetation and atmosphere. Albedo exhibits seasonal patterns with development and senescence of the vegetation canopy that differentially reflect photosynthetically active and near-infrared radiation. In deciduous forests, leaf-out increases albedo by 20%-50% from the spring minima to growing season maxima, followed by rapid decrease during senescence; in contrast, in grasslands, green-up causes albedo decreases and then increases with senescence (Hollinger et al. 2010). The seasonal patterns of sensible and latent heat fluxes are also driven by LAI cycle in temperate deciduous forests: sensible heat fluxes peak in spring and autumn and latent heat fluxes peak in mid-summer (Moore et al. 1996). Increased transpiration accompanying leaf-out causes surface cooling and puts water vapour into the lower atmosphere that increases lower atmosphere heat capacity (Schwartz, 1990). In areas with good soil water availability and extensive vegetation, increased evapotranspiration contributes enough moisture into atmosphere, resulting in increased frequency of cumulus clouds during the growing season (Richardson et al. 2013).

Whereas LAI increases in warmer climate result in overall cooling effects to the climate, the greening of high latitudinal regions with vegetation may lead to positive feedback to climate, known as Arctic amplification, mainly through decrease of albedo (Pearson et al. 2013). The warming effect of albedo change is maximum in boreal summer when incoming solar radiation is high (Pielke et al. 2011; Chae et al. 2015). In contrast, the increased growing-season greening on Tibetan Plateau has induced dominant evaporative cooling in daily maximum temperature (Shen et al. 2015a). Globally, the continuously increased growing season LAI since 1982 mitigated 12% (0.09±0.02°C) of global land-surface warming for the past 30 years, via the combined cooling effects from increased evapotranspiration (70%), changed atmospheric circulation (44%) and decreased shortwave transmissivity (21%), and warming effects from increased longwave air emissivity (-29%) and decreased albedo (-6%) (Yang et al. 2017; Zeng et al. 2017).

2.2.5 Coupling of water in soil-plant-atmosphere continuum and drought mortality

The response of plants to changing environmental drivers, such as soil moisture and vapour pressure deficit, fundamentally mediates ecosystem responses to climate and land-atmosphere interactions (Sellers et al. 1996; Bonan 2008). When stomatal conductance and leaf area change, the stand-level fluxes of carbon and water, as well as latent and sensible heat fluxes change (Seneviratne et al. 2018). Stomatal response to environmental conditions has been studied for decades (Wong et al. 1979) and could be incorporated into photosynthesis component of ESMs (Farquhar 1989). A critical role of plant water transport through the soil-plant-atmosphere continuum, particularly during drought, is widely recognised(Sperry and Love 2015; Brodribb 2009; Choat et al. 2012). New models now link plant water transport with canopy gas exchange and energy fluxes, leading to improved prediction of climate change impacts on forests and land-atmosphere interactions (Wolf et al. 2016; Sperry et al. 2017; Anderegg et al. 2016).

The importance of regionally widespread tree mortality triggered directly by drought and heat stress, which are often exacerbated by insect outbreak and fire was well recognised at the time of AR5 (Allen et al. 2010; Breshears et al. 2005; Kurz et al. 2008). For example, the massive climate-driven bark beetle outbreak in western Canada in the early 2000s may have flipped a large region of Canadian boreal forest from a net carbon sink to a carbon source for over a decade (Kurz et al. 2008). Tree mortality will also alter land albedo, roughness, and other biophysical properties of forests, often in complicated ways (Anderegg et al. 2012).

Current vegetation and land surface models do not adequately capture tree mortality and the response of forests to climate extremes like drought (Hartmann et al. 2018). Most vegetation models use climate stress envelopes or vegetation carbon balance estimations to predict climate-driven mortality and loss of forests (McDowell et al. 2011), which are unlikely to provide robust projections of biome shifts and impacts of disturbance in future climates. For example, a suite of vegetation models was compared to a field drought experiment in the Amazon on mature rainforest trees and all models performed poorly in predicting the timing and magnitude of biomass loss due to drought (Powell et al. 2013). More recently, the loss of water transport in tree xylem due to embolism (Sperry and Love 2015) is receiving attention as a key physiological process relevant for drought-induced tree mortality (Hartmann et al. 2018). A recent meta-analysis documented that a set of plant traits related to tree water transport explained drought-induced tree mortality rates in many sites across the world (Anderegg et al. 2016). Large uncertainties remain around how forests recover from climate stress and interactions among drought, temperature, rising CO_2 concentrations and other disturbances (e.g. fire) (Allen et al. 2015).

2.2.6 Soil organic matter decomposition and nutrients dynamics

The sensitivity of soil organic matter (SOM) stocks to changes in climate and plant productivity has been identified as a major uncertainty in global carbon cycle projections *(robust evidence, high agreement)*. Todd-Brown et al. (Todd-Brown et al. 2013) identified high variation in soil organic carbon (SOC) stocks among CMIP5 ESMs, with model estimates of contemporary SOC stocks ranging from 510 to 3040 Pg C. Projections of changes in global SOC stocks during the 21st century by CMIP5 models also ranged widely, from a loss of 37 Pg to a gain of 146 Pg, with differences largely explained by initial SOC stocks, differing C input rates, and different decomposition rates and temperature sensitivities (Todd-Brown et al. 2014). With respect to land-climate interactions, the key processes affecting SOC stocks are warming (which is expected to accelerate SOC losses through microbial respiration) and acceleration of plant growth (which increases inputs of C to soils). However, complex mechanisms underlying SOC responses to both warming and carbon addition drive considerable uncertainty in projections of future changes in SOC stocks. The processes involving C sequestration into the soil as well as microbial community responses to warming have to be adequately understood when modelling the global carbon cycle (Singh et al. 2010).

Three existing data bases (SoiGrids, the Harmonized World Soil Base, Northern Circumpolar Soil Database) substantially differ in estimated size of global soil carbon stock (SOC) down to 1 m depth, varying between 2500 Pg to 3400 Pg (Tifafi et al. 2018). This amount is larger than the global soil carbon stock size reported as the best estimate in AR5 WGI (1500-2400 Pg), and represents four to eight times larger than the carbon stock associated with the terrestrial vegetation. Carbon stored in permafrost and deep mineral soil layers is a substantial in addition to this. Annually, 119 Pg C is estimated to be emitted from soil to the atmosphere, of which 50% is attributed to soil microbial respiration (Auffret et al. 2016; Shao et al. 2013).

Meta-analyses of warming experiments have shown significant variability in temperature responses across biomes and climates. Crowther *et al.* (2016) found that warming effects were most sensitive to initial carbon stocks, while van Gestel et al. (2018) suggested that SOC responses to warming were not significant in an expanded version of the same dataset. Studies of SOC responses to warming over time have also shown complex responses. In a multi-decadal warming experiment, Melillo et al. (2017) found that soil respiration response to warming went through multiple phases of increasing and decreasing strength, which were related to changes in microbial communities and available substrates over time. Knorr et al. (2005) and Conant et al. (2011) suggested that transient decomposition responses to warming could be explained by depletion of labile substrates, but that long-term SOC losses could be amplified by high temperature sensitivity of slowly decomposing SOC components. Overall, long-term SOC responses to warming remain uncertain: "*although it is well established that,* *within reasonable limits, the biological processes which drive decomposition will be more rapid at greater temperatures, being able to assign a thermal coefficient or set of coefficients to decomposition and nutrient mineralisation has proved remarkably difficult* (Davidson and Janssens 2006)" (Dungait et al. 2012). Thus, in the absence of a commonly accepted and broadly validated concept to describe SOM decomposition, projections of the impact of climate change on SOC by process-based terrestrial ecosystem models remain uncertain.

While current ESM structures mean that increasing C inputs to soils drive corresponding increases in SOC stocks, long-term carbon addition experiments have found contradictory SOC responses. Some litter addition experiments have observed increased SOC accumulation (Lajtha et al. 2014a; Liu et al. 2009), while others suggest insignificant SOC responses (Lajtha et al. 2014b; van Groenigen et al. 2014). Microbial dynamics are believed to have an important role in driving complex responses to C additions. The addition of fresh organic material can accelerate microbial growth and SOM decomposition via priming effects (Kuzyakov, 2010; Cheng et al., 2014). Priming effects in the soil directly surrounding living roots (rhizosphere) have been shown to increase under elevated CO_2 and N-limited conditions due to acceleration of root exudate production, contributing to accelerated soil C and N cycling as a plant-mediated response (Drake et al. 2011; Phillips et al. 2011).

SOM cycling is dominated by "hot spots" including the rhizosphere as well as areas surrounding fresh detritus (Finzi et al. 2015; Kuzyakov and Blagodatskaya 2015). This complicates projections of SOC responses to increasing plant productivity; increasing C inputs could promote higher SOC storage, but these fresh C inputs could also deplete SOC stocks by promoting faster decomposition (Hopkins et al. 2014; Sulman et al. 2014; Bertrand et al. 2018). A meta-analysis by van Groenigen et al. (2014) suggested that elevated CO_2 accelerated SOC turnover rates across several biomes. These effects could be especially important in high-latitude regions where soils have high organic matter content and plant productivity is increasing (Hartley et al. 2012), but have also been observed in the tropics (Sayer et al. 2011).

Microbial processes are also important in the context of warming. Acclimation (*via* physiological or community-level changes) to changing temperature regimes could reduce SOC losses under warming (Bradford et al., 2008; Zhou et al., 2011). However, experimental studies of microbial acclimation to warming have found contradictory results (Luo et al. 2001; Carey et al. 2016) with no acclimation observed in C-rich calcareous temperate forest soils (Schindlbacher et al. 2015) and arctic soils (Hartley et al. 2008). Indeed, research on soils from a variety of ecosystems from the Arctic to the Amazon indicated that microbes, in fact, could enhance the temperature sensitivity of soil respiration in Arctic and boreal soils, thereby releasing even more carbon than currently predicted (Karhu et al. 2014). In tropical forests, P limitation of microbial processes is a key factor influencing soil respiration (Camenzind et al. 2018). Temperature responses of symbiotic mycorrhizae differ widely among host plant species, without a clear pattern that may allow generalisation across plant species and vegetation types (Fahey et al. 2016).

Observational and modelling studies have highlighted the importance of temperature responses of microbial parameters such as carbon use efficiency and soil N dynamics in determining SOC responses to warming (Allison et al. 2010; Frey et al. 2013; Wieder et al. 2013; García-Palacios et al. 2015). More complex community interactions including competitive and trophic interactions could drive unexpected responses to SOC cycling to changes in temperature, moisture, and C inputs (Crowther et al. 2015; Buchkowski et al. 2017). Competition for nitrogen among bacteria and fungi could also suppress decomposition (Averill et al. 2014). Overall, the roles of soil microbial community and trophic dynamics in global SOC cycling remain very uncertain.

Along with biological decomposition, the other major process controlling SOC stabilisation and responses to climate change is stabilisation via interactions with mineral particles. Historically, conceptual models of SOC cycling have centred on the role of chemical recalcitrance, the hypothesis that long-lived components of SOC are formed from organic compounds that are inherently resistant to decomposition. Mathematical models, including all CMIP5 ESMs, have reflected this framework through their use of pseudo-first-order linear kinetics that represented SOC as a combination of pools with different fixed turnover rates modified by temperature and moisture functions. However, "*Empirical evidence is building against the notion of intrinsic molecular recalcitrance as a concept in understanding the stability of SOM*" (Ingrid et al. 2008; Marschner et al. 2008; MARKUS et al. 2011; Schmidt 2011) .

Under the emerging paradigm, stable SOC is primarily formed by the bonding of microbially-processed organic material to mineral particles, which limits the accessibility of organic material to microbial decomposers (Kallenbach et al. 2016; MARKUS et al. 2011; Francesca et al. 2012). SOC in soil aggregates can be protected from microbial decomposition by being trapped in soil pores too small for microbes to access (Blanco-Canqui and Lal 2004; Six et al. 2004) or by oxygen limitation (Keiluweit et al. 2016). Alternatively, organic materials can be stabilised through chemical bonds with mineral surfaces and metal ions (Lützow et al. 2006). These organo-mineral bonds are highly stable and are thought to make bonded organic matter inaccessible to microbial decomposition, although there is some evidence that root exudates such as oxalic acid can release mineral-associated organic matter (Keiluweit et al. 2015). While some emerging models are integrating these mineral protection processes into SOC cycling projections (Wang et al. 2013; Sulman et al. 2014; Tang and Riley 2014; Cleveland et al. 2015), the sensitivity of mineral-associated organic matter to changes in temperature, moisture, and carbon inputs is highly uncertain.

The effect of fire on soils is also a potentially important factor in soil-atmosphere feedbacks. While some soil and litter C is lost to the atmosphere as smoke and gases, fires also chemically transform organic matter into decomposition-resistant forms (pyrogenic C). Pyrogenic C is a common feature of soils around the world (Schmidt and Noack 2000) and has long residence times, although it can be decomposed and assimilated by microbes (Kuzyakov et al. 2014; Santos et al. 2012).

Deep soil layers (below 30 cm) can contain 46-63% of total profile C stocks, making them an important component of global terrestrial C stocks. Based on radiocarbon measurements, deep SOC can be very old, with residence times up to several thousand years (Rumpel and Kögel-Knabner 2011). More recently, Strey et al., (2017) show that in deep Amazon oxisols, only 21% of the soil carbon occur in the top 0.3 m (the depth considered in the standard IPCC protocol and UNFCC guidelines) of the vertical soil profile, whereas 84% of soil carbon can be accounted by going down to 3m. Dynamics associated with such deeply varied carbon remain understudied and ignored by the models, and not addressed in most of the studies assessed in this subsection. Deep soil C is thought to be stabilised by mineral interactions, but recent experiments suggest that CO_2 production from deep soils can be increased by warming (Hicks Pries et al. 2017) or additions of fresh carbon (Fontaine et al. 2007). While erosion is not typically modelled as a carbon flux in ESMs, erosion and burial of carbon-containing sediments is likely a significant carbon sink (Berhe et al. 2007, 2008; Wang et al. 2017d).

2.2.7 Agricultural land management and climate

Agricultural activities impact land-climate interactions not only through land cover changes, but also through changes in land management under intensification achieved with new technology. During 20th century, total global crop production nearly tripled, with major crop breeding improvements specifically targeting maize, rice, wheat, and other major grains (and later on, soybean) (Pingali 2012). By the late 20th century, these crops accounted for about 63% of the total global cropped area, with large expansions and land conversions across the developing world. Agriculture now occupies about 38% of the Earth's land surface (Foley et al. 2011; Ramankutty et al. 2008) (Figure 2.2.2). Alongside these land conversions were increased use of chemical fertilisers and irrigation infrastructure to increase agricultural productivity, which resulted in substantial climate and environmental impacts (Campbell et al. 2017; Pingali 2012; Foley et al. 2011).

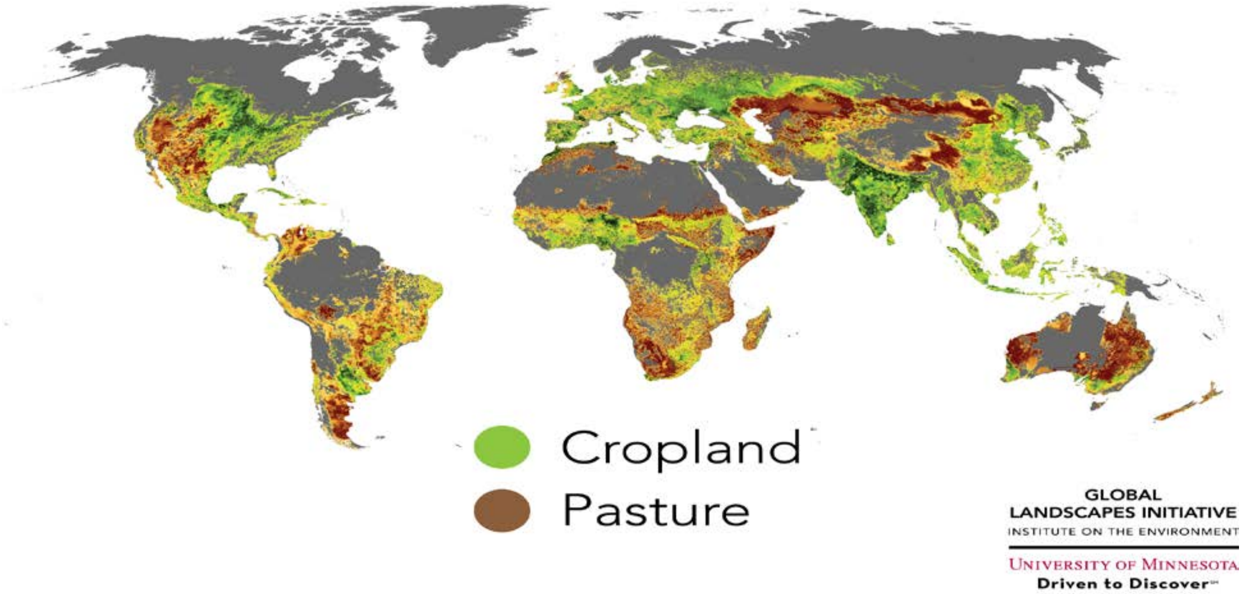

Figure 2.2.3: Extent of crop and pasture areas

Enteric fermentation associated with livestock production and rice paddy cultivation are major drivers agricultural CH_4 emissions, while N_2O emission largely result from agricultural soils, fertiliser applications, and manure management (Smith et al. 2008a; Carlson et al. 2016). There are still outstanding uncertainties in the biogeophysical climate impacts of various agricultural land management strategies and the response of managed vegetation to global environmental change. Improvements in observational datasets, however, are now elucidating important trends and processes by which agricultural land management is impacting regional and global climate systems (Duveiller et al. 2018a). For example, a non-trivial amount (about 20%) of land carbon sink strength may also be explained by intensifying agricultural production trends that involve the prodigious use of nitrogenous fertilisers and irrigation (Mueller et al. 2014). These trends are most pronounced in areas of rapid agricultural LCC and development over this time period, such as those in South and East Asia, as well as portions of Europe and South America (Liu et al. 2015a; Zeng et al. 2017). More study is needed to disentangle the effects of intensive management also embedded in observed greening signals.

CO_2 fertilisation effects may also have increased increase water use efficiency and thus reduced agricultural water per unit amount of crop produced (Deryng et al. 2016; Nazemi and Wheater 2015; Elliott et al. 2014) *(medium confidence, medium evidence)*. This effect may be quite pronounced in semi-arid and arid environments, which could lead to near-term continued greening of agricultural areas alongside modifications to water management, however current assessments of these effects are based on limited datasets from mostly temperate growing regions (Deryng et al. 2016).

Agriculture-driven soil fertility loss and soil degradation may also affect local and regional hydro-climate (Amundson et al. 2015; Lal 2011a). Agricultural soils in some of the most productive regions have exhibited carbon losses due to include ploughing and tillage, over-fertilisation, and disappearance of long fallow-periods (Arneth et al. 2017b; Pugh et al. 2015; Lal 2011a). These practices may have resulted in soil organic carbon losses ranging from 25%-75% across global agricultural regions (Sanderman et al. 2017; Lal 2011a), although much uncertainty still exists (Pongratz et al. 2014) (*medium confidence, medium evidence*). The removal of organic matters can also impact the soil's capacity to store and filter water throughout the column and within the root zone (Amundson et al. 2015), but the magnitudes of these effects on climate processes remain uncertain (Minasny and McBratney 2018a).

Emerging land management options for mitigation of climate impacts include deliberately planned crop rotations, timing, and water/irrigation (Hirsch et al. 2017; Seneviratne et al. 2018). Additionally, regionally degraded agricultural soils could potentially serve as carbon sinks by implementation of improved nutrient and water management techniques that enable high agricultural productivity and organic matter return (Mercedes et al. 2014; Paustian et al. 2016a; Minasny et al. 2017). However, outstanding uncertainties exist in quantifying the amount of carbon that can be stored locally and regionally, which depend on the confluence of biogeophysical, biogeochemical, and socio-economic conditions (Powlson et al. 2014).

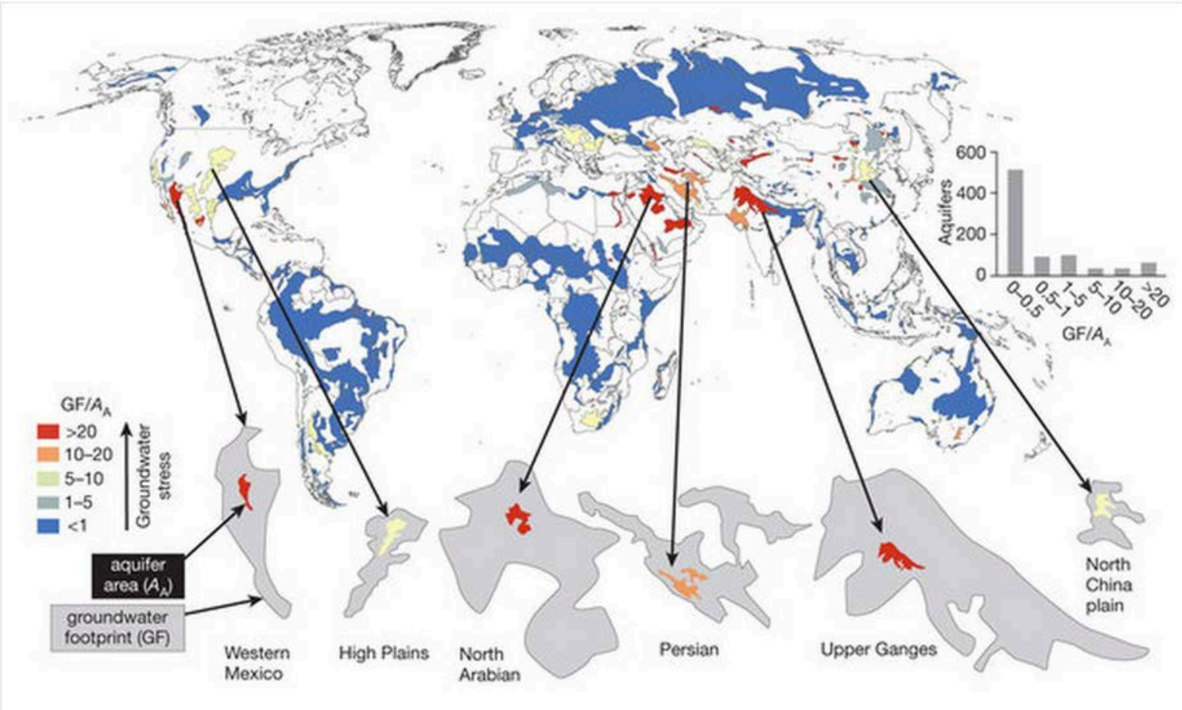

Figure 2.2.4: Groundwater footprint of major aquifers used for agricultural irrigation. Higher values indicate stressed conditions. Adapted from (Gleeson et al. 2012).

Climate patterns and processes related to agricultural irrigation

An increasing body of climate modeling work demonstrates that intensive irrigation potentially exerts a strong climate forcing (Cook et al. 2015; Guimberteau et al. 2012) (*high confidence*, *robust evidence*). Nearly 70% of global freshwater withdrawals, approximately 3300 km^3/year in 2010, are currently used for agricultural irrigation with groundwater accounting for about 30%-40% of this total (Pokhrel et al. 2016; Wada et al. 2014). In some regions, such as South Asia, year-round irrigation consumes about 90% of freshwater withdrawals from surface and groundwater stores combined (Wisser et al. 2008; Rodell et al. 2009; Gleeson et al. 2012). The most intensive irrigation regimes may be found in water-limited regions, where about 45% of global agricultural productivity takes place (Pokhrel et al. 2016). Addition of such vast amounts of water to the land surface can substantially modify regional energy and moisture balances, particularly in conjunction with highly productive agricultural crops with high rates of evapotranspiration. In general, climate studies and assessments of irrigation have sought to quantify and understand how irrigation-induced enhancements in surface latent heat fluxes can impact overall regional energy and moisture balances and interact with larger-scale atmospheric circulation processes, particularly in water-limited domains. However, most CMIP5 models did not account for water management.

2.2.8 Urban ecosystems and climate change

Urbanisation, one of the major LCCs, is becoming increasingly important because of its impacts on local climates in urban areas (Wang et al. 2016a; Zhong et al. 2017), with a variety of subsequent implications for human societies such as health and building energy demand (Li et al. 2017b; Santamouris et al. 2015). Urban heat island (UHI), with temperature in urban areas higher than that in the surrounding rural areas, has intensified as anthropogenic heat discharges have increased, whereas albedo and vegetation coverage have decreased (Mohajerani et al. 2017; Phelan et al. 2015). With the time series of satellite observations of land surface temperature, surface UHI (SUHI), especially its trend (Estoque & Murayama, 2017; D. Zhou et al., 2016) and regional variations (Zhou et al. 2017) have been investigated. The intensity of SUHI varies across regions and study areas, for example, less than 0.5°C in Mediterranean cities (Polydoros et al. 2018) and higher than 8°C in Baguio City, Philippines (Estoque and Murayama 2017). Negative SUHI effects have been found in hot subtropical desert cities (Fan et al. 2017; Rasul et al. 2015). Although SUHI may not be comparable across studies due to methodological differences and inter-annual variations of human activities, a consistent increase of SUHI has been confirmed in multiple studies (Estoque and Murayama 2017, Polydoros et al. 2018, Zhou et al. 2016). For example, SUHI could increase as high as 0.7°C when urban area size doubles in the conterminous United States, and this effect is most pronounced during the daytime in summer at high latitudes (Zeng et al. 2017). The patterns of SUHI along the urban-rural gradient are influenced by local climate-vegetation conditions, SUHI can be modeled by its relationship with impervious surface area (Li et al. 2018a).

Urbanisation alters the stock size of soil organic carbon (SOC) and its stability by converting natural vegetation to urban land cover. Overall, carbon densities or stocks decreases from natural land areas to urban core along the rural-urban gradient (Tao et al., 2015; Zhang et al., 2015). The conversion of vegetation, to urban land results in a loss of carbon stored in plants, and stresses associated with urban environment (e.g., heat, limited water availability and pollution) may reduce plant growth and survival (Xu et al. 2016b). However, urban soils may serve as an important carbon sink in some areas (Yesilonis et al. 2017). Urban soils may exhibit high levels of SOC, significant enough to be considered in earth system models (Zhai et al. 2017; Vasenev et al. 2018). Urbanisation *per se* may not result in loss of carbon already present in the soil (Liu et al. 2018), although there is a wide variation across different urban landscapes. For example, a tenfold difference in SOC stock across land cover types was reported for Seoul Forest Park (urban park)(Bae and Ryu 2015). In Changchun in Northeast China, SOC density is higher in recreational forests within urban areas compared to a production forest (Zhang et al. 2015).

Urbanisation changes precipitation patterns, frequency, and intensity (Zhong et al. 2015, 2017), as a results of changes in thermodynamic, aerodynamic, and cloud microphysics. Divergent results have been reported from different areas using different detection methods. Some report that high temperature of UHI increases the formation of convective clouds over urban areas, leading to an increase in the frequency of extreme summer precipitation (Shimadera et al. 2015; Dou et al. 2014; Zhong et al. 2017). A similar finding is reported based on the satellite observation of the urban area of the China Pearl River Delta; increases in short-duration heavy rain is observed but less so compared to surrounding rural areas (Chen et al. 2015). The urbanisation-induced convection may result in stronger effects on precipitation near large water bodies from which humid atmosphere may be drawn into (Kusaka et al. 2013; Yang et al. 2013). On the other hand, during the weak UHI periods, summer thunderstorms may bifurcate and bypass the urban center because of the building-barrier effect, producing a minimum of regional-normalised rainfall in the urban center and directly downwind of the urban area (Dou et al. 2015). Additionally, increased aerosols in urban areas may counter the effect of UHI on precipitation (Zhong et al. 2015; Zhong et al. 2017) (*limited evidence*).

Box 2.1. Fire and Climate Change

Fires have been a natural part of Earth's geological past and its biological evolution since at least the late Silurian, about 400 million years ago (Scott 2000), while human-caused controlled fires have been routinely used since the Middle Pleistocene, about 700,000 years ago (Roebroeks and Villa 2011; Bond et al. 2005). Presently, roughly 3% of the Earth's land surface burns annually which affects both energy and matter exchanges between the land and atmosphere (Stanne et al. 2009). Climate is a major determinant of fire regimes through its interaction with vegetation structure and productivity which provide fuel for burning. The basic climate-vegetation-fire relationship is similar at the global scale (Krawchuk and Moritz 2011), the regional biome scale (Pausas and Paula 2012) and even a more localised landscape scale (Mondal and Sukumar 2016). Presently, humans are the main cause of fire ignition with lightning playing a lesser role (Bowman et al. 2017; Harris et al. 2016). The inter-annual variability of fire spread and frequency responds to large-scale climate fluctuations (Fernandes et al. 2011; Gutiérrez-Velez et al. 2014; Fanin and Van Der Werf 2017). The expansion of agriculture and deforestation in humid tropics is making these regions more vulnerable to drought-driven fires (Davidson et al. 2012; Brando et al., 2014).

Emissions from wildfires and biomass burning are a significant source of greenhouse gases (CO_2, CH_4, N_2O), CO, carbonaceous aerosols, and a vast array of other gases including non-methane organic compounds (NMOC) (Akagi et al. 2011; Van Der Werf et al. 2010a). Fires also indirectly influence climate by changing land-atmosphere energy exchange through altering land surface temperature and albedo post-burn (Bremer and Ham 1999; Veraverbeke et al. 2012). Other indirect influences of fire on climate include post-burn vegetation growth response, CO_2 fertilisation of vegetation and soil-litter decomposition.

Historical trends and drivers in land area burnt

In spite of public perceptions to the contrary, there was less biomass burning during the 20th century than at any time during the past two millennia (Doerr and Santín 2016). During the first half of the 20th century the average land area burned globally decreased by about 7% largely due to fire suppression and land use change, but then increased by about 10% during the second half of the century due to land use change in the tropics (Mouillot and Field 2005). While precipitation has been the major influence on the wild fire regimes at the pre-industrial times, human activities become dominant drivers since the dawn of the Industrial Age.

Climate variability and extreme climatic events such as severe drought, especially those associated with the El Niño Southern Oscillation (ENSO), play a major role in fire upsurges. Fire emissions in tropical forests increased by 133% during and following El Niño compared to La Niña and that this was due to reductions in precipitation and terrestrial water storage (Chen et al. 2017). Temperature increase and precipitation decline would be the major driver of fire regimes under future climates as evapotranspiration increase and soil moisture decrease (Pechony and Shindell 2010 ; Aldersley et al. 2011 ; Abatzoglou and Williams 2016; Fernandes et al. 2017; Fernandes et al. 2017)

In recent decades the trends in land area burnt have varied regionally (Giglio et al. 2013). There is a fire decrease of 1.7 Mha yr^{-1} (–1.4% yr^{-1}) in Northern Hemisphere Africa since 2000 but an increase of 2.3 Mha yr^{-1} (+1.8% yr^{-1}) in Southern Hemisphere Africa during the same period. Southeast Asia witnessed a slight increase of 0.2 Mha yr^{-1} (+2.5% yr^{-1}) 1997, while Australia experienced a rapid decrease of about 5.5 Mha yr^{-1} (-10.7% yr^{-1}) during 2001-11, followed by a major upsurge in 2011 that exceeded the annual area burned in the previous 14 years. The global burned area from 2000 to 2012 showed a modest net decreasing trend of 4.3 Mha yr^{-1} (-1.2% yr^{-1}). A more recent analysis using the Global Fire Emissions Database v.4 that includes small fires also came to a similar conclusion; the net reduction in land area burnt globally was -24.3$\pm$ 8.8% (-1.35 $\pm$ 0.49% yr^{-1}) (Andela et al. 2017). Improved estimates of land area burnt (Giglio et al. 2013), fire emission factors (Akagi et al. 2011; Urbanski 2014), etc. have become available (section 2.4).

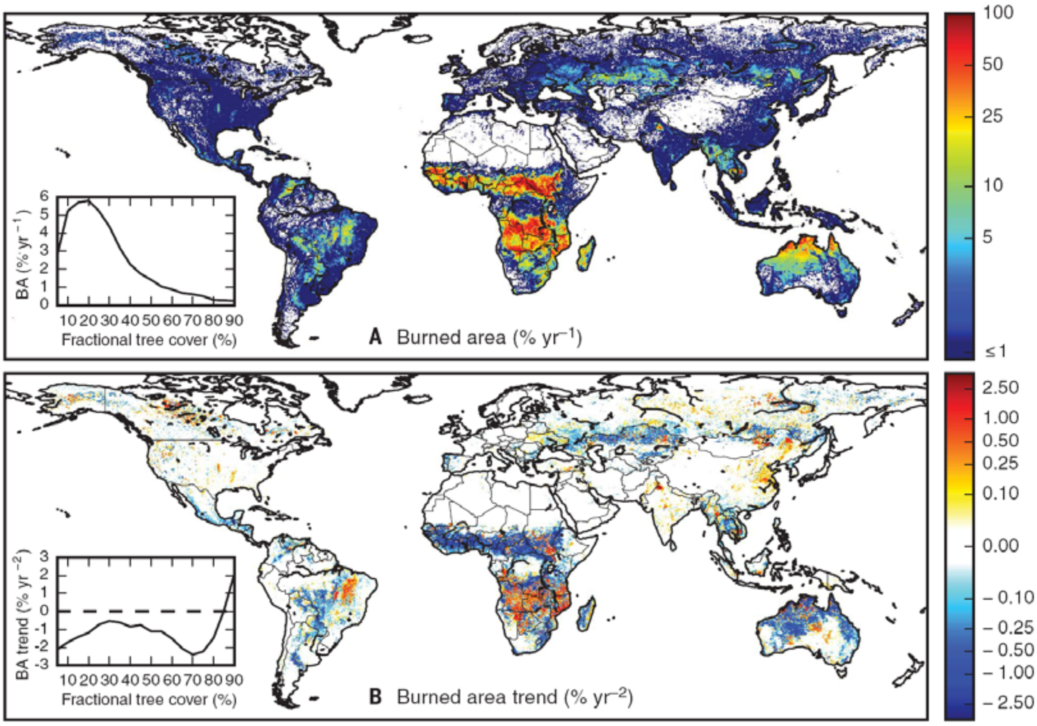

Figure 2.2.5 Satellite observations show a declining trend in fire activity across the world's tropical and temperate grassland ecosystems and land use frontiers in the America and Southeast Asia. (A) mean annual burned area and (B) trends in burned area (GFED4s, 1998 through 2015). Line plots (insert) indicate global burned area and trends by fractional tree cover. From (Andela et al. 2017)

Fires under future climate change

The risk of wildfires in future could be expected to change under future climates, increasing significantly in the United States, South America, central Asia, southern Europe, southern Africa, and Australia (Liu et al. 2010). There is emerging evidence that recent surges in wildland fires are being driven by changing weather extremes, thereby signalling geographical shifts in fire proneness (Jolly et al. 2015). Fire weather season has already increased by 18.7% globally between 1979 and 2013, with statistically significant increases across 25.3% but decreases only across 10.7% of Earth's land surface covered with vegetation; even sharper changes have been observed during the second half of this period (Jolly et al. 2015). Correspondingly, the global area experiencing long weather fire season (defined as experiencing fire weather season greater than 1 standard deviation (SD) from the mean global value) has increased by 3.1% per annum or 108.1% over the above study period. Fire frequencies under the 2050 conditions are projected to increase by approximately 27% globally relative to the 2000 levels, with changes in future fire meteorology playing the most important role in enhancing the future global wildfires, followed by land cover changes, lightning activities and land use while changes in population density exhibits the opposite effects during the period of 2000 to 2050 (Huang et al. 2014).

Until recently most land-climate models ignored or inadequately incorporated fire into their simulations. Improved models include the complex nature of human-fire relationships across regions and societies for more realistic projections of fire regimes under global change (Bowman et al. 2011). Recent simulations with the LPJ-GUESS-SIMFIRE global dynamic vegetation-fire model found no clear fire trends the climate scenario (RCP 4.5) and the rise in fires after 2020 under RCP 8.5 scenario (Knorr et al. 2016b). On the contrary, human exposure to wildland fires could increase because of population expansion into areas already under high risk of fires (Knorr et al. 2016a). There are still major challenges in projecting future fire regimes using the newly developed DGVMs. In particular these need improvements in representing present-day vegetation, plant community responses to fire, ecosystem dynamics and future land use change and management, ultimately requiring a “trans-disciplinary synthesis of the biological, atmospheric and socioeconomic drivers of fire”(Harris et al. 2016).

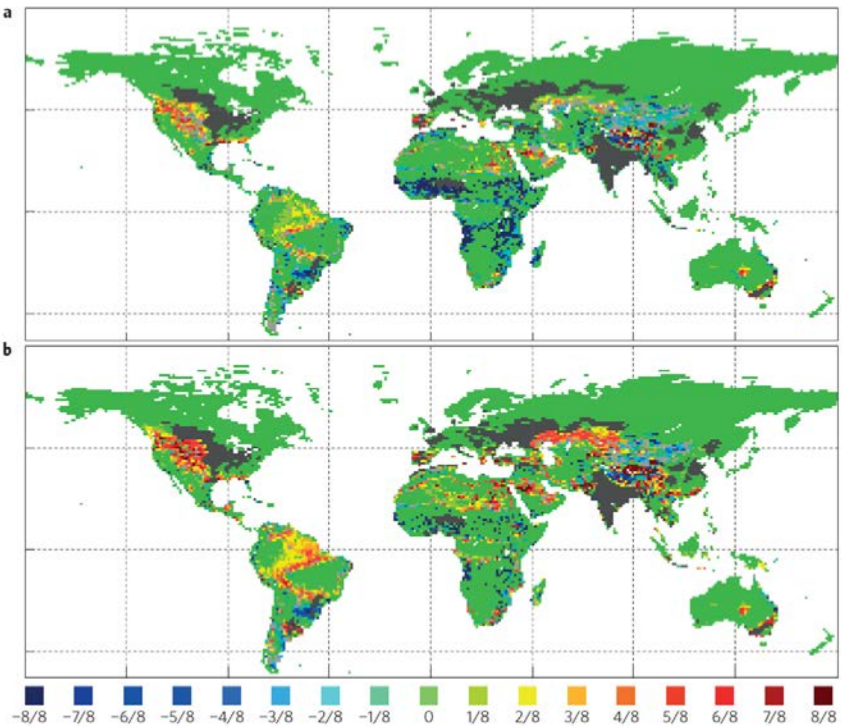

Figure 2 | The probability of low-fire regions becoming fire prone (positive values), or of fire-prone areas changing to a low-fire state (negative values) between 1971–2000 and 2071–2100 based on eight-ESM ensembles. Light grey: areas where at least one ensemble simulation predicts a positive and one a negative change (lack of agreement). Dark grey: areas with >50% past or future cropland. Fire-prone areas are defined as having a fire frequency of >0.01 yr^{-1}. **a**, RCP4.5 emissions with SSP3 demographics. **b**, RCP8.5 emissions with SSP5 demographics.

Figure 2.2.6 from (Knorr et al. 2016a)

2.3 Climate change and variability, including extremes, that influence desertification, land degradation, food security, sustainable land management and GHG fluxes in terrestrial ecosystems

2.3.1 Overview of climate impacts on land

More energy from the sun reaches equatorial regions of the earth than Polar regions. Energy is redistributed poleward through large-scale atmospheric and oceanic processes such as the Hadley circulation and Gulf stream (Oort and Peixóto 1983; Carissimo et al. 1985; Yang et al. 2015a). Subsequently, a number of global climate zones have been classified ranging from large-scale primary climate zones (tropical, sub-tropical, temperate, sub-polar, polar) to much higher-resolution, regional climate zones (e.g. the Koppen-Geiger classification, Kottek et al. 2006). **The regional climate determines the regional land characteristics and functioning** (e.g. geomorphology, hydrology, terrestrial ecosystems distribution) including global biomes (Figure 2.3.1). Functioning within these biomes is subject to modes of natural variability in the ocean-atmosphere system that results in wetter/dryer or hotter/cooler periods regionally, spanning seasons to decades.

This variability is driven by variability in oceanic and atmospheric phenomena, typically sea surface temperature and atmospheric pressure anomalies respectively. Oceanic examples include the El Niño Southern Oscillation (ENSO), Indian Ocean Dipole (IOD), North Atlantic Oscillation (NAO) and Pacific Decadal Oscillation (PDO) and atmospheric examples include the Southern and Northern Annular Modes (SAM/NAM), Quasi-biennial oscillation (QBO) and Madden-Julien Oscillation (MJO). Temporal scales of these natural variability modes vary from weeks to months (SAM), months to seasons (MJO), years (ENSO) and decades (PDO). Climate change alters the drivers of natural climate variability within the ocean-climate system with consequent impacts on these (Hulme et al. 1999; Parmesan and Yohe 2003).

Climate is a primary determinant of regional land characteristics and functioning, climate change due to natural or anthropogenic causes can alter these. It is *very likely* that land-based systems will be exposed to disturbances beyond the range of current natural variability, which will alter the structure, composition and functioning of the system (Settele et al. 2015). It is expected that tropical and sub-tropical regions will see the emergence of novel climates that are beyond the envelope of current natural variability as a result of warmer temperatures (Mora et al. 2013, 2014; Hawkins et al. 2014; Colwell et al. 2008; Maule et al. 2017). Polar climates and those of major mountains and mountain ranges are projected to warm and shrink and hot, arid climates of the Sahara, southern Africa, and Australia are projected to expand.

Assessing the impacts of climate variability and change on land use and functioning requires the analysis of observations (both *in situ* and satellite derived observations) as well as results from models (e.g. vegetation, agriculture and hydrology models). Modelled data may be sourced from (i) climate models coupled with an impact model or (ii) offline dynamic impact models that are forced by data from global or regional climate models. For (ii), climate model data are usually bias-corrected and/or interpolated to the required horizontal spatial resolution of the impact model before it is used by the impact model, however this is not without problems (Maraun et al. 2017).

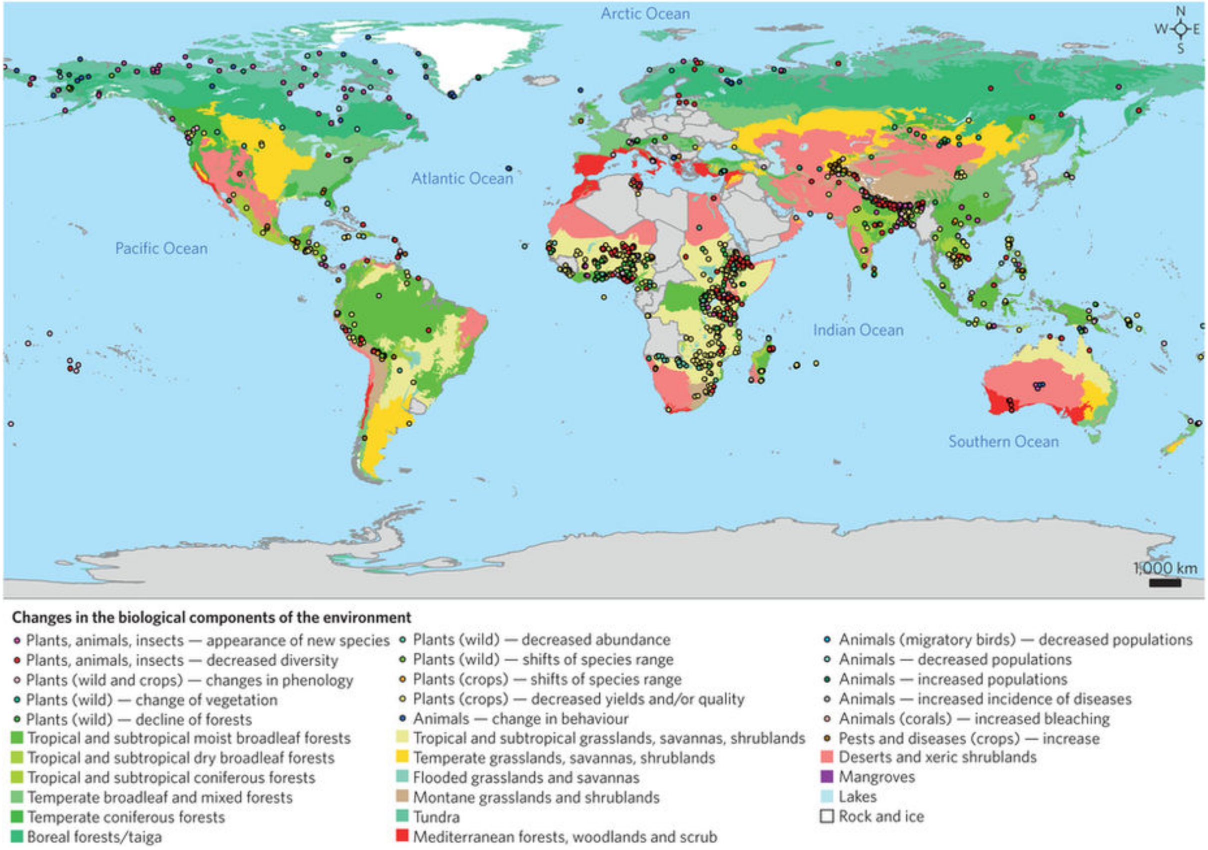

Figure 2.3.1. Global biomes with historical changes in biological components of the environment (Savo et al. 2016). Shaded areas represent different biomes and coloured dots indicate some change in the biological components of the environment (for example, distributional shifts in plant and animal species).

2.3.2 Desertification and land degradation

Desertification is defined by the IPCC as “Land degradation in arid, semi-arid, and dry sub-humid areas resulting from various factors, including climatic variations and human activities.” Land degradation in these three areas is further defined as a “reduction or loss of the biological or economic productivity and complexity of rainfed cropland, irrigated cropland, or range, pasture, forest, and woodlands resulting from land uses or from a process or combination of processes, including processes arising from human activities and habitation patterns, such as (1) soil erosion caused by wind and/or water; (2) deterioration of the physical, chemical, biological, or economic properties of soil; and (3) long term losses of natural vegetation.” From this definition the primary driver of land degradation in drylands (hyper-arid, arid, semi-arid, and dry sub-humid areas) is “human activities and habitation patterns” and the climate is a background stressor.

Drylands are generally situated in regions of subsiding air (such as the descending limbs of the Hadley and Ferrel cells) that inhibits convection and rainfall, are far from oceans and atmospheric moisture sources, in a rain shadow on the leeward side of mountain chains or near cold ocean surfaces also characterised by subsiding air and low atmospheric moisture (D’Odorico et al. 2013). Drylands are usually characterised by strong seasonal and interannual variability with a relatively short summer rainfall season and no rain in the rest of the year. They are particularly sensitive to climatic variability as the relative scarcity of precipitation means that small changes can have large impacts, most drylands exist along “climate ecotones,” the transition zones between a wet and a dry climatic regime often with sharp gradients in precipitation and dryland environments are the consequence of complex feedback loops involving climatological, biological, geomorphological, hydrological, and human systems (Nicholson 2011).

Although methods and metrics to assess extents and rates of desertification vary (Thorstensson 2001; Safriel 2007) and it is currently difficult to distinguish between current climate-caused and anthropogenic desertification (D'Odorico et al. 2013), **future projections show an increase in aridity across the globe**, attributable to greenhouse gas emissions (Burke et al. 2006; Dai 2011). Furthermore, the extent of global drylands has increased over the last 60 years and is projected to accelerate in the 21st century, with most of this expansion expected to occur in developing countries. Worryingly, dryland expansion has been underestimated in the historical simulations of the CMIP5 GCMs (Feng and Fu 2013) and (Huang et al. 2016) estimate 56% and 50% of total land surface will be covered by drylands by 2100 under RCP8.5 and RCP4.5, respectively.

Projected warming trends over drylands are twice the global average which, along with extensive land use and rising temperatures, is *likely* to exacerbate the risk of land degradation and desertification affecting approximately 70% of the Earth's agricultural drylands (Huang et al. 2017a and citations therin). **Dryland expansion will *likely* lead to reduced carbon sequestration and enhanced regional warming, result in decreased agricultural yields and runoff and increased drought frequency and persistence** (Huang et al. 2017b).

2.3.3 The influence of climate on food security

The UN Food and Agricultural Organization (FAO) define global food security as the 1) availability of enough nutritious food for regional and global populations, 2) comprehensive access to that food supply, 3) populations' ability and capacity to utilise and consume accessed food in a timely way, and that all these components are stable over time (FAO, also in Wheeler and von Braun 2013). As food security is a function of climatic factors (temperature, rainfall, CO_2, ozone), non-climate factors (soil fertility, irrigation, demography, economics), production factors (crops and livestock) and non-production factors (processing, transport, storage, retail, income), the overall impact of climate on food security is complex, being potentially greater than impacts on agricultural productivity alone (Conway 2012b; Beer 2018).

Mean climate change, even under aggressive mitigation, is expected to have regionally-distributed impacts on agricultural production, which may impact food security globally (Howden et al. 2007; Rosenzweig et al. 2013; Challinor et al. 2014; Parry et al. 2005; Lobell and Tebaldi 2014; Wheeler and Von Braun 2013). At middle and higher latitudes, the lengthening of growing seasons, reduced frost damage, CO_2 fertilisation effects, potential for increased rainfall and expansion of the crop climate envelope through warmer temperatures (Gregory and Marshall 2012; Yang et al. 2015b) may serve to improve crop productivity and/or mitigate climate-induced losses (Parry et al. 2004; Rosenzweig et al., 2014; Deryng et al. 2016) (*medium confidence, medium evidence*). However, enhanced climate variability and the propensity for negative impacts of climate trends on yield to be more common than positive ones, nutrient limitation, and non-climatic environmental conditions, such as soil composition and health, caveat these potential benefits and introduce uncertainty in the magnitude and sign of agricultural impacts (Leakey et al. 2012; Wheeler and Von Braun 2013; Porter et al. 2014; Gray et al. 2016).

Elsewhere in the sub-tropics, tropics, and water-limited environments, changes in rainfall variability, drought, and growing season temperature increases are expected to negatively impact agricultural production both in magnitude and variability, though there remains outstanding uncertainty in quantifying the magnitude the regional impacts (Schlenker and Lobell 2010; Challinor et al. 2014;

Wheeler and Von Braun 2013; Parry et al. 2004; IFPRI 2009; Müller et al. 2017).

Over 60% of the world's crop production is dominated by maize, rice, wheat and soybean (Pingali 2012). Analyses of historical crop production trends indicate climate-induced 20th century reductions in overall global wheat and maize yields, while rice and soybean responses showed much regional variation (Lobell et al. 2011; Zhao et al. 2017). Globally, in the absence of adaptation, there is agreement that most crops exhibit yield declines and enhanced variability after 2˚C increases in globally averaged temperature or mid-century under high GHG emissions trajectories, with outstanding uncertainty due to CO_2 fertilisation effects(Conway 2012b; Challinor et al. 2014; Deryng et al. 2014; Lobell and Tebaldi 2014) (*high confidence, medium evidence*). Continued rising temperatures are expected to impact global wheat yields by about 4%-6% reductions for every degree of temperature rise (Liu et al. 2016a; Asseng et al. 2015a) (*medium confidence, limited evidence).* Temperature increases are also expected to be a controlling factor for maize productivity by the end of the century, resulting in potential yield reductions across both mid- and low latitude regions (Bassu et al. 2014; Zhao et al. 2017).

However, several sources of uncertainties exist in these projected climate change-induced crop impacts, partly stemming from differences between the utilised tools and models, sparse observations to current climate trends, and other agro-ecosystem responses (e.g. to CO_2 effects) (Asseng 2013; Li et al. 2015c; Mistry et al. 2017; Bassu et al. 2014). The uncertainty in climate simulation is generally larger than, or sometimes comparable to, the uncertainty in crop simulations using a single model (Iizumi et al. 2011), but can be less than crop model uncertainty when multiple crop models are used, however, the use of multiple crop models in agricultural studies is relatively rare (Koehler et al. 2013).

In addition to the direct climate impacts on crop production (e.g., temperature and precipitation), pests, diseases, and weeds are also expected to present further challenges to agricultural production in a warmer climate. These include enhanced crop losses and productivity, which in some cases might lead to geographic shifts in land use and crop distribution (Ziska and Runion 2006; Rosenzweig and Tubiello 2007). Furthermore, food access within countries relies not just on local or domestic production, but also by changes in imports and distribution, which may be impacted by both mean climate change and, in particular, shocks and extremes. The latter may limit the import of critical foodstuffs and/or impact pricing and scarcity, leading to regional food insecurity and instability, particularly for rice and wheat which have relatively complex trade connectivities between a few exporting and many importing states (Puma et al. 2015; Nelson et al. 2014; Wheeler and Von Braun 2013).

In the face of climate shocks, and in particularly severe drought and its subsequent trade disruption, least-developed countries experience the greatest import losses which thereby impact their food security and access (Puma et al. 2015). In other regions, modeling results indicate that technology and management improvements and adaptation can help to alleviate some of the risks associated with major drought events (Elliott et al. 2017). However, while most models show consistent economic stresses in the face of climate shocks that impact food access, there is low agreement on the magnitude of changes between models (Nelson et al. 2014; Wiebe et al. 2015).

2.3.4 Climate-driven changes in terrestrial ecosystems

There is *high confidence* that the earth's biota and ecosystem processes have been strongly affected by past climate changes at rates of climate change lower than those projected during the 21st century under high warming scenarios like RCP8.5 and most ecosystems are vulnerable to climate change even at rates of climate change projected under low- to medium-range warming scenarios (Settele et al. 2015). There is *high confidence* that in response to the observed climate change over recent decades ranges of many plant and animal species have moved, abundance altered, and seasonal activities have shifted. However, in a warming climate many species will be unable to track their climate niche as it moves, especially those in extensive flat landscapes and with low dispersal capacity (Warszawski et al. 2013). While climate change will be the principal driver of range contractions at higher latitudes, land conversion (e.g., deforestation, conversion of grasslands to croplands, etc.) will have a much larger effect on species that inhabit the tropics (Jetz et al. 2007). Expansion of forest at higher elevations occurs as a result of abandoned land use and climate change (Grace et al. 2002; Harsch et al. 2009; Landhäusser et al. 2010; Alatalo and Ferrarini 2017). However, this effect can be countered by intense and frequent drought which accelerates rates of taxonomic change and spatial heterogeneity in an ecotone than would be expected under gradual climate change and land- use changes only (Tietjen et al. 2017).

Increased CO_2 in the atmosphere has both a direct and indirect effect on terrestrial ecosystems through vegetation. The direct effect for most C3 plants results in increased photosynthesis. The indirect effects include decreased evapotranspiration through stomatal closure (Zhu et al. 2017a). Rising CO_2 concentrations may offset the projected impact of drought in some water-stressed plants through modification of stomatal conductance and plant water use in temperate regions (Swann et al. 2016) suggesting that rain-fed cropping systems will benefit from elevated atmospheric CO_2 concentrations. In grasslands projected elevated CO_2 concentrations compensated for the negative impact of extreme heat and drought on net carbon uptake during the growing season (Roy et al. 2016). Increased flowering activity in tropical forests is associated primarily with increased atmospheric CO_2 concentrations and secondarily with rainfall, solar radiation and ENSO. In recent decades flowering activity in mid-story trees and shrub species has continued with increasing CO_2 concentrations but diminished for lianas and canopy trees. Given projected increasing atmospheric CO_2 levels a long-term increase in flowering activity may persist in some vegetation until checked by nutrient availability or climate factor like drought frequency, rising temperatures and reduced insolation (Pau et al. 2018).

PLACEHOLDER (Table 2.3.1. Summary of climate driven changes in land type and function.)
(This table is under development, and moved to appendix)

2.3.5 Climate extremes that impact land type and functioning

Extreme climate events may be taken as being the upper or lower ends of the observed range of values of a single variable (e.g. temperature, rainfall, wind) or a combination of variables (e.g. drought and aridity indices). Extreme events occur across a wide range of time and space scales and may be individual weather events that are relatively short-lived (e.g. extreme thunderstorms storms and frost events) or an accumulation of extreme climate events that may be short or long-lived (e.g. floods, heat waves and drought).

Extreme climate events typically have extreme impacts on land type and functioning at different scales in space and time (Figure 2.3.2). However, extreme impacts may also occur through a combination of variables that are not necessarily in an extreme state (Colwell et al. 2008; Kundzewicz and Germany 2012). Combinatory processes leading to a significant impact is referred to as a 'compound event' and are a function of the nature and number of physical climate and land variables, the range of spatial and temporal scales, the strength of dependence between processes, and the perspective of the stakeholder who defines the impact (Leonard et al. 2014). Current *confidence* in the impact of compound events on land functioning and type is *low* as the multi-disciplinary approaches needed to address the problem are few (Zscheischler et al. 2018).

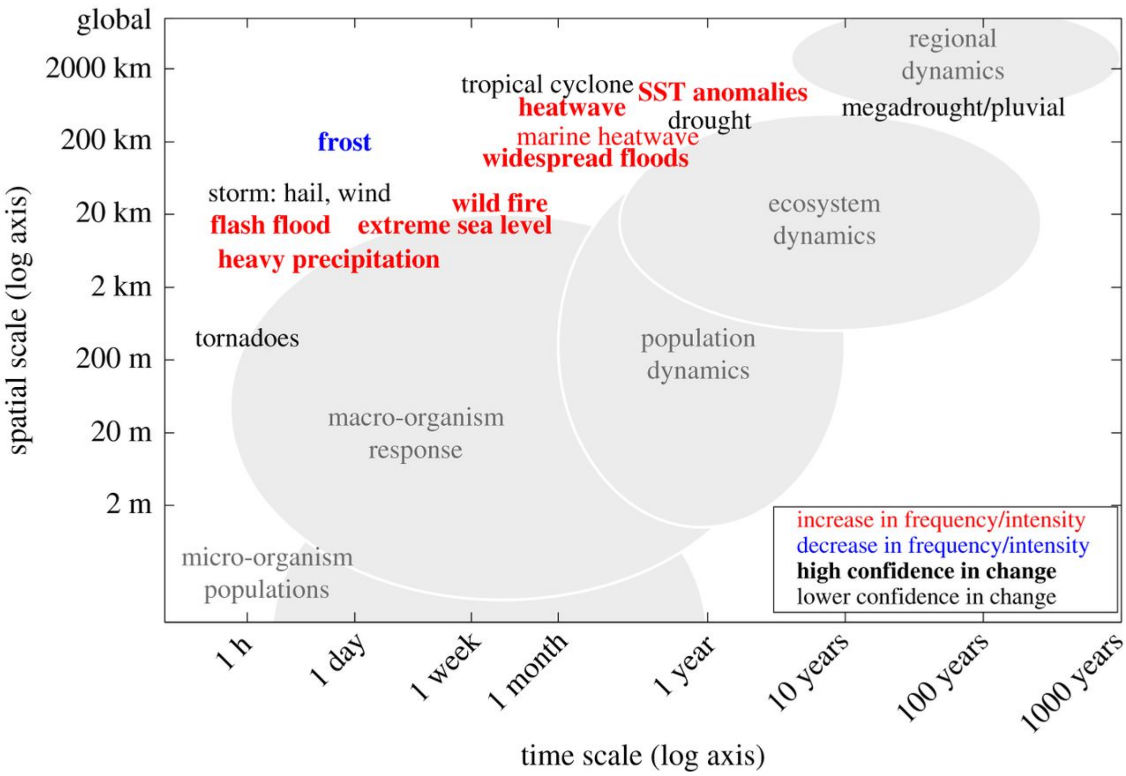

Figure 2.3.2. Spatial and temporal scales of typical extreme climatic events (ECEs) and the biological systems they impact (shaded grey). Individuals, populations and ecosystems within these space-time ranges respond to relevant climate stressors. Red (blue) labels indicate an increase (decrease) in the frequency or intensity of the event, with bold font reflecting confidence in the change. For each ECE type indicated in the figure, ECEs are likely to affect biological systems at all temporal and spatial scales located to the left and below the specific ECE position in the figure. From Ummenhofer and Meehl (2017).

2.3.5.1 Changes in extreme temperatures, heat waves and drought

From an atmospheric perspective, extreme heat events in the extra-tropics are usually associated with extra-tropical, transient high-pressure anticyclones that have become semi-stationary or "blocked" (Barnes et al. 2012, 2014; Grotjahn et al. 2016) that are in turn associated with subsiding, warming air (through adiabatic compression) and clear skies that result in warming during high-insolation summer. Blocking anticyclones greatly reduce the weather variability in a region and allow the heat event time to build and intensify (Photiadou et al. 2014). The intensity of heat events may also be modulated by the land cover (see section 2.6.3). A temperature rise results in a decrease in soil moisture, which reduces latent heat flux, allowing temperatures to rise further. However, if the land surface is irrigated the feedback is diminished through the introduction of latent heat (Mueller et al. 2015; Siebert et al. 2017).

Although there is no consensus definition of heat waves (some heat wave indices are percentile-based with relative thresholds and others are based on absolute temperatures having absolute thresholds), there is significant correlation in observed heat wave trends between indices of the same type (Smith et al. 2013b). **Recent heat-related events have been made more frequent or more intense due to anthropogenic greenhouse gas emissions**. It is *very likely that* most land areas have experienced a decrease in the number of cold days and nights, and an increase in the number of warm days and nights (Seneviratne et al. 2012a; Mishra et al. 2015; Ye et al. 2018). Globally increasing trends in unusually hot nights and extremely hot daytime temperatures have been attributed to greenhouse gas emissions (Zwiers et al. 2011), although, at regional and local scales, trends in daytime maximum are more difficult to attribute to greenhouse gas emissions because of the prominent role of soil moisture and clouds in driving these trends (Christidis et al. 2005; Zwiers et al. 2011). Over Africa and South America *confidence* remains *low* to *medium confidence* and varies regionally as a consequence of a poor observational record.

Temperature means and extremes tend to be underestimated at the regional level (Orlowsky and Seneviratne 2012; Lehner and Stocker 2015; Seneviratne et al. 2016) and 50-80 % of the global land fraction is projected to experience significantly more intense hot extremes (Fischer et al. 2013; Diffenbaugh et al. 2017). **Projections indicate an increase in the number, spatial extent and duration of heat waves** (Russo et al. 2016; Ceccherini et al. 2017; Herrera-Estrada and Sheffield 2017) and by the end of the century heat waves may become extremely long (more than 60 consecutive days) and frequent (once every two years) in large areas of central Africa, the Sahel, the Horn of Africa, and the Arabian Peninsula (Dosio 2017) and unusual heat wave conditions today will occur regularly by 2040 under the RCP 8.5 scenario ((Russo et al. 2016). Therefore, *confidence* in the increased number and duration of heat waves in recent decades is *medium* and that heat waves will increase in frequency and duration into the 21st century there is *high confidence*. It is *very likely* that temperature extremes will become more common in the 21st century in most land regions of the globe.

Drought is defined by the IPCC as "A period of abnormally dry weather long enough to cause a serious hydrological imbalance" recognising that "Drought is a relative term, therefore any discussion in terms of precipitation deficit must refer to the particular precipitation-related activity that is under discussion" (Qin et al. 2013). Droughts are a normal component of climate variability (Hoerling et al. 2010; Dai 2011) and may be seasonal, multi-year (Van Dijk et al. 2013) or multi-decadal (Hulme 2001) with increasing degrees of impact on the regional activity. Droughts impact many aspects of land functioning and type including agriculture (Lesk et al. 2016), hydrology (Mosley 2015; Van Loon and Laaha 2015), vegetation (Xu et al. 2011; Zhou et al. 2014) and carbon and other biogeochemical cycles (Frank et al. 2015; Doughty et al. 2015; Schlesinger et al. 2016). Although systems may demonstrate resilience to a climate stressor like drought, the compound effect of deforestation, fire and drought potentially lead to losses of carbon storage and changes in regional precipitation patterns and river discharge and a transition to a disturbance-dominated regime (Davidson et al. 2012b). Additionally, adaptation to seasonal drought may be overwhelmed by multi-year drought (Brando et al. 2008; da Costa et al. 2010).

There are conflicting messages about how drought has changed historically (Sheffield et al. 2012; Dai 2013), which is a function of potential deficiencies in drought indices (especially in how evapotranspiration is treated), discrepancies in and availability of precipitation data and the role of natural variability, especially ENSO, which biases the land precipitation towards wetter conditions, and with less drought globally under La Niña conditions (Trenberth et al. 2014). However, it is expected that **the extra heat from global warming will increase the rate of drying causing natural drought to set in quicker, become more**

intense, last longer, become more widespread and result in an increased global aridity (Dai 2011; Prudhomme et al. 2014). Drought risk over the Mediterranean, central Europe, the Amazon and southern Africa increases significantly compared to present day for both 1.5°C and 2°C warming levels, and the additional 0.5°C from a 1.5°C to 2°C climate leads to significantly higher drought risk here (Lehner et al. 2017). However, over the US. Southwest and Central Plains a two-degree increase in global temperature results in only a small change in drought risk.

2.3.5.2 Impacts of heat extremes and drought on land types and functioning

Heat extremes impact land type and functioning. In **agricultural areas** they have become more common where exposure to extreme heat, particularly during key growth phases such as the reproductive period, can severely damage crop production (Gourdji et al. 2013; Jagadish et al. 2015). These adverse heat conditions have been observed to reduce crop yield in many regions of the globe and will continue to do so in the future in the absence of adaptive interventions, particularly in regions dependent on rain-fed agriculture (Durigon and de Jong van Lier 2013; Siebert et al. 2014; Trnka et al. 2014; Asseng et al. 2015b; Kimball et al. 2015; Schauberger et al. 2017; Zhang et al. 2017e). Unusually hot nights are damaging to most crops (Peng et al. 2004; Wassmann et al. 2009) and extremely high daytime temperatures are also damaging and occasionally lethal to crops (Porter and Gawith 1999; Schlenker and Roberts 2009). Heat stress over wheat cropping regions increased significantly in the period 1980–2010, especially since the mid-1990s and is in general as important as drought a predictor of observed and projected crop yield. Heat waves in combination with drought are common and intrinsically linked through a positive feedback (Stéfanon et al. 2014). Drought, however, has a larger detrimental effect on wheat yield than heat stress in Mediterranean countries (Zampieri et al. 2017) and affects both harvested area and yield (Lesk et al. 2016). Heat stress in irrigated crops is reduced due to surface cooling and is overestimated in modelling studies (Siebert et al. 2017).

Trees are more resilient to heat stress although extreme heat events can impact a wide variety of tree functions including reduced photosynthesis, increased photooxidative stress, leaves abscise, a decreased growth rate of remaining leaves decreases, decrease growth of the whole tree and a shift biomass allocation (Teskey et al. 2015).

Extreme heat events have an impact on **fire**. Fires affect energy and matter exchanges between the land and atmosphere (Archibald et al. 2017) impacting living systems and the terrestrial carbon budget (through which tropical fires may be viewed as a carbon source) (Le Quéré et al. 2009; Ward et al. 2012). While ignition is largely related to human activities, the inter-annual variability of fire spread and frequency responds to large-scale climate fluctuations (Fernandes et al. 2011; Gutiérrez-Velez et al. 2014; Fanin and Van Der Werf 2017). Droughts have clear impact on fire occurrence (Davidson et al. 2012b), although anomalously active fire seasons also occur during non-drought years, for example in Indonesia and in the Amazon (Gaveau et al. 2014; Brando et al. 2014). High temperatures increases the risk of fire through increase evapotranspiration rates that lead to greater soil and vegetation water depletion (Abatzoglou and Williams 2016; Fernandes et al. 2017; Aldersley et al. 2011). Even though humid tropical forest landscapes typically do not burn, the expansion of agriculture and deforestation into these landscapes make them vulnerable to drought-driven fires (Davidson et al. 2012; Brando et al. 2014). Seasonal fire anomalies are currently driven through seasonal to decadal fluctuations in rainfall (Fernandes et al. 2011), however, temperature is expected to become a more important factor than rainfall deficit as regional temperatures rise, especially in the humid tropics (Fernandes et al. 2017). In temperate and boreal regions fire seasons are lengthening and this trend is *likely* to continue in a warmer world (Flannigan et al. 2009; Williams and Abatzoglou 2016). However, **future trends in future fire frequency, area and intensity especially at the regional scale are difficult to determine as there are complex and non-linear interactions** between climate processes such as blocking highs and variables such as temperature and humidity, atmospheric CO_2, fuels and human behaviour.

2.3.5.3 Heavy precipitation and flooding

A large number of extreme rainfall events have been documented over the past decades (Coumou and Rahmstorf 2012; Seneviratne et al. 2012b; Trenberth 2012; Westra et al. 2013; Guhathakurta et al. 2017; Taylor et al. 2017; Thompson et al. 2017; Zilli et al. 2017) and the observed shift in the trend distribution for precipitation extremes is more distinct than for annual mean precipitation (Fischer and Knutti 2014). The number of record-breaking rainfall events globally has increased significantly by 12% during the period 1981 to 2010 compared to those expected due to natural multi-decadal climate variability as a result of the warming climate (Lehmann et al. 2015) and the global land fraction experiencing more intense precipitation events is larger than expected from internal variability (Fischer et al. 2013).

The hydrological cycle is expected to intensify in a warming climate as a warmer climate facilitates more water vapour in the atmosphere, as approximated by the Clausius-Clapeyron relationship, with subsequent effects on extreme precipitation events (Berg et al. 2013; Pall et al. 2007; Christensen and Christensen 2003; Wu et al. 2013; Thompson et al. 2017; Taylor et al. 2017; Zilli et al. 2017; Guhathakurta et al. 2017). However, the Clausius-Clapeyron (C-C) relationship is an approximation and precipitation extremes are expected to deviate from it. In regions with low to intermediate temperatures, precipitation intensity can be up to twice the C-C relationship (Westra et al. 2014) but at very high temperatures the effect is opposite, particularly in tropical regions (Maeda et al. 2012; Zhang et al. 2017d) However, this does not imply a potential upper limit for future precipitation extremes (Wang et al. 2017a). Furthermore, changing atmospheric dynamics amplify or weaken future precipitation extremes at the regional scale (Pfahl et al. 2017).

Continued warming as a result of anthropogenic greenhouse gas emissions is *very likely* to increase the frequency and intensity of extreme rainfall in many regions of the globe (Seneviratne et al. 2012b; Stott 2016; Abiodun et al. 2017; Mohan and Rajeevan 2017; Prein et al. 2017). Rainfall intensity in regions with high heavy rainfall intensity is underestimated by many CMIP5 models suggesting a substantially stronger intensification of future heavy rainfall than the multimodel mean in these regions (Min et al. 2011; Borodina et al. 2017) and regionally, spatially aggregated trends in extremes are statistically more significant than single grids or point based trends (Fischer and Knutti 2014).

2.3.5.4 Impacts of precipitation extremes on land types and functioning

A number of studies have attributed extreme rainfall observed events to human influence (Min et al. 2011; Pall et al. 2011; Sippel and Otto 2014; Trenberth et al. 2015). However, the evidence for human influence on the probability of observed extreme precipitation events and storms is less robust than for temperature extremes as extreme rainfall events are often poorly observed, models usually do not represent them adequately, and their relationship with climate variability and change is often not well understood (Stott 2016). Consequently, **the impact of changes in flood hazard due to anthropogenic climate change is uncertain and flood damage in many regions of the world is dominated by increased exposure** (Bouwer 2011; Lavell et al. 2012). The climate signal might be masked by a counteracting decrease in vulnerability, as suggested by studies at global and regional scales (Di Baldassarre et al. 2015; Jongman et al. 2015; Mechler and Bouwer 2015; Kreibich et al. 2017). However, climate models indicate an increase in the frequency and intensity of extreme rainfall in many regions of the Earth (see Section 2.3.2.3) and may even underestimate this change as they underestimate observed increased trends in heavy precipitation (Min et al. 2011).

Flooding as a result of extreme rainfall affects **wheat production** more than drought in several countries, particularly in tropical regions (e.g. India) and in some mid/high latitude regions such as China and parts of France (Zampieri et al. 2017). Waterlogging of croplands and **soil erosion** also negatively affect farm operations and block important transport routes (Vogel and Meyer 2018; Kundzewicz and Germany 2012). However, **the impact of extreme rainfall on crops is less than that of temperature extremes** (Lesk et al.

2016).

Although many **soils** on floodplains regularly suffer from inundation, the increased magnitude of flood events means that new areas with no recent history of flooding are now becoming severely affected (Yellen et al. 2014). Surface flooding and associated soil saturation causes considerable losses in soil quality and plant productivity and induces changes in nutrient cycling with increased potential for nutrient loss, meso- and macro-faunal abundance, stimulates microbial growth and microbial community composition, negatively impacts redox and increases greenhouse gas emissions (Bossio and Scow 1998; Niu et al. 2014; Sánchez-Rodríguez et al. 2017; Barnes et al. 2018). The impact of flooding on soil quality is influenced by management systems that may mitigate or exacerbate the impact. Although soils tend recover quickly after floodwater removal, the impact of repeated extreme flood events over longer timescales on soil quality and function is unclear.

Heavy precipitation inundation in **agricultural systems** can delay planting, increases soil compaction, and causes crop losses through anoxia and root diseases and in tropical regions flooding associated with tropical cyclones can lead to crop destruction and failure. Heavy precipitation events also result in greater erosion of land surfaces, more landslides, and a decrease in the protection afforded by levees. However, flooding can be beneficial in drylands as the floodwaters infiltrate and recharge alluvial aquifers along ephemeral river pathways, extending water availability to dry seasons and drought years and support riparian systems and human communities (Kundzewicz and Germany 2012).

Grassland ecosystem responses to extreme rainfall patterns expected with climate change are likely to be variable as the response is dependent on the interval between rainfall events, variation in rainfall total quantity, and individual event size which combine to effect soil water content, but will likely result in changes in ecosystem carbon cycling (Fay et al. 2008).

There is *low confidence* in the detection of long-term observed and projected seasonal and daily trends in extreme snowfall as a result of a relatively narrow range of temperatures below the rain–snow transition at which extreme snowfall can occur and subsequent large interdecadal variability (O'Gorman 2014; Kunkel et al. 2013).

2.3.6 The effect of the El Niño Southern Oscillation on land functioning

The El Niño/Southern Oscillation (ENSO) is a dominant mode of interannual climate variability the tropical Pacific (McPhaden et al. 2006; Christensen et al. 2013) with regional impacts on land functioning primarily through extreme rainfall and temperature variability. During El Niño (La Niña) phases there is increased (decreased) precipitation in the south Pacific Ocean, whereas dry (wet) conditions occur in Australia, Southeast Asia, South Africa and northern South America (Vicente-Serrano et al. 2011). Over tropical and sub-tropical land regions rainfall is generally below average during El Niño (Mason and Goddard 2001), although the timing and magnitude varies regionally as a result of meridional and zonal atmospheric circulation (Curtis and Adler 2003). The IPCC reports that there is *high confidence* that the El Niño-Southern Oscillation (ENSO) will remain the dominant mode of interannual variability in the tropical Pacific, with impacts on precipitation variability globally.

ENSO has a complex impact on fire occurrence and emissions in different regions of the world (Van Der Werf et al. 2010b; van der Werf et al. 2008; Duffy et al. 2005; Andela and Van Der Werf 2014; Shabbar et al. 2011; Armenteras-Pascual et al. 2011; Greenville et al. 2009; Liu et al. 2013; Goodrick and Hanley 2009). In pan-tropical forests, during and following an El Niño, fire emissions increase as a result of reductions in precipitation and terrestrial water storage as compared with La Niña (Chen et al. 2017b).

ENSO is a strong driver of extra-tropical drought. Regions affected by La Niña drought are southern USA/northern Mexico and southern Russia/eastern Europe, whereas for El Niño drought the most affected areas are South Africa, Indonesia and the western Pacific area, Australia, the northern part of South America and the Amazon, India and the Indochina peninsulas, central and western Canada, and large areas of the Sahel (Vicente-Serrano et al. 2011). Furthermore, ENSO drives interannual variability in the land carbon sink through vegetation changes in semi-arid ecosystems (Zhang et al. 2017a). ENSO impacts may be compound-the 2015 El Niño led to drought in many parts of Indonesia, resulting in elevated fire occurrence comparable with the previous catastrophic event in 1997/1998 (Lohberger et al. 2018). Extreme drought events in the western Amazon have been related to both El Niño and warm condition in North tropical Atlantic SST (Espinoza et al. 2011).

The IPCC AR5 report future changes in El Niño intensity in CMIP5 models are model and not significantly distinguished from natural modulations result in *low confidence* in any specific projected change in ENSO and related regional phenomena for the 21st century (Christensen et al. 2013). However, recent work has reported robust modeled increases in the occurrence of extreme El Niño and La Niña events like the 1982/1983 and 1997/1998 El Niño events and 1998/1999 La Niña events (Cai et al. 2014, 2015). The frequency of extreme El Niño and La Niña events are projected to double from one in every 20 years to one in every 10 years for El Niño and one in every 23 years to one in every 13 years for La Niña. These extreme ENSO events have significant impacts on land type and functioning including flooding and drought with associated impacts on food security including agriculture, ecosystems and human and animal mortality. **It is therefore *more likely than not* that extreme ENSO events will become more frequent in the future with implications for twenty-first century land type and functioning (*medium evidence*).**

2.4 GHG fluxes from unmanaged and managed land

The land is simultaneously a source and sink for several greenhouses gases. Both natural and anthropogenic fluxes are an important component of the global budgets of CO_2, CH_4, and N_2O. Since preindustrial period the anthropogenic components of these budgets have become more prominent, with Agriculture, Forestry and Other Land Use (AFOLU) creating both sources and sinks of different gasses due to different activities (Figure 2.4.1). In AR5, it was found that AFOLU was responsible for approximately 25% of GHG emissions in 2000-2010 (Smith et al. 2013a; Ciais et al. 2013). The spatial and temporal variations of these exchanges and the influences of land-climate feedbacks continue to be major sources of uncertainty in understanding anthropogenic impacts on the climate system. However, an emerging area of uncertainty highlighted since AR5 is the difficulty in defining and attributing "anthropogenic" fluxes in the land sector.

(IPCC 2010) have previously noted that it is impossible with any direct observation to separate anthropogenic from non-anthropogenic fluxes in the land sector. They have divided natural and anthropogenic processes into three categories (IPCC 2010): (1) natural climate variability and natural disturbance processes (e.g. fire, windrow, disease); (2) the direct effects of anthropogenic activity due to changing land cover or land management; and (3) the indirect effects of anthropogenic environmental change such as climate change, CO_2 and N fertilisation. A variety of different definitions, methods and approaches are used for estimating the anthropogenic fluxes from land, each including different data sources and processes, in part dependent on the purpose for which they were designed (Smith et al. 2014; Houghton et al. 2012a; Gasser and Ciais 2013; Pongratz et al. 2014; Tubiello et al. 2015; Grassi et al. 2018).

The different approaches lead to a wide range of estimates that need to be better understood and reconciled to ensure transparency and credibility in monitoring, reporting and verifying GHG fluxes under the UNFCCC (Grassi et al. 2018). The long-term temperature stabilisation goal of the Paris Agreement (PA) is to hold "the increase in the global average temperature to well below 2°C" (Article 2) and requires achieving "…a balance between global anthropogenic greenhouse gas emissions by sources and removals by sinks of greenhouse gas in the second half of this century." (Serrano-Cinca et al. 2005a). The PA includes an Enhanced Transparency Framework, to track countries' progress towards achieving their individual targets (i.e., the Nationally Determined Contributions, NDCs), and a Global Stocktake (every five years starting in 2023), to assess the countries' collective progress towards the long-term goals of the PA. This implies a need to have credible estimates of what is "anthropogenic" (which is generally understood to apply to both "emissions" and "removals" (Fuglestvedt et al. 2018). It is also expected that the global stocktake will assess progress to date using country data officially submitted to the UNFCCC, and compare it with modelled pathways of the long-term goal (i.e. 1.5°C and 2°C pathways). This further implies a need to ensure consistency between different approaches or, if they are not consistent to assess why and if they can be reconciled. The details of the Transparency Framework and of the Global Stocktake will be included in the PA's "rulebook" (decisions that will rule its implementation), currently being elaborated by the United Nations Framework Convention on Climate Change (UNFCCC).

The terrestrial biosphere absorbs about 20% of fossil-fuel CO_2 emissions. However, the land sink is actually composed of two largely counteracting fluxes that are poorly quantified: fluxes from land use change and CO_2 uptake by terrestrial ecosystems. Dynamic global vegetation model simulations suggest that CO_2 emissions from land use change have been substantially underestimated because processes such as tree harvesting and land clearing from shifting cultivation have not been considered (Arneth et al. 2017a). It was reported that the rate of net biome productivity (NBP) has significantly accelerated from -0.007 ± 0.065 PgC yr^{-2} over the warming period (1982 to 1998) to 0.119 ± 0.071 PgC yr^{-2} over the warming hiatus (1998-2012) (Ballantyne et al. 2017). The global greening may have slowed down the rise in global land-surface air temperature by 0.09 ± 0.02 °C since 1982 (*moderate confidence*) (Zeng et al. 2017).

It was estimated that vegetation currently stores around 450 petagrams of carbon. In the hypothetical absence of land use, potential vegetation would store around 916 PgC, under current climate conditions. This difference highlights the massive effect of land use on biomass stocks (Houghton and Nassikas 2017; Mao et al. 2016). Deforestation and other land-cover changes are responsible for 53-58% of the difference between current and potential biomass stocks. Land management effects (the biomass stock changes induced by land use within the same land cover) contribute 42%-47% (Erb et al. 2018). Terrestrial ecosystems respond to climate change and variability in very different ways cross hemispheres (Zhang et al. 2017b), regions, and biomes (*high confidence*).

According to CMIP6 (BB4CMIP) estimates, global biomass burning emissions were relatively constant, with 10-year averages varying between 1.8 and 2.3 Pg C yr^{-1} from 1750 to 2015. Carbon emissions increased only slightly over the full time period and peaked during the 1990s after which they decreased gradually (*high confidence*) (Van Marle et al. 2017).

This section therefore aims to assess both updates of anthropogenic land fluxes from the science literature that have typically been included in past IPCC ARs along-side flux estimates as reported by countries in their Greenhouse Gas Inventories (GHGIs) to the UNFCCC. The major GHGs exchanged between the biosphere and the atmosphere discussed in this chapter are carbon dioxide (CO_2), methane (CH_4) and nitrous oxide (N_2O).

2.4.1 Carbon dioxide

2.4.1.1 The Global Carbon Budget

The continuous exchange of CO_2 between land and the atmosphere as part of the natural global carbon cycle is a gross sink of about 60 GtC (220 $GtCO_2$ yr^{-1}) due to photosynthesis, and gross emissions of about the same amount to the atmosphere due to respiration (Ciais et al. 2013). AFOLU has altered this cycle changing carbon fluxes and carbon storage.

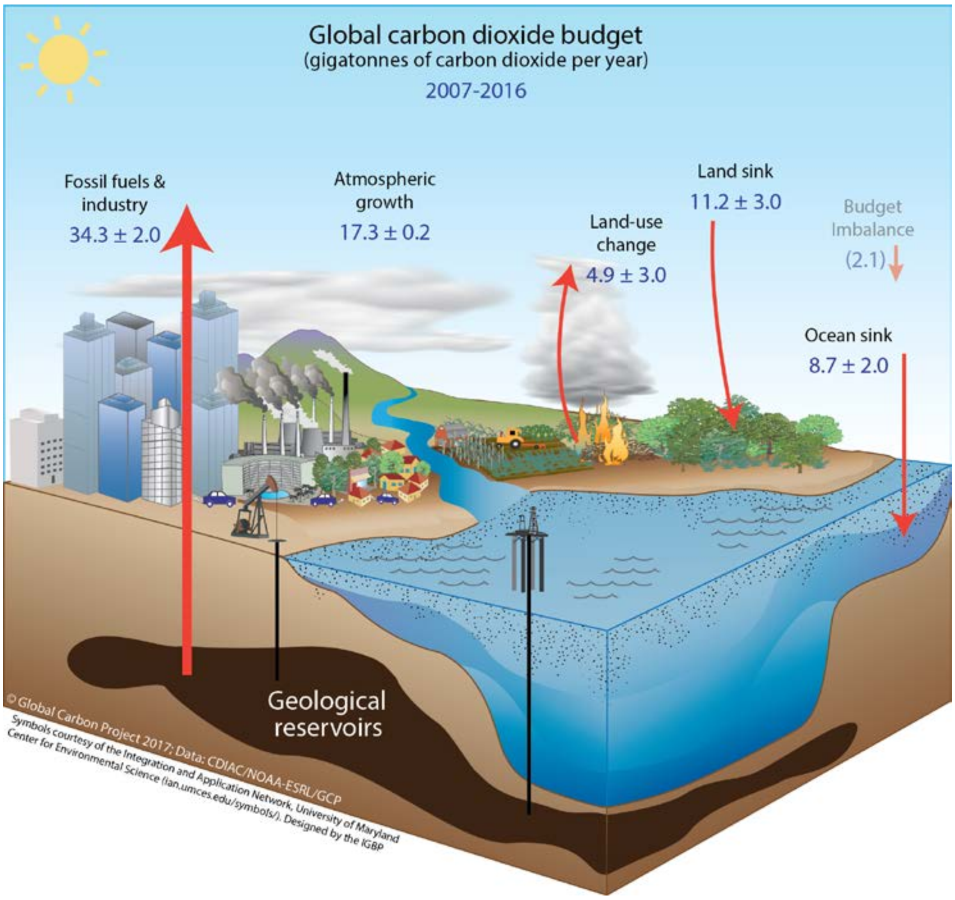

Figure 2.4.1. Perturbation of the global carbon cycle caused by anthropogenic activities, averaged globally for the decade 2007-2016 ($GtCO_2$ yr^{-1}) (Le Quéré et al. 2017) *(note : update with numbers from 2018 budget when available)*

Anthropogenic influences on the carbon budget are calculated each year by the Global Carbon Project as used in AR5 (Ciais et al. 2013; Conway 2012a). The 2017 carbon budget (Le Quéré et al. 2017) estimates that the average net anthropogenic flux of carbon dioxide from "land use change[1]" was a source of 4.9 ± 3.0 $GtCO_2$ yr^{-1} for 2007-2016, approximately 12% of total anthropogenic emissions (Figure 2.4.1) *(note will update with 2018 budget numbers)*. This "land use change" source is the net flux due to direct anthropogenic activities, predominated by tropical deforestation, but also including afforestation/reforestation sinks, and fluxes due to forest management (e.g. wood harvest) and other land management dependant on what is included in the models. It is calculated as the mean across two bookeeping models (Houghton and Nassikas 2017; Hansis et al. 2015) including an update to the single bookkeeping model that was used in AR5 (Houghton et al. 2012a). The bookkeeping model mean very similar to mean across a range of Dynamic Global Vegetation Models (DGVMs) run using the same driving data through the TRNEDY model

[1] Footnote: CO_2 flux from "land is change" as used in the science literature is similar to the UNFCCC LULUCF (Land Use, Land use Change and Forestry) sector in that it combines changes in land cover and some management. IN AR5 it was referred to as the FOLU part of AFOLU.

intercomparison exercise, even though the DGVMS are all individually quite different(Le Quéré et al. 2017, Box 2.4.1, Fig 2.4.2).

Just under half (47%) of total CO_2 emissions (AFOLU and fossil fuels) remain in the atmosphere. The rest is taken up by ocean and land sinks. These sinks are driven by the indirect effects of environmental change (climate, CO_2, N) on the land-both managed and unmanaged land. As described in 2.2, rising CO_2 concentrations have a fertilising effect on land, while climate has a mixture of effects e.g. rising temperature increases respiration rates and may enhance or reduce photosynthesis depending on location, while longer growing seasons allow for higher photosynthesis. The net land sink due to indirect effects of environmental change was -11.2 ± 3.0 $GtCO_2\ yr^{-1}$ in 2007 to 2016, absorbing 22% of global anthropogenic emissions. This sink was referred to in AR5 as the "residual terrestrial flux" as it was not estimated directly but calculated as the residual of all the directly estimated fluxes in the budget. In the 2017 budget it is estimated by DGVMs. There is a budget imbalance in that the estimated emissions are 0.6 Gt C yr^{-1} greater than estimated sinks (including the atmosphere). In AR5, the budget imbalance would have been included in the residual terrestrial flux. The imbalance implies either emissions have been overestimated or the sinks have been underestimated.

The land appears twice in the budget-a net source due to direct AFOLU activity, and a net sink due to the indirect effects of environmental change. Thus overall, combined direct and indirect anthropogenic effects on all managed and unmanaged lands means that the land is a net sink of -6.3 $GtCO_2\ yr^{-1}$ for 2007-2016. This is corroborated with estimates of the total net land flux from atmospheric inversions based on observations (1.8/1.4/2.3 GtC yr^{-1} 2007 to 2016 from CTE/Jena CarboScope/CAMS) – while atmospheric inversion can separate the net land flux from fossil fuel flux and ocean fluxes, they are unable to further disaggregate land CO_2 fluxes (Box 2.1 methods)

Gross versus net emissions: The flux of 4.9 ± 3.0 $GtCO_2\ yr^{-1}$ from land use change over the period 2007 and 2016 represents a net value. It consists of both gross emissions of carbon from, for example, deforestation and forest degradation, and gross sinks of carbon from, for example, carbon accumulation in forests recovering from harvests. Gross emissions from changes in land use, globally may be as high as 20.2 PgC yr^{-1}(Houghton and Nassikas 2017).

Satellite land-cover and biomass-based estimates of CO_2 emissions from tropical forests loss during 2000-2010 are quite variable: 4.8 $GtCO_2\ yr^{-1}$ (Tyukavina et al. 2015), 3.0 $GtCO_2\ yr^{-1}$ (Harris et al. 2015) 3.2 $GtCO_2\ yr^{-1}$ (Achard et al. 2014) and 1.6 $GtCO_2\ yr^{-1}$ (Baccini et al. 2017b). Differences in estimates can be explained to a large extent by the approaches used. For example, the analysis by (Tyukavina et al. 2015) had a higher estimate because they used a higher spatial resolution, and small changes in area add considerably to the total. All of the estimates above (except (Baccini et al. 2017b) considered losses in forest area and ignored degradation and regrowth of forests. (Baccini et al. 2017b), on the other hand, included both losses and gains in forest area and losses and gains of carbon within forests (i.e., forest degradation and growth). Together, these processes yielded a lower total loss, presumably because of forest growth. Some of the growth in carbon stocks results from recovery of forests following harvest of wood or agricultural abandonment (i.e., direct anthropogenic effect)(Houghton and Nassikas 2017; Le Quéré et al. 2009), and some is thought to result from CO_2 fertilisation (an indirect effect) (Schimel et al. 2015). The four studies cited above also reported committed emissions; i.e., all of the carbon lost from deforestation was assumed to be released to the atmosphere in the year of deforestation. In reality, some of the carbon in trees is not released immediately to the atmosphere but transferred to dead and downed vegetation. Both bookkeeping models and DGVMs account for these delayed emissions in growth and decomposition.

Carbon emissions from fires

Emissions from fires and biomass burning are a significant source of greenhouse gases. These emissions may result from anthropogenic or natural wildland fires or from burning of agricultural waste, and directly influence the radiative balance of the atmosphere in complex ways through their potential for warming (e.g. CO_2, CH_4). For several decades the net effect of fire on global terrestrial carbon storage and fluxes had been either ignored or inadequately incorporated into land-climate models with the possible exception of considering future fire risks from a changing climate. Our ability to understand past and present drivers of fires as well as future projections of fires under a changing climate at global and regional scales is thus important.

The Global Fire Emissions Database V.3 (GFED3), widely used in various fire models, estimated C emissions of 2.0 PgC yr^{-1} during 1997-2001 with significant inter-annual variability (2.8 PgC yr^{-1} in 1998 and 1.6 PgC year^{-1} in 2001), relative stability at 2.1 Pg C yr^{-1} during 2002-2007, declining subsequently to 1.7 Pg C yr^{-1} in 2008 and 1.5 Pg C yr^{-1}in 2009 because of reduced deforestation in South America and tropical Asia (Van Der Werf et al. 2010a). Further, the contributions of fire carbon emissions from various land cover and land use sectors for the period (2001-2009) when data were available from MODIS were determined as follows: Grassland and savannahs (44%), tropical deforestation and degradation (20%), woodland fires mostly in the tropics (16%), forest fires mostly in the extratropics (15%), tropical peat fires (3%) and agricultural waste burning (3%) (Van Der Werf et al. 2010a). In spite of some underestimation of fires in agricultural land because of non-detection of small fires, and an interaction between forest (especially tropical) deforestation/degradation because of land clearing for agriculture, it is clear that wildland fires make by far the greatest contributions to carbon emissions from biomass burning.

Since then, better estimates from land area burnt (Giglio et al. 2013), fire emission factors (Akagi et al. 2011; Urbanski 2014), etc. have become available. Most recently, GFDB4s has updated fire-related emissions estimates biome-wise, regionally and globally, using higher resolution input data gridded at 0.25˚, the new burned area dataset with small fires, improved fire emission factors and better fire severity characterisation of boreal forests (van der Werf et al. 2017). The new estimates for the period 1997-2016 are 2.2 Pg C yr^{-1}with a high of 3.0 Pg C yr^{-1} in 1997 and a low of 1.8 Pg C yr^{-1}in 2013, figures that are about 11% higher than those from GFDB3 for the common period 1997-2011, mainly because of 37% increase in burned area estimated through inclusion of small fires, and a -19% change in fuel consumption factor from field-based studies especially in grassland and savannas.

2.4.1.2 Historical trends in anthropogenic CO_2 flux

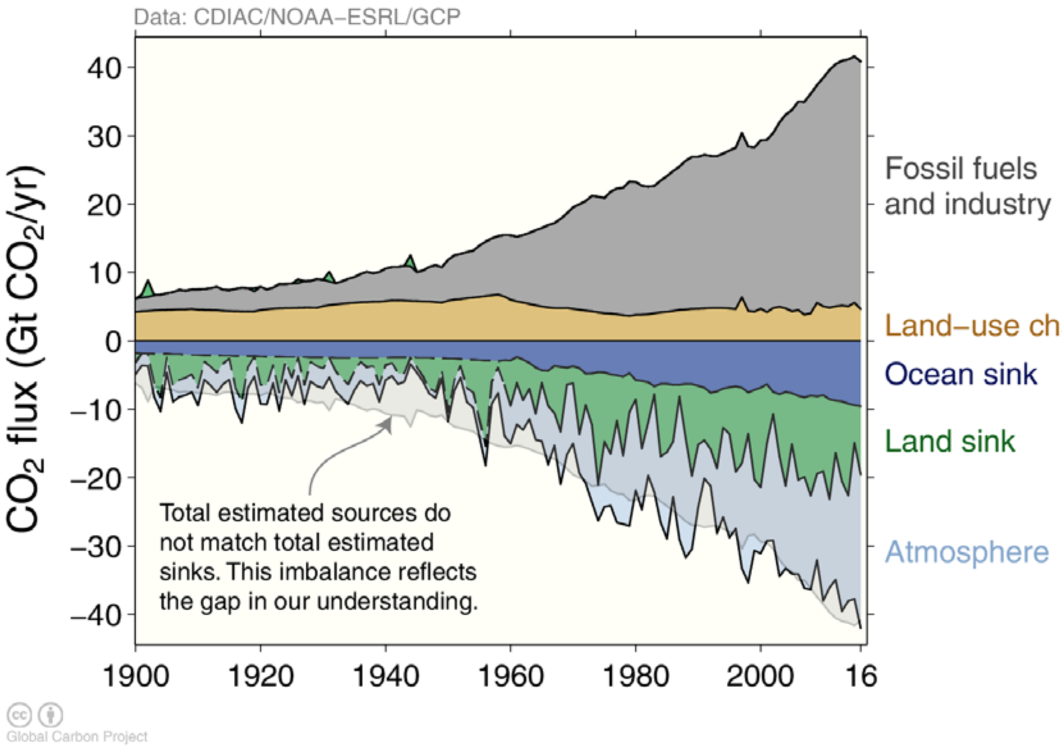

Figure. 2.4.2 Trends in anthropogenic CO_2 flux from combined components of the global carbon budget since 1900. Figure from (Le Quéré et al. 2017). Data from CDIAC; NOAA-ESRL/GCP (Houghton and Nassikas 2017; Hansis et al. 2015; Khatiwala et al. 2013; Devries 2014; Le Quéré et al. 2016a; Saunois et al. 2016; Marland et al.)

Land use change emissions used to be the dominant anthropogenic source until around the middle of the last century when fossil fuel emissions became more dominant (Figure 2.4.2). According to bookkeeping models (Houghton and Nassikas 2017; Hansis et al. 2015), the land use change flux (due to direct anthropogenic activities) declined from the 1960 to 1980s, (Figure 2.4.3) then (Houghton and Nassikas 2017) so a very slight decrease while (Hansis et al. 2015) show a slight increase, with the mean showing little trend (figure 2.2.3). Individual DGMS show high variability, with no trend over this period (Figure 2.2.3) (*low certainty*). This is in contrast to results in AR5 which showed a declining trend in land use change emissions from the Houghton bookkeeping model (Houghton et al. 2012a)and the DGVMs. in part because of reduced deforestation in Brazil and afforestation in other countries (Gasser and Ciais 2013; Conway 2012a). BLUE and the DGVMs use the spatially explicit harmonised land use change data (LUH2) data set (Hurtt et al. 2017) based on HYDE 3.2, the older version of which (HYDDE 3.1, (Klein Goldewijk and Verburg 2013) had higher gross transitions in individual countries around the year 2000. The Houghton bookkeeping approach uses FAO Forest Resource Assessment data which was updated in 2015 (FAO 2015)– this has net change in forest areas over 5 year periods. (Houghton and Nassikas 2017) also do not include shifting cultivation which was included in the AR5 version, but they do include Indonesian and Malaysian peat burning and drainage.

In addition to differences in land cover data sets between models, and indeed satellites, there are many other methodological reasons for differences (See box 2.4.1) (Conway 2012a; Houghton et al. 2012b; Gasser and Ciais 2013; Pongratz et al. 2014; Tubiello et al. 2015). There are different definitions of land cover type and indeed forest e.g. FAO uses a tree cover threshold for forests of 10%. (Tyukavina et al. 2017b) used 25%, different estimates of biomass and soil carbon density, different approaches to tracking emissions through time (legacy effects), different types of activity included (e.g. forest harvest, peatland drainage and fires). Most DGVMS only fairly recently included forest management which has been found since AR5 to have larger impacts on global fluxes than was previously realised (Arneth et al. 2017b; Luyssaert et al. 2014a; Erb et al. 2018). Grazing management has likewise been found to have large effects not included in most DGVMs (Pugh et al. 2015).

In contrast to the global model results, estimates of LULUCF flux based on IPCC methodologies, both those calculated by FAO and those reported by countries to UNFCCC in the National Greenhouse Gas Inventories (GHGI), show a smaller net source and show a declining trend (Figure 2.4.3, panel b). This is discussed in more detail below.

The trends in the global carbon budget since 1900 (Figure 2.4.2) show the "land sink" has increased due to ongoing increases in climate change and CO_2 concentration. Note the high variability in the land sink as it is very sensitive to interannual climate variability. However overall model fluxes are far more influenced by CO_2 fertilisation effects than climate change effects. The DGVM TRENDY intercomparison in (Sitch et al. 2015) for 1990 to 2009 fund that CO_2 only contributed to mean global NBP sink of -2.875 ± 1.003 PgC yr^{-1}, trend 0.121 ± 0.055PgC yr^{-2} while climate only contributed a source of 0.497 ± 0.523 PgC yr^{-1}, trend 0.039 ± 00.022PgC yr^{-2}, to give a net indirect effect of -2.378 ± 00.721 PgC yr^{-1}, trend -0.055 ± 00.03PgC yr^{-1}.

Panel (a)

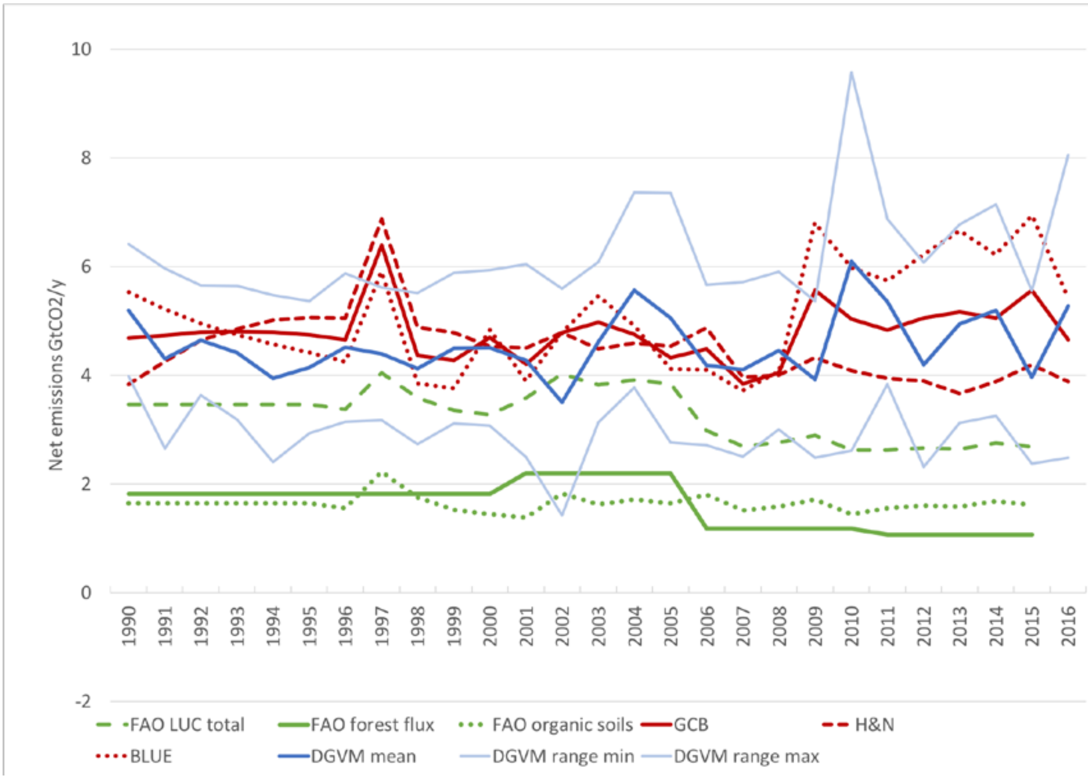

Panel (b)

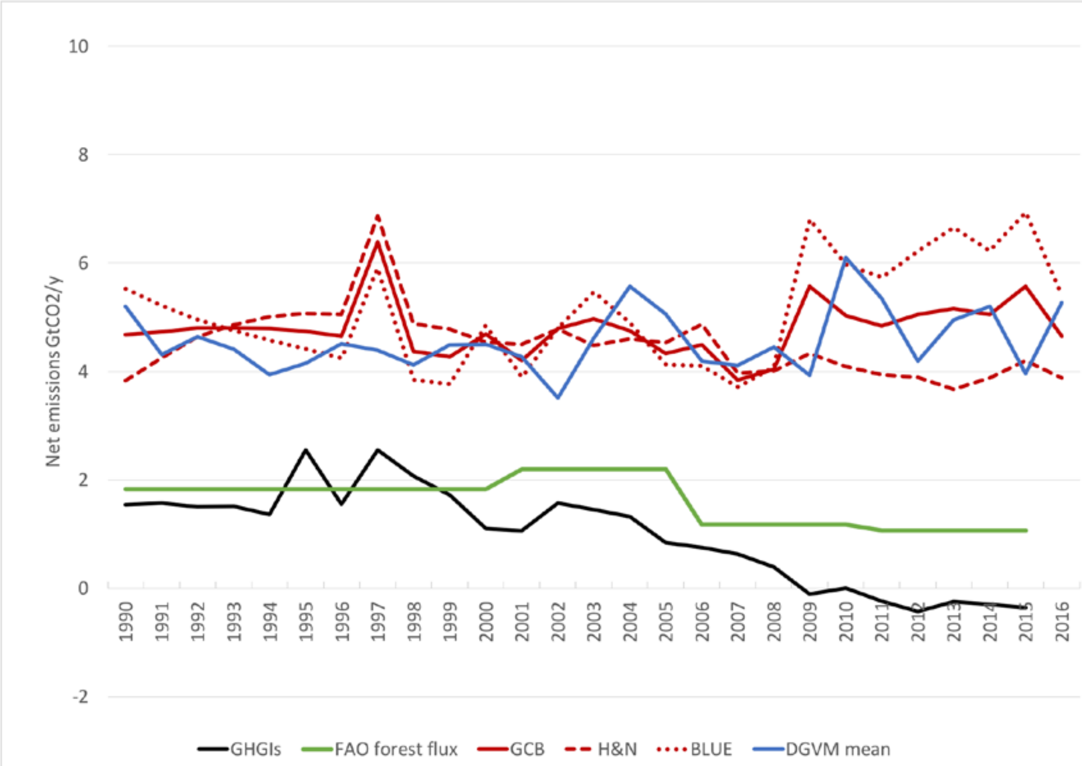

Figure 2.4.3. Global net CO_2 emissions from AFOLU from 1990 (in $GtCO_2$ yr^{-1})

Panel (a) shows global estimates from models and FAO (which represents a globally consistent methodological approach). FAO (green line - downloaded from FAOSTAT website, see also (FAO 2015). GCB (red line): Global Carbon Budget (Le Quéré et al. 2017), the mean between the two bookkeeping models, H&N (Houghton and Nassikas 2017) and BLUE (Hansis et al. 2015). DGMV mean (dark blue line) is the mean of the Dynamic Global Vegetation Models (individual pale blue lines) included in Le Quéré et al. 2017 and the pale blue lines show the 1 standard deviation range. Panel (b) shows the Greenhouse Gas Inventories GHGI (black line): based on individually reported country data compiled by (Grassi et al. 2018). *(Note: panel a) to add ESM models that did runs with/without climate change e.g.* (Lawrence and Vandecar 2015a) *and other globally consistent/global coverage estimates (e.g. GFED and EDGAR when new versions become available). Could add AR5 to discuss difference. Panel b, take out FAO, add in AR5)*(Houghton et al. 2012b; Hansis et al. 2015).

Box 2.2 Methodological Approaches for estimating national to global scale anthropogenic land carbon fluxes

Bookkeeping/accounting models track changes in biomass and soils that result from changes in land activity using data on biomass density and rates of growth/decomposition, typically from ground-based inventory data collection (field measurements of carbon in trees and soils). The approach is to include only those changes directly caused by land-use change and management. The models do not respond to changing environmental conditions as the data reflects the conditions at the time of collection, which will implicitly include some degree of indirect effects. Thus it may overestimate biomass density in the past (before CO_2 fertilization), and underestimate it in the future.

Dynamic Global Vegetation Models (DGVMs) model the processes of photosynthesis and respiration driven by both environmental conditions (climate variability, climate change, CO_2, N concentrations) and data sets of changing anthropogenic activity (land cover and management). Models vary with respect to the processes included with many since AR5 now including forest management, fire, N, and other management (Sitch et al. 2005; Le Quéré et al. 2017). Models are run with and without land use to differentiate the direct effects of anthropogenic land use from the indirect effects of climate and CO_2 change. This approach implicitly includes a "lost atmospheric sink capacity", or the carbon uptake due to environmental effects on forests (captured in the model run without land use) that does not happen if the forests are removed.

Earth System Models (ESMs) couple (often simplified) versions of DGVMs with a climate model enabling feedbacks between climate change and the carbon cycle (e.g., temperature effects on respiration). They are fewer experiments run with/without land use change to diagnose the anthropogenic AFOLU flux. **Integrated Assessment Models** also include simplified DGVMs

Satellite data can be used to map land cover, the photosynthetic activity (greenness) of vegetation, vegetation fires and biomass density. Algorithms, models and independent data can be used to convert satellite data to net changes in carbon flux. Some active satellite sensors (LiDAR) are able to measure three-dimensional structure in woody vegetation, which is closely related to biomass density (Zarin et al. 2016a; Baccini et al. 2012; Saatchi et al. 2011) increasing the number of biomass density estimates from a few hundred measured field sites to more than 40,000 GLAS footprints (for the tropics)(Baccini et al. 2017b). Together with land cover change data, these can be used to provide increasingly high resolution observational-based estimates estimate of fluxes due to change in forest area (e.g. (Tyukavina et al. 2015; Harris et al. 2015; Baccini et al. 2012) or degradation (Baccini et al. 2017a). Data is only available for recent decades, methods generally assume that all losses of carbon are immediately released to the atmosphere, and belowground biomass and soil carbon changes have to be modelled. The approach implicitly includes indirect and natural disturbance effects.

Atmospheric Inversions use observations of atmospheric concentrations with a model of atmospheric transport and data on wind speed and direction to calculate backward to the implied initial emissions that resulted in the observed concentrations. Since AR5 there has been enormous progress in availability of concentration data from flux towers networks and satellite data, enabling better global coverage at finer spatial scales and some national estimates (e.g. in the UK where they are used along-side national GHG inventories). A combination of concentrations of different gases and isotopes enables the separation of fossil, ocean and land fluxes. However, inversions give only the net flux of CO_2 from land, they cannot separate natural and anthropogenic fluxes.

FAOSTAT: The United Nations Food and Agricultural Organization has produced country level estimates of greenhouse gas emissions from 1990 using IPCC Tier 1 methods (see main text 2.4.1.3). For CO_2: Countries report change in forest area and forest carbon stock every 5 years (Tian et al. 2015a).

The carbon flux is estimated due to forest cover change (assuming instantaneous emissions in the year of forest area loss) and change in carbon stock in extant forests, but without distinguishing "managed" and "unmanaged" forest areas (Federici et al. 2015). Some large countries may define remote areas as unmanaged and do not account for emissions there. FAO also estimate CO_2 loss from agricultural soils and biomass burning, and non-CO_2 GHG flux from agriculture (see 2.4.2 and 2.4.3).

2.4.1.3 Regional variations in emissions

(note to be expanded with regional figures and data from different sources eg TRENDY models, FAO, Satellite tropical deforestation)

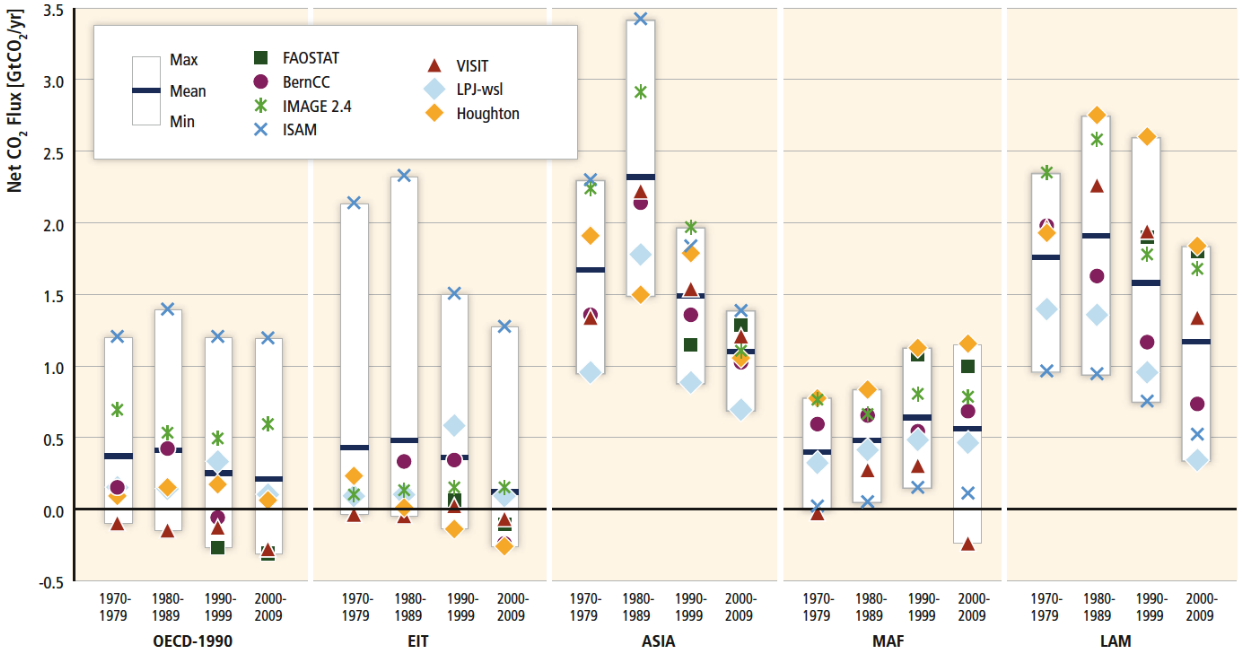

Figure 2.4.4 Regional trends in net CO_2 fluxes from LULUCF *(placeholder to update with new bookeeping model data, TRENDY runs, FAOSTAT (and EDGAR if available))* This figure was from AR5 WGIII chapter 11 (Conway 2012a)

The estimated annual emissions of carbon from land use change vary through time and across regions (Figure 2.4.4). The average emissions from predominantly tropical regions averaged 1.4 GtC yr^{-1} for the 2006-2015 period, while regions outside the tropics were a net sink of 0.3 GtC yr^{-1}(from (Houghton and Nassikas 2017). Countries with the highest area of deforested lands include Brazil, Indonesia and the Democratic Republic of Congo (DRC), while countries with the highest deforestation rates include West African and Southeast Asian countries, as well as Paraguay in South America. There are areas of afforestation in China, India, the USA and Europe. *(Placeholder – for a figure of afforestation/deforestation rates in key countries/regions)*. Tropical peatland forests have a deforestation rate of 4% per year, significantly higher than the average rate for tropical forests at 0.5% (Miettinen et al. 2016; Achard et al. 2014).

Soils store high amounts of carbon and are strongly affected by land use change. Forest soils lose significant amount of Soil organic carbon (SOC)-up to 70 % of their original topsoil amount – very rapidly after conversion to agricultural land (Recha et al. 2013; Poeplau et al. 2011) In contrast, forest land has been quantified to sequester significant amounts of SOC (Pan et al. 2011). Sequestered carbon and SOC stocks from well managed grassland systems (re-) sometimes surpass that of comparable forests (Poeplau and Don 2013; Mosquera et al. 2012; Soussana et al. 2010; Tubiello et al. 2007), with exceptions especially in the tropics (Stahl et al. 2017). Conversion of grasslands to croplands has repeatedly been reported to trigger significant losses of SOC (*high agreement and robust evidence*). Analogously in turn, conversion of cropland to grassland was reported to come along with significant SOC increases (Don et al. 2011; Wang et al. 2011).

Peatlands and coastal wetlands store up to 44% to 71% of the world's terrestrial biological carbon pool (Zedler and Kercher 2005). Although wetlands represent a significant sink for CO_2, they have also historically been a significant source of methane (2.4.2). Peatland conversion (fires and peat decomposition from drainage) account for 0.6-1.2 $GtCO_2e$ a year (Hooijer et al. 2010; Carlson et al. 2016; Tian et al. 2015b). While only 10% of peatlands are located in the tropics, they account for more than 80% of peatland soil emissions, primarily in Indonesia (about 60%) and Malaysia (about10%) (Hooijer et al. 2006, 2010; Page et al. 2011). Wetlands (mangroves, tidal marshes, and seagrasses) have also been converted, with over 25%-50% of wetlands lost in the last 50-100 years due to aquaculture, agriculture, industrial use, upstream dams, dredging, eutrophication of overlying waters, and urban development (McLeod et al. 2011; Pendleton et al. 2012).

Mangrove forests occur in tropical and subtropical coastal regions, with about 75% in 15 countries; their total area was estimated from Landsat imagery to be 138,000 km^2 in 2000 (Giri et al. 2011). Whilst above- and below-ground biomass values are within the range of other forest ecosystems, mangrove soil carbon levels are unusually high, typically at 200-700 tC ha^{-1} (Hutchison et al. 2014). Such carbon stores have accumulated under anaerobic, saline conditions over centuries to millennia (Mckee et al. 2007). Together, living and non-living components of mangrove ecosystems are estimated to store a global total of 4-6 GtC (Kauffman et al. 2011; Alongi 2014; Hamilton and Friess 2018). Following mangrove clearance, at least half is likely to be released relatively rapidly (Lovelock et al. 2017). The historical global loss of mangrove forests due to human disturbance and habitat degradation is estimated at 30%-50% (Pendleton et al. 2012; Alongi 2014; Duarte et al. 2013), with current global loss rates estimated at 0.2% - 3% yr^{-1} (Hamilton and Friess 2018; McLeod et al. 2011). Estimates of associated emissions cover an even wider range, at 0.007-0.029 Gt CO_2 yr^{-1} (Atwood et al. 2017); 0.24 Gt CO_2 yr^{-1} (Pendleton et al. 2012) and 0.33-3.66 Gt CO_2 yr^{-1} (Alongi 2014) At a national level, such carbon releases can represent 10-30% of land use emissions (Murdiyarso et al. 2015).

2.4.1.4 Reconciling global model estimates and UNFCCC reporting of the AFOLU CO_2 flux

(to note: the analysis below is from Grassi et al, in press. However for the SOD will repeat with updated model runs being carried out for the 2018 GCP enabling a more direct estimate of sinks in managed forests in DGVMs)

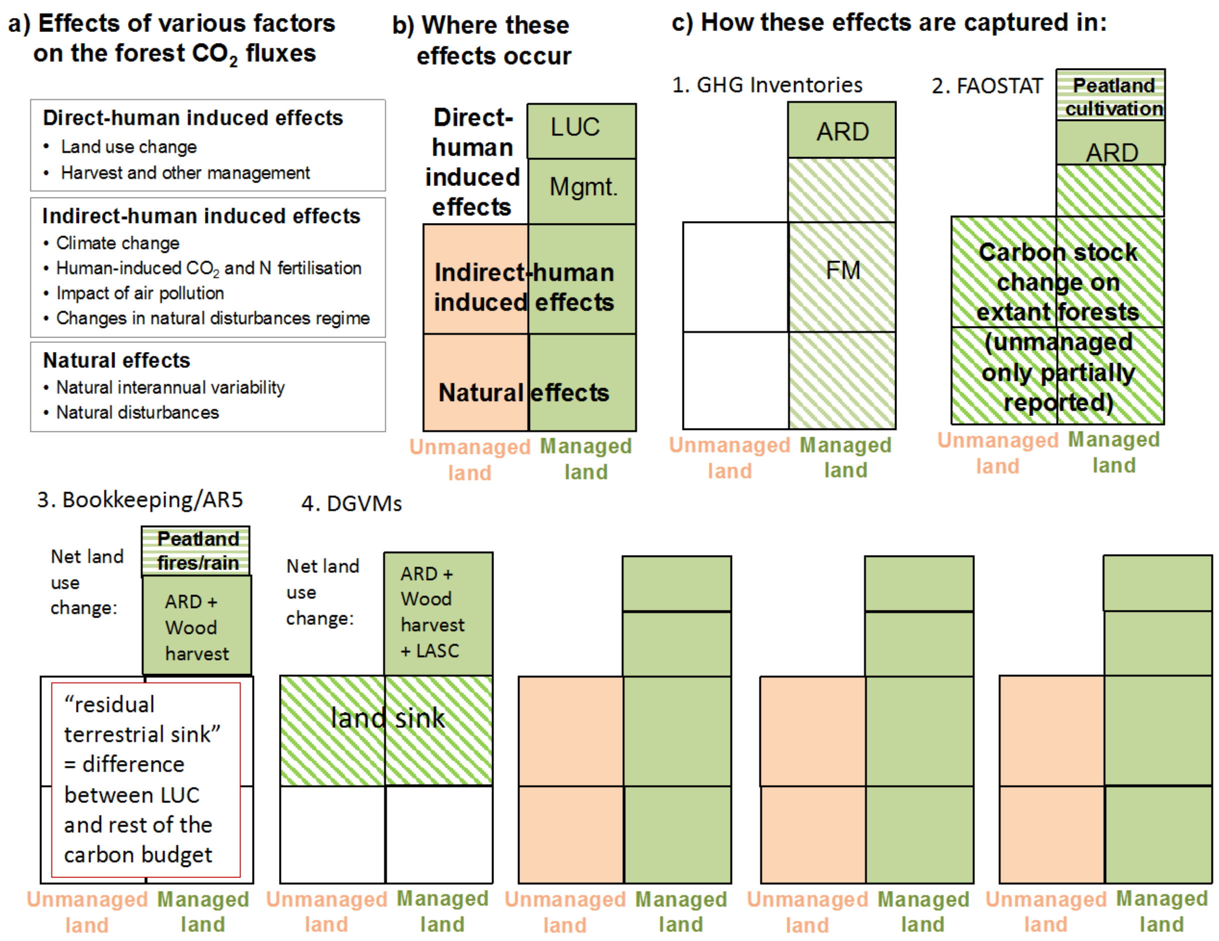

Figure 2.4.5. (Adapted from (Grassi et al. 2018)) Summary of the main conceptual differences between country Greenhouse Gas Inventories (GHGIs) and independent estimates in considering what is the "anthropogenic land CO_2 flux": (a) Effects of key processes on the land flux as defined by IPCC (2010); (b) Where these effects occur (in unmanaged/primary lands, vs. managed/secondary lands); (c) How these effects are captured in and country GHGIs reported to UNFCCC (under the "Land Use, Land use Change and Forestry" sector, LULUCF), in IPCC AR5 (Ciais et al. 2013; Conway 2012a) and earlier versions of the Global Carbon Budget (Le Quéré et al. 2016b) (the anthropogenic "net land use" from bookkeeping models (Houghton et al. 2012b), and the "residual sink", calculated by difference from the other terms in the global carbon budget) and in other methods.

All Parties to the UNFCCC are required to report national GHGIs of anthropogenic emissions and removals Recent studies (Grassi et al. 2017; Grassi et al. 2018) highlighted a discrepancy in global anthropogenic land-related net flux estimates, with fluxes reported in country GHGIs to the UNFCCC (Grassi et al. In press, Figure 2.4.5 panel B) ≈4.3GtCO_2 yr^{-1} lower compared to global modelling approaches (Houghton et al, 2012) used in AR5 (Ciais et al. 2013; Conway 2012a) and updated in Figure 2.4.5 (Houghton and Nassikas 2017). Updated model(Houghton and Nassikas 2017) and GHGI estimates (Grassi et al. In press)shown in Figure 2.4.3 panel (b) widen this gap to for the period 2005-2014 (Figure. 2), equivalent to ≈11% (Fossil fuel + land use: 38.7 GtCO_2 from 2005-2014) of all anthropogenic emissions in this period(Le Quéré et al. 2016b).

The PA includes an Enhanced Transparency Framework, to track countries' progress towards achieving their individual targets (i.e., the Nationally Determined Contributions, NDCs), and a Global Stocktake (every five years starting in 2023), to assess the countries' collective progress towards the long-term goals of the PA. The details of the Transparency Framework and of the Global Stocktake will be included in the PA's "rulebook" (decisions that will rule its implementation), currently being elaborated by the United Nations Framework Convention on Climate Change (UNFCCC). It is expected that that the Global Stocktake will assess the collective countries' progress using independent scientific GHG estimates as the "benchmark" against which the country data will be compared to identify the future "emission gap" and the need for increased policy ambition (Grassi et al. 2018). If a large discrepancy exists in the historical period, the future emission gap may be underestimated.

Under the UNFCCC, **c**ountries report fluxes using methodological guidelines outlined by the IPCC (Intergovernmental Panel on Climate Change 2006; IPCC 2013) with different levels of complexity (Tiers 1 to 3) to reflect country capabilities. Annex I (Developed) countries must report regularly and are expected to use higher tier methods. Tier 1 approaches use activity data (such as country-level land cover change, area of managed land, number of livestock, etc.) and simple approaches to calculating flux (such as carbon stock change, emissions factors, etc.). Tier 3 approaches typically use spatially explicit data and more complex modelling approaches based on field and or satellite data. As countries are able to use their own methods and to some extent definition, these are not globally consistent.

Due to the difficulty in providing widely applicable and scientifically robust methods to disentangle direct and indirect human-induced and natural effects on land-based GHG fluxes, the IPCC GL adopted the "managed land" concept (Ipcc 2003; IPCC 2006) as a pragmatic proxy to facilitate GHGI reporting. "Anthropogenic" land GHG fluxes (direct and indirect) are defined as all those occurring on "managed land", i.e. "where human interventions and practices have been applied to perform production, ecological or social functions"(IPCC 2006) (see SI section 1). The contribution of natural effects on managed lands is assumed negligible over time(IPCC 2010). GHG fluxes from "unmanaged land" are not reported in GHGIs because they are assumed non-anthropogenic. The specific land "effects" included in GHGIs depend on the estimation method used, which differ in approach and complexity among countries (SI section 2). Most countries report both direct and indirect human-induced and natural effects on managed lands (see Table 1 and Figure 3b). The reported estimates may then be filtered through agreed "accounting rules" - i.e. what countries actually count towards their mitigation targets (Grassi et al. 2012; Lee, D. and Sanz 2017a). These may aim to better quantify the additional mitigation actions by, for example, factoring out the impact of natural disturbances and of forest age-related dynamics (Canadell et al. 2007; Grassi et al. 2018)

The conceptual differences between IPCC AR5 and GHGIs in estimating the "anthropogenic land flux" are illustrated in Figure 2.4.5c. Due to differences in purpose and scope, the largely independent scientific communities supporting the IPCC GL (reflected in country GHGIs) and the IPCC ARs have developed different approaches to identify "anthropogenic" GHG fluxes (Figure 2.4.5). Most GHGIs include the majority of fluxes occurring on "managed lands" (i.e., direct, indirect and natural effects), with some differences in practice depending on methods applied. The IPCC AR5, in contrast, disaggregates GHG fluxes into a "net land use" (mostly associated with direct effects) and a "residual sink" (associated with responses of all land to indirect and natural effects). Thus, in the IPCC AR5 most of the indirect effects are included as part of the "residual terrestrial flux", while in most GHGIs they are largely included in the estimated fluxes from managed lands.

While global models and the GHGIs are conceptually similar in considering deforestation and afforestation/reforestation as direct anthropogenic (and even use the same FAO FRA data (FAO 2015), the differences lie mostly in the treatment of extant "managed" forests. The bookkeeping model (Houghton and Nassikas 2017) and some DGVMs (Attribution et al. 2015; Le Quéré et al. 2016b) directly model land management (wood harvest and regrowth). The GHGIs' "managed land" concept is, however, broader and may also include activities related to the social and ecological functions of land. Therefore, the "managed land" area considered by GHGIs is generally larger than that of global models (figure 2.4.6 panel b). (Grassi et al. 2018) use a simple post-processing approach to analyse the carbon uptake in managed forest areas in the DGVM output from Le Quéré et al. (2017). The indirect (climate and CO_2) effects on the larger areas of managed forests in the DGVMS Form the LUH data set, (Hurtt et al. 2011) accounted for $\approx$3.3 $GtCO_2$ yr^{-1} or 75 % of the global-level discrepancy, in both developed and developing countries (Figure 2.4.6).

Reconciliation of the differences would enable a more credible Global Stocktake. It is possible for GHGIs to provide more transparent and complete information on managed forests (including maps, harvested area, harvest cycle, forest age and if/how indirect and natural effects are included), *(note to update with outcomes of 2019 update to methodological guidelines)*. Since the bookkeeping model(Houghton and Nassikas 2017) uses forest data submitted by countries to FAO, it would enhance comparability if countries report consistently between UNFCCC and FAO, which currently is not always the case (Frederici et al., 2017) There are similarly opportunities for the global modeling community to design future models and model experiments to increase their comparability with historical GHGIs and thus their relevance in the context of the PA in time for AR6, including more models including forest management, and providing more disaggregated results on areas of fluxes from primary and secondary forests. This includes the Integrated Assessment Models used for developing mitigation pathways (2.7)

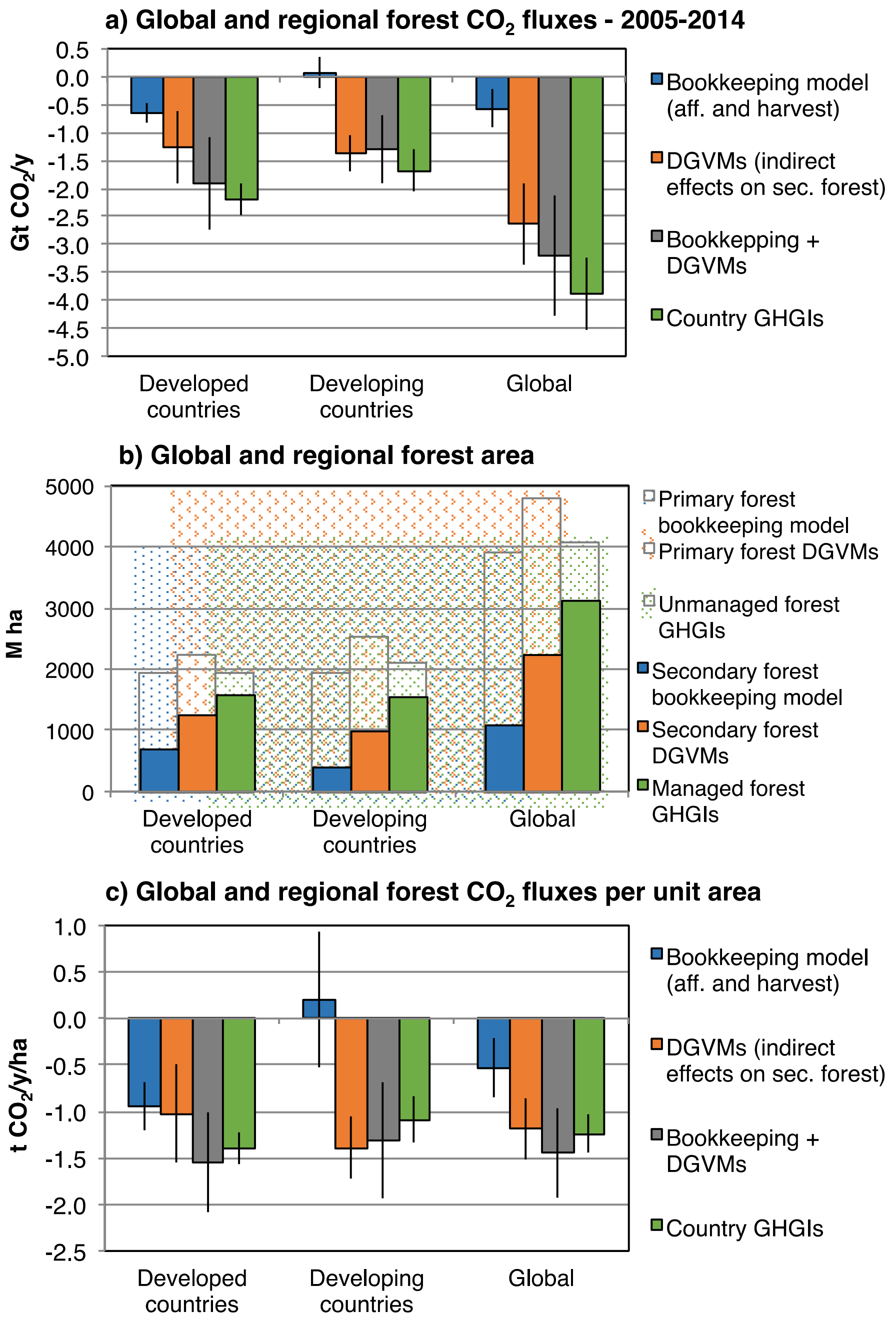

Figure 2.4.6. Reconciling global models and UNFCCC Greenhouse Gas Inventory data. (Figure (Grassi et al. 2018) Estimates of (a) forest net CO_2 flux estimates (including afforestation, but excluding deforestation, peat

fire and peat decomposition) from secondary/managed forests, (b) forest area (primary/unmanaged and secondary/managed) and (c) CO_2 fluxes from existing secondary/managed forests per unit area, in developed countries, developing countries and at global level, from bookkeeping model (Houghton and Nassikas 2017), DGVMs (Le Quéré et al. 2017), and country data submitted to UNFCCC (Grassi et al. 2018). The grey column in (c) is estimated as the grey column in (a) divided by the area of secondary forest from DGVMs (b). While our analysis does not include all developing countries, it covers about the 85% of the FAO-FRA's global "secondary forest" area (see Methods). Whiskers in panel (a) express +/-1 SD (see Methods).

2.4.2 Methane

2.4.2.1 Methods – CH_4

As for CO_2, several methods are applied to estimate methane fluxes. Process models for wetlands and fire emissions are parameterised for local conditions which are then driven by global climate data or satellite observations of burned area. These data are complimented by emissions inventories of agricultural activities, energy production and use, and sector specific emission factors to provide yearly or periodic average emissions estimates. Many studies combine top-down atmospheric measurements and inversions with the "bottom-up" model and inventory estimates to look for consistency between the approaches for the different terms of CH_4 budgets. These approaches are not completely independent as bottom-up estimates are typically used in inversion modelling to describe "prior" spatial distributions of sources and sinks, which are then modified by the inverse model (Combal et al., 2003; Bergamaschi et al., 2013).

In global CH_4 budgets, the atmospheric OH sink is difficult to quantify because the radical has a lifetime on the order of 1 second and its distribution is controlled by different precursor species that have non-linear interactions (Taraborrelli et al., 2012; Prather et al., 2017). Results from the Atmospheric Chemistry and Climate Model Intercomparison Project (ACCMIP) (http://www.giss.nasa.gov/projects/accmip/) produced a series of bottom-up, time-slice experiments that estimated long-term changes in atmospheric composition. As most models do not produce year to year estimates of the OH variability, time-slice results are used in most CH_4 budgets. These bottom-up estimates can be adjusted at large scales using inversion models based on measurements of tracers such as methyl chloroform or chloromethanes that have known emissions and that are removed through reactions with OH (Kirschke et al. 2013).

2.4.2.2 Atmospheric trends

In 2016, the globally averaged atmospheric concentration of CH_4 was 1843 ± 1 ppbv. Systematic measurements of atmospheric CH_4 concentrations began in the mid-1980s and trends show a steady increase between the mid-1980s and early-1990s, slower growth thereafter until 1999, a period of no growth between 1999 and 2006, followed by a resumption of growth in 2007 that continues (Figure 2.4.7A). The growth rates show very high inter-annual variability with a negative trend from the beginning of the measurement period until about 2006, followed by a rapid recovery and continued high inter-annual variability through 2016 (Figure 2.4.7B).

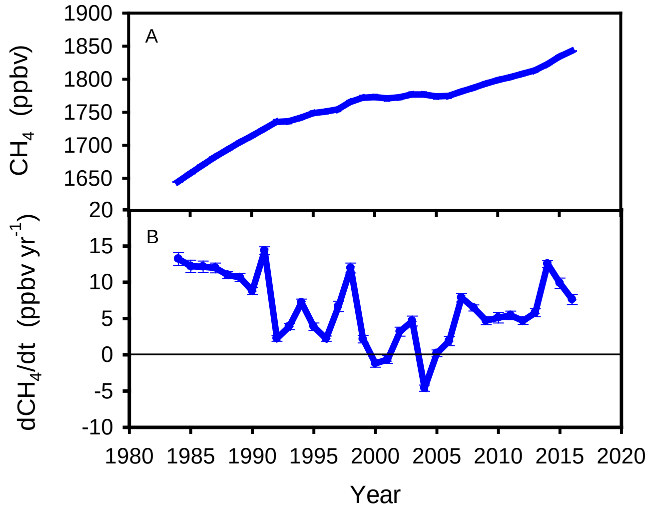

Figure 2.4.7. Globally averaged atmospheric CH_4 mixing ratios (Frame A) and instantaneous rates of change (Frame B) Data source: NOAA/ESRL (www.esrl.noaa.gov/gmd/ccgg/trends_ch4/)(Dlugokencky et al. 1994).

Understanding the underlying causes of temporal variation in atmospheric CH_4 concentrations is an active area of research. To estimate temporal emission trends, Bergamaschi et al. (2013) used column averaged CH_4 mixing ratios from the Scanning Imaging Absorption Spectrometer for Atmospheric Cartography (SICAMACHY) on board Envirosat (Frankenberg et al. 2011) for inversion sensitivity experiments. The modelled global emissions showed small anomalies between 2000 and 2006 (±10 Tg y^{-1}). There was a significant increase after 2006 and emissions between 2007 and 2010 were between 16 and 20 Tg y^{-1}. The increase was mainly attributed to anomalies in the tropics (9-14 Tg y^{-1}) and the mid-latitude northern hemisphere (6-8 Tg y^{-1}). Half of the increase in anthropogenic emissions in the EDGAR v4.2 dataset was attributed to China – 11Tg from coal mining and 5Tg from agriculture (rice cultivation and enteric fermentation). The inversion estimate by Bergamaschi et al. (2013) attributed about 1/3 less emissions to China. Superimposed on the rising emissions trend were significant inter-annual variations attributed to wetlands (±10 Tg y^{-1}) and biomass burning (±7 Tg y^{-1}).

Inter-annual variability of CH_4 growth was thought to be driven mostly by variations in natural emissions from wetlands (Rice et al. 2016; Bousquet et al. 2006), particularly during the pause in CH_4 growth between 2000 and 2006. Bousquet et al. (2011) used two inverse modelling approaches to analyse the changes in the CH_4 budget between 2006 and 2008, during the stable phase of atmospheric accumulation. The two inversions showed that tropical wetlands were responsible for between 50 and 100% of the inter-annual fluctuations, but results were inconsistent for the geographic distribution of the wetland source. The authors also used the global vegetation model ORCHIDEE, which gave results that were inconsistent with the inversion models in both magnitude and geographic distribution of the source of the anomaly. The model responded to precipitation changes in the tropics and to both temperature and precipitation changes in the boreal zone. The authors concluded that OH variation over the period analysed accounted for <1% of the variation.

The importance of fossil fuel emissions in the global atmospheric accumulation rates continues to be debated. Rice et al. (2016) used measurements of the stable isotopic composition of atmospheric CH_4 ($^{13}C/^{12}C$ and D/H) in the northern hemisphere between 1977 and 2009 to constrain the sources of CH_4 estimated in an inversion that used a 3D chemical transport model to apportion the fluxes across sources. These authors found an increase in fugitive fossil fuel emissions since 1984 with most of this growth occurring after 2000. They also found that wetlands were the largest contributor to inter-annual variability.

Studies attributing the cause of inter-annual variability to wetlands assumed that the atmospheric OH sink was approximately time invariant, but recent studies suggest that this is inappropriate. Pison et al. (2013) used two atmospheric inversion models and the ORCHIDEE model and found greater uncertainty in the role of wetlands in inter-annual variability between 1990 and 2009 and the 1999-2006 pause. In particular, the authors found a positive trend in Amazon Basin emissions between 2000 and 2006 from the process-based model and a negative trend from the inversion estimates. McNorton et al. (2016) further weakened the argument for the role of wetlands in determining temporal trends since 1990. These authors used a 3-D global chemical transport model, driven by meteorological re-analyses and variations in global mean OH concentrations derived from methyl chloroform (CH_3CCl_3) observations to show that changes in the atmospheric sink explained a large portion of the suppression in global CH_4 concentrations relative to the pre-1999 trend. Atmospheric transport of CH_4 to its sink region and atmospheric temperature were minor contributors to inter-annual variability. Turner et al. (2017) found that there was a 35 Tg y^{-1} increase in CH_4 emissions between 1993 and 2003, the majority of which was found to be in the Northern Hemisphere. This was accompanied by a 7% increase in global mean OH between 1991 and 2000. They attribute the 1999-2006 stabilisation to slowing of the increase of CH_4 emissions after 1998 and the enhanced OH sink.

The reasons behind the reprise of the growth trend in 2007, which continues, is unclear. The emerging picture is that it is likely that inter-annual variations in the OH sink play a role. Turner et al. (2017) found that the most likely explanation for this sudden increase is a 25 Tg y^{-1} decrease in methane emissions from 2003 to 2016 that is offset by a 7% decrease in global mean OH concentrations. Rigby et al. (2017) also attribute part of the reprise of growth to changes in OH concentrations. They suggest that CH_4 emissions increased steadily during the 1990s and early 2000s. Contrary to Turner et al. (2017) Rigby et al. (2017) find that emissions increases continued at a more modest pace after the early 2000s. It is impossible to rule out that a change in emissions after 2006 explains the renewed CH_4 growth and Rigby et al. (2017) conclude that the change in the OH sink does not fully explain the inflection.

Changes in the isotopic signature of CH_4 in the atmosphere suggests a shift from fossil-fuel to biogenic sources (Schaefer et al. 2016; Schwietzke et al. 2016). The depletion of $\delta^{13}C_{atm}$ beginning in 2009 could be due to changes in several sources. (Schaefer et al. 2016) suggested that lower fire emissions combined with higher tropical wetland emissions could explain the $\delta^{13}C$ perturbations to atmospheric CH_4 sources. However, because tropical wetland emissions are higher in the southern hemisphere, and the remote sensing observations show that CH_4 emissions increases are largely in the tropics north of the equator (Bergamaschi et al. 2013; Melton et al. 2013; Houweling et al. 2014), an increased wetland source does not fit well with the $\delta^{13}C$ observations. Schaefer et al. (2016) suggested that agriculture is a more likely source of increased emissions, and particularly livestock in the tropics, which is consistent with inventory data[2].

With respect to atmospheric CH_4 growth rates, we conclude that there is significant and ongoing accumulation of CH_4 in the atmosphere (*very high confidence*). Contrary to the findings of AR5, wetlands are not the primary drivers of inter-annual variability or the cause of the pause in growth rates in the early 2000s (*high confidence*). We also conclude that variation in the atmospheric OH sink plays an important role in the year to year variation of the CH_4 growth rate, but does not explain the entirety of the changes in the growth rates (*medium confidence*); that growth in biogenic CH_4 sources explains part of the current growth (*very high confidence*); and that increases in other tropical sources may be playing a role in the reprise of the growth rate (*medium confidence*).

2.4.2.3 Global CH_4 budget

AR5 presented decadal global CH_4 budgets beginning in 1980; the Kirschke et al. (2013) budget in Table

[2] European Commission, Joint Research Centre/Netherlands Environmental Assessment Agency, Emission Database for Global Atmospheric Research (EDGAR) (version 4.2) (2011); http://edgar.jrc.ec.europa.eu.
Note to myself: The paper by Rice et al.2016 assumes a constant OH sink, so wetlands come back and they do not include the uptick in CH4 after 2006 in this analysis.

2.4.1 represents the most recent decade reported. A new budget has been developed, covering the period 2000 to 2012 (Saunois et al. 2016). We present the revised budget for the final decade reported in AR5 and for the final year of the new analysis. The main sources of CH_4 are natural emissions from wetlands and anthropogenic sources, with significant emissions from agriculture, forestry and other land use. Global emissions are between 600 and 700 Tg CH_4 yr^{-1} and 60-70% of this is due to anthropogenic sources (Kirschke et al. 2013; Bruhwiler et al. 2014; Janssens-Maenhout et al. 2017). The primary sink for atmospheric CH_4 is consumption by tropospheric OH; stratospheric reactions with chlorine and atomic oxygen radicals, and consumption in soils by methanotrophic bacteria are minor sinks. However, these minor sinks are 3 to 5 times greater than the current rate of annual increase of CH_4 in the atmosphere, so changes to them could affect atmospheric accumulation rates. Increasing atmospheric concentrations are largely driven by anthropogenic emissions, which appear to be increasing. Estimates derived from inverse modelling vary, and they suggest that the current annual rates of increase are between 6 and 14 Tg CH_4 yr^{-1} between 2000 and 2012 (Kirschke et al. 2013; Saunois et al. 2016). Observations show that annual rates of increase have varied between 3.84 and 10.30 Tg since 2010 (NOAA/ESRL, www.esrl.noaa.gov/gmd/ccgg/trends_ch4).

Table 0.4.1. Bottom-up and top-down estimates of the components of the global CH_4 budget by source type (Tg CH_4 yr^{-1}) for 2000-2009 and 2012. The numbers in brackets represent the minimum and maximum values in reported studies. The atmospheric annual increase reported is the assumed value for inversions that do not report the global sink.

	Kirschke et al. 2013		**Saunois et al. 2016**			
	2000-2009		2000-2009		2012	
	Bottom Up	Top-down	Bottom-up	Top-down	Bottom-up	Top-down
Natural sources	**347 (238–484)**	**218 (179–273)**	**382 (255–519)**	**234 (194–292)**	**386 (259–532)**	**221 (192–302)**
Natural wetlands	217 (177–284)	175 (142–208)	183 (151–222)	166 (125–204)	187 (155–235)	172 (155–201)
Fresh water	40 (8–73)		122 (60–80)			
Wildlife	15 (15–15)		10 (5–15)			
Termites	11 (2–22)		9 (3–15)			
Wildfires	3 (1–5)		3 (1–5)			
Permafrost	1 (0–1)		1 (0–1)			
Non-land based)	61 (35 – 85)		68 (40–106)			
Anthropogenic sources	**331 (304–368)**	**335 (273–409)**	**338 (329–342)**	**319 (255–357)**	**370 (351–385)**	**347 (262–384)**
Agriculture and waste		209 (180–241)		183 (112–241)		200 (122–213)
Enteric fermentation & manure	101 (98–105)		103 (95–109)		107 (100–112)	
Landfills & waste	63(56–79)		57 (51–61)		60 (54–66)	
Rice cultivation	36 (33–40)		29 (23–35)		29 (25–39)	
Biomass burning	35 (32–39)*	30 (24–45)*	18 (15–20)		17 (13–21)	
Non-land based	96 (85–105)	96 (77–123)	112 (107–126)*	136 (93–179)*	134 (123–141)*	147 (118–188)*
Sinks						
Soils	28 (9–47)	32 (26–42)		32 (27–38)		36 (30–42)
Atmospheric chemical loss	604 (483–738)	518 (510–538)		514		518
TOTALS						
Sum of sources	678 (542–852)	548 (526–569)	719 (583–861)	552 (535–566)	756 (609–916)	568 (542–582)
Sum of sinks	632 (592–	540 (514–		546		555

	785)	560)		
Imbalance (sources−sinks)		8 (−4–19)	6	14
Atmospheric growth rate		6	6.0 (4.9-6.6)	14.0 ()

* Includes biofuel burning

2.4.2.4 Land use effects

There are several datasets that are typically used for tracking emissions for agriculture, forestry and other land use (AFOLU). In Figure 2.4.8 we present national greenhouse gas inventory data, EDGAR (Emissions Database for Global Atmospheric Research) and FAOSTAT (Food and Agriculture Organization Corporate Statistical Database). Whereas there is generally good agreement between these datasets for agriculture (Roman-Cuesta et al. 2016), we can conclude that in the agricultural sector, emissions are higher in non-Annex 1 countries than in Annex 1 countries (*high confidence*). (A fuller discussion of AFOLU will be developed in the SOD as well as a stronger discussion of the differences between datasets)

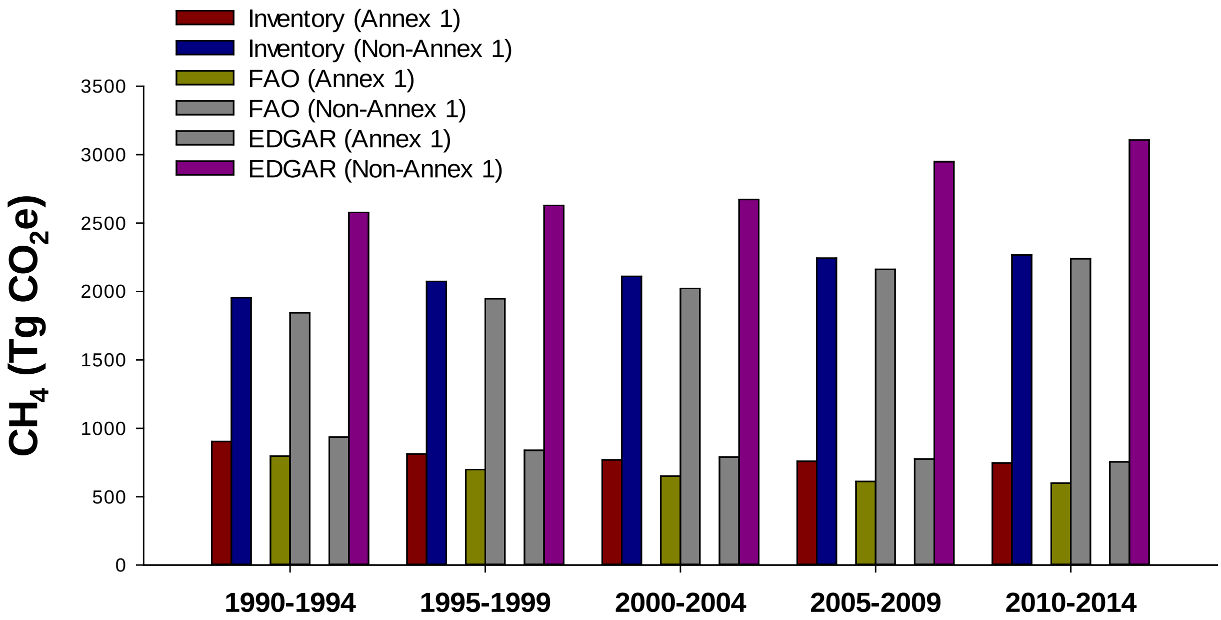

Figure 2.4.8. Agricultural CH_4 emissions for Annex 1 and Non-Annex 1 countries from national GHG inventory data, FAOSTAT (FAO 2015), and EDGAR databases (Janssens-Maenhout et al. 2017).

Agricultural emissions are predominantly from enteric fermentation and rice, with manure management and waste burning contributing small amounts (Figure 2.4.9). Livestock production is responsible for 33% of total global emissions and 66% of agricultural emissions (Source: EDGAR 4.3.2 database, accessed May 2018). Most of the livestock emissions are from developing countries (EDGAR 4.3.2, USEPA, 2013; Tubiello et al. 2014). Asia has the largest livestock emissions (37%) and emissions in the region have been growing by around 2% per year. Africa is responsible for only 14%, but emissions are growing fastest in this region at around 2.5%. In Latin America and the Caribbean, livestock emissions are decreasing at around 1.6% per year and the region makes up 16% of emissions. Developed countries are responsible for about 17% of emissions and these are decreasing by about 1.5% per year. Rice emissions are responsible for about 24% of agricultural emissions, and 89% of these are from Asia. Rice emissions are increasing by 0.9% per year in that region. These trends are predicted to continue through 2030 (USEPA 2013).

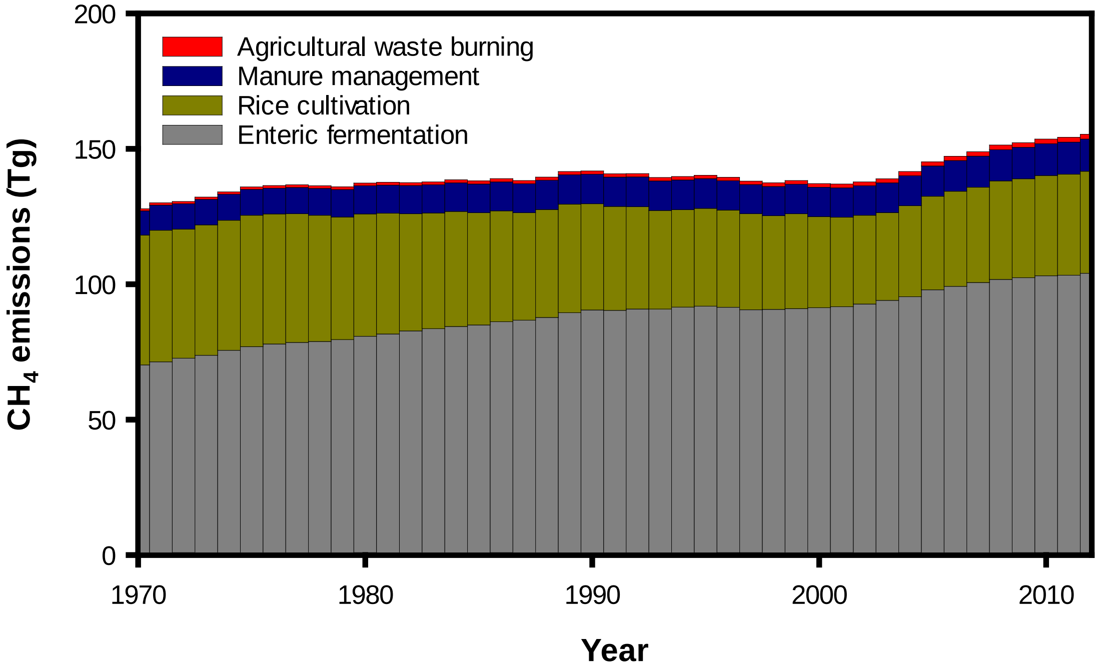

Figure 2.4.9. Agricultural CH_4 emissions between 1970 and 2012. Source: Edgar database 4.3.2.

Upland soils are a net sink of atmospheric CH_4, but soils both produce and consume the gas. The net soil–atmosphere flux is the result of the balance between the two offsetting processes of methanogenesis (microbial production) and methanotrophy (microbial consumption) (Serrano-Silva et al. 2014). Microbial consumption requires aerobic conditions because the biochemical process requires a monooxygenase enzyme. Methanogenesis is the process of microbial production of CH_4 in anaerobic conditions. Methanogenesis is an important process in wetland soils and rice paddies and these systems are usually sources of CH_4 for the atmosphere. However, methanogenesis can also occur in upland soils in anaerobic 'microsites' inside soil aggregates. Methanotrophy is the dominant process in upland soils, where oxidation generally exceeds production. Methanotrophy is also an important process in wetland and rice paddy soils at the oxic soil-water interface and in the rhizosphere, and this limits the amount of CH_4 emitted by these soils. Between 40% and 80% of the CH_4 that diffuses through the oxic zones in soils and sediments is consumed therein (Laanbroek, 2018; Serrano-Silva et al. 2014).

On the global scale climatic zone, soil texture, and land cover have an important effect on CH_4 uptake in upland soils (Tate 2015; Yu et al. 2017; Dutaur and Verchot 2007). Boreal soils take up less than temperate or tropical soils, coarse textured soils take up more CH_4 than medium and fine textured soils, and forests take up more than other ecosystems. Low levels of nitrogen fertilisation can stimulate soil CH_4 uptake, while higher fertilisation rates decrease uptake (Edwards et al. 2018). The effect of N additions is cumulative and repeated fertilisation events have progressively greater suppression effects. Zhuang et al. (2013) estimated that between 1998 and 2004, that N fertilisation suppressed CH_4 oxidation by 26 Tg. Soil CH_4 consumption has been increasing during the second half of the 20th century and it is expected to continue to increase by as much as 1 Tg in the 21st century

Northern peatlands (40°-70°N) constitute a significant source of atmospheric CH_4, emitting about 48 Tg CH_4, or about 10% of the total emissions to the atmosphere (Zhuang et al. 2006; Wuebbles and Hayhoe 2002). CH_4 emissions from natural northern peatlands are highly variable with the highest rate from fen ecosystems. The rate of CH_4 emissions from natural peatlands depends on many factors including water table depth, temperature, vegetation (direct release via vascular plants as well) and other factors. Under the climate change, interactions of these complex factors will be the main determinant of emissions from northern peatlands. However, management of undisturbed peatlands, as well as the restoration of disturbed ones, alter the exchange of CH_4 with the atmosphere. Abdalla et al. (2016) reviewed 87 studies with paired observations on drained and undrained sites and found that on average drainage reduced CH_4 emissions by

84%. They also reviewed 1 sites with restoration by rewetting and found that emissions increased by 46% above pre-drainage levels. Most direct uses of northern peatlands, such as peat extraction, agriculture and forestry require drainage. Lowering the water table usually turns peat soils from CH_4 sources to sinks as a result of reduced methanogenesis in the waterlogged peat and enhanced methanotrophy in the aerated zone of the surface peat (Augustin et al. 2011; Strack and Waddington 2008). Drained peatlands which usually considered as negligible or "zero" methane sources, still emit CH_4 under wet weather conditions and especially in the drainage ditches (Drösler et al. 2013; Sirin et al. 2012), which cover only a small percent of the drained area. In some cases drainage ditch emissions are so high that drained peatlands are comparable to natural one (Sirin et al. 2012; Wilson et al. 2016).

Because of the large uncertainty in the tropical peatland area, estimations of the global flux are highly uncertain. Hergoualc'h and Verchot (2012) conducted a meta-analysis on peat CH_4 fluxes before and after land use change. Conversion of primary forest to rice production increased emissions from 29±10 kg CH_4-C ha^{-1} y^{-1} to 108±60 kg CH_4-C ha^{-1} yr^{-1}. For land uses that required drainage emissions decreased to 9.5+6.1 kg CH_4-C ha^{-1} yr^{-1}. Methane fluxes displayed an exponential response to water table depth changes across all land uses. There are no representative measurements of emissions from drainage ditches in tropical peatlands.

2.4.3 Nitrous Oxide

2.4.3.1 Atmospheric trends

The atmospheric abundance of N_2O has increased since 1750, from a pre-industrial concentration of 270 ppbv to 328 ppbv in 2016 (Dlugokencky 2003) Figure 2.4.10). The rate of increase has also increased, from approximately 0.15 ppbv yr^{-1} 100 years ago, to 0.85 ppbv yr^{-1} over 2001-2015 (Wells et al. 2018). Recent measurements of isotopic N_2O composition ($^{14/15}$N) show a decrease in the δ^{15}N to N_2O ratio over 1940-2005, which confirms that consumption of synthetic nitrogen (N) fertiliser is largely responsible for the observed increase in N_2O concentrations (Park et al. 2012). Increased nitrogen deposition and climate warming have also contributed, particularly since 1980 (Tian et al. 2016a). The increase in atmospheric N_2O concentrations is concerning not only because N_2O is responsible for approximately 6% of global radiative forcing from anthropogenic greenhouse gases; its ozone-depletion potential-weighted emissions of 0.47 Mt CFC-11-equivalent in 2008 outweighs the sum of emissions from all other ozone-depleting substances controlled by the Montreal Protocol (Saikawa et al. 2014). Moreover, as noted in AR5, the long atmospheric lifetime of N_2O (118-131 years) means that atmospheric concentrations would take more than a century to stabilise following the stabilisation of global emissions (Ciais et al. 2013).

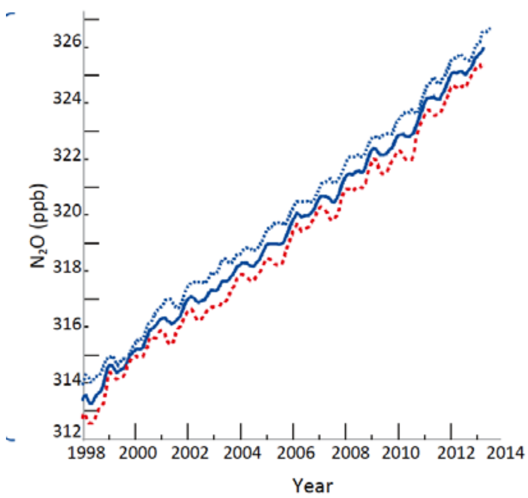

Figure 2.4.10. Global N_2O accumulation (placeholder figure)

2.4.3.2 Global N_2O budget

Recent estimates using inversion modelling and process models estimate total global N_2O emissions of 15.3-17.3 (bottom-up) and 15.9-17.7 Tg N (top-down), demonstrating relatively close agreement (Davidson and Kanter 2014; Wells et al. 2018). Microbial denitrification and nitrification processes are responsible for more than 80% of total global N_2O emissions, which includes natural soils, agriculture, and oceans, with the remainder coming from non-biological sources such as biomass burning and fossil-fuel combustion ((Fowler et al. 2015). A recent development since AR5 is the ability to combine these methodologies using a multi-inversion approach and an ensemble of surface observations to better constrain the regional and temporal distribution of emissions (Saikawa et al. 2014; Wells et al. 2018).

N_2O has both natural and anthropogenic sources (Table 2.4.2). Natural emissions have terrestrial, marine and atmospheric sources. Recent estimates of terrestrial sources suggest a higher and slightly more constrained emissions range than reported in AR5: approximately 9 (7-11) Tg N_2O-N yr^{-1} (Saikawa et al. 2014; Tian et al. 2016b) versus 6.6 (3.3-9.0) Tg N_2O-N $year^{-1}$ (Ciais et al. 2013). Similarly, recent estimates of marine N_2O emissions (2.5 ± 0.8 Tg N_2O-N yr^{-1}; Buitenhuis et al. 2017; 4.6 ± 0.3 Tg N_2O-N yr^{-1}; Saikawa et al. 2014) show a more well constrained range than AR5, although the AR5 estimate (3.8 Tg N_2O-N yr^{-1} with uncertainty bounds of 1.8-9.4 Tg N_2O-N yr^{-1}) is within the range.

Table 2.4.2. N_2O inventories by sector, all units in Tg (Source: Davidson and Kanter, 2014)

	FAO	EDGAR	EPA 2012
Agriculture	4.1	3.8	4.6
Fertiliser	1.4		
Direct	1.1		
Indirect	0.3	3.6	
Manure	1.8		
Direct	1.4	4.2	2.8
Indirect	0.4		
Organic soils	0.2		
Crop residues	0.3		
Manure	0.3	0.2	0.4
Biomass burning		1.1	
Residue burning	0.01		1.6
Other			0.1
Industry, energy and transport		1.7	0.9
Wastewater		0.2	0.2
Solvent and other product use			0.2
Total	11.31	14.8	10.8

Both top-down and bottom-up approaches can differentiate natural from anthropogenic N_2O contributions (Davidson and Kanter 2014). For the top-down analyses, changes in the atmospheric abundance of N_2O from pre-industrial to the present are assumed to be entirely anthropogenic. Natural emissions are assumed to have remained stable over this period (~11 Tg N yr^{-1}) and are subtracted from the total to yield an estimate of anthropogenic emissions. The bottom-up approach uses protocols developed by the IPCC that, in their simplest and most widely applied form, multiply measures of activity in agriculture, energy generation, industry and other sectors by emission factors (EFs) to estimate the N_2O emitted per unit of activity (de

Klein et al. 2014). Recent estimates using both approaches suggest net anthropogenic emissions of approximately 5.3 Tg N_2O-N yr^{-1} (Davidson and Kanter 2014). This estimate also accounts for lower tropical forest soil emissions of approximately 0.9 Tg N_2O-N yr^{-1} as a result of deforestation, both past and present (Davidson 2009)

2.4.3.3 Anthropogenic contributions

Agriculture is the predominant source of anthropogenic N_2O and is responsible for approximately two-thirds of emissions. Recent studies estimate emissions of 4.1 Tg N_2O-N yr^{-1} (3.8-6.8 Tg N_2O-N yr^{-1}; Oenema et al. 2014). Total emissions from this sector are the sum of direct and indirect emissions. Direct emissions from soils are the result of mineral fertiliser and manure application, manure management, deposition of crop residues, cultivation of organic soils and biological nitrogen fixation. Indirect emissions come from downstream and downwind water bodies and soils after nitrate has been leached or nitrogen oxides and ammonia emissions have been deposited back on agricultural land. The main driver of agricultural N_2O emissions (and other agricultural N losses) is a lack of synchronisation between crop N demand and soil N supply, with approximately 50% of N applied to agricultural land not taken up by the crop (Zhang et al. 2017c). Recent findings at regional scales confirm significant increases in agricultural N_2O emissions from the Asian agricultural sector in recent years, likely driven by an increase in synthetic N fertiliser use (Saikawa et al. 2014; Wells et al. 2018)

Agricultural N_2O emissions (and soil N_2O emissions generally; Figure 2.4.11) are characterised by hot spots and hot moments (Groffman et al. 2009) meaning that they are often concentrated in brief periods and small areas where conditions are optimal (e.g. high soil moisture after springtime N application). Since AR5, our understanding of these conditions has improved, particularly with regards to freeze-thaw cycles outside of the growing season. Between 35% and 65% of total annual N_2O emissions from terrestrial sources may result from thaw-related fluxes, as a result of increased substrate availability, changes in denitrifying enzymes, and the release of previously produced N_2O. Neglecting these emissions could lead to an underestimation of global agricultural N_2O emissions by 17%-28% (Wagner-Riddle et al. 2017). (Note: A fuller discussion of AFOLU will be developed in the SOD as well as a stronger discussion of the differences between datasets)

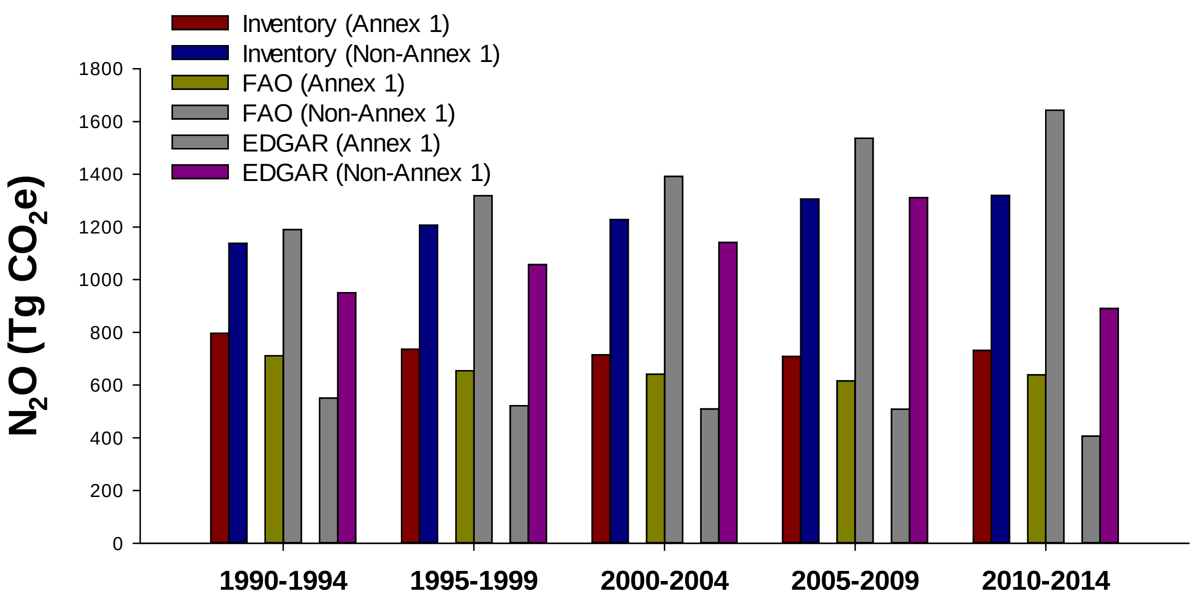

Figure 2.4.11. Agricultural N_2O emissions for Annex 1 and Non-Annex 1 countries from national GHG inventory data, FAOSTAT, and EDGAR databases.

Industry and fossil fuel combustion is the largest non-agricultural source of anthropogenic N_2O emissions, responsible for approximately 0.9 Tg N_2O-N yr^{-1} (3.8-6.8 Tg N_2O-N yr^{-1}) or 15% of total gross anthropogenic N_2O emissions (Wiesen et al. 2013). Nitric and adipic acid production are the major industrial sources, while stationary combustion (mainly from coal power plants) is the energy sector's main source. In both cases N_2O emissions are the result of the oxidation of atmospheric N_2 and organic N in fossil fuels. Biomass burning (see Box) is responsible for approximately 0.7 Tg N_2O-N yr^{-1} (0.5-1.7 Tg N_2O-N yr^{-1}) or 11% of total gross anthropogenic emissions due to the release of N_2O from the oxidation of organic N in biomass (van der Werf et al. 2013) . This source includes crop residue burning, forest fires, household cook stoves, and prescribed savannah, pasture and cropland burning. Emissions from wastewater are approximately 0.2 Tg N_2O-N $year^{-1}$ or 3% of total gross anthropogenic emissions, emitted either directly from wastewater or wastewater management facilities (Bouwman et al. 2013). Aquaculture, while currently responsible for less than 0.1 Tg N_2O-N yr^{-1}, is one of the fastest growing sources of anthropogenic N_2O emissions (Williams and Crutzen, 2010; (Bouwman et al. 2013). Finally, increased N deposition onto the ocean is estimated to have increased the oceanic N_2O source by 0.2 Tg N_2O-N yr^{-1} or 3% of total gross anthropogenic emissions (Suntharalingam et al. 2012).

2.4.3.4 Uncertainties

Studies since AR5 highlight two major uncertainties in the estimation of anthropogenic N_2O emissions using bottom-up methods, particularly from the agricultural sector: emission factors and indirect emissions. First, the Tier 1 EFs assume a linear relationship between N application rates and N_2O emissions, with a 1% EF applied to synthetic N fertiliser rates to estimate direct emissions. However, recent studies are increasingly finding nonlinear relationships, suggesting that N_2O emissions per hectare are lower than the Tier 1 EFs at low N application rates, and higher at high N application rates – likely due to the greater excess N unused by crops, which is then available to be emitted as N_2O (Shcherbak et al. 2014; Satria 2017). For example, applying the IPCC Tier 1 EF to a 50 kg N ha^{-1} reduction in N application rate would generate an estimated reduction in N_2O emissions of 0.5 kg N_2O-N ha^{-1}, regardless of the initial application rate. However, using a non-linear EF for upland grain crops derived via meta-analysis, a reduction from 50 kg N ha^{-1} to zero would reduce emissions by 0.37 kg N_2O-N ha^{-1}, while a reduction from 300 kg N ha^{-1} to 250 kg N ha^{-1} would reduce emissions by 0.84 kg N_2O-N ha^{-1}, suggesting greater mitigation potential in regions with higher N application rates. This not only has implications for how agricultural N_2O emissions are estimated in national and regional inventories, it also suggests that in regions of the world where low N application rates dominate, such as sub-Saharan Africa and parts of Eastern Europe, relatively large increases in N fertiliser use would generate relatively small increases in agricultural N_2O emissions. Other factors that impact EF magnitude include crop and fertiliser type, soil carbon, pH, mean annual temperatures, and organic amendment type (Charles et al. 2017; Shcherbak et al. 2014). Nevertheless, there is evidence that errors in emission estimates from applying the Tier 1 EF at small scales are largely cancelled when aggregated to larger scales (Del Grosso et al. 2010).

The second major uncertainty in estimating agricultural N_2O emissions comes from indirect emissions. Recent studies suggest that the Tier 1 EFs are low, especially the 0.75% EF for indirect N_2O from leached nitrate. One study in the U.S. Corn Belt estimates an EF closer to 2% and emissions are highly dependent on stream hierarchy, which would imply an underestimation of current indirect emissions of up to nine fold and translate to a total underestimation of agricultural N_2O emissions in the region of up to 40% (Turner et al. 2015). The gap between estimated and actual EFs will become increasingly important in a changing climate, as described below.

2.4.3.5 Future trends in CO_2, CH_4 and N_2O flux due to climate change

Climate change is expected to impact the key terrestrial biogeochemical cycles, via an array of complex feedback mechanisms that will act to either enhance or decrease future CO_2, CH_4 and N_2O emissions (described in Section 2.2 and 2.3). The balance of these positive and negative feedbacks remains uncertain. Estimations from climate models included in AR5, CMIP5 and C^4MIP exhibit large differences for the different carbon and nitrogen cycle feedbacks and how they change in a warming climate (Anav et al. 2013;

Friedlingstein et al. 2006; Friedlingstein et al. 2014). The differences are in large part due to the uncertainty regarding how primary productivity will evolve, with many of the models not even agreeing on the sign of change. Furthermore, many models do not include a nitrogen cycle, which limits the CO_2 fertilisation effect. These uncertainties are further exacerbated by the lack of observational constraints (Prentice et al. 2015a).

The CO_2 fertilisation effect is expected to increase CO_2 uptake, which in addition to a decrease in stomatal conductance may drive an increase in productivity and consequent greening effect. However, given that plant biomass has fixed C:N ratios (which vary by plant and soil type), the magnitude and persistence of the CO_2 fertilisation effect depends on the availability of mineral N and the ability of plants to acquire it. N limitation, particularly in natural ecosystems, is a key limiting factor on C storage capacity, which is not yet well represented in many Earth System models (Zaehle et al. 2015). Similarly, CO_2 fertilisation is likely to be limited by an upper limit to the efficiency of photosynthesis (Heimann and Reichstein, 2008). In contrast, increased temperature may encourage greater microbial decomposition and greater CO_2 release from soils (Heimann and Reichstein, 2008), in addition to enhanced degradation of permafrost and wetland ecosystems. The shift in vegetation distribution due to climate change may also impact the carbon and nitrogen cycles.

The future of the CH_4 budget will depend in large part on changes in the atmospheric OH sink. Methane trajectories in AR5 were based on calculations of the MAGICC model that accounted for changes in the OH sink, anthropogenic CO emissions, NO_x, VOCs, temperature, and the negative feedback of increasing CH_4 concentrations on OH (Meinshausen et al. 2011). A more recent analysis based on three chemical transport models showed that atmospheric lifetime of CH_4 is likely to increase through about 2070 and decrease slightly thereafter (Holmes et al. 2013). While the trajectory is similar to that in AR5, the atmospheric lifetime is predicted to be approximately one year shorter in the new analysis. Sensitivity analyses of the models lead to an upward revision in the 100-yr GWP estimate to 32. This study assumes that all other sinks remain constant, but other analyses suggest that increased atmospheric abundance will also increase the global soil sink. Similar results were found in simulations performed for the Atmospheric Chemistry and Climate Modeling Intercomparison Project (ACCMIP) (Voulgarakis et al. 2013). Mean tropospheric lifetime for the year 2000 was estimated to be 9.8±1.6 yr^{-1}, which was lower than AR5 estimates. Future projections were made using the four Representative Concentration Pathways (RCPs). Decreases in global methane lifetime of 4.5±9.1% were projected for RCP 2.6, the scenario with lowest radiative forcing by 2100. Simulation with the high radiative forcing RCP8.5 produced increases of 8.5±10.4%. In this latter scenario, atmospheric CH_4 concentration was the key driver of the evolution of OH and methane lifetime because CH_4 concentration more than doubled by 2100, which resulted in significantly greater consumption of atmospheric OH.

Climate change is expected to impact N_2O emissions in several ways. Warmer and wetter conditions will enhance the conditions for soil N_2O emissions, acting as a positive feedback to climate change. These conditions have already led to indirect N_2O emissions dominating interannual variability of total emissions (Griffis et al. 2017). Changes in soil moisture driven by changes in precipitation patterns and totals as well as evapotranspiration fluxes will likely dominate the N_2O response to climate change, overshadowing the direct temperature effects on denitrification and nitrification (Fowler et al. 2015). Indeed, changes in precipitation alone are projected to increase total N loading to rivers by 19% within the continental United States by the end of this century, with important implications for indirect N_2O emissions. Offsetting this increase would require a 33% reduction in N application rates (Sinha et al. 2017) A similar dynamic is expected in regions with high N consumption and projected increases in precipitation, such as China, India, and Southeast Asia. However, N_2O emissions are not expected to increase proportionally with N loading, especially as a river becomes N saturated due to an inverse relationship between N loading and removal efficiency, with a doubling in nitrate concentrations estimated to increase N_2O emissions by 40% (Mulholland et al. 2008; Turner et al. 2015) Climate change is also expected to cause changes in land use and management, which will likely impact terrestrial biogeochemical cycles. An increase in the area of irrigated agricultural land could stimulate N_2O emissions increases of 50%-150%, likely a result of increased denitrification activity (Trost et al. 2013; Fowler et al. 2015) .

Analysis by Prentice et al. (2015b) that looked specifically at the land CO_2 feedbacks in the CMIP5 and C^4MIP models under a range of scenarios indicate that the negative feedbacks associated with increased productivity outweighs the positive feedbacks throughout the 21st century. Arneth et al. (2010) came to a similar conclusion, showing that the feedback range for CO_2 fertilisation was between -0.17 to -1.9 Wm^{-2} compared to 0.1 to 0.9 for the positive feedbacks. In both studies however, the inclusion of the nitrogen cycle reduces this CO_2 fertilisation effect significantly due to nutrient limitations. Arneth et al. (2010) showed that the negative feedbacks decreased to -0.4 to -0.8 Wm^{-2}, which for some models removes the net carbon loss completely. Similarly, when including the feedbacks associated with methane, fire and ozone, the total radiative forcing between the atmosphere and terrestrial biosphere was positive, ranging between 0.9 to 1.5 $Wm^{-2} K^{-1}$ at the end of the 21st Century. Other studies suggest that the cumulative warming effect of methane (CH_4) and N_2O emissions over the period 2001-2010 was a factor of two larger than the cooling effect that resulted from CO_2 fertilisation (Tian et al. 2016a), suggesting that mitigation efforts should be as focused on reducing emissions of these non-CO_2 GHGs as on increasing carbon storage capacity. Nevertheless, studies highlight the uncertainty in carbon-cycle estimates from ESMs and the need for more realistic carbon and nutrient cycling in models.

Permafrost and wetlands

A warming climate and conversion of the land surface can influence permafrost and wetland ecosystems. Thawing permafrost and degradation of wetlands is expected to increase atmospheric greenhouse gases and act as a positive feedback. Although current wetland methane emissions remain uncertain, they may account for up to 40% of total global methane emissions (Saunois et al., 2016), and for much of annual variability (McNorton et al., 2016). A warming climate may act to enhance this release, with modelling studies indicating a 78% increase in wetland emissions for a doubling of CO_2 (Ciais, 2013).

High latitude permafrost stores a significant quantity of carbon that can be released in a warming climate via the exposure of long-protected (i.e. frozen) organic matter to decay. (Burke et al., 2018; Burke et al., 2017; Schuur et al., 2015; von Deimling et al., 2015). Under the 2°C warming target, the extent of permafrost has been estimated to decrease by up to 40% (Chadburn et al., 2017), and under RCP2.6 contribute between 4% to 18% of the global temperature anomaly (Burke et al., 2017). However significant uncertainty remains regarding the consequent extent of greenhouse gas emissions (e.g., (Davies-Barnard et al. 2015; Schneck et al. 2015; Crowther et al. 2016b; Schuur et al. 2015) estimated that 130-160 Pg C would be released by 2100 as a result of the thawing permafrost. However, other studies show that an increase in vegetation productivity might offset permafrost emissions to some degree (Koven et al. 2015; Abbott et al. 2016)

The emissions from ecosystems such as peatlands and wetlands are countered by the size of the vegetation carbon sink. The time at which emissions exceed the sink remains uncertain; some models indicate that it is already happening (Hayes et al. 2014; Mauritz et al. 2017) some that it will happen later this century (Lawrence and Vandecar 2015a), and some that it will happen between 2100 and 2200 (McGuire et al. 2016) The latter model showed substantial declines in the accumulation of stored carbon by 2100 in Alaska (but not substantial releases). Other key uncertainties in projecting the rate of release include the interactions of permafrost with fire, thermokarst, decomposability of newly exposed permafrost soil (including its response to temperature and the impacts of unfrozen water), and changes in hydrology.

Impacts of mitigation on carbon sinks

Under future low emission levels and large negative emissions, the global land and ocean sinks are expected to weaken (or even reverse) (Jones et al. 2016). Carbon today absorbed by the oceans following increases in atmospheric CO_2 concentration will partially be released back to the air when concentration declines (Cao and Caldeira, 2010; Ciais et al. 2013; Jones et al. 2016). This means that to maintain atmospheric CO_2 and temperature at low levels, both the excess CO_2 from the atmosphere and the CO_2 progressively outgassed from the ocean and land sinks need to be removed (Cao and Caldeira, 2010). This outgassing from the land and ocean sinks is called the "rebound effect" of the global carbon cycle (Ciais et al. 2013). It will reduce the effectiveness of negative emissions and increase the deployment level needed to achieve a climate stabilisation target (Jackson et al. 2017; Jones et al. 2016). *(add text to link to SR1.5 when published)*

Table 2.4.3. Emissions and removals summary from land use aggregated from 2003 to 2012. Values in bold were used to calculate total-land use emissions.

Land use emissions	Gtonnes CO_2(e)
Land use CO_2	
Bookkeeping model average (H&N, Blue)*	**4.69**
DGVM average	4.75
FAOSTAT	3.09
Non-CO_2 GHGs	
Agricultural CH_4	
FAOSTAT	2.78
USEPA	3.02
EDGAR	3.72
Average	**3.17**
Agricultural N_2O	
FAOSTAT	2.17
USEPA	2.76
EDGAR	1.82
Average	**2.25**
Total emissions (2003 to 2012) from land use	**10.12**
Total anthropogenic emissions (2003 to 2012) from all sources†	42.07
Land use emissions : Total emissions	**24%**

* Data sources: Hansis et al. 2015; Houghton & Nassikas 2017.
† Total anthropogenic emissions were calculated using CDIAC values for fossil fuel, cement and flaring emissions from the 2016 budget (http://cdiac.ess-dive.lbl.gov/GCP/carbonbudget/2016/) and the land use emissions calculated here.

We calculated the contribution of land use emissions to total anthropogenic emissions over the decade 2003 to 2012 (Table 2.3.4) using several global datasets. The non-CO_2 GHG data available in EDGAR do not yet extend beyond 2012. We calculated emissions over the decade to account for inter-annual variability due to ENSO and other sources of variability. We note that land use CO_2 emissions values in FAOSTAT, which included emissions from organic soils, are lower than those of both the book keeping models and the DGVMs. To calculate total land use emissions we combined the average emissions from the book keeping models with the average non-CO_2 GHG data from the different data sources and we calculated total anthropogenic emissions using CDIAC data for non-land use emissions. Similarly to AR5, we find that global land use emissions are 24% of total anthropogenic emissions (*high confidence*), with slightly more than half these emissions coming as non-CO_2 GHGs from agriculture. Since publication of the IPCC Fourth Assessment Report (AR4), land use emissions have remained relatively constant; however, the share of land use in anthropogenic emissions has decreased due to increases in emissions in the energy sector. Increasing non-CO_2 emissions in non-Annex I countries may be offsetting decreases in deforestation emissions (placeholder: this will be developed more fully in the SOD).

2.5 Historical and future non-GHGs fluxes and precursors of short-lived species from unmanaged and managed land

While the atmospheric concentration of greenhouse gases is the largest factor affecting modern climate, the levels of atmospheric aerosol particles (diameters between about 0.002 μm to about 100 μm), can significantly modulate regional climate and are considered in mitigation strategies (Rogelj et al. 2014; Kok et al. 2018) . While there was a progress in quantifying regional emissions of anthropogenic and natural land aerosols, considerable uncertainty still remains about their historical trends, their inter-annual and decadal variability and about any changes in the future (Calvo et al. 2013).

Depending on the chemical composition and size, aerosols can absorb or scatter sunlight and thus directly affect amount of absorbed and scatted radiation. In the troposphere, aerosols can affect clouds formation and development, and thus change precipitation. In addition, deposition of aerosols has implication for surface reflectance, particularly snow, and biogeochemical cycling such as nitrogen and phosphorus deposition. Primary land atmospheric aerosols are emitted directly into the atmosphere due to natural or anthropogenic processes and include mineral aerosols (or dust), volcanic dust, smoke and soot from combustion, several organic compounds. Secondary atmospheric aerosols (not discussed here) are particulates that formed in the atmosphere by gas-to-particles conversion processes from land emissions (Hodzic et al. 2016; Manish et al. 2017)

2.5.1 Temporal trends, spatial patterns, and variability

Mineral dust

One of the most abundant atmospheric aerosols is mineral dust, which is emitted into the atmosphere from arid and semi-arid regions and then transported over long distances across continents and oceans (Ginoux et al. 2001). Depending on the dust mineralogy and size, dust particles can absorb or scatter shortwave and long-wave radiation. Dust particles served as cloud and ice condensation nuclei and modulate the optical properties of clouds and the rate of precipitation. In addition, dust particles have shown to alter the cloud cover through changes in evaporation of cloud droplets (i.e. the cloud burning effect) (Boucher et al. 2013) New and improved understanding of processes controlling emissions and transport of dust, its regional patterns and variability as well as its chemical composition has been developed since AR5 *(robust evidence, high agreement).*

Characterisation of spatial and temporal distribution of dust emissions is essential for weather prediction and climate projections *(robust evidence, high agreement).* Satellite observations have been the most effective way of identifying and quantifying regional dust sources, which were initially derived by analysing Aerosol Index (AI) or Aerosol Optical Thickness (AOT) (e.g. from the Total Ozone Mapping Spectrometer (TOMS) the Moderate Resolution Imaging Spectroradiometer (MODIS), the Ozone Monitoring Instrument (OMI), the Multi-angle Imaging Spectroradiometer (MISR). The AI/AOT approach is relying on optical methods that typically measure column-integrated quantities during daytime and is unable to distinguish newly released dust from previously released long range transported dust (Kocha et al. 2013). The infrared-based method (e.g. Infrared Atmospheric Sounder Interferometer (IASI) improves the ability to capture dust sources at night, however has biases in the boundary layer measurements.

The new 'dust source activation' (DSA) frequency method was developed and applied over the Sahara desert by analysing output from the Spinning and Enhanced Visible and Infrared Imager (SEVIRI) sensor on the geostationary Meteosat Second Generation (MSG) satellites (Ashpole and Washington 2013; Ian and Richard 2013)). Characterisation of dust emission further improved with analysis of aerosol vertical profiles from the Cloud-Aerosol Lidar with Orthogonal Polarization (CALIOP) instrument on board the Cloud-Aerosol Lidar and Infrared Pathfinder Satellite Observation (CALIPSO) satellite (Todd and Cavazos-Guerra 2016), enabling detection of night-time emissions and the overall diurnal cycles, peaking in the mid-mornings. The Dust Emission Index derived from the CALIOP time series shows that the highest emissions over Sahara occur during June-September over a more restricted area, than AOT/AI estimates previously indicated, with the night-time emission, driven by convective cold pools, exceeding the day-time emissions. The highest emissions are occurring between 5W-10E and 16N-24N, to the south and southwest of the main Saharan mountains. Although there is a growing confidence in characterising the seasonality and peak dust emissions (i.e. spring-summer, (Wang et al. 2015) and how the meteorological and soil conditions control dust sources, an understanding of long-term future dust dynamics, inter-annual dust variability and how they will affect future climate still requires work.

While satellites remain the primary source of information about the dust distribution in the atmosphere and are used to derive emissions of dust, new surface observations improve process understanding and reduce uncertainty about optical and mineralogical properties of the dust (Rocha-Lima et al. 2018). Dust particles include several minerals with different physical and chemical properties, which affect how dust interacts with radiation and hydrological cycle. Mineralogy of dust is strongly linked to mineralogy of soils where dust is emitted. New global databases were developed to characterise mineralogical composition of soils for use in the weather and climate models (Journet et al. 2014; Perlwitz et al. 2015) New field campaigns as well as new analysis from prior campaign have produce accurate characterisation of optical properties and insights into role of dust in climate system: i) the SHADOW (study of SaHAran Dust Over West Africa) campaign at the IRD (Institute for Research and Development) in Mbour, Senegal (14◦ N, 17◦ W) in March–April 2015 (Veselovskii et al. 2016); ii) the SALTRACE (Saharan Aerosol Long-range Transport and Aerosol-Cloud interaction Experiment) in Barbados, June and July 2013, to characterise long-range transported transport of Saharan Dust across the Atlantic Ocean (Groß et al. 2015), ii) the UK Ice in dust clouds experiment took place in Cape Verde, August of 2015, to characterise aerosol particles and their ability to act as ice nuclei (IN) and cloud condensation nuclei (CCN) within convective and layered clouds (Price et al. 2018).

Carbonaceous Aerosols

Carbonaceous aerosols are one of the most abundant components of particles in the continental areas of the global atmosphere. It can comprise about 60 to 80% of PM1 in urban and remote atmosphere. It comprises of an organic fraction (Organic Carbon-OC) and a refractory light absorbing component, generally referred as Elemental Carbon (EC). Organic carbon (OC) is a major component of aerosol mass concentration, and it originates from different anthropogenic (combustion processes) and natural (biogenic emissions) sources (Robinson et al. 2007). A large fraction of OC in the atmosphere has a secondary origin, since OC can be both primarily emitted but also formed in the atmosphere through condensation to the aerosol phase of low vapour pressure compounds emitted as primary pollutants or formed in the atmosphere. Organic carbon is also characterised by a high solubility with a high fraction of water soluble organic aerosol (WSOA) and it is one of the main drivers of the oxidative potential of atmospheric particles. This makes OC an efficient CCN in most of the conditions (Pöhlker et al. 2016; Thalman et al. 2017). In terms of radiative effects and optical properties, organic carbon is important for the scattering properties of aerosols and EC is important for the absorption component (Tsigaridis et al. 2014; Fuzzi et al. 2015). A third components is the so-called brown carbon (BrC) that has assumed an increasing importance because this organic material shows enhanced absorption at short wavelengths. As it absorbs solar radiation at shorter wavelengths and scatters in the red region giving a brown colour (Liu et al. 2016b; Bond et al. 2013).

Biomass burning is a major global source of carbonaceous aerosols (Bowman et al. 2011; Harrison et al.

2010; Reddington et al. 2016) As knowledge of past fire dynamics improved through new satellite observations, new fire proxies' datasets (Marlon et al. 2013), and process-based models, a new historic biomass burning emissions dataset starting in 1750 has been developed (Van Marle et al. 2017). OC emissions (Van Marle et al. 2017) show in general more variability and smaller trends than emissions developed by (Lamarque et al. 2010) for CMIP5.

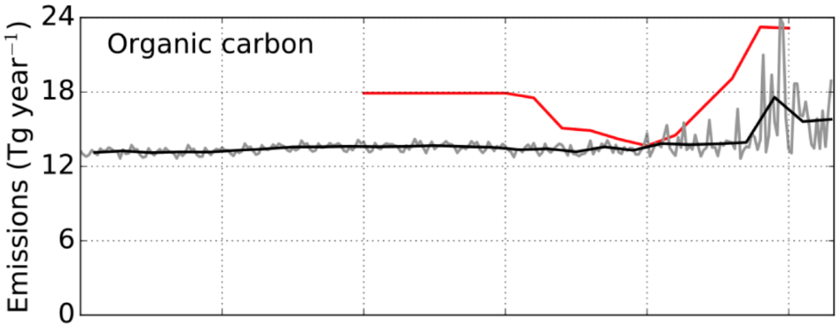

Figure 2.5.1 Total global biomass burning emissions for organic carbon estimated by (Lamarque et al. 2010), in red, developed for CMIP5 and (Van Marle et al. 2017), in black, developed for CMIP6 on annual and decadal time steps.

Previous emission inventories of BC were mostly obtained in a bottom-up framework (Jacobson 2012; Wang et al. 2014a)), an approach that derives emissions based on categorised emitting sources and emission factors used to convert burning mass to emissions. (Bond et al. 2013) estimated that at pre-industrial time (around 1750s) emission from biofuel and biomass burning were approximately 1400 Gg of black carbon per year. Although it's not clear how much of such discrepancy is related to the underestimates of biomass burning BC. (Wang et al. 2014a) estimated a substantial contribution of agricultural fires and wildfires to BC emissions for 1960 to 2007 period.

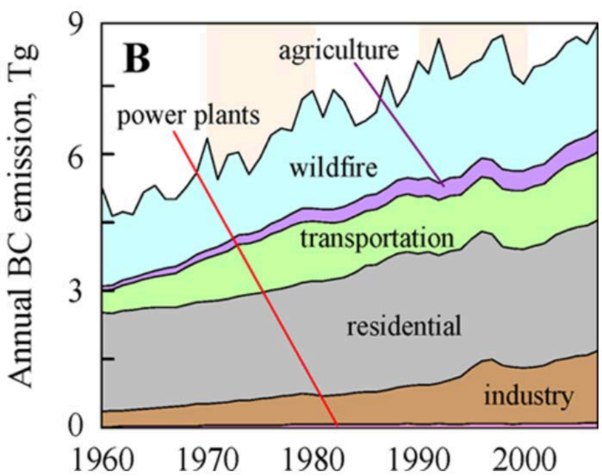

Figure 2.5.2 Global temporal trends of annual BC emissions (B) in various sectors, from Wang 2014.

A top-down total (biomass burning, fossil fuel consumption, etc.) global estimate of BC emission17.8 ± 5.6 Tg/yr was obtained using a fully coupled climate-aerosol-urban model constrained by aerosol absorption optical depth and surface concentrations from global and regional networks (Cohen and Wang 2014). Cohen and Wang 2014 estimate is a factor of 2 higher than previous estimates (e.g. 7.662-8.800, (Bond et al. 2007;

Van Der Werf et al. 2010b)), with considerably higher BC emissions for Eastern Europe, Southern East Asia, and Southeast Asia mostly due to higher anthropogenic BC emissions.

(Giglio et al. 2013) found a gradual fire area decrease of 1.7 Mha /yr (–1.4% yr^{-1}) in Northern Hemisphere Africa since 2000, a gradual increase of 2.3 Mha yr^{-1} (+1.8% yr^{-1}) in Southern Hemisphere Africa also since 2000, a slight increase of 0.2 Mha yr^{-1} (+2.5% yr^{-1}) in Southeast Asia since 1997, and a rapid decrease of approximately 5.5 Mha yr^{-1} (-10.7% yr^{-1}) from 2001 through 2011 in Australia, followed by a major upsurge in 2011 that exceeded the annual area burned in at least the previous 14 years. The net trend in global burned area from 2000 to 2012 was a modest decrease of 4.3 Mha yr^{-1} (-1.2% yr^{-1}).

Biogenic Volatile Organic compounds (BVOCs)

Plants emit a substantial amount of biogenic volatile organic compounds (BVOCs) into the atmosphere including isoprene, terpenes, alkanes, alkenes, alcohols, esters, carbonyls and acids (Peñuelas and Staudt 2010). These BVOCs emissions represent a carbon loss to the ecosystem; their emission can represent up to 10% of the carbon fixed by photosynthesis under stressful conditions. The global average for vegetated surfaces is 0.7g C m^{-2} yr^{-1} but could exceed 100 g m^{-2} per year in some tropical ecosystems (Peñuelas and Llusià 2003). These BVOC emissions strongly depend on temperature. We know that, in the short term at least, a rise in temperature exponentially increases the emission rates of most BVOCs (Peñuelas and Llusià 2003). It does so not only by enhancing the enzymatic activities of synthesis but also by raising the BVOCs vapour pressure and by decreasing the resistance of the diffusion pathway. BVOC emissions are thus expected to increase sharply as global temperatures rise *(moderate evidence, high agreement)*.

By applying the most frequently used algorithms of emission response to temperature, it can be estimated that climate warming over the past 30 years could have already increased BVOC global emissions by 10% since the preindustrial times. A further 2-3^{o} C rise in the mean global temperature, which is predicted to occur during this century (IPCC 2013) could increase BVOC global emissions by an additional 30-45% (Peñuelas and Llusià 2003). Furthermore, global warming in boreal and temperate environments not only means warmer average and warmer winter temperatures but also implies an extended plant activity season (Peñuelas 2009) increasing total annual emissions even further. Other results, however, suggest that previous regional model inventories based on one fixed emission factor probably overestimate regional emissions, and species-specific expressions of seasonality in temperature response can be necessary (Kreuzwieser et al. 2002). There is, moreover, a lack of precise and complete data on the effects of all the other global change components such as land use changes or global fertilisation with increasing CO_2 and N inputs, but everything seems to indicate that the most likely overall effect will be to increase BVOC emissions (Peñuelas and Staudt 2010). BVOC are the most important precursors of secondary organic aerosols, via oxidation and chemical processes. Isoprene, terpenes and sesquiterpenes are the most important BVOCs in terms of aerosol particle production. The SOA over boreal and tropical forests are mostly originated from BVOC emissions(Manish et al. 2017). The same with cloud condensation nuclei, making a strong link between BVOC emissions by plants and climate/hydrological cycle-(Fuentes et al. 2000).

2.5.2 Dust, BVOC and carbonaceous aerosols in Coupled Climate and Earth System Models

Coupled Model Intercomparison Project, phase 5 (CMIP5, Taylor) included a number of models with representation of aerosol emission, transport, and deposition. Such models either specify emissions of short-lived gases into their atmospheric components or had prognostic capabilities for some precursors such as dust. Since CMIP5 a number of coupled and atmospheric modelling studies included prognostic emissions for dust, carbonaceous aerosols, and BVOC. Earth System Models (ESM) have difficulties in properly model BVOCs and SOA production. Actually all CMIP5-class ESM did not include explicitly SOA formation, due to the chemical complexity and diversity of process that depends heavily on land use (Arneth et al. 2011). BVOC emissions are very sensitive to temperature and radiation fields, and models such as MEGAN version 2.1 (Model of Emissions of Gases and Aerosols from Nature) (Guenther et al. 2012) been incorporated in the

Community Land Model version 4 (CLM4), but they are too computationally intensive to be included in ESM. MEGAN take into account about 150 specific compounds that are still a fraction of ecosystem and climatic relevant BVOCs (Isaacman-Vanwertz et al. 2018; Park et al. 2013).

Analysis of the 23 CMIP5 models reveals that all models systematically under-estimate dust emissions, amount of dust in the atmosphere and its inter-annual variability (Evan et al. 2014). The vertically integrated mass of atmospheric dust per unit area (i.e. mean dust mass path DMP, g m^{-2}) , obtained from the advanced very high resolution radiometer (AVHRR) (Stowe et al. 2002) for 1982-2004 and the Moderate Resolution Imaging Spectroradiometer (MODIS) (Remer et al. 2005)Terra instrument for 2000–2013 was approximately 0.6 to 1.0 g m^{-2}, while the 23 CMIP models range for DMP was only 0.05 to 0.46 g m^{-2} (Evan et al. 2014). The relationship between CMIP5 multi-model DMP and total northern Africa emissions implies that the AVHRR- and MODIS-based dust emissions are 3 times as high as those used in the models, i.e. 4500 ± 1500 Tg yr^{-1} (Evan et al. 2014). General circulation models (GCMs) typically do not reproduce inter-annual and longer time scales variability seen in observations (Evan et al. 2016).

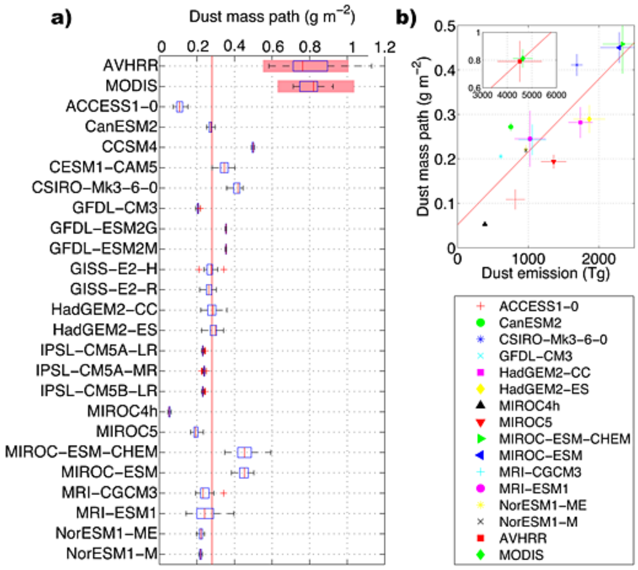

Figure 2.5.3 Comparison of modelled and remotely sensed dust mass paths and emissions, from Evan et al 2014.

2.5.3 Contribution of non-GHG fluxes from managed and unmanaged lands to atmospheric composition and climate

Mineral dust

Usually mineral dust is considered as a "natural" aerosol as it is produced by wind over dry regions with low-density vegetation; although soil and vegetation cover could be altered by human land use land cover changes or agricultural practices. (Stanelle et al. 2014) used a global climate-aerosol model and found that global annual dust emissions have increased by 25% from preindustrial to present day (e.g., from 729 Tgyr^{-1} to 912 Tg yr^{-1}) with 56% increase driven by climate change and 40% by land use cover change such as conversion of natural lands to agriculture. Approximately 10% of present day dust emissions originate from agricultural regions.

In North Africa most dust is of natural origin with 15% increase in dust emissions attributed to climate change. In North America two thirds of dust emissions take place on agricultural lands and both climate change and land use change jointly drive the increase. In Australia land use is the primary driver of increase in dust emissions due to the biogeophysical feedbacks. Between pre-industrial and present-day the overall effect of changes in dust is - 0.14 Wm^{-2} cooling of clear sky net radiative forcing on top of the atmosphere, with -0.05 W m^{-2} form land use and -0.083 W m^{-2} from changes in climate.

The observed decreasing trends in Sahel dust emissions and transport has been attributed to reduction in surface winds primarily due to increased vegetation surface roughness ("stilling" effect) with secondary effects form changes in turbulence and evapotranspiration, and changes large-scale circulation (Cowie et al. 2013). Similarly the observed decreasing trends in dust storms in Northeast Asia since the 1950s, with the exception of beginning of the 21st century, has been attributed to surface wind stilling. In addition, analysis of relationship of vegetation green-up dates derived from the satellite observation and dust storms from 1982 to 2008 over Inner Mongolia, Northern China showed a significant dampening effect of earlier spring greening on dust storms (r = 0.49, p = 0.01), with a one-day earlier green-up date corresponding to a decrease in annual spring dust storm outbreaks by 3%.

One commonly suggested reason for the lack of dust variability in climate models is the models' inability to simulate the effects of land surface changes on dust emission (Stanelle et al. 2014). There has been progress in incorporating effects of vegetation, soil moisture, surface wind and vegetation on dust emission source functions and show more agreement with the satellite observations both in terms of AOD and DMP (Kok et al. 2014). New prognostic dust emissions models now able to account for both changes in surface winds and vegetation characteristics (e.g. leaf area index and steam area index) and soil water, ice, and snow cover (Evans et al. 2016). As a result, the new modelling studies (e.g. Evans et al. 2016) indicate that in regions where soil and vegetation respond strongly to ENSO events, such as in Australia, inclusion of dynamic vegetation characteristics into dust emission parameterisations improves comparisons between the modelled and observed relationship long-term climate variability (e.g. ENSO) and dust levels (Evans et al. 2016).

While inter-annual climate variability, particularly precipitation, often is the primary driver of regional dust variability, changes in the dust radiative forcing induce climate feedbacks that affect regional precipitation, as it been illustrated for the summer precipitation during the 2000–2009 over southern India (Solmon et al. 2015).

Carbonaceous aerosols

Carbonaceous aerosols are important in urban areas as well as pristine continental regions. In boreal and tropical forests, OC originates from BVOC oxidation, being isoprene and terpenes the most important precursors (Claeys et al. 2004). In particular, isoprene epoxydiol-derived secondary organic aerosol (IEPOX-SOA) is being identified in recent studies in North America and Amazonian forest as a major component in the oxidation of isoprene. The largest global source of BC aerosols is open burning of forests, savannah and agricultural lands with about 2700 Gg yr^{-1} in the year 2000 (Bond et al. 2013).

Land use change is critically important for carbonaceous aerosols, since biomass burning emissions consist mostly of organic aerosol. Additionally, urban aerosols are also mostly carbonaceous, because of the source composition (traffic, combustion, industry, etc.). Burning of fossil fuel, biomass burning emissions and SOA from natural BVOC emissions are the main global sources of carbonaceous aerosols. Any change in each of these components in a future climate will influence directly the radiative forcing (Boucher et al. 2013).

BVOCs

BVOCs' possible climate effects have received little attention because it was thought that the short lifetime of BVOCs would preclude them from having any significant direct influence on climate. However, there is emerging evidence that this influence might be significant at different spatial scales, from local to global, through aerosol formation and through direct and indirect greenhouse effects *(little evidence, moderate agreement)*. Either directly, by reflecting more solar radiation, or indirectly, by increasing Cloud Condensation Numbers (CCN), the increase in aerosols reduces the amount of solar radiation reaching the surface of Earth with a consequent cooling effect. A recent study (Goldstein et al. 2009) observed aerosol optical thickness resulting from BVOCs which in summer is sufficient to form a regional cooling haze over the South-eastern US (i.e. it constitutes a significant potential for a regional negative feedback on climate warming). Furthermore, aerosols scatter the light received by the canopy, increasing CO_2 fixation (Niyogi 2004) and providing another indirect, potentially negative feedback on warming. As a result, there should be a net cooling of the Earth's surface during the day because of radiation interception.

However, it has also been observed that BVOCs help to slow down nocturnal cooling in areas with relatively dry air masses and active photosynthesis (Hayden 1998). Makkonen et al. 2012 used the global aerosol-climate model ECHAM5.5-HAM2 to explore the effect of BVOC emissions on new particle formation, clouds and climate and found that the change of shortwave cloud forcing from year 1750 to 2000 ranged from -1.4 to -1.8 Wm^{-2}, and that from the year 2000 to 2100 ranged from 1.0 to 1.5 Wm^{-2}. Due to simulated decreases in future cloud cover, the increased CCN concentrations from BVOCs cannot provide significant additional cooling in the future.

Apart from the direct local BVOC greenhouse effect, which has detectable effects only when canopy-scale BVOC emissions are high, an additional global indirect greenhouse effect must also be considered because BVOCs increase the production of ozone and the atmospheric lifetime of methane, and hence enhance the greenhouse effect of these other gases. It therefore seems that the increases in BVOC emissions expected as a result of the current warming and global changes could thus significantly contribute (via negative and positive feedbacks) to the complex processes associated with global warming. Whether the increased BVOC emissions will cool or warm the climate depends on the relative weights of the negative (increased albedo and CO_2 fixation) and positive (increased greenhouse action) feedbacks (Peñuelas and Llusià 2003). The net chemical forcing of global climate due to all known anthropogenic influences on BVOC emissions has been estimated in 0.17 Wm^{-2} (cooling). This magnitude is comparable to that of the surface albedo. Many questions about these BVOC relationships with climate remain to be solved, so laboratory experiments, global climate modelling and extensive international measurement campaigns are necessary to quantify BVOC emissions, aerosol formation and reactions with hydroxyl radicals and ozone, among other processes including soil or water deposition. The still scarce available data indicate though that BVOC emissions should be included in assessments of anthropogenic radiative forcing.

2.6 Evidence that changes in land cover – uses – functioning influence climate and weather at various spatial and temporal scales

The evidence that land cover matters for the climate system have long been known, especially from early paleoclimate modelling studies.

The studies that have examined the respective roles of oceans and land on the initiation of the last glaciation, that occurred 115,000 years ago, concluded that vegetation feedbacks played a major role during that specific climatic transition. They agreed that glacial inception would not have been possible without the existence of feedbacks from changes in land-cover distribution (Kageyama et al. 2004). *(to be updated with more recent papers)*

6000 years ago, during the mid-Holocene, the Sahara was quite greener than today and climate models have confirmed that this greening contributed to maintain a rather intense African monsoon ((De Noblet-Ducoudré et al. 2000)). *(to be updated with more recent papers)*

At the regional scale, and looking at recent climate evolution, the pioneering work of (Charney 1975) examined the role of desertification on the Sahelian climate. Charney hypothesised that the observed reduction in rainfall may be linked to overgrazing north of 18°N in northern West Africa. The grazing-induced increase in land surface albedo indeed resulted in increased radiative cooling of the atmosphere and compensating sinking motion. This sinking motion tends to suppress rainfall and thus sustain the desertified system.

Since then there have been many modeling works that reported impacts of idealised or simplified land cover changes on weather patterns (Pielke et al. 2011). However, the number of publications dealing with such issues increased significantly over the past 10 years, with more and more studies that address realistic past or projected land changes. The fraction of those papers that addresses the impacts of changes in land management remains however quite low as very few land surface models, embedded within climate models (whether global or regional), include a representation of land management.

The search for evidence of land-induced climate impacts from observations is even more recent (e.g. (Forzieri et al. 2017b)) and the literature is therefore limited.

In this section we will essentially report on what we know regarding the influence land has on climate via biophysical exchanges as reports on how it influences the GHG content in the atmosphere can be found in section 2.4 and the ways it can influence non-GHG gas and aerosols can be found in section 2.5.

(Place Holder: This section may be enlarged for the Second order draft with additional papers that report on how land impacts climate dynamics through exchanges of GHGs and non GHGs).

2.6.1 Land-induced changes in global climate

Three types of studies in the literature address the impacts of land changes on climate at the global scale.

The first ones examine how climate-induced changes on land feeds back to the global GHG-induced climate change. For example, the warming-induced reduction in snow cover and extent in the boreal regions is known to positively feedback on the original warming. Those will be discussed in section 2.6.5 as they either amplify or dampen initial GHG-induced climate change.

The second set of studies is meant to understand the processes underlying the influence of land functioning on climate and to bracket the maximum climate changes one can expect from changes in Land. They all make use of global climate models with simulations of one of the following types:

- The climate model is forced with extreme land-cover changes (essentially global deforestation / afforestation; e.g. (Davin and de Noblet-Ducoudre 2010; Devaraju et al. 2015)) ;
- The climate model is run with one specific land characteristic kept prescribed compared to another in which the same land characteristic is interactive. A number of simulations have examined for example the effect of allowing vegetation cover to respond to climate as opposed to simulations where the land-cover distribution is kept unchanged from one year to another (O'ishi et al. 2009). Others have imposed a fixed seasonal (and climatological) behaviour of e.g. soil moisture or leaf area index from year to year, as opposed to simulations with fully interactive soil moisture or LAI (Delire et al. 2011; Lorenz et al. 2016a).

The third set of studies, more realistic, embeds simulations using global climate models, forced with either historical reconstructions or future global scenarios of land-cover change (e.g. (Pitman et al. 2009; Brovkin et al. 2013)).

The second set of experiments is often referred to as **idealised (or extreme) experiments**. They have been initially designed to understand the mechanisms through which land influences climate. The magnified perturbations, or isolated parameters/parameterisations, ensure large enough, or targeted, climatic changes to be analysed (hopefully above the natural climatic variability). Such experiments a) **provide upper limits to land-induced climatic changes**, and b) **allow the identification of models that are sensitive to land changes** (e.g. extreme global deforestation experiments proposed in the LUMIP project (Lawrence et al. 2016)).

2.6.1.1 Impacts on climate of global historical land use changes

Historical land use induced land cover changes (HLULCC) have been shown to cool down mean global climate annually via their influence on wind speed, on the energy and water cycles (Strengers et al. 2010; Matthews et al. 2004; De Noblet-Ducoudré et al. 2012; Pongratz et al. 2010; Brovkin et al. 2013)) *(robust evidence, high agreement)*. The range of annual cooling globally though is quite large as it can be as low as -0.03°C and as large as -0.26°C depending on the model. Cooling over land only is larger, especially regionally where it can exceed -0.5°C as reported by (Pongratz et al. 2010) and (De Noblet-Ducoudré et al. 2012). Figure 2.6.1 for example shows that the seasonal and regional HLUCC-induced cooling in ambient air temperature for 7 climate models is as large as the GHG-induced warming in those same regions, and of opposite sign. There *is robust evidence and high agreement* that this cooling has dampened the historical anthropogenic warming in many regions of the world.

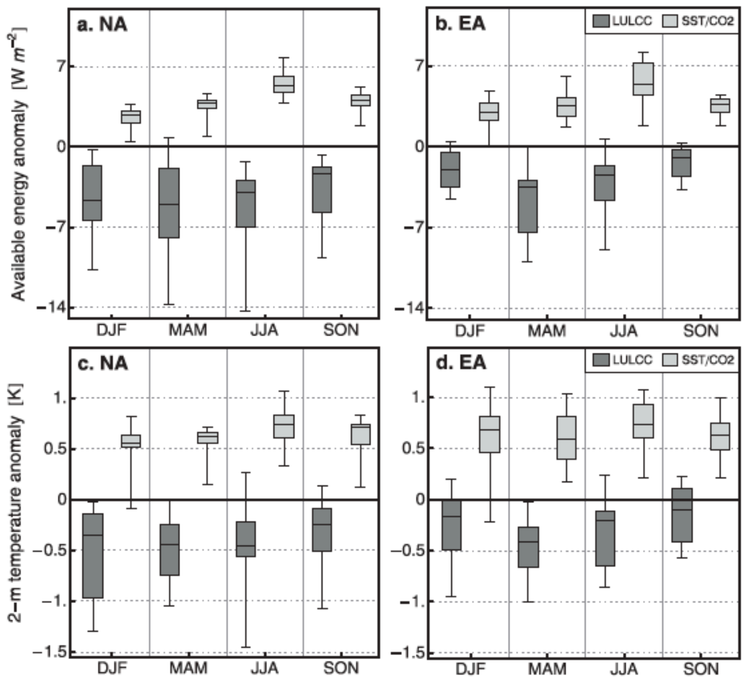

FIG. 3. Box-and-whisker plots of the simulated changes between the PI period and PD in (a),(b) available energy (W m^{-2}) and (c),(d) surface air temperature (°C) for all seasons and for (a),(c) North America and (b),(d) Eurasia. The mean ensemble values of each individual model and each set of experiment (i.e., PD − PIv and PDv − PI for the CO2SST impacts; PD − PDv and PIv − PI for the LULCC impacts) have been used to create this plot. The bottom and top of the box are the 25th and 75th percentiles, and the horizontal line within each box is the 50th percentile (the median). The whiskers (straight lines) indicate the ensemble maximum and minimum values.

Figure 2.6.1.: modelled changes in surface air temperature showing that land-induced changes are as large as GHG-induced changes in North America (NA) and Eurasia (EA). Figure from (De Noblet-Ducoudré et al. 2012)

The other effect HLULCC has on global climate is through its contribution to the increase in atmospheric CO_2 content, as discussed in section 2.4, that has led to global annual warming. When this biogeochemical effect on climate is combined with the biophysical one discussed above, estimates of the net contribution of HLULCC on ambient air temperature go from net annual and global cooling (about -0.05°C, (Brovkin et al. 2013; Pongratz et al. 2010)) to warming (about 0.15°C to 0.18°C, (Brovkin et al. 2013; Pongratz et al. 2010)). There is therefore *no agreement* on this net effect today, although there is *high agreement and high confidence* that at the regional and seasonal scales there are areas where the HLULCC-induced net cooling is the dominant signal.

None of those estimates account for the evolution of natural vegetation in non anthropised areas, while many studies have shown a greening of the lands in boreal regions resulting from both extended growing season and poleward migration of tree lines (see section 2.3). This greening enhances global warming essentially via a darkening of the land through the snow-albedo feedbacks (see sections 2.6.2 and 2.6.5). When feedbacks from the poleward migration of treeline is accounted for together with the HLULCC-induced biophysical effects, the biophysical annual cooling (about -0.20 to -0.22°C on land, -0.06°C globally) is significantly dampened by the warming (about +0.13°C) resulting from the movements of natural vegetation ((Strengers et al. 2010)). Accounting simultaneously for both HLULCC and the dynamics of natural vegetation reduces the cooling impacts of HLULCC globally, while still reporting regional cooling as large as -1.5°C.

2.6.1.2 Impacts on climate of global future land use scenarios

The impacts of **future land use induced land cover changes (FLULCC)** have been studied for some SRES scenarios as well as for some more recent RCP ones. The strong tropical deforestation projected in the SRES

A2 scenario for the end of the century was shown to provoke a global biophysical cooling of -0.14°C while the HLULUCC induced cooling in the same model was only of -0.05°C ((Davin et al. 2007)). This global cooling occurred while, over the deforested regions, warming was predicted. Oceanic feedbacks were shown to play a significant role in transmitting to other regions and latitudes the deforestation-induced cooling of the upper atmosphere. The authors calculated an overall cooling effect of ~0.3°C/W.m^{-2} as a result of LULCC, while the response of their models to GHG forcing is of about 1°C/W.m^{-2}. This means that **FLULCC has the potential to dampen significantly GHG-induced warming in this scenario and model, through its impacts on the energy and water cycles**. Including biogeochemical effects in addition to the biophysical ones (Sitch et al. 2005) concluded that although biophysical cooling was large (reaching ~ -0.5°C regionally), biogeochemical impacts led to a net warming effect of FLULCC in SRES A2 that amplified the GHG-induced warming. In SRES B1, land abandonment in temperate regions induced regional and global warming through biophysical processes. The relative net contributions of FLULCC to global climate changes projected by SRES A1B, A2, B1 and B2 amount respectively 9, 10, 13 and 16% of the total global annual temperature change in this study.

The more recent RCP scenarios project relatively small FLULCC in comparison to the former SRES. Their impacts on global climate are therefore of lesser magnitude. (Brovkin et al. 2013) have analysed the net FLULCC impacts on climate changes for 6 climate models and 2 RCPs (RCP2.6 and RCP8.5). They show a systematic warming effect of HLULCC in both scenarios mainly through the net release of CO2 from land, even in the RCP2.6 scenario that largely expanded the growth of bioenergy crops. Biophysical effects were negligible in all models, except very locally where FLULCC is the largest. The additional warming expected from FLULCC was of ~0.1 to 0.3°C for RCP 2.6 and of less than 0.1°C for RCP8.5. **There is therefore some evidence that FLULCC may contribute to enhance globally and annually the GHG-induced warming through an additional contribution to atmospheric CO2 content.** Using the RCP8.5 scenario and a more limited set of models (Boysen et al. 2014) looked at the regional importance of net FLULCC. They concluded that **FLULCC hold a potential for climate mitigation in some areas where the biophysical effects of FLULCC are the largest and can decrease by -11 to -23% the GHG-induced warming**. However where those dampening effects occur is not consistent among the models.

There are very few studies that go beyond analysing the changes in surface or ambient air temperature. Some studies attempted to look at global changes in rainfall and found no significant influence of FLULCC. (Quesada et al. 2017b,a) however carried out a systematic analysis of a number of atmospheric variables (e.g. rainfall, sea level pressure, geopotential height, horizontal and vertical wind speed). They found a systematic reduction of rainfall in 6 out of 8 monsoon regions studied (Figure 2) of about 1.9% to 3% which is up to 0.5mm/day in some areas. This dampens by about 9% to 41% the increased rainfall in those same regions in response to increased atmospheric GHG. In addition they found a shortening of the monsoon season of one to four days. They conclude that the projected future increase in monsoon rains may be overestimated by those models that do not yet include FLULCC.

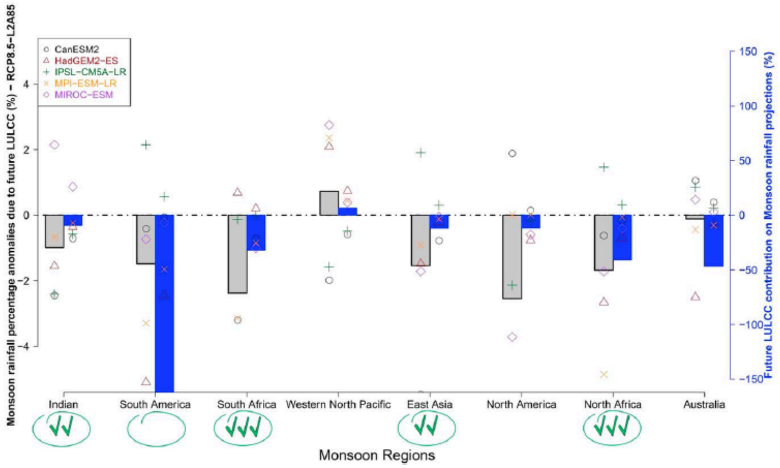

Figure 1. ENS-FUT changes in monsoon rainfall and their relative contribution to future projections (RCP8.5-HIST) in the eight monsoonal regions. Results are shown in DJF for Southern Hemisphere regions and in JJA for Northern Hemisphere regions averaged over 2071–2100 period. On the left axis, grey bars indicate monsoon rainfall anomaly percentage ($\frac{RCP8.5-L2A85}{RCP8.5}$) due to future LULCC. On the right axis, blue bars indicate the contribution of future LULCC (RCP8.5-L2A85) relative to future projections with all forcings (RCP8.5-HIST). Both units are percent. Symbols are shown for individual results of each LUCID-CMIP5 model. Note that simulated precipitations are first arithmetically averaged among the five LUCID-CMIP5 models before the calculation of the rainfall anomaly percentage and the relative contribution. Statistical significance is given by green tick marks and circles. One, two, and three green tick marks are displayed for the regions where at least 80% of LUCID-CMIP5 models have regional changes significant at 66th, 75th, and 80th confidence level, respectively (see section 2). Green circles are added when ENS-FUT regional values are also significant at 90th confidence level.

Figure 2.6.2: Changes in monsoon rainfall in eight monsoonal regions ((Quesada et al. 2017b)). The figures illustrates the contribution of land use induced land cover changes to the total change in monsoon rains in RCP8.5 using five different Earth System Models used in both CMIP5 and LUCID-CMIP5

2.6.2 Land-induced changes in regional climate and weather

The impacts of changes in either land cover (e.g. conversion of forests to crops) or land uses (e.g. irrigation) on regional climate or weather have been quite extensively studied in many regions of the world (e.g. West Africa, Europe, Amazon, Australia, India). In addition specific studies that solely change one or few land parameters (e.g. albedo, roughness, foliage density, soil moisture) have often been carried out to further understand the paths of changes from land to the atmosphere. Most studies used a regional climate model, forced on its boundaries by either recent climate years or future global scale scenario, and carried out two simulations with two different land scenarios. Some studies used a global climate model where land changes have been imposed in a specific region of the world.

Almost none of those experiments are comparable as they generally a) do not use the same climate model, b) nor the same land scenario, c) nor the same synoptic climate forcing. Moreover contradictory changes can be obtained between global models and regional models for similar area of change as both models do not include the exact same atmospheric processes and have different horizontal resolutions (e.g. about 200 kms for the global model and about 40 kms for the regional one; (Lawrence and Vandecar 2015b)). There is therefore little material to allow a robust assessment of the land-induced weather impacts on specific regions. Strict confidence can therefore not be reported below.

Focusing on regional aspects is particularly important as it is the relevant scale for impacts on ecosystems and societies, and the scale at which most decisions are made. In addition, there is *high confidence and high agreement* that historical land use induced land cover changes (HLULCC) are invisible at the global scale through their biophysical effects (using the standard IPCC metric: change in mean global annual ambient air temperature) but are important and statistically significant at the regional scale. Results from the international intercomparison project LUCID ((De Noblet-Ducoudré et al. 2012; Boisier et al. 2012)) have indeed shown that conversion of natural vegetation to crops in North America and Eurasia has been as large as, and opposite to, the global warming induced changes in those same regions (of the order of 0.5°C on average, see Figure 2.6.1). Moreover, there is also *high agreement and high confidence* that the same LULCC leads to different changes depending on where it occurs. What we name the background climate influences the sign and magnitude of the changes triggered by LULCC (Pitman et al. 2011a; Hagos et al. 2014).

In the following we have chosen to highlight the known impacts of some key human-induced land changes (e.g. deforestation / afforestation, deployment of bioenergy crops).

2.6.2.1 The impacts of afforestation / deforestation

Deforestation (or afforestation), wherever it occurs, triggers simultaneously warming and cooling of the surface and of the atmosphere via changes in its various characteristics.

Warming effects result from a) the release of CO_2 in the atmosphere that follows (biogeochemical impact) and subsequent increase in incoming infrared radiation at surface (greenhouse effect), b) decreased total loss of energy through turbulent fluxes (latent and sensible heat fluxes) resulting from reduced surface roughness, c) increased incoming solar radiation following reduced cloudiness that often (but not always) accompanies the decreased total evapotranspiration.

Cooling occurs in response to i) increased surface albedo that reduces the amount of absorbed solar radiation, ii) reduced incoming infrared radiation triggered by the decreased evapotranspiration and subsequent decrease in atmospheric water vapour. b-c-i-ii are referred to as biophysical feedbacks.

All those compensating effects make it very difficult to assess whether deforestation cools or warms climate as a) few analyses have been done combining both biophysical and biogeochemical effects, b) the net biophysical effect depends on what is referred to as the background climate, i.e. where the deforestation occurs ((Pitman et al. 2011b; Hagos et al. 2014)there are recent evidence ((Devaraju et al. in prep.)) that biophysical effects are immediate following deforestation while warming through the release of CO2 may not start immediately and may increase through time. This implies that **impacts of deforestation on local/regional climate evolve and may change sign through time** (*high confidence* although not enough literature yet).

However some consistencies can be found in the literature, starting from the pioneering work of (Claussen et al. 2001), and there is *high agreement and high confidence* that **boreal deforestation has a cooling effect on boreal climate through biophysical feedbacks**, as opposed to a **warming regional effect from tropical deforestation at the annual scale** ((Davin and de Noblet-Ducoudre 2010), (Li et al. 2015d)).

There is *no agreement* on the sign the impact temperate deforestation has on mean annual climate as, at those latitudes, the albedo-induced cooling is often compensated by the evapotranspiration-induced warming. This apparent absence of agreement at the annual scale is however masking rising agreement regarding seasonal and diurnal impacts of deforestation at those latitudes. Temperate and boreal deforestation both lead to moderate summer warming via decreases in evapotranspiration, while they both show cooling during winter time but with relatively strong cooling in boreal regions and moderate one at temperate latitudes ((Li et al. 2015d)).

Looking only at changes in ambient air temperature however is too restrictive as afforestation/deforestation are known to also impact a number of atmospheric a) variables e.g. air humidity, cloudiness, rainfall, winds, incident solar and thermal radiations, and b) processes e.g. convection, monsoons, as discussed below.

Historical deforestation was significant in Europe and North America before mid-20th century and its impacts on climate have essentially been discussed through global scale simulations (see section 2.6.1.2). Tropical deforestation is more recent and its impacts on climate are discussed below.

Observed deforestation in Rondonia since ~1970 has shifted the onset of the rainy season by ~18 days over 30 years (that is between 0.4 and 0.6 daysyr^{-1}, (Butt et al. 2011)). This resulted in an extension of the dry season in this region. It occurred because evapotranspiration from pasture during the dry season is much smaller than that from forests, and does not provide sufficient moisture to the atmosphere to trigger convection as early as when forests are present. Lower evapotranspiration results in surface warming, despite the competing effect from increased surface albedo. This warming sharpens the vertical gradient of temperature in the boundary layer, and should theoretically promote convection ((Wu et al. 2017b)). But this is inhibited by the lack of atmospheric moisture. When the impacts of deforestation are analysed at a larger scale (contrasting present-day forest extent to pre-deforestation times) over the Amazon, the evapotranspiration-induced warming during the dry season, is enhanced by reduced cloudiness (+2.2°C all together). This increases the land-ocean thermal gradient and increases the oceanic influx. It results in a contrasted picture where moisture flux (and therefore rainfall) is reduced over the NW Amazon, while it increases over the SE part (Wu et al. 2017b).

Similar deforestation-induced strengthening of the land-ocean thermal contrast has also been found in Africa, when the Congo basin lost substantial amounts of forests between 2000 and 2007 (Nogherotto et al. 2013). The local warming resulting from decreased evapotranspiration and cloudiness deepened the continental thermal law and increases the monsoonal flow. As a result, precipitation was increased further north, towards sahelian regions. Changes in the circulation of winds and therefore moisture are also obtained along forests/deforested borders where similar thermal contrasts are found ((Lawrence and Vandecar 2015b)).

Historical conversion from trees and shrubs to pasture and crops in drier regions such as the Sahel does not produce such a consistent signal as it occurred in semi-arid regions where dryness is already limiting evapotranspiration (Boone et al. 2016; Hagos et al. 2014). However, there are evidence that, when surface warming occurs in the Sahel, it increases the meridional surface temperature gradient and enhances the African easterly jet, a key feature of the African monsoon. The stronger AEJ then transports moisture out of the Sahel region and decreases rainfall.

The impacts of **Future afforestation** on climate were tested in many regions of the world (e.g. Africa, China, Europe) using either global or regional climate models, but not always combined with climate change scenarios.

Afforestation using a variety of forest types (deciduous or evergreen trees, broad or needle leaved) has been tested (numerically) in China in the Jiangxi Province (Ma et al. 2013). It has shown that while evergreen trees may induce local warming, deciduous trees tend to produce cooling. Although changes are not very large at the annual level (from -0.25°C to +0.18°C) **the choice of trees used to afforest may change the biophysical local/regional effect on climate**. In another study, afforestation of Eastern China led to cooler summers of both land (-1.21°C) and ambient air (-0.16°C) via increases in latent heat flux (+4.14 Wm^{-2}), while surfaces were slightly warmer during winter time (+0.29°C) in response to increases in surface roughness length and therefore in the sum of turbulent fluxes (changes in the sum of latent and sensible heat flux is -1.31 Wm^{-2}). The most remarkable impact of the reduced land roughness is the slowing down of the winds coming from adjacent oceans thereby exporting less moisture away from the region. Such study illustrates the **importance of accounting for oceanic feedbacks even when studying the impacts of land changes on climate**.

Idealised **afforestation scenarios in West Africa**, combined with future climate projections using SRES A1B GHG emissions, have shown the **potential to dampen the GHG-induced warming and drying** in three west African regions: the Sahel, the southward Savannah area, and Guinea (Abiodun et al. 2012). When one of those regions is experiencing large forest increases, its surface temperature decreases (by -2.5°C in the Sahel and -1°C in the Savannah area). In the case of Savannah afforestation this decrease entirely compensates the GHG-warming (+1°C). Cooling is accompanied with increases in rainfall that more than compensates the GHG-drying. However, because those regions are affecting and affected by the monsoon system, consequences occur outside the afforested areas and lead to warming and drying in those adjacent areas.

Similar experiment has been carried out in **Hungary where reforesting the entire country** under SRES

A1B **partly compensates for the warming-induced drought**: the -25% decrease in rainfall is limited to -17% following afforestation (Gálos et al. 2011). In addition the number of dry summers are reduced.

Large scale afforestation in Europe shows more contrasted hydrological responses with cooling and moistening in Central Europe and Ukraine, dampening the GHG-induced warming and drying, while Spain, Belarus and Russia experience enhanced drought ((Gálos et al. 2013)). Annual European afforestation induced cooling is quite small (-0.3°C) compared to the +3°C GHG-induced warming. However changes in precipitation are relatively larger (-10 to +10% compared to -25% to + 25% resulting from increased GHG). **Locally afforestation-induced rainfall increases can more than compensate the GHG-induced decrease** (+45 compared to -36mm, +36 versus -69 mm, +18 versus -39 mm respectively in three different locations).

Progressive afforestation of the 30-60°N latitudinal band, adding successively 3.5, 7, 11.2 and 15.3 million km^2 of trees, leads to contrasting effects on the atmosphere ((Laguë and Swann 2016)). Although all scenarios imply increases in annual evapotranspiration, this increase is levelled of above ~11.2 Mkm^2 additional tree cover. This signs up the shift in this area from energy- to moisture-limited evapotranspiration as trees pump massive quantities of water from the soil. For the lowest additional amount of trees, the increase in evapotranspiration is compensated by decreases in sensible heat fluxes. The soil temperature is not significantly changed, the ambient air cools down and is more humid. For larger amount of additional trees, sensible heat flux experiences large increases (as large as latent heat flux). Soil and ambient air temperatures also increase, the relative air humidity decreases and so does cloudiness. **The surface and atmospheric effects of afforestation are therefore strongly dependent upon the magnitude of the change in tree cover, not only for the magnitude of the change, but also for the sign**.

2.6.2.2 The impacts of land management

Accounting for land management (LM) in regional or global climate models is still quite rare. There is therefore very little literature to report on. We focus our attention below on two LM that have been studied, with respect to their impacts on climate: irrigation (one form of crop intensification) and forest management.

Figure 2.6.3 from (Chen and Jeong 2018) summarises the findings from observations in many regions of the World (India, China, North America and eastern Africa). There is a consistent cooling of maximum daytime ambient air temperature observed in response to irrigation, wherever it occurs (e.g. (Bonfils and Lobell, 2007; Alter et al. 2015; Mueller et al. 2016)), together with an increase in dew point temperature of the ambient air ((Mahmood et al. 2008)). Daytime maximum cooling can be as low as about -0.007°C/decade in China and as large as about -0.25°C in California. Cooling occurs via significant increases in evapotranspiration accompanied by decreased sensible heat flux. There is however less consistency in the measured impact on nighttime temperature that shows non-significant change or contradictory changes in most observations. However (Chen and Jeong 2018)recently reported warming of lowest nighttime values from observations, that they were able to reproduce using a regional climate model. Wetter soils are able to store more heat during daytime and they restore it during nighttime. They even report a daily irrigation-induced warming, therefore dominated by the nighttime warming and conclude that irrigation has the potential to enhance GHG-induced warming. This finding however is contradicting all previous studies but none were carried out over the same regions.

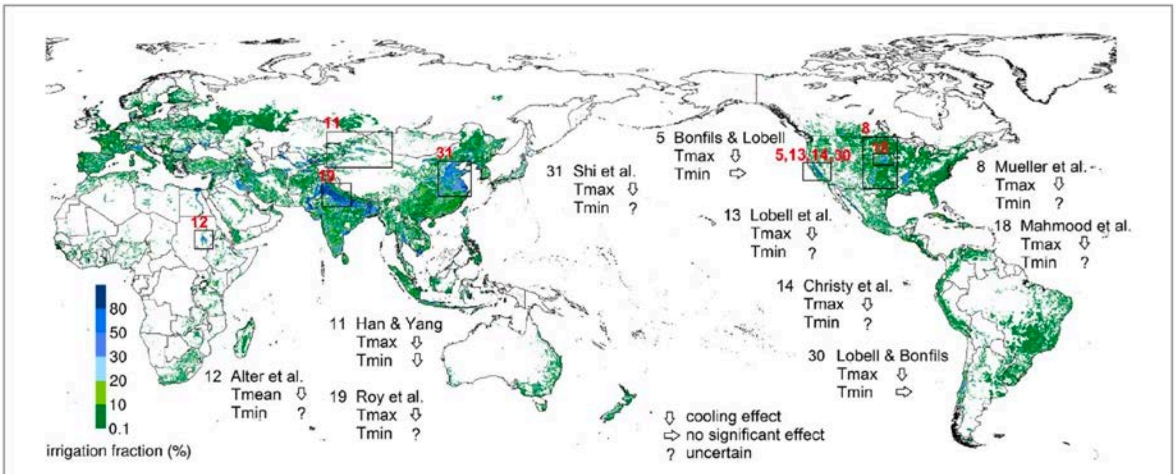

Figure 1. Summary of the observational studies focusing on the irrigation impact on temperature. The area equipped for irrigation around the year 2005 expressed as a percentage of total area (irrigation fraction) [20] is shown in the map. The boxes indicate the research regions of previous observational studies. References and results are summarized in this map.

Figure 2.6.3: Impact of historical irrigation on daily maximum and minimum temperatures, as derived from observations in many regions of the world (Chen and Jeong 2018)

In addition to changes in surface temperature, there are many evidence from both modelling studies and observation that irrigation changes horizontal gradients of temperature, ambient air specific and relative humidity, vertical gradient of air temperature and humidity, as displayed Figure 2.6.4. Such changes have impacts on horizontal winds and convective activity. Monsoon systems for example are affected by irrigation in India (Niyogi et al. 2010; Guimberteau et al. 2012), Eastern and Western Africa (Alter et al. 2015; Im et al. 2014). Land cooling following irrigation decreases the land-sea temperature contrast that delays the onset of the Indian monsoon by about six days (Guimberteau et al. 2012).

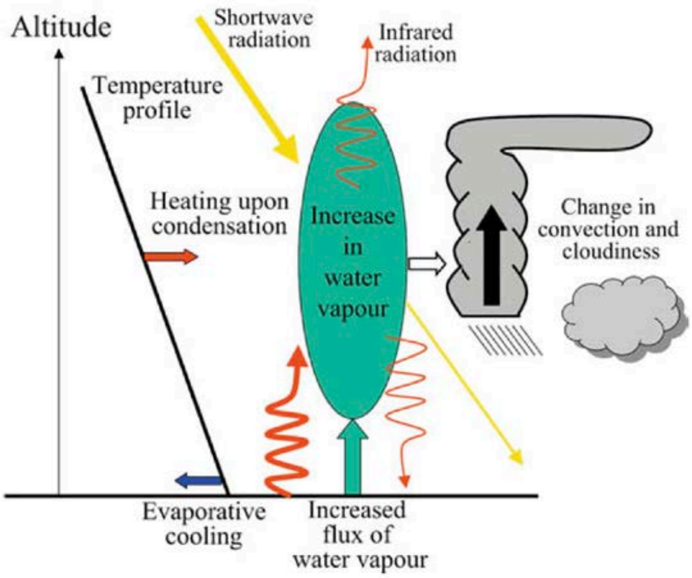

Fig. 1 Schematic of the atmospheric properties and processes potentially induced by irrigation

Figure 2.6.4: Schematic illustration of how irrigation impacts surface/atmosphere fluxes, atmospheric variables and processes (Boucher et al. 2004)

Forest management has been reported to affect water and energy fluxes to the atmosphere to the same extent as changes in land cover do. Indeed (Luyssaert et al. 2014b) have shown that changes in forest management induce effects on surface temperature of the same order of magnitude as those resulting from changes in land cover pointing to the importance of including not only scenarios of land cover change in climate models but also of land management change. Combining models and observations of European afforestation over the past decades, (Wilfert et al. 2016) showed that although increasing forests drew CO_2 down from the atmosphere, the resulting effect at the ambient air level was a warming of Europe over the afforested areas, in response to the choice of tree species.

(Place Holder for other Land Management Changes, e.g. double cropping?)

2.6.2.3 The impacts of deploying bio-energy crops, or geo-engineering the land

<u>Combining afforestation and irrigation</u>

Complete afforestation of the Saharan and the Australian deserts, through the large-scale deployment of irrigation and of desalination plants, have been proposed to increase the net land sink of CO_2 ((Ornstein et al. 2009; Kemena et al. 2017)). Large local cooling, resulting from the sole biophysical feedbacks, was obtained (up to -8°C in western Sahara) together with significant increases in rainfall. Those were however not sufficient to sustain the planted forests without irrigation: in the Sahara 26% to 50% of the produced evapotranspiration could be recycled.

The role of forests as providers of water vapor for the atmosphere and therefore as catalysts for increasing terrestrial precipitation has been questioned by (Ellison et al. 2017 and Layton and Ellison, 2016) based on a literature survey. They bring forward the potential of combined ‘small-scale’ afforestation and irrigation to boost the precipitation-recycling mechanism in the semi-arid region of Los Angeles California, and to provoke the growth of natural vegetation down-wind of the afforested area but up-wind of the ‘mountains’ (Figure 2.6.5).

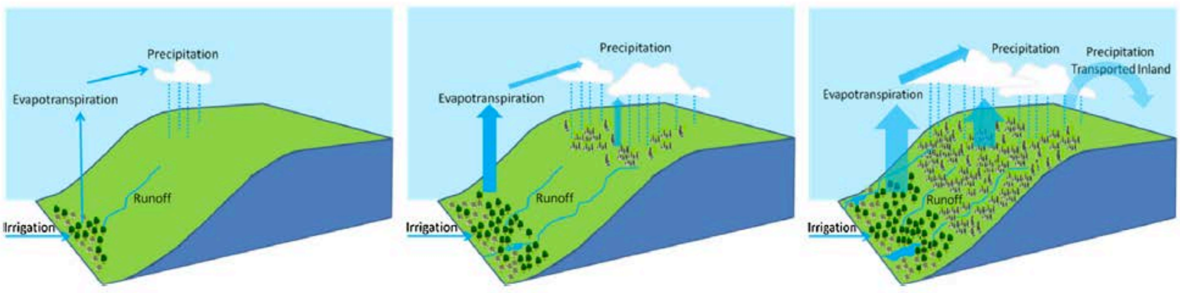

Fig. 4. The virtuous cycle of increased precipitation and forest growth initiated by IPR.

Figure 2.6.5: Schematic illustration of how combined afforestation and irrigation in Los Angeles (California) area can influence down wind precipitation on mountainous areas, and feeds back to the afforested area via increased runoff (Layton and Ellison 2016)

<u>Deploying or Expanding bioenergy crops</u>

Sugar cane is the main bioenergy crop deployed in Brazil up to now. When grown at the expense of existing cropland, it has been shown to cool down the surface during daytime conditions by about -0.93°C (-0.78 to about -1.07°C) locally (Loarie et al. 2011). This is the result of the larger evapotranspiration rates of sugar cane (+about 0.43mm/day), combined with larger surface albedo (+0.20%). If however sugar cane is deployed at the expense of natural vegetation (Brazilian Cerrado), then warming is expected through decreased evapotranspiration rates even if albedo increases. **The cooling potential of such bioenergy crops can thus be increased when considering both biophysical and biogeochemical effects**, **but this depends on what the previous land cover is on those areas**.

In a modeling study carried out under present-day climatic conditions (Georgescu et al. 2013a) tested the effects of replacing both natural cerrado and crops by sugar cane and pointed to large seasonal variations of the biophysical impacts, while effects at the annual scale were negligible. Sugar cane has a well marked seasonal cycle, and this induces a cooling of ambient air (as large as 1°C) during its growing season, essentially in response to larger albedo. However, post-harvest, the decrease in evapotranspiration (-0.5 to -1mm/day) induces atmospheric warming of about +1°C. Such seasonal contrast is often reported in the most recent literature: **sticking to annual analysis may hide important seasonal climate warming mitigation potential (CWMP) of land changes**.

Replacing annual crops with perennial switchgrass or miscanthus in North America increases both albedo and evapotranspiration during the growing season, thereby cooling down the land and the overlying atmosphere (~-0.45°C regionally with values as large as -1.5°C locally; (Georgescu et al. 2011)). This has the potential to offset, regionally, the GHG-induced warming until around 2040. In addition, biophysical cooling effects are larger than the biogeochemical ones during the 1st 7 years after planting. Neglecting those biophysical effects (BPHE) therefore leads to underestimate the CWMP as discussed in (Zhu et al. 2017b) who have estimated that equivalent carbon storage with and without accounting for BPHE shift from +49.1 and 69.3 gCm^{-2} to 78.5 and 96.2 gCm^{-2} respectively for switchgrass and miscanthus.

2.6.2.4 Urban-induced climate and weather changes

Cities affect the local weather by perturbing the wind, temperature, moisture, turbulence, and surface energy budget field. Another unique feature of cities is the release of the anthropogenic heat flux from energy consumption ((Ichinose et al. 1999; Bohnenstengel et al. 2014; Ma et al. 2017a)). One well known phenomenon is the so-called urban heat island (UHI) where urban air temperatures are substantially higher than corresponding temperatures in the surrounding rural areas. Three main factors contribute to the establishment of the UHI: 3-D urban geometry, thermal characteristics of impervious surfaces and anthropogenic heat. In addition and as for any land cover or use change (see section 2.3), ((Zhao et al. 2014; Ward et al. 2016)) have shown that the magnitude and diurnal amplitude of the UHI depends on the local background climate. Cities can also experience another phenomenon: the urban dryness island refers to conditions where the lower relative humidity are observed in cities relative to more rural locations, or the urban wind island where cities experience slower wind speeds compared to their adjacent suburbans and countryside ((Bader et al. 2016; Wu et al. 2017a)).

Global climate modelling groups consider that the impact of urban land cover on the global weather and climate is negligible compared to that due to other types of land cover, since the cities cover only 0.2% of the world's land area. Zhang et al. (2013a) and Chen et al. (2016a) introduced an estimate of the anthropogenic heat release globally as an external energy source into the lowest model layer of a global climate model. They found that while the global mean surface air temperature responses are insignificant (0.01K annual mean), there are statistically significant change by as much as 1K in mid and high latitude in winter and autumn over North America and Eurasia. There is also an equatorward shift of the winter mid-latitude jet, with increasing westerly wind at 20°N and decreasing westerly wind at 40°N. This suggests that the global anthropogenic heat could disturb the normal atmospheric circulation pattern and produce a remote effect on surface air temperature (*limited evidence, low agreement*).

At the regional scale, a percentage of the warming trend can be linked to historical urbanisation in rapidly industrialised countries such as China (*robust evidence*, *high agreement*). Sun et al. (2016) found that while China's recorded annual mean temperature increased by 1.44°C during the period 1961 to 2013, urban warming influences account for about a third (0.49°C; Figure 2.6.6). The annual-mean maximum temperature is substantially less affected by urbanisation than the minimum temperature (*robust evidence, high agreement*) (Liao et al. 2017; Wang et al. 2017b). In the United States, (Hausfather et al. 2013) found that urbanisation accounted for between 14 and 21% of the increase of minimum temperatures since 1895, and 6 to 9% since 1960 (trend between 0.2°C and 0.6°C per century for the period 1960-2010). Over Europe, (Chrysanthou et al. 2014) show that urbanisation explains 0.0026 °C/decade of the annual averaged pan-European temperature trend of 0.179 °C/decade. The strongest effect of urbanisation was found in the summer (0.0070°C/decade) where the trend is more than twice the annual values. Similar effect was reported in other regions (Japan - (Fujibe 2009); PuertoRico – (Torres-Valcárcel et al. 2015)) and other cities ((Bader et al. 2016)). Therefore, if observations of near-surface air temperatures in growing cities are used in the assessment of global warming trends, these trends may be overestimated (*robust evidence, high agreement*) (Hamdi, 2010; Alizadeh-Choobari et al. 2016; Arsiso et al. 2018; Elagib, 2011; Lokoshchenko, 2017; Robaa, 2013; Sachindra et al. 2016), while this urban warming is smaller for a station that originally was established in a densely built-up area (Jones and Lister 2009). Adjusting global temperature data to remove the impacts of urban affects revealed that for 42% of global stations urban areas warmed at slower rates compared to the surrounding non-urban areas ((Bader et al. 2016)).

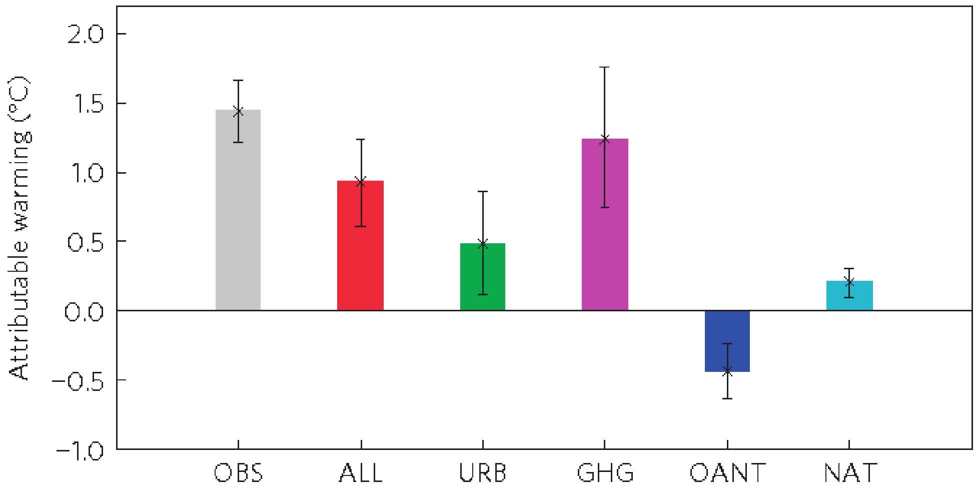

Figure 2.6.6: Attributable warming from different contributors in China (from (Sun et al. 2016)): urbanisation (URB), green-house gases (GHG), other anthropogenic forcing (OANT, predominantly aerosols) and natural forcing (NAT, solar and volcanic combined), along with their 5-95% uncertainty range.

There is evidence from recent observational studies that statistically significant positive anomalies in mean but also in extreme precipitations are found over and downwind of the urban areas (medium evidence, medium agreement) in different climate regions of the world and especially in the afternoon and early evening: Atlanta (McLeod et al. 2017; M. et al. 2014); different inland and coastal US cities (Ganeshan and Murtugudde 2015); Dutch coastal cities (Daniels et al. 2016); Hamburg (Schlünzen et al. 2010); Shanghai (Liang and Ding 2017)). Over Beijing, (Dou et al. 2014) found, however, that depending on the strength of the UHI, maximum precipitation values were found either over the most urbanised area of Beijing in the case of strong UHI (>1.25 °C) or along its downwind lateral edges for a weak UHI (<1.25 °C). Theoretical analysis ((Han et al. 2011)) and regional climate models using urban canopy parameterisations (Ganeshan and Murtugudde, 2015; Li et al. 2017; Pathirana et al. 2014; Song et al. 2016; Trusilova et al. 2008; Zhong and Yang, 2015; Zhu et al. 2017b; Seino et al. 2018; Zhong et al. 2017; Ooi et al. 2017) have been used to simulate the impact of urbanisation on the precipitation patterns near urban centres. Three mechanisms could be assessed: (i) upward motion induced by the urban heat island circulation can initiate moist convection by creating an urban-induced convergence which may interact with sea-breeze for coastal cities, (ii) increased urban roughness which may attract propagating storms toward the urban centres, and (iii) urban aerosols which may interact synergistically with the previous mechanisms producing a rainfall enhancement (Schmid and Niyogi 2014) but other studies suggest that increased aerosols concentrations in urban areas can interrupt precipitation formation process and thereby reducing heavy rainfall (Zhong et al. 2017; Daniels et al. 2016). Recently, there are new studies on the urbanisation impact on Indian summer monsoon rainfall extremes (Shastri, H., Paul, S., Ghosh, S., Paul, S., Ghosh, S., Karmakar 2015) and on the East Asian summer monsoon ((Chen et al. 2016b; Jiang et al. 2017)). Overall, the studies reveal the sensitivity of extreme monsoon rainfall events to the increased urbanisation but further studies are still needed to reduce uncertainties (*limited evidence, high agreement*). Finally, urban areas affect also the other components of the water cycle by increasing the evapotranspiration demand for plants in cities by as much as 10% (Zipper et al. 2017) and increasing the surface runoff (Hamdi et al. 2011).

Zhang et al. (2009) reported that upstream urbanisation exacerbates (*medium evidence, high agreement*) UHI effects along the Washington-Baltimore corridor in the US. Similar effect was found in the Suzhou-Wuxi area (China) by Zhang and Chen (2014) and more recently over the UK by (Bassett et al. 2017) where the urban heat advection from small urban is found to increase mean nocturnal air temperature by 0.6°C at a horizontal distance of 0.5 km. There are also example of interaction between sea breeze front penetration and urban areas (*medium evidence, low agreement*), either enhancing the sea-breeze front (Li et al. 2015b) or decelerating its penetration inland (Hamdi et al. 2012; Flores Rojas et al. 2018; Yamato et al. 2017) and therefore impacting the spatial distribution of the urban heat island. Finally, there are also evidence of synergistic interactions between UHI and heat wave episodes (*robust evidence, high agreement*) making the heat wave more intense in urban than rural areas and the nocturnal UHI during heat wave stronger than its climatological mean: along the Washington-Baltimore corridor in the US (Li and Bou-Zeid 2013), across the Yangtze River Delta in China (Wang et al. 2017b), Western Europe, Brussels (Hamdi et al. 2016) and in the Mediterranean climate, Athens (Founda and Santamouris 2017).

It is very uncertain (*limited evidence, low agreement*) to estimate the UHI under climate change conditions because several studies using different methods report contrasting results. (McCarthy et al. 2010; Oleson et al. 2011; Oleson, 2012) investigated the changes in the UHI using global climate models coupled to urban canopy parameterisations. The results show that under simulation constraints of no urban growth both urban and rural areas warm substantially in response to greenhouse gas induced climate change but generally the rural areas warm more and reduce then the urban to rural contrast. The larger storage capacity of urban areas was found to buffer the increase in long-wave radiation, sensible heat flux is reduced accordingly so that urban air temperature warms less than rural air temperature at night. (Adachi et al. 2012; Hamdi et al. 2014; KUSAKA et al. 2012a, 2012b; Mccarthy et al. 2012; Arsiso et al. 2018) used a regional climate model coupled to a single-layer urban scheme, the results show that the relative magnitude of UHIs in the UK and Japan would remain the same, while for Brussels, summertime rural areas were found to warm more than urban due to a soil dryness over rural areas limiting then the evapotranspiration. Other studies generally employ a dynamical downscaling of global climate model information with a regional climate model, while further high-resolution simulations are performed using statistical downscaling approach (Früh et al. 2011; Hoffmann et al. 2015; Sachindra et al. 2016; Hatchett et al. 2016; Arsiso et al. 2018). These studies found an increase of the UHIs in both Hamburg and Melbourne and a decrease during the summer in Addis Ababa under climate change conditions and no urban growth. Finally, in some studies the regionally downscaled model output is used to force an off-line urbanised land surface scheme (Lemonsu et al. 2013; Rafael et al. 2017; Lauwaet et al. 2015). These studies report also contrasting results about the changes in the UHIs. However, because of the offline mode of these simulations, the contribution and feedback processes by urban heat island and climate change are not taken into account. Finally, there are clear evidence that future urbanisation may amplify the air temperature in different climatic regions (*robust evidence, high agreement*) (Mahmood et al. 2014) either under present (Kaplan et al. 2017; Doan et al. 2016; Li et al. 2018) or future conditions (Georgescu et al. 2013b; Argüeso et al. 2014; Kim et al. 2016); Kusaka et al. 2016; Grossman-Clarke et al. 2017) with a strong impact on minimum temperatures that could be comparable to the climate change signal only for the near future over western Europe (+0.6 °C, Berckmans et al. to be submitted).

2.6.3 Land-induced changes in extreme weather events

There is emerging evidence that, in absolute terms, **land affects local temperature extremes more than mean climate conditions** (*medium confidence; e.g. high agreement but limited evidence as the type of evidence is essentially model-based with few observational confirmation*). Observational evidence suggests that trees dampen seasonal and diurnal temperature variations at all latitudes and even more so in temperate regions compared to short vegetation ((Lee et al. 2011; Li et al. 2015a; Chen et al. 2018; Duveiller et al. 2018b)). Furthermore trees also locally dampen the amplitude of hot extremes (Zaitchik et al. 2006; Renaud and Rebetez 2008) although this result depends on the forest type, coniferous trees providing less cooling effect than broadleaf trees(Renaud and Rebetez 2008; Renaud et al. 2011).

There is no direct observational evidence of the effect of historical deforestation on extreme temperature trends since the effect of land forcing and of other climate forcings are intertwined. Based on results from four climate models, the impact of historical land cover change on temperature and precipitation extremes was found to be locally as important as changes arising from increases in atmospheric CO_2 and sea-surface temperatures, but in the absence of observational constraints models disagree on the sign of changes due to land cover changes (Pitman et al. 2012). Using an observational constraint for the local biogeophysical effect of land cover change applied to a set of CMIP5 climate models, (Lejeune et al. 2018) found that historical deforestation increased extreme hot temperatures in northern mid-latitudes. The results also indicate a stronger impact on hot temperatures compared to mean temperatures. (Findell et al. 2017) reached similar conclusions, although using only a single climate model. Importantly, the climate models involved in these three studies did not consider the effect of management changes which have been shown to be important, as discussed below.

Beyond land conversions the impact of land management (for a given land cover type) is also crucial. For instance, irrigation provides evaporative cooling which can locally mitigate the effect of heatwaves (Wim et al. 2017; Mueller et al. 2015). The suppression of tillage as in conservation agriculture, or the use of cover crops, was also shown to provide local cooling effect due to surface albedo increase (Davin et al. 2014; Ceschia 2018). This cooling effect increases with increasing maximum temperature and is therefore more intense during hot summer days (Figure 2.6.7). The cooling effect from conservation agriculture was found to be potentially more pronounced in dry regions (Hirsch et al. 2017).

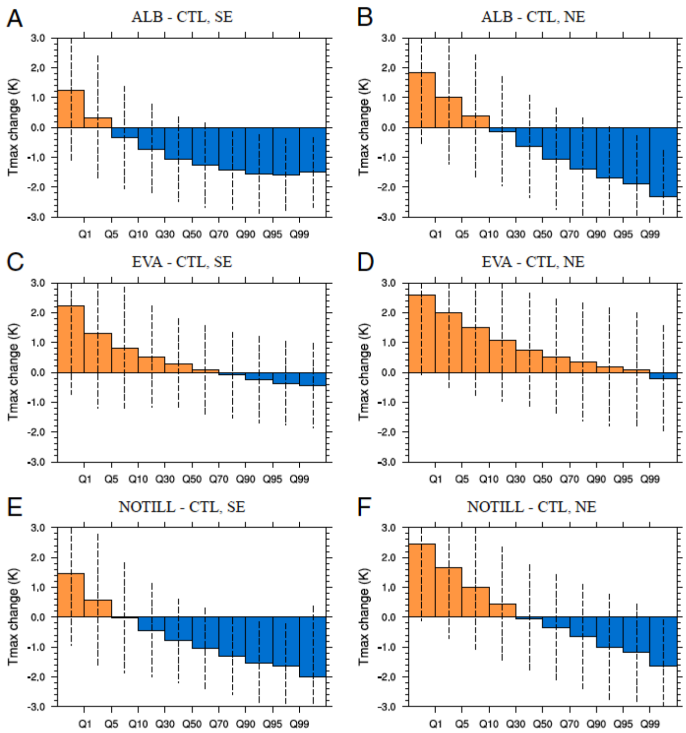

Figure 2.6.7: Changes in daily maximum temperature resulting from suppressed ploughing in Europe (Davin et al. 2014)

(Place holder to add discussion about the role of forest management).

There is *robust evidence and high agreement* in the fact that the process of urbanisation has increased vulnerability to extreme events because it concentrates human populations in areas that physically amplify these extremes. For instance, the SREX SR states that "urbanisation exacerbates the negative effects of flooding through greatly increased runoff concentration, peak, and volume, the increased occupation of flood plains, and often inadequate drainage planning". Conversions to urban environments also exacerbate temperature, moisture, and wind gradients that act as a source of vorticity for storm inception and development into tornadoes (Kellner and Niyogi 2014; Niyogi et al. 2017). Cities are also a source of aerosols that stimulate atmospheric water condensation and favour thunderstorm initiation (Haberlie et al. 2015). Furthermore, there is high confidence that hot heatwave days are warmer in urban compared to rural areas due to the Urban Heat Island (UHI) effect (Li et al. 2015a; Zhao et al. 2018).

In addition to changes in extremes triggered by altering land cover or uses, climate change-induced land perturbations (such as soil moisture, snow extent and duration) can also influence the frequency and magnitude of extremes. GHG-induced climate change is associated with changes in the frequency and strength of extreme events. In particular, IPCC AR5WG1 concluded that "it is virtually certain that there will be more frequent hot and fewer cold temperature extremes over most land areas on daily and seasonal timescales as global mean temperatures increase". In some regions, part of the projected increase in hot extremes may be due to land-atmosphere feedbacks involving soil moisture (Seneviratne et al. 2012b, 2013). There is indeed robust evidence that dry soil moisture conditions favour summer heat waves, in particular in regions where evapotranspiration in limited by moisture availability (Mueller and Seneviratne 2012). Quantitative estimates are however very uncertain due to the low confidence in projected soil moisture changes (AR5WG1) and to methodological uncertainties associated with the model-based framework used to attribute soil moisture impacts on temperature trends (Hauser et al. 2017). The role of land processes in changes in precipitation extremes remain largely uncertain (Tuttle and Salvucci 2016; Yang et al. 2018) and requires further research.

2.6.4 Land-induced teleconnections, non-local and down-wind effects

The potential of land changes to induce teleconnections within the climate system has been questioned for years in the scientific community. If Human-induced land changes do not just have local consequences (through biophysical processes), but also affect adjacent or more remote areas, then any action on land (to e.g. dampen global warming effects) needs to be anticipated not only for its local impacts but also for how it may affect other countries.

Extreme afforestation under present-day climatic conditions for example, per latitudinal band (0°-15°N, 15°-30°N, 30°-45°N, and 45°-60°N) lead (**through biophysical effects**) to **systematic annual warming** where afforestation occurs (from +0.8°C to + 4.4°C in small regions), but also **globally** (from +0.68°C to +1.38°C) although the global effects is larger when afforestation occurs in boreal regions than when it occurs in tropical regions ((Wang et al. 2014b)). Such global warming induces the known consequences on sea-ice extent that is reduced, on sea-surface temperatures that are increased and on the meridional transport of heat by the oceanic circulation that is decreased in response to the decreased equator to pole temperature gradient. **The ability of changes in land cover to influence oceanic temperatures that then feedback on the land-induced climate change** has also been reported by (Davin and de Noblet-Ducoudre 2010) in response to a change from globally forested to herbaceous Earth under pre-industrial GHG conditions.

Tropical deforestation, whether regional (in Africa, the Amazon, or Asia) or latitudinal (the entire tropics being deforested) has been reported to have impacts in many subtropical and temperate regions as illustrated Figure 2.6.8 and reported by (Lawrence and Vandecar 2015b). Those changes occur because deforestation **triggers perturbations in large-scale atmospheric transport**. (Cowling et al. 2009; Laguë and Swann, 2016) have indeed showed changes in the transport of atmospheric energy towards the pole or across the equator in response to large-scale greening of the Earth. In (Cowling et al. 2009) an additional warming of about 3°C in the 75-90°N latitudinal band was attributed to increased atmospheric inflow of heat. In (Laguë and Swann 2016) afforestation in the 30-60°N latitudinal band, whatever the magnitude (increases in tree cover from 1.5 to 15.3 Mkm^2), induces increases in cross equatorial atmospheric energy transport and consequently a northward shift of the annual mean location of the ITCZ (intertropical convergence zone).

Similarly afforestation in West Africa or irrigation in India have been shown to influence monsoon winds (see section 2.6.2), while historical or future land use induced land cover changes have a global influence on temperature via oceanic feedbacks (section 2.6.1).

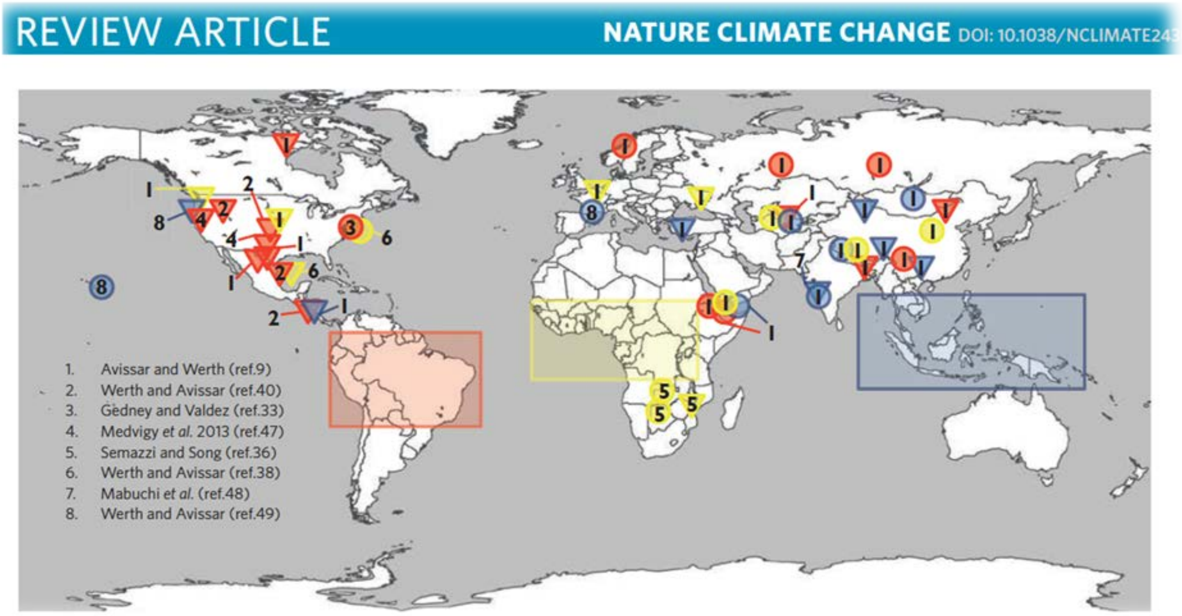

Figure 2.6.8: Evidences of extra-tropical influences of tropical deforestation as reviewed by (Lawrence and Vandecar 2015b)

(Lorenz et al. 2016b) however warned the community that existence of such teleconnections is biased by a) the size of the imposed deforestation that is often exaggerated in most studies, b) the magnitude of the internal climatic variability that is often not well accounted for in the statistical tests applied to estimate the significance of the changes simulated.

Using two climate models and similar latitudinal deforestation scenarios, (Devaraju et al. 2018) have demonstrated that boreal (resp. temperate) deforestation significantly affect ambient air temperature in the tropics and in the temperate (resp. boreal and tropical) regions. Temperate cooling in both models results from boreal deforestation and varies between -0.8°C and -1.5°C. The response of boreal regions to temperate deforestation varies from warming of about +0.3°C to cooling of -1°C depending on the model. Tropical deforestation on the other hand has little impacts in boreal and temperate regions. This is in disagreement with other modeling experiments that have reported remote impacts of amazon deforestation (Werth and Avissar 2005) through changes in large-scale atmospheric transport such as the Pacific/North Atlantic Oscillation (Lean and Warrilow 1989; Poveda and Salazar 2004).

Evidence is discussed in sections 2.6.2.1 and 2.6.2.5 that **afforestation scenarios and urbanisation trigger up stream and downstream changes** in e.g. temperature, rainfall, humidity through for example changes in wind speed and sometimes direction (e.g. (Ma et al. 2013; McLeod et al. 2017; Abiodun et al. 2012)).

(De Vrese et al. 2016) demonstrated, using a global climate model, that irrigation in India affected regions as remote as eastern Africa through changes in the atmospheric transport of water vapour. At the onset of boreal spring (February-March) evapotranspiration is already large over irrigated crops and the resulting excess moisture in the atmosphere is transported south-westward by the low-level winds. This resulted in increases in precipitation as large as 1mm/day in the horn of Africa. Such finding implies that if irrigation is to decrease in India, rainfall may decrease in eastern Africa where the consequences of drought are already disastrous.

Evidence of existing teleconnection is impossible to get from observations. They can only be identified using regional or global climate models and carefully designed experiments. However, a) as there is *high confidence and agreement* that land changes trigger significant impacts on surface and air temperature (section 2.6.2) and b) as loosened (resp. sharpened) temperature gradient decrease (resp. increase) horizontal wind, **there is *agreement* that land changes can have up-wind and/or down-wind effects**. Moreover **as**

land changes also trigger changes in atmospheric moisture and vertical motion, chances are that they cascade in downward motion elsewhere with consequences on atmospheric moisture, temperature and cloudiness. But more work is requested to carefully identify and quantify those remote changes.

2.6.5 Amplifying / dampening climate effects through land/atmosphere feedbacks

Section 2.2 illustrates the various mechanisms through which land can affect the atmosphere and thereby climate. Section 2.3 illustrates the many impacts climate changes have on the functioning of land ecosystems. Sections 2.6.1 to 2.6.4 show the many effects changes in land cover, uses or functioning have on atmospheric processes (e.g. convection) or states (e.g. air temperature, rainfall). Few papers (many are not recent) have shown that land significantly contributes to increase low frequency variability of precipitation relatively to the high frequency one (Delire et al. 2011) and increase the persistent of dry and wet events (Wang et al. 2004; Zeng et al. 1999). This occurs through the responses and feedbacks of either vegetation greening/browning (through leaf area index growth/decay or growth/disappearance of herbaceous vegetation), and/or soil moisture, to changes in weather variables (e.g. rainfall, temperature). Those effects are more prominent in regions of strong moisture gradient, that is within semi-arid regions.

Land has therefore the potential to dampen or amplify either the greenhouse-induced climate warming or its regional consequences (e.g. drought or moistening), as schematically illustrated Figure 2.6.9. It can also be used as a tool to mitigate (attenuate) some unpleasant regional climatic consequences of global warming (e.g. extreme weather events). **It has essentially been thought of, up to now, as a tool to increase the amount of CO_2 pumped from the atmosphere** (see section 2.7), and thereby decrease the atmospheric CO_2 concentration and global warming. However such strategy has been shown to potentially have the unintended consequence of further increased warming over the afforested regions and also potentially globally (e.g.(Betts 2000)).

Despite its clear importance in climate changes, vegetation dynamics (interannually through changes in foliage seasonality, annually through disappearance/appearance of vegetation types in each pixel) is represented in only a few of the GCMs that participated in CMIP5 ensemble simulations/projections conducted for IPCC AR5. It is even less common among the RCMs participating in CORDEX for various regions. The findings below are therefore based on a limited number of peer-reviewed papers. The robustness of the features discussed is therefore questionable although many share strong agreement among modellers.

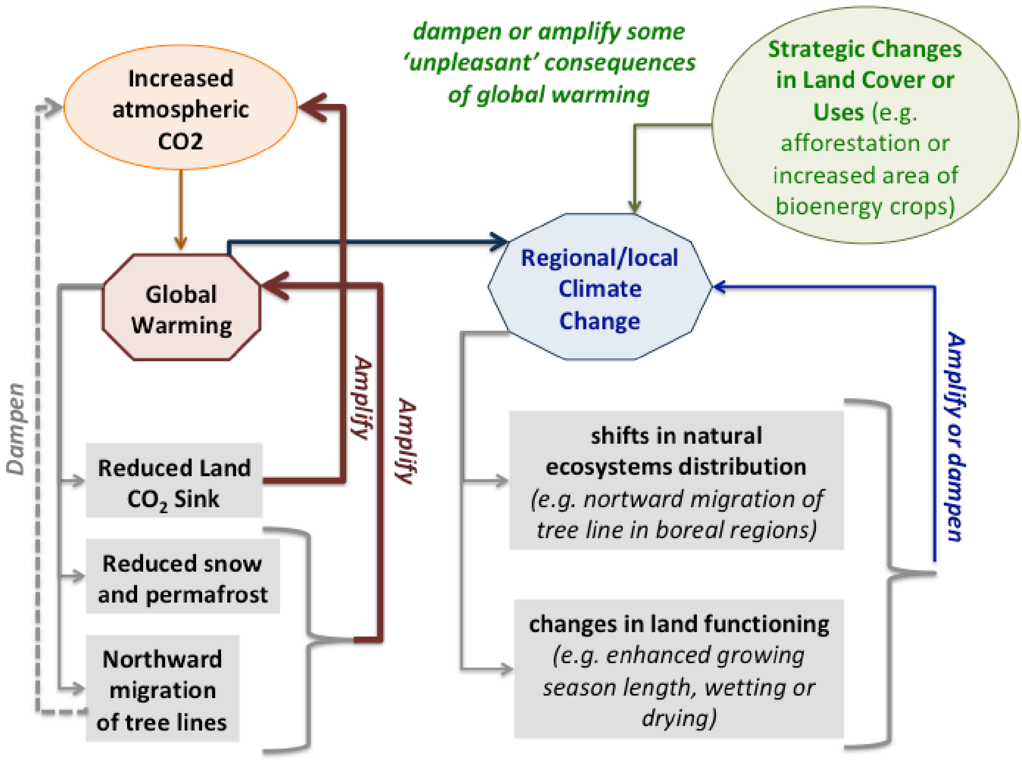

Figure 2.6.9: schematic of the various ways Land has been shown to either amplify or dampen the initial climate change, at the global scale (left panel) or at the regional/local levels (right panel).

2.6.5.1 Land feedbacks on global warming

There are essentially three ways (reported in the literature) through which land can amplify global warming.

The **first** one is via the expected **reduced land sink caused by rising atmospheric CO_2**. (Ciais et al. 2013) have indeed concluded that "*there is high confidence that climate change will partially offset increases in global land and ocean carbon sinks caused by rising atmospheric CO_2*". That in turn will cause more CO_2 to be stored in the atmosphere, creating a positive feedback, which would further amplify global warming (Friedlingstein et al. 2006).

The **second** one is classically discussed in other IPCC reports and goes **through the reduction of snow extent and depth in many regions of the world**, **as well as the reduction of areas experiencing permafrost** (see section 2.6.5.2).

The **third** one occurs in response to **enhanced vegetation activity** in high northern latitudes. GHG-induced warming in boreal regions provokes an increased growing season length of all vegetation types north of 60°N as well as, in many regions, a northward migration of the tree line (Jeong et al. 2014). The immediate effect of those changes in vegetation activity and distribution is a significant reduction in surface albedo especially in late winter and early spring (Figure 2.6.10). The presence of more tree vegetation at those latitudes darkens the snowy ground and allows more solar radiation to be absorbed (Loranty et al. 2014). As a consequence, the duration and the amount of snow on the ground further reduces enhancing warming at those seasons (winter and spring). On the contrary during late spring and early summer denser vegetation increases the loss of energy from the surfaces in the form of evapotranspiration (or latent heat flux) and this tends to dampen the GHG-induced warming regionally. At the annual scale however, as at the global scale, the snow-albedo-induced warming remains the dominant signal. **There is high confidence that the growth of vegetation in boreal regions will enhance late winter / early spring warming, while dampen the late spring / early summer one**, despite some findings that the growth of vegetation in boreal regions may be overestimated by climate models ((Snyder and Liess 2014)).

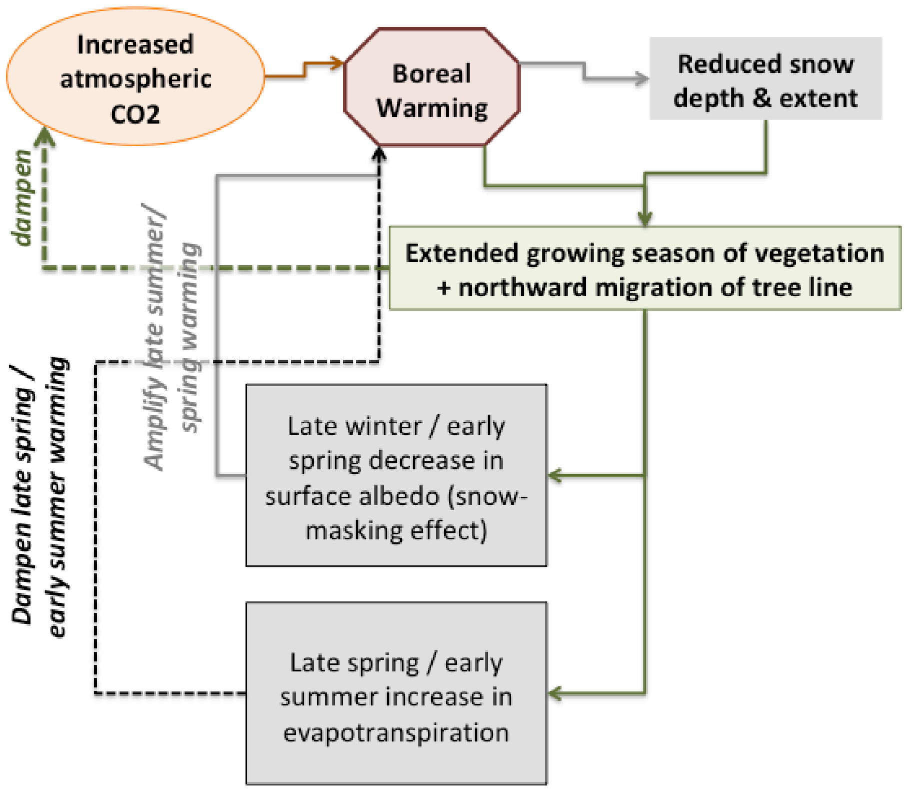

Figure 2.6.10: Schematic illustration of how climate-induced changes in vegetation distribution in the boreal regions feedback on boreal warming. The sign of the feedbacks depends on the season, although annually global warming is further enhanced in those regions. Dashed lines illustrate negative feedbacks while plain lines indicate positive feedbacks

However, at the global scale, there are evidences that **global land greening** (GLG) **dampens global annual mean temperature.** Greening essentially refers to a combination of three main changes: larger values of foliage density (often referred to as leaf area index), extended growing season length, and expansion of denser vegetation in new areas (e.g. northward expansion of treeline). Those changes can either result from global warming or from man-made changes (e.g. afforestation or changes in agricultural practices).

Historical GLG has been observed and reported **since about 1982** (see section 2.3). There is some evidence that it **has contributed to dampen the historical climate warming** since 1982 (Zeng et al. 2017) by 0.009±0.02°C. Increased latent heat flux, following greening, explains 70% of this increase, while changes in shortwave radiation only explains 21% and changes in atmospheric circulation 44%. The warming induced by those 3 processes has been counteracted by cooling-induced changes from albedo (-6%) and atmospheric long wave radiation (-29%). This greening has been shown to influence not only global warming but also the global hydrological cycle as it enhances it: wetter regions have increased both evapotranspiration and precipitation (Zeng et al. 2018). On the other hand, an enhanced warming of ~0.11°C is reported by (Strengers et al. 2010) in response to large increases in tree cover between 1871 and 2007 in their modeling study, but their analysis does not account for the net increase in CO_2 sink resulting from land greening. Moreover oceanic feedbacks are not accounted for.

Future climate-induced GLP has been examined by (Port et al. 2012) in a RCP 8.5 world with natural vegetation dynamics but no land use induced land cover changes. The global greening draws CO_2 down from the atmosphere, inducing cooling of the ambient air temperature. Greening is no realised everywhere on Earth as tropical trees tend to decrease due to increased drought, especially in the Amazon. Biophysical warming is simulated in response to increased tree cover in high northern latitudes, and decreased tree cover in the tropics. This warming however does not entirely compensate for the biogeochemically-induced cooling. A **net mean global annual cooling of ~-0.22°C** is obtained at the end of the 23rd century. In idealised experiments where atmospheric CO_2 is either doubled or quadrupled, (O'ishi et al. 2009) reported that letting natural vegetation interact with climate change amplifies the initial warming through increased land greening, and thereby enhances by ~10% the climatic sensitivity of their model. This however only accounts for biophysical effects. Inclusion of biogeochemical effects would lower this increase in sensitivity.

2.6.5.2 Relevant effects of, and feedbacks from, high-latitude land-surface changes

In the high latitudes, there is little land use and thus very little directly induced land cover change. However, past climate changes had, and future global changes are projected to have, large effects on high-latitude surface processes and characteristics, and these had, in turn, large-scale effects. A number of climate feedbacks involving high-latitude land surfaces have been identified. Of these feedbacks, the most well-known, and arguably the most important ones because of the large-scale impacts, are the snow albedo feedback and the permafrost carbon feedback. Here we assess recent progress in the quantification of regional and global effects of high-latitude land-surface changes.

A critical element of the snow albedo feedback is the shortwave radiative forcing exerted by the highly reflective snow. Following Flanner et al. (2011), Singh et al. (2015) recently evaluated the all-sky global land snow shortwave radiative effect to be around -2.5 ± 0.5 Wm^{-2}. In the Southern Hemisphere, the Antarctic contribution ($\approx$ -3.1 ± 0.3 Wm^{-2}) is by far dominant, while in the Northern Hemisphere, this is essentially attributable to seasonal snow ($\approx$ -1.5 ± 0.5 Wm^{-2}), with a smaller contribution ($\approx$ -0.45±0.10 Wm-2) from glaciated areas. Ongoing (e.g., (Derksen and Brown 2012)) and projected (e.g., (Brutel-Vuilmet et al. 2013)) decrease of seasonal snow cover in the Northern Hemisphere will lead to a reduction of this radiative forcing (e.g., (Perket et al. 2014)) within the 21st century (*robust evidence, strong agreement*).

The second element of the snow albedo feedback loop is the sensitivity of snow cover to temperature. (Mudryk et al. 2017) have recently shown that in the high latitudes, climate models tend to correctly represent this sensitivity, while in mid-latitude and alpine regions, the simulated snow cover sensitivity to temperature variations tends to be biased weak. In total, the global snow albedo feedback is about $0.1Wm^{-2}K^{-1}$, which amounts to about 7% of the strength of the globally dominant water vapour feedback (e.g., (Thackeray and Fletcher 2015). As the dominant part of the surface albedo feedback in the high latitudes, the snow albedo feedback is thus an important contributor to the Arctic Amplification (Pithan and Mauritsen 2014). While climate models do represent this feedback, a persistent spread in the modelled feedback strength has been noticed (Qu and Hall 2014), and on average, the simulated snow albedo feedback strength tends to be somewhat weaker than in reality (Flanner et al. 2011; Thackeray and Fletcher 2015); interestingly, this also appears to be the case for the broader global land surface albedo feedback (Crook and Forster 2014). Various reasons for the spread and biases of the simulated snow albedo feedback have been identified, notably inadequate representations of vegetation masking of snow in forested areas (Loranty et al. 2014; Thackeray and Fletcher 2015; Wang et al. 2016b)

Besides snow masking, recent literature highlights other snow-vegetation interactions: a) variations of snow melt dates on the regional spring carbon uptake (Pulliainen et al. 2017), and b) vegetation impacts on snow structure, with lower average snow density and thermal conductivity in shrub-dominated areas than on herb tundra (Domine et al. 2016) Observed shrub encroachment on low-growth tundra (e.g., (Frost and Epstein 2014; Myers-Smith et al. 2015; Myers-Smith and Hik 2018) an important aspect of the generally observed Arctic vegetation biomass increase known as “Arctic Greening” (see section 2.2), which is partly compensated by more local “Arctic Browning” events induced by climate extremes and perturbations such as fire (Phoenix and Bjerke 2016), can thus lead to a better insulation of underlying soil in winter and thus possibly accelerate permafrost thaw (e.g., (Wang et al. 2016b)). More generally, an analysis of observed relationships between vegetation and albedo, evapotranspiration and biomass (Pearson et al. 2013) suggests overall feedbacks to climate change from expected future Arctic Greening, consistent with model projections (Bonfils et al. 2012).

Recent years have seen large progress in the quantification of the permafrost carbon feedback, which is caused by the decomposition of organic matter in previously frozen soil after permafrost decay in a warming climate, which, depending on the soil moisture state, leads to the emission of carbon dioxide and/or methane and thus further warming. The magnitude of this feedback in reality and models depends on several critical factors, among which the most important ones are the size of the permafrost carbon pool, its decomposability, the characteristics of future high-latitude climate change and the correct identification and model representation of the processes at play (Schuur et al. 2015). The most recent comprehensive estimates establish a total soil organic carbon storage of about 1500 ± 200 PgC (Hugelius et al. 2014, 2013; Olefeldt et al. 2016), which is about 300 PgC lower than previous estimates. Important progress has been made in recent years at incorporating permafrost-related processes in complex Earth System Models (e.g., (McGuire et al. 2018), but representations of some critical processes such as thermokarst formation are still in their infancy (Schuur et al. 2015). Recent model-based estimates of future permafrost carbon release, based on offline land simulations (e.g., (Koven et al. 2015; McGuire et al. 2018) have converged on the insight that substantial carbon release of the coupled vegetation-permafrost system will likely not occur before about 2100, because carbon uptake by increased vegetation growth will initially compensate for beginning release of old permafrost carbon. Another important emerging insight is that the permafrost carbon feedback will probably amplify the expected global-mean surface air temperature increase by 2100 by less than about 20% compared to its assessed value in the absence of this feedback (Crichton et al. 2016; Burke et al. 2017) because of slow carbon decomposition at depth and compensation by vegetation growth; however, currently neglected abrupt processes such as thermokarst formation might induce faster changes (Schuur et al. 2015). Furthermore, the few available studies tend to consistently suggest that the permafrost carbon feedback is relatively more important (in terms of additional warming with respect to the directly induced warming by human greenhouse gas emissions) in heavy-mitigation climate change scenarios (Crichton et al. 2016; Burke et al. 2017), essentially because the quantity of carbon released from permafrost will be approximately a linear function of the expected warming, while the additional permafrost-induced warming is a logarithmic function of the additionally emitted carbon.

2.6.5.3 Land feedbacks on regional climate changes

Many studies have emphasised the role of climate-induced changes in soil moisture on the enhancement or dampening of regional climate changes. **There is for example (high) confidence that the climate-induced aridity in the subtropics and temperate latitudes is significantly enhanced by the existence of soil moisture feedbacks** ((Berg et al. 2016)). Figure 2.6.11 shows how the initial warming-induced decrease in precipitation (Pdec) and increase in potential evapotranspiration and latent heat flux (Einc) leads to decreased soil moisture at those latitudes and amplifies both Pdec and Einc. Soil moisture is also key to the amplification of projected extreme heat waves or drought events especially in south European regions as discussed in section 2.6.3.

Such feature is consistent with more and more evidence that in a warmer climate land and atmosphere will be more strongly coupled via both the water and the energy cycles (Dirmeyer et al. 2014; Guo et al. 2006). This increased sensitivity of atmospheric response to land perturbations implies that changes in **land uses and cover are expected, in the future, to have more impact on climate than they do today**.

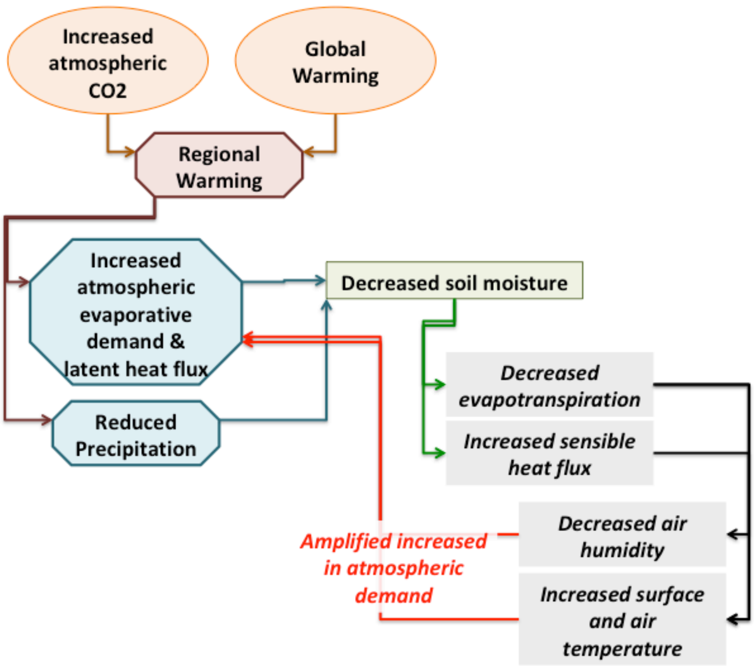

Figure 2.6.11: schematic illustration of how land/atmosphere feeds back on the warming-induced aridity in the subtropics and some temperate regions, via climate-induced changes in soil moisture

In the Amazon, despite the CO_2 fertilisation effects, future tropical warming and reduced precipitation will provoke decreases in tree cover and shortened growing season (Figure 2.6.12; (Port et al. 2012)). This in turn will decrease evapotranspiration and atmospheric humidity, with positive feedbacks on rainfall that may be further reduced, thereby amplifying the GHG-induced change. Feedbacks on GHG-induced warming are less certain as decreased latent heat flux warms the land & the overlying atmosphere, while decreased air humidity has both warming and cooling effects: cooling via decreases in incoming long-wave radiation, warming via decreases in cloudiness and thereby increased incoming solar radiation. **There is very *little agreement and confidence* on amplified drying from vegetation feedbacks but there is medium *agreement and high confidence* that those changes will amplify tropical warming.**

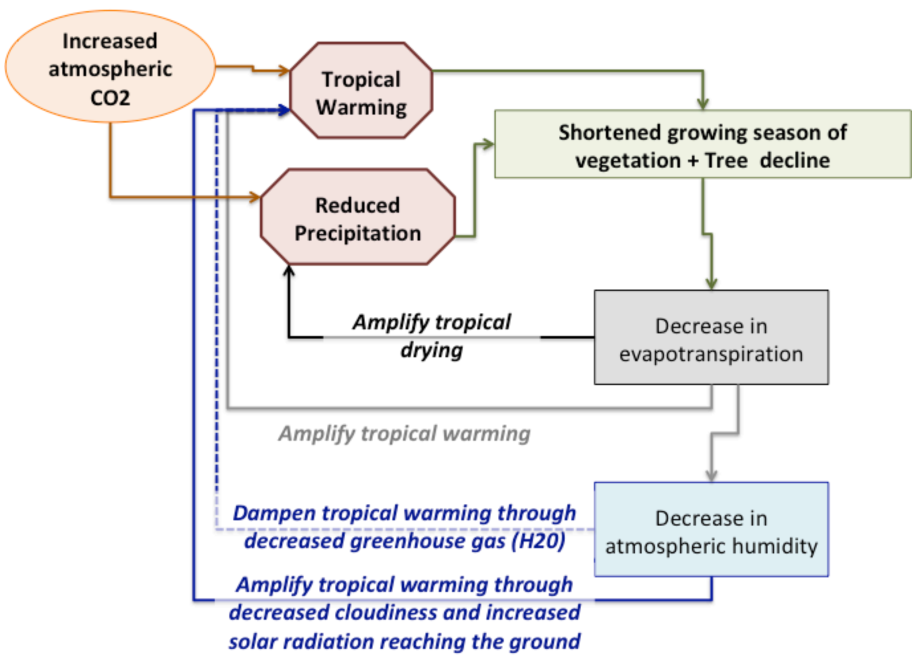

Figure 2.6.12: Schematic illustration of how climate-induced changes in vegetation distribution in the Amazon region feedback on tropical warming and drying. Despite many feedbacks occur simultaneously and in opposite

direction, it is very likely that tree decline will amplify tropical warming while there is no agreement regarding the amplification of tropical drying. Dashed lines illustrate negative feedbacks while plain lines indicate positive feedbacks

In moisture limited regions (e.g. **at the margin of desertic regions**) CO_2 fertilisation increases water use efficiency and therefore the growth of vegetation. If this is accompanied with GHG-induced changes in precipitation, positive feedbacks are activated and leads to both enhanced rainfall and greening ((Port et al. 2012)). Models that simulate increases in **African monsoon** rains northward of their today's position in response to future global warming scenarios induce greening in the southern margin of the Sahara, that is further amplified by increases in evapotranspiration and rainfall (Wu et al. 2016;Yu et al. 2016). **There is *high agreement* that such feedbacks will be triggered if rainfall is increased in those regions in response to global warming.** Confidence on the right direction of such feedbacks is based on a significant number of paleoclimate studies that analysed how vegetation dynamics helped maintain a northward position of the african monsoon during the Holocene time period (9 to 6 kyr BP) (De Noblet-Ducoudré et al. 2000; Rachmayani et al. 2015).

In **North America**, increased CO_2 and warmer conditions in both RCP4.5 and RCP8.5 induce longer growing season in mid and high latitudes through earlier leaf onset (21 days in RCP4.5 and 27 days in RCP8.5; (Garnaud and Sushama 2015)). This **greening enhances the initial GHG-induced warming in scenarios and both spring and summer seasons (+4.3°C and +5 °C respectively for spring and summer in RCP4.5; +4.9 and +5.6 in RCP8.5)**. In south eastern US, in RCP8.5, warming induces summer temperatures that often exceed 34°C by the end of the century and are thus limiting vegetation growth. In this region and scenario there is no significant change in vegetation greenness and no feedback on ambient air temperature. Those simulations however do not account for changes in natural vegetation distribution.

(Refer to chapter 3 that should report on e.g. desert amplification of climate change, or include such discussion herein)

2.6.5.4 Combining land uses or management options with projected regional climate change

Future global afforestation has been tested for SRES A2 in a fully coupled global climate model. Afforestation of either 50% or 100% of the total agricultural area has been gradually prescribed between years 2011 and 2060. In addition boreal, temperate and tropical deforestation have been tested separately. Both biophysical and biogeochemical effects have been accounted for (Arora and Montenegro 2011).**The net impacts of afforestation was quite marginal compared to the GHG-induced global warming** (+3°C at the end of the 21st century) but was indeed the expected cooling effect (from -0.04°C to -0.45°C depending on the location and magnitude of the additional forest cover). Consistent with previous experiments, increasing forests in boreal regions induced biophysical warming and biogeochemical cooling while increasing tree cover in the tropics led to both biophysical and biogeochemical cooling. The authors conclude that **tropical afforestation is three times more effective in cooling down climate than are boreal or temperate afforestation**.

Less extreme afforestation has been tested in the warmer world predicted by RCP 8.5 scenario, and the net impact of afforestation was examined, combining both biophysical and biogeochemical effects (Sonntag et al. 2016, 2018). 8Mkm2 of forests were added globally, following the land use RCP 4.5 scenario. **The global cooling resulting from this increase in forest area is too small (-0.27°C annually) to dampen the RCP8.5 warming**. It however reaches ~-1°C in some temperate regions and -2.5°C in boreal ones. This is accompanied by a reduction in the number of extremely warm days. Detailed regional analysis of this global run however shows that **dampening in the densely populated areas is quite small, while it can be very large in sparsely populated areas**. (Such scenarios may therefore not directly benefit societies.)

As discussed in section 2.6.2.1 **afforestation in West African countries** have the potential to **dampen partially, or even totally at some places, the GHG-induced warming and drying in the deforested regions** (Abiodun et al. 2012). However **this is compensated by enhanced warming and drying in adjacent countries**.

Large-scale **afforestation of western Europe in the SRES A2 scenario** shows small damping potential of additional forest on ambient air temperature (land-induced cooling of ~-0.5°C versus GHG-induced warming larger than 2.5°C; Figure 2.6.**13**; (Gálos et al. 2013)). Influence on rainfall was however much larger and significant. While Germany, France and Ukraine experienced decreases in **annual rainfall** following warming, afforestation **can revert this signal in Germany and significantly dampen it in both France & Ukraine** (Figure 2.6.**13**). In addition the warming-induced increase in the number of dry days is dampened by afforestation while the number of extreme precipitation events is amplified.

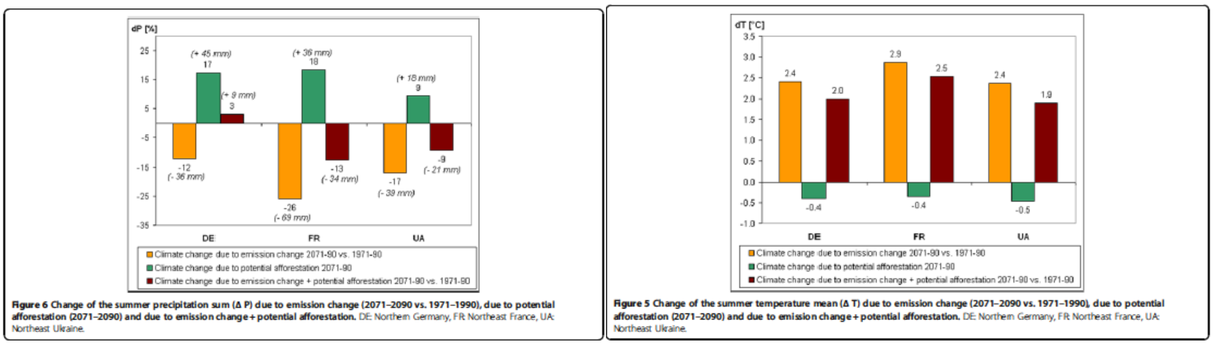

Figure 2.6.13**: Afforestation induced changes in ambient air temperature and total rainfall in three part**s of Europe (Germany, France and Ukraine), compared to GHG-induced changes following SRES A2 scenario **(Gálos et al. 2013)**

2.7 Climate consequences of land-based mitigation and adaptation

In this section we assess the climate impacts of land based mitigation and adaptation activities. Land management often affects mitigation and adaptation simultaneously. Adaptation options specific to desertification, degradation and food security are described in more detail in chapters 3, 4 and 5. Chapter 6 explores the interplay between mitigation and adaptation in terms of sustainable land management as well as other non-climate synergies and trade-offs including impacts on a range of ecosystem services, planetary boundaries and sustainable development goals. Climate mitigation in the land sector aims to decrease net GHG emissions and enhance carbon stocks. Climate adaptation measures also often protect or increase vegetation cover or soil carbon stocks and aim to increase agricultural productivity thereby decreasing the need for agricultural expansion and associate emissions from land use change.

Climate mitigation options in the AFOLU sector in AR5 chapter 11(Conway 2012a) were separated into supply-side mitigation options (e.g. reducing GHG emissions per unit of land / animal, or per unit of product), or demand-side options (e.g. reducing demand for food and fibre products that have high GHG emissions, reducing waste. We follow that approach below. Options that result in a net removal of GHGs from the atmosphere and storage (in living or dead plant material, soils, timber, biochar or in underground storage through Carbon Capture and Storage associated with bioenergy – BECCS) are frequently referred to in the literature as carbon dioxide removal (CDR), Greenhouse Gas Removal (GGR) and negative emissions technologies (NETs).

Since AR5 there is a wealth of new literature on individual management options. Different options interact with each other; they may have additive effects or compete with each other land or other inputs. Several assessments have aggregated across the literature to assess mitigation potential of individual of single options building on AR5 updating the literature and including new options (Section 2.7.1). The demand for, and potential of, land based mitigation under given climate mitigation targets is influenced by wider socioeconomic conditions, the interplay between different land-based mitigation options as well as with mitigation options in other sectors (such as energy or transport) and interaction with other sustainability goals. Thus in section 2.7.2 we look at modelled integrated assessment pathways highlighting the role of the land sector in contributing to specific mitigation pathways (2.7.2). At the end of this section we deal with policy issues related specifically to GHG flux under the Paris Agreement (2.7.3). Chapter 7 deals further policy and governance issues.

2.7.1 Land management options for climate mitigation

Estimates of available land plays a large part in uncertainty of the mitigation potential. Most mitigation estimates prioritise food production, fiber and some degree of habitat protection before implementing mitigation options. Thus estimates of mitigation potential are very sensitive to what is considered "available" land, and assumptions about future agricultural intensification (high crop yields, intensified pasture management and livestock production systems may decrease the need for agricultural expansion and in consequence free up more land for mitigation), use of fertilisers and irrigation, approaches to land protection or restoration (e.g. REDD+ projects), diet shifts away from high land intensity products, and reduction of waste. The amount of land converted, the prior land cover, the location of activity and the required inputs (fertiliser, energy, etc.) alter the net GHG flux across the lifecycle of the mitigation option, and also biophysical climate effects. Differences in estimates also stem from varying definitions of land cover or activity, time periods assessed, assumptions in population or demand for food and timber products, and carbon pools included (some only include aboveground biomass, while others include belowground biomass, dead wood, litter and soil, and even whether soil is peat). Some also include full life-cycle analysis from change in land cover, through inputs used to transport and product disposal.

Permanence is a key uncertainty regarding longevity of land based mitigation and adaptation options as carbon stored in biomass and soils are at risk of climate change (e.g. increase soil decomposition at higher temperatures) and natural disturbances, which may increase in future due to climate change e.g. fire, disease, wind throw, drought (section 3, 2.4). Furthermore, management may change in the future e.g. harvesting of forests.

When combining estimates from multiple bottom-up studies and sources, there are a range of methodologies reflected that may not be directly comparable or additive. Some of the studies assesses a technical mitigation potential only ("the amount of emissions reductions and carbon sequestration possible with current technologies without economic and political constraints" (Roe et al. 2018)). Some include biophysical or resource constraints (e.g. limits to yields or irrigation), or assess mitigation at different carbon prices – "economic mitigation potential". The multi-option assessment of Smith et al. (2017) focused land-based CDR options and explored resource and sustainability issues (Chapter 6). (Griscom et al. 2017) focused on "Nature based solutions", calculating potentials broken down by country after accounting for constraints around the production of food, fiber hand habitat for biological diversity (Fig 2.7.1). They explored 2 carbon prices 10 US$/Mg$CO_2$e to approximate existing prices, and 100 US$/Mg$CO_2$e as a maximum cost of emission reduction. Roe et al. (In press) used data from (Griscom et al. 2017)., FAOSTAT and other literature (see Figure 2.7.2) to produce technical mitigation potential estimates globally and by country. They further combined their literature based assessment with their own model estimates and that of published integrated assessment models to highlight possible optimised future land based mitigation.

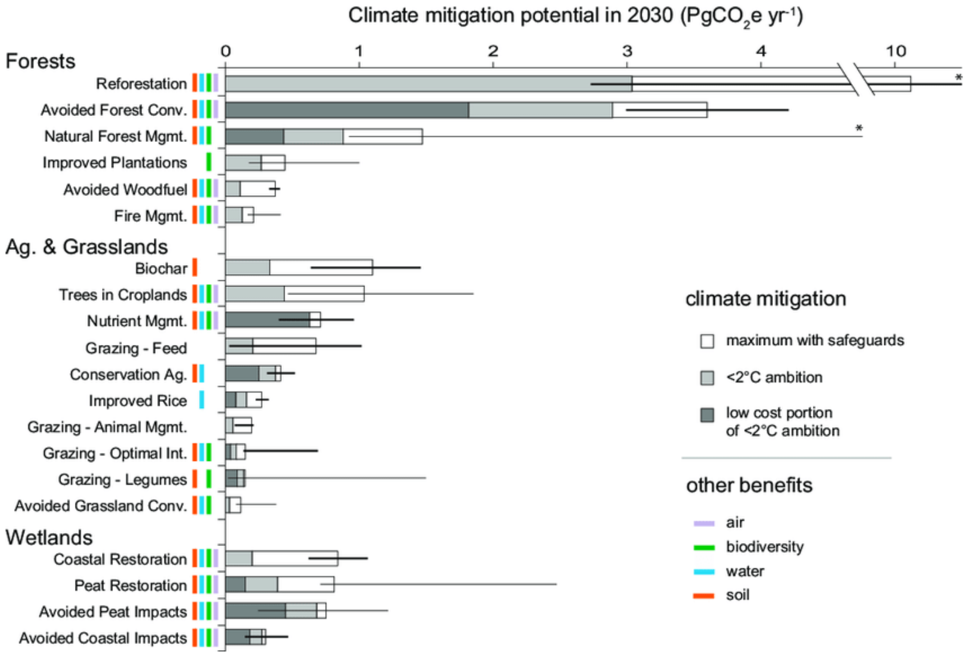

Figure 2.7.1. Climate mitigation potential of 20 "natural pathways" (Griscom et al. 2017). Maximum climate mitigation potential with safeguards for reference year 2030. Light gray portions of bars represent cost-effective mitigation levels assuming a global ambition to hold warming to <2 °C (<100 USD $MgCO_2\,e^{-1}\,y^{-1}$). Dark gray portions of bars indicate low cost (<10 USD $MgCO_2\,e^{-1}\,y^{-1}$) portions of <2 °C levels. Wider error bars indicate empirical estimates of 95% confidence intervals, while narrower error bars indicate estimates derived from expert elicitation. Ecosystem service benefits linked with each pathway are indicated by colored bars for biodiversity, water (filtration and flood control), soil (enrichment), and air (filtration). Asterisks indicate truncated error bars.

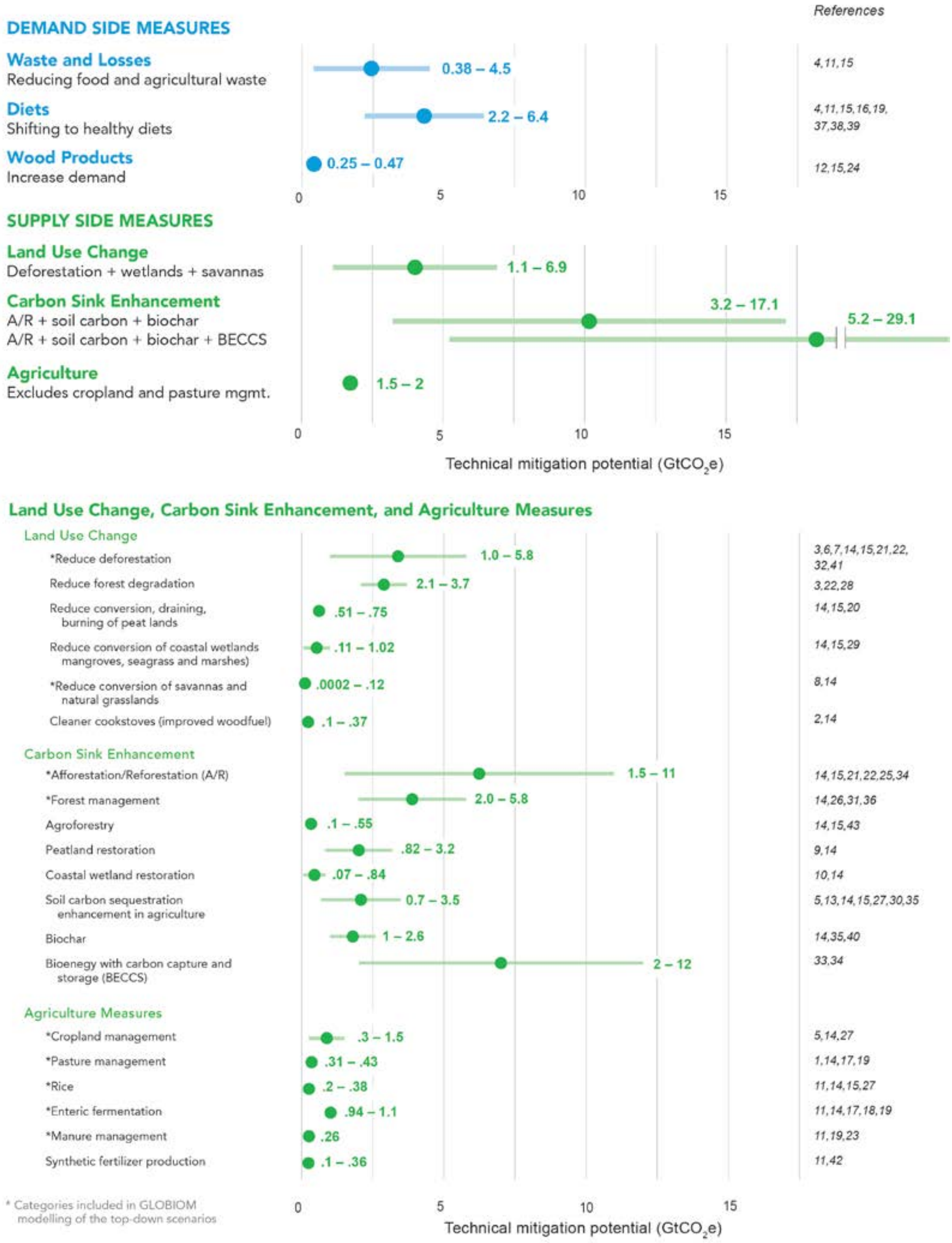

Figure 2.7.2. Land-based mitigation potential by activity type, measured in GtCO$_2$e/yr reflecting the full range of low to high estimates from literature (Roe et al. 2018) (will work with Roe to update and adapt for SOD). Includes both technical (possible with current technologies) and economic (possible given economic constraints) mitigation potential. Only includes references that explicitly provide mitigation potential estimates in CO$_2$e/yr. Provides separate estimates for total supply-side and demand-side measures as these two categories are not additive. Elements of the analysis were designed to avoid potential double-counting of emissions reductions – the summed categories are highlighted in the supply-side and demand-side measures Supply-side measures are activities that require a change in land use and/or management. Demand-side measures, are activities that require a change in consumer behaviour. References: (United Nations University 2015; Bailis et al. 2015; Baccini et al. 2017b; Change 2015; Review 2011; Busch and Engelmann 2015; Carter et al. 2015; Diaz et al. 2012; Couwenberg et al. 2010; Crooks et al. 2011; Dickie et al. 2014; Miner 2010; Obersteiner 2017; Griscom et al. 2017; Hawken 2017; Hedenus et al. 2014; Henderson et al. 2015; Herrero et al. 2013, 2016; Hooijer et al. 2010; Houghton and Nassikas 2017; Hristov et al. 2013; Kauppi et al. 2001; Lenton 2014; Nabuurs et al. 2007; Paustian et al. 2016a; Pearson et al. 2017; Pendleton et al. 2012; Sanderman et al. 2017; Sasaki et al. 2016; Smith et al. 2013a; Pete et al. 2015; Baron et al. 2009; Springmann et al. 2016; Stehfest et al. 2009; Tilman and Clark 2014; Das et al. 2014; Zarin et al. 2016b; Zhang et al. 2013b; Gharajehdaghipour et al. 2016)

2.7.1.1 Forestry-based mitigation and adaptation options:

Reduced deforestation, afforestation/reforestation, forest management, forest restoration and timber products.

The main strategies for forestry-based climate change mitigation include: (a) reducing emission from deforestation and degradation (REDD) (b) increasing stock though Afforestation (A), the conversion of non-forested land into forests, and reforestation (R), restoring and replanting deforested or degraded forests (c) enhancing the existing forest-related carbon sinks and stocks through Forest Management (FM), and (c) using wood-based products to reduce emissions in other sectors such as timber in buildings and bioenergy with or without long term storage. Many of these options are widely practiced already throughout the world. They are thus often used in modelled scenarios as immediately available mitigation methods, while other technologies are being developed and deployed. While the costs of implementing A/R and REDD may in themselves be low (not accounting for macro-economic consequences), finance is often needed to compensate for loss of alternative income.

The maximum potential for reduced deforestation and degradation is equal to current net emissions. When deforestation and degradation are halted, some gross emissions would continue, because of ongoing decomposition of residues and soil carbon on the deforested or logged areas, and because of the large pools of wood products that would continue to decay and burn. Mitigation would be further enhanced if forests were allowed to recover on deforested lands. There are upper limits for restoration of carbon on land and it can take many decades to recover the biomass initially present in native ecosystems. (Houghton and Nassikas 2018b) have estimated a technical (upper limit) sequestration potential of 120 PgC between 2016 and 2100 if deforestation and wood harvest were stopped and secondary forests were allowed to recover. The estimate does not consider possible expansion of forest areas. Once plants grow to maturity, they can be harvested and used for bioenergy offsetting fossil fuels (with or without carbon capture and storage) (Section 2.7.1.5), long-lived products such as timber (See below), or buried as biochar (Section 2.7.1.1), enabling areas of land to be used continuously for mitigation.

Afforestation/Reforestation can increase carbon sequestration in both vegetation and soils by 1.5-11 Gt CO_2 yr^{-1} in (Houghton 2013; Lenton 2014; Smith et al. 2016b; Griscom et al. 2017; Hawken 2017; Houghton and Nassikas 2017). The lower estimate takes into consideration the competition for land use in agriculture, and the high estimate allows all secondary forests and shifting cultivation fallow areas to naturally regenerate. The most recent mitigation potential estimates for A/R provide "realistic" figures of 4.04 $GtCO_2$ yr^{-1} by 2100 (Smith et al. 2016a) by averaging model results that factor in deployment costs in a 2°C scenario, and 3.04 $GtCO_2$ yr^{-1} by 2030 (Griscom et al. 2017)by considering spatially explicit environmental and social constraints as well as economic constraints of <\$100 per tCO_2. Future sequestration potentials for afforestation, reforestation and forest management modelled in line with the 1.5°C and 2°C scenarios, were found to increase to around 4 $GtCO_2e$ yr^{-1} by 2070, with more "realistic" bottom up estimates of about 2 $GtCO_2e$ yr^{-1} in 2050 (Roe et al. 2018). A/R takes some time for full carbon removal to be achieved as the forest grows, with net uptake of carbon slowing as forests reach maturity. While initial costs of establishing plantations can be high, the costs of regeneration and management are low. Cost estimates for afforestation and reforestation for 2100 range from \$65-108 / t C-eq (Smith et al. 2016b). Significant amounts of land are required to achieve substantial CO_2 capture, with land intensity of afforestation and reforestation estimated at 0.29 ha $tCeq^{-1}$ yr^{-1} (Smith et al. 2016b). (Boysen et al. 2017) estimated that to sequester about 100 GtC by 2100 would require 1300 Mha of abandoned cropland and pastures. The annual reforestation in 2015 was reported at 27 Mha (Section 2.4), and countries have committed to restore another 161 Mha of forests by 2030 led by China, Brazil, India and the US (FAO 2015; Climate Focus 2016).

Improving forest management includes extending rotation cycles between harvests, reducing damage to remaining trees when harvesting, reducing logging waste, implementing soil conservation practices, fertilisation, and using wood more efficiently. Forest management could potentially mitigate 2-5.78 Gt CO_2

yr^{-1} in 2030, although the upper estimate also includes other A/R interventions (Nabuurs et al. 2007; Baron et al. 2009; Sasaki et al. 2016; Griscom et al. 2017) A new study asserts that Climate Smart Forestry, a technique addressing the ecosystem, wood products and the energy supply chain in Europe, could double the forest management climate mitigation potential by 2050 (Nabuurs et al. 2007) .

Agroforestry is a land management system that combines woody biomass (e.g., trees or shrubs) with crops and/or livestock, and can include fruit or timber trees for harvest, windbreaks, riparian buffers, and silvopasture. Agroforestry systems have a long tradition in temperate regions around the world, and have also been developed as a land management practice in many developing countries, particularly for smallholder systems. The mitigation potential ranges between 0.55 – 1.04 Gt CO_2 yr^{-1} , with the higher estimate representing the tree biomass carbon increase between 2000 and 2010 (Gharajehdaghipour et al. 2016; Griscom et al. 2017; Hawken 2017) .

2.7.1.2 Use of wood products for offsetting and storage

Using wood products in construction to substitute for more GHG intensive materials like cement and steel has a two-fold effect of (a) increasing carbon storage in Harvested Wood Products (HWP) that often have a long life-cycle (Over 100 years) (Höglmeier et al. 2015; Sikkema et al. 2013), and (b) avoiding emissions from the production of concrete and steel (Sathre and O’Connor 2010; Smyth et al. 2017). If biomass harvest is followed by regrowth, then net impacts on land storage are zero over time, and the carbon going into long term storage represents negative emissions, the magnitude of which depends on the type of biomass and storage period (Cherubini et al. 2012; Earles et al. 2012; Marland et al. 2010). The displacement factor, or the substitution benefit in CO_2, when wood is used instead of another material estimated in the literature ranges range from -2.3 to 15 tCO_2 of emission reduction per tC in wood product (Sathre and O’Connor 2010). Displacements factors, as well as calculations of carbon storage from HWPs have been used to calculate mitigation potential of wood substitution in various countries including Canada (Smith et al. 2016c), the EU (Pilli et al. 2015), Germany (Knauf 2015) , the US (Mckeever 2009) and Japan (Kayo et al. 2015). However, there are limited estimates of global mitigation potential from increasing the demand of timber products to replace construction materials (Sathre and O’Connor 2010) . Roe et al.’s (in press) range of 0.25- 0.48 $GtCO_2$ of mitigation potential is relatively small compared to other demand-side measures, with the low estimate assuming a material substitution effect of $0.28tC/m^3$ of final wood product, and a roundwood volume of 0.9 billion m^3 annually (based on 2000 level demand) (Kauppi et al. 2001) and the high estimate assuming 40% of global wood products were used for construction (Miner 2010) There is concern that increased demand for wood products may reduce forest stocks, however studies have shown that increased wood demand led to higher wood prices and investments in forest management in some parts of Europe, China and New Zealand(Galik and Abt 2016; Nabuurs et al. 2017) Additional studies are needed to better understand the global dynamics (GHG emissions, trade, deforestation impacts) of increasing wood products in construction.

Combined biophysical and GHG effects of changes in forest cover: changes in forest cover can have large effects on climate not only though changes in GHG flux but also through biophysical effects (section 2.5). These should be considered in determining the overall climate mitigation effects of forests (although in reality one would also need to account for non GHG gas effects such as aerosols). In tropical areas, ground and satellite-based observational studies (refs) and modelling studies (Nobre et al. 2009; Davin and de Noblet-Ducoudre 2010) consistently indicate that deforestation causes a net biophysical warming where trees are removed and around, while globally a cooling is generally simulated when oceans are interacting (Perugini et al. 2017); section 2.6). Therefore avoided deforestation or afforeestation in the tropics contributes to climate mitigation through both biogeochemical and biophysical effects. It also maintains rainfall recycling to some extent though not always in areas afforested as discussed in section 2.6 (increases in rainfall may in neighbouring regions). In contrast, in higher latitude boreal areas observational and modelling studies show that afforestation and reforestation lead to local and global warming effects, particularly in snow covered regions in the winter as the albedo is lower for forests than bare snow.

However global effects are quite small when compared to CO_2-induced changes in temperature. Thus the biophysical effects run counter to the GHG effects in terms of climate mitigation at the local to regional scale with implications for adapation *(section 2.6).* The biophysical impacts of forest area change in mid-latitudes are complex, because of the opposite effects on climate from the typical changes in albedo and surface evapotranspiration (Ma et al. 2017b). Below 35°N, afforestation and reforestation are considered to decrease near-surface temperature because the warming effect of decreased albedo is weaker than cooling effect of increased latent heat, roughness length and rooting depth (Pielke et al. 2007; Peng et al. 2014). Therefore for recent trends of afforestation in mid-latitude regions such as China, Russia, USA and Europe(Liu et al. 2015b) the biophysical effects support the climate mitigation mediated through biogeochemical effects during the vegetation growing period, although less strongly than in tropical areas (Perugini et al. 2017). It does not support climate mitigation when there is snow on the ground. (Kreidenweis et al. 2016) showed that excluding boreal regions from afforestation does not affect carbon dioxide removal significantly. Even restricting afforestation only to tropical regions would still allow 60% of carbon sequestration in comparison to a scenario not accounting for albedo effects in boreal and temperate regions.

2.7.1.3 Soil Organic Carbon Management in agriculture and other soils

Improved management practices can turn soils into C-sinks, provided that sufficient organic matter (including plant litter, residues and manure) is retained or added to allow for balancing losses of soil organic carbon (SOC) in response to the continuing decomposition of soil organic matter (SOM). Land management practices include improved rotations with deeper rooting cultivars, low tillage, and addition of organic materials(Lal 2011b, 2013; Smith et al. 2008b; Conway 2012a). Physical protection by formation of organo-mineral soil aggregates (Six et al. 2002) and/or complexes involving fine (clay & silt) soil particles (Feng et al. 2013; Hassink and Whitmore 1997) affect SOC stabilisation and the capacity of soils to stabilise additional SOC (Beare et al. 2014), which limits increases in SOM (and associated SOC sequestration) with increased organic matter inputs. Hence, not all will sequester SOC at the same rate and length of time. Potential for soil carbon sequestration varies considerably, depending on prior and current land management approaches, soil type, resource availability, environmental conditions microbial and fungi composition and nutrient availability among other (Smith and Dukes 2013; Palm et al. 2014; Lal 2013) There is considerable uncertainty around long -term storage capacity, with sequestration rates potentially declining to negligible levels over as little as a couple of decades as they reach a new higher equilibrium carbon concentration (West et al. 2004; Smith and Dukes 2013).

There is *high agreement and medium evidence* that adoption of green manure cover crops, while increasing cropping frequency or diversity, helps sequestering SOC (Poeplau and Don 2015; Mazzoncini et al. 2011; Luo et al. 2010). In sub-Saharan Africa, agroforestry systems were shown to (re-)sequester SOC (Corbeels et al. 2018). There is medium evidence that conservation agriculture, i.e. the simultaneous adoption of minimum tillage, (cover) crop residue retention and associated soil surface coverage, and crop rotations, can contribute to SOC sequestration; both, positive (Powlson et al. 2016; Zhang et al. 2014) and inconclusive cases (Cheesman et al. 2016; Palm et al. 2014; Govaerts et al. 2009), have been published. In a systematic review of literature covering the global boreo-temperate regions, reduced tillage alone was shown to lead to an increase stock of SOC in the topsoil only, but differences were no longer significant if observation reference was extended to 60 cm depth (Haddaway et al. 2017). Likewise, no significant increase in SOC was observed comparing no-till and conventional tillage in a meta-analysis using global data set of soils where sampling extended to below 40 cm (Luo et al. 2010). The benefit of conservation or no till agriculture was shown to be often an artefact of shallow sampling or comparison of soil layers that differ in bulk density and hence mass (Luo et al. 2010), and the lack of robust comparisons of soils on an equivalent mass basis continues to be an problem for credible estimates (Wendt and Hauser 2013; Powlson et al. 2011).

When scaled globally, the technical potential for soil carbon sequestration has been estimated between 1.1 and 11.4 $GtCO_2$ pa, with more conservative estimates between 3.6 and 6.9 $GtCO_2$ pa (Conant et al. 2011; Lal 2011b, 2013; Minasny and McBratney 2018b). Roe et al. (2018) estimated the soil mitigation potential in agricultural systems through conservation agriculture practices (including reduced tillage, crop residue management, use of perennials or deeper rooted cultivars, organic amendment and fire management), and pasture management (including managing stocking rates, timing and rotation of livestock, higher productivity grass species or legumes, and nutrient management) to be 0.7-3.5 Gt CO_2/yr (Review 2011; Frank et al. 2017; Smith et al. 2016b; Griscom et al. 2017; Hawken 2017; Paustian et al. 2016b; Sanderman et al. 2017) Assuming unit costs limited to between 5 and 25 US$ per tCO_2 yields estimates of global carbon emission mitigation potentials of soil carbon sequestration between 1.5 and 2.6 $GtCO_2$ pa for a period of 10-20 years (Smith et al. 2008b, 2016b).

Soil carbon management does not have specific land requirements as it happens in situ on existing land use, but it requires changes in practices that may affect other aspects of lad management. Soil carbon management interacts with- N_2O emissions. For example, (Li et al. 2005) estimate that the management strategies required to increase C sequestration (reduced tillage, crop residue, and manure recycling) would increase N_2O emissions significantly, offsetting 75%-310% of the C sequestered.

Biochar

Biochar is produced by thermal decomposition of biomass in the absence of oxygen (pyrolysis) into a stable, long-lived product like charcoal that is relatively resistant to decomposition (Lehmann et al. 2015) and which can stabilise organic matter added to soil (Han Weng et al. 2017) Although it is an established technology, it is not widely practiced. It is estimated that, on a life cycle basis, biochar produced from different crops can remove between 2.1 to 4.8 tCO_2 per tonne of biochar (Hammond et al. 2009; Roy and Dias 2017). This takes into account crop cultivation, biochar production by pyrolysis, carbon sequestration by biochar used as a soil improver and system credits for electricity generation by pyrolysis. Scaled globally, biochar to use for soil amendment has the potential to mitigate 1-2.57 Gt CO_2/yr (Das et al. 2014; Smith et al. 2016b; Griscom et al. 2017) (the higher end of the estimate) assumes bioenergy crops can be used to make biochar and includes syn-gas production as offsetting fossil fuel usage. Griscom et al. (2017) (the lower estimate) uses a bottom up calculation of available residues and pyrolysis efficiency.

2.7.1.4 Agriculture-based mitigation options

(note the following text is primarily adapted from Roe et al, need to incorporate other sources for SOD. Need to link with chapter 5)

Due to increasing demand for food, fuel, and fiber, agricultural emissions are projected to increase by 30% relative to the 2001-2010 average by 2050 (Tubiello et al. 2014). Since agriculture accounts for 56% of methane emissions, and 27% of all potent short-lived gases (Sections 2.4 and 2.5), measures addressing enteric fermentation, manure management and rice CH_4 emissions would reduce global warming effects sooner and may offset some delays in reducing emissions or increasing sinks for CO_2 or enable etra allowable CO_2 emissions in meeting the goals of the Paris Agreement (Montzka et al. 2011; Collins et al. 2018).

Sustainable intensification reduces the emissions intensity of agriculture by using inputs more efficiently or adding new inputs that address limiting factors of production. These practices are typically based on changes or increases in the use of direct inputs, such as improved varieties/breeds, nutrient and organic amendments, water and mechanisation. In addition, a variety of farming practices can be adopted that optimise density, rotations and precision of inputs. In addition, sustainable intensification could lower agricultural expansion rates and hence GHG emissions from land use change (Garnett et al. 2013).

Reducing emissions intensity from enteric fermentation, manure management, rice fields and fertiliser production has a total mitigation potential of 1.5-2.1 Gt CO_2 yr^{-1} (Roe et al. 2018) from references(Hristov et al. 2013; Zhang et al. 2013a; United Nations University 2015; Dickie et al. 2014; Henderson et al. 2015;

Herrero et al. 2016; Paustian et al. 2016a; Griscom et al. 2017). The mitigation potential of cropland management (plant, nutrient and soil management) is 0.3-1.5 Gt CO_2 yr^{-1} (Review 2011; Paustian et al. 2016b) , and pasture management (plant, manure and fire management) is 0.31-0.43 Gt CO_2 yr^{-1} (Anderson and Peters 2016; Henderson et al. 2015; Paustian et al. 2016b; Griscom et al. 2017; Herrero et al. 2016). Enteric fermentation is responsible for over 40% of direct agricultural emissions with beef and dairy cattle accounting for approximately 65% (Herrero et al. 2016). The three main measures to reduce enteric fermentation include improved diets (higher quality, more digestible livestock feed), supplements and additives (reduce methane by changing the microbiology of the rumen), and animal management and breeding (improve husbandry practices and genetics) (Dickie et al. 2014). Applying these measures can mitigate 0.94-1.08 Gt CO_2 yr^{-1} (Dickie et al. 2014; Henderson et al. 2015; Herrero et al. 2013, 2016; Griscom et al. 2017). Most livestock production systems in highly developed countries (e.g., the U.S., E.U., Australia, and Canada) have intensified systems and thus have lower mitigation potential per unit compared to developing countries with large livestock herds managed at low productivity levels, suboptimal diets, nutrition and herd structure (e.g., India, Latin America and Sub-Saharan Africa). These developing countries have higher mitigation potential gains from sustainable intensification.

Manure from livestock cause both nitrous oxide and methane emissions, and account for roughly one quarter of direct agricultural GHG emissions (Dickie et al. 2014). Although stored manure accounts for a relatively small amount of direct agricultural emissions, it is technically possible to mitigate a very high percentage of these emissions (as much as 70% for most systems), or approximately 0.26 Gt CO_2 yr^{-1} (Hristov et al. 2013; Dickie et al. 2014; Herrero et al. 2016). The highest manure management emissions come from China, India, the US and the EU. Measures to manage manure include anaerobic digestion for energy use, composting as a nutrient source, reducing storage time, and changing livestock diets. Improved manure management practices have important co-benefits including reducing water and air pollution, and increased yields and income from nutrient and energy inputs produced.

Rice production contributes about 11% of emissions from agriculture and 90% of this is from Asia (FAO 2015). The top rice producing countries-China, India, Indonesia, Thailand, Philippines, Vietnam Bangladesh, and Myanmar-account for more than 85% of global rice emissions. Reducing emissions from rice production through improved water management (periodic draining of flooded fields to reduce methane emissions from anaerobic decomposition), and straw residue management (apply in dry conditions instead of on flooded fields, avoid burning to reduce methane and nitrous oxide emissions) has the potential to mitigate up to 60% of emissions (Hussain et al. 2015), or 0.2-0.38 Gt CO_2 yr^{-1} (Dickie et al. 2014; Paustian et al. 2016b; Griscom et al. 2017; Hawken 2017). While well managed rice fields can increase yields and reduce water needs, correct management of water levels requires precise control of irrigated systems and high technical capacity that may present barriers to adoption (Dickie et al. 2014)

Synthetic fertiliser production is a major source of GHG emissions and air pollution as it requires a large amount of energy to produce, and uses fossil fuels (natural gas or coal) as feedstocks. China has the largest emissions from synthetic fertiliser production as they have older, less efficient plants and use coal feedstocks (Dickie et al. 2014) . Improvements in industrial efficiency are typically cost effective, would improve the productivity of the sector, reduce pollution, and have the potential to mitigate 0.10 to 0.36 Gt CO_2e yr^{-1} in China (there are no global estimates) (Zhang et al. 2013b; Dickie et al. 2014)..

Efficiency improvements from sustainable intensification generally produce productivity gains and improve farmers' livelihoods, especially smallholders. If managed well, intensification can also spare land/avoid land conversion because greater agricultural production occurs on the same area of land. However, efficiency improvements also carry the risk of environmental and social trade-offs that need to be managed. Intensification will likely produce an increase in fertiliser use and other agrochemicals which may increase emissions and pollution. Further, more efficient production methods can reduce costs and increase yields, and therefore, may encourage farmers to further increase production and expand land use (deforest) (Lambin and Meyfroidt 2011).

2.7.1.5 Protection and restoration of wetlands, peatlands and coastal habitats (blue carbon)

Protection and restoration of wetlands, peatlands and coastal habitats (such as Manrove forests, salt marshes and seagrass meadows) reduces net carbon loss (primarily from sediment/soils) and provides continue or enhanced natural CO_2 removal. Wetland drainage and rewetting was included as a flux category under the second commitment Period of the Kyoto protocol, this incentivising activity, with significant management knowledge gained over the last decade (IPCC 2014). However there are high uncertainties as to the carbon storage and flux rates, in particular the balance between CH_4 sources and CO_2 sinks, with implications for confidence in monitoring reporting and verification of GHX flux within national carbon accounting schemes (Spencer et al. 2016). Restoring some wetlands could induce a short-term net warming effect, due to increased emissions of methane and nitrous oxide. Dedicated and sustained research is needed to resolve or reduce these uncertainties. Permanence is a key risk in these ecosystems as peatlands in particular may be vulnerable to changes in temperature and precipitation (Clark et al. 2010; Gallego-Sala and et 2010).

Reducing annual emissions from peatland conversion, draining and burning would mitigate 0.51-0.75 Gt $CO_2e\ yr^{-1}$ (Griscom et al. 2017; Hooijer et al. 2010). Approximately 1 Gt $CO_2\ yr^{-1}$ can be mitigated if 30% of the 65 Mha of drained peatlands were rewetted to stop continued emissions from carbon oxidation, and about 3.2 Gt $CO_2\ yr^{-1}$ if all ongoing CO_2 emissions from continued peat oxidation were ceased (Joosten and Couwenberg 2008). Griscom et al. (2017) estimate 0.81 Gt $CO_2\ yr^{-1}$ as a feasible target (<USD100 tCO_2e^{-1}) for rewetting and biomass enhancement.

The climate mitigation potential of mangrove forests is considered in Chapter 5 of the IPCC Special Report on the Ocean, Cryosphere and Climate Change, in a wider ‘blue carbon’ context. There is *high confidence* that climatically-significant carbon losses from mangrove land use change (Section 2.4) can be prevented, primarily by increased enforcement of existing regulatory measures (Miteva 2016; Howard et al. 2017; Herr et al. 2017). Commitments to strengthen mangrove protection and conservation have been made in many Nationally Determined Contributions (NDCs) to the Paris Agreement (Gallo et al. 2017). The ongoing benefits provided by mangroves as a natural carbon sink can also be nationally-important for Small Island Developing States (SIDS), based on estimates of high carbon sequestration rates per unit area (McLeod et al. 2011; Duarte et al. 2013; Duarte 2017) although global totals are small compared to other ocean and land-based mitigation options (Griscom et al. 2017; Gattuso and et al 2018). Reducing the conversion of coastal wetlands (mangroves, seagrass and marshes) would realise mitigation of 0.11-1.02 Gt $CO_2e\ yr^{-1}$ of emissions (Pendleton et al. 2012; Griscom et al. 2017). Mangrove restoration can mitigate the release of 0.07 Gt $CO_2\ yr^{-1}$ through rewetting (Crooks et al. 2011) and 0.84 Gt $CO_2\ yr^{-1}$ from biomass and soil enhancement (Griscom et al. 2017);. There is only *medium confidence* in the effectiveness of enhanced carbon uptake using mangroves, due to the many uncertainties regarding the response of mangroves to future climate change (Jennerjahn et al. 2017); dynamic changes in distributions (Kelleway et al. 2017) and other local-scale factors affecting longterm sequestration and climatic benefits (e.g. methane release; Dutta et al. 2017).

2.7.1.6 Biomass provision for bioenergy and BECCS

Bioenergy production mitigates climate change by delivering an energy service, therefore avoiding combustion of fossil energy. It is the most common renewable energy source used today in the world and the one with the largest future potential deployment (Chum et al. 2011; Creutzig et al. 2015; Slade et al. 2014). Bioenergy is produced from dedicated forest or agricultural systems and residues or municipal solid waste. It is a key option for climate change mitigation of the energy and transport sector in many future scenarios (Chum et al. 2011; Clarke et al. 2014; Creutzig et al. 2015; Popp et al. 2017; Serrano-Cinca et al. 2005b; Sims et al. 2014), especially those aiming at a stabilisation of global climate at 2°C or less (Edelenbosch et al. 2017; Popp et al. 2017, 2014, van Vuuren et al. 2010, 2011; Van Vuuren et al. 2016). In the different Shared Socio-economic Pathways (SSPs), the demand for 2nd generation bioenergy crops can range from less than 5,000 up to about 20,000 million tons per year by 2100, requiring between 200-1500 million ha of land (Popp et al. 2017).

The steps required to cultivate, harvest, transport, process and use biomass fuels require the use of energy and material resources, thereby generating emissions of GHGs and other climate pollutants (Staples et al. 2017). The magnitude of these impacts largely depends on the type of biomass, transportation distances, conversion technologies, applications, and location (Chum et al. 2011; Creutzig et al. 2015; Muñoz et al. 2014; Müller-Langer et al. 2014). They are usually lower for forest-based resources and agricultural residues, whereas for dedicated bioenergy crops the agricultural phase can be more energy, water and GHG intensive (Chum et al. 2011; Gerbrandt et al. 2016). However, direct life-cycle emissions of most bioenergy alternatives still constitute net savings in comparison to fossil fuels (Chum et al. 2011; Creutzig et al. 2015). At a global level, an optimal reduction of life-cycle GHG emissions from biofuels relative to fossil fuels ranges from 18% to 61%, depending on biomass availability and temperature stabilisation policy (Staples et al. 2017).

When annual crops or short rotation coppice are used for bioenergy, the carbon balance between emissions and plant regrowth is fast enough to avoid significant perturbations to the global carbon cycle. When bioenergy is sourced from biomass with longer turnover times, especially from forest plantations and managed forests, there can be an initial period where carbon accumulates in the atmosphere because emissions from biomass combustion occur at a faster rate than CO_2 uptake by vegetation re-growth (Berndes et al. 2013; Cherubini et al. 2016b; Hudiburg et al. 2011). Many studies investigated this temporal asymmetry and find a misbalance in carbon fluxes that is frequently referred to as the initial carbon debt of forest-based bioenergy systems (Bernier and Paré 2013; McKechnie et al. 2011; Mitchell et al. 2012). This can range from a few years to more than a century depending on specific system characteristics such as rotation period, plant species, location, residue management, or fossil fuel displaced (Guest et al. 2013b; Lamers and Junginger 2013; Ortiz et al. 2016; Ter-Mikaelian et al. 2015). Other studies focus on the links between forest management and the influence of bioenergy incentives, showing the diverse implications when accounting from a forest ownership perspective and their expectations about market development for bioenergy and other wood-based products (Berndes et al. 2013; Cintas et al. 2017).

In terms of climate system response, whereas CO_2 emissions from fossil fuels cause a nearly irreversible warming (Eby et al. 2009; Solomon et al. 2009), the forcing from carbon cycle dynamics in bioenergy systems is temporary and does not significantly contribute to long-term perturbations of the global carbon cycle or future temperature stabilisation providing the biomass is regrown, and it does not cause loss of slow-recovery high carbon stores such as peatlands (Cherubini et al. 2014; Jones et al. 2013; Mackey et al. 2013). For instance, bioenergy systems reach climate neutrality when sourced from biomass products that remain stored in the anthroposphere for approximately half of the biomass rotation period (Guest et al. 2013a).

Direct GHG emissions from land use changes (LUC) such as deforestation or afforestation, as well as those from changes in above-ground or soil carbon content after a change in management, shape full life-cycle climate impacts of bioenergy products (Berndes et al. 2013; Elshout et al. 2015; Popp et al. 2011). Mitigation benefits of energy crop plantations are site specific and strongly affected by agricultural factors and soil carbon dynamics, including prior land use, harvesting techniques, harvest timing, and fertilisation (Davis et al. 2013). Removal of forests to establish bioenergy crops results in high emissions of carbon, especially in the tropics, which may take from a few years up to a century to be re-paid in terms of net CO_2 emission savings due to displacing fossil fuels (Elshout et al. 2015). Harper et al. (in press) found carbon payback times varied from insignificant when replacing agricultural crops in temperate areas, through 10 to 100+ years replacing tropical forests, and over 100 years due to high loss of soil carbon in high latitudes. Since a 1.5 ˚C scenario meant more high latitude land was used for bioenergy than in a 2˚C scenario, the land carbon loss largely offset the additional CCS storage, and AR and D were found to be more efficient for atmospheric removal than BECCS on a century time scale.

Use of agriculture and forest residues for bioenergy can decrease soil carbon stocks and nutrient levels, potentially contributing to reduced crop yields and curtailing mitigation benefits of some bioenergy options

(Gerbrandt et al. 2016; Pourhashem et al. 2016, Liska et al. 2014). On the other hand, short rotation coppice species and perennial C4 grasses, such as *Miscanthus* and switchgrass, typically accumulate carbon in soils thanks to their deep root system, and if established on former cropland they can increase soil carbon at rates between 0.4 and 0.7 tC per ha per year (Don et al. 2012). Their cultivation often require application of N-containing fertilisers to achieve high yields, thereby enhancing soil emissions of N_2O, although at usually lower rate than conventional annual crops (Lai et al. 2017; Oates et al. 2016; Robertson et al. 2017; Rowe et al. 2016; Popp et al. 2011).

The potential for bioenergy with carbon capture and storage in 2 degrees scenarios developed for AR5 was found to be between 2 and 12 $GtCO_2e\ yr^{-1}$ (Conway 2012a; Smith et al. 2016a). However, BECCS has been the focus of a great many integrated assessment studies since AR5, including for the IPCC SR1.5. Since the potential is so intertwined with mitigation scnearios, energy sector and food production and trade, it is discussed in more detail in 2.7.2.

Impacts on climate - indirect land use change (iLUC): Bioenergy crops can be responsible for GHG emissions resulting from possible indirect land use changes i.e., the bioenergy activity may replace forest or agricultural activity that is then displaced to another location, driven by market-mediated effects. While this is true of many land based mitigation options (e.g. afforestation or froest protection), is a concern most commonly raised in relation to bioenergy. These indirect emissions are a major concern for food-based feedstocks such as corn, wheat and soybean, than for advanced biofuels from lignocellulosic materials (Ahlgren and Di Lucia 2014; Chum et al. 2011; Valin et al. 2015; Wicke et al. 2012). Estimates of emissions from indirect land use change are inherently uncertain and highly dependent on modelling assumptions, such as supply/demand elasticities, productivity estimates, incorporation or exclusion of emission credits for coproducts, and are widely debated in the scientific community (Finkbeiner 2014; Kim et al. 2014; Rajagopal and Plevin 2013; Zilberman 2017; Wise et al. 2015). A review of dozens of iLUC studies shows major variations in results for biodiesel fuels, whereas there is a gradual convergence for bioethanol from maize, wheat and sugarcane (Ahlgren and Di Lucia 2014). For example, iLUC values for corn bioethanol were originally calculated as 104 g $CO_2\ MJ^{-1}$ fuel (Searchinger et al. 2008), but a review of articles on the topic finds convergence towards about 20 g CO_2MJ^{-1} fuel, or even lower (Ahlgren and Di Lucia 2014).

Impacts on climate - biophysical effects: Biophysical changes can be incurred due to deforestation (for bioenergy crops) or afforestation (for wood based bionergy) as described for forest area change in 2.7.1.1 above and in more detail in 2.5. Land use changes due to future biofuel scenarios over the first half of the 21st century show a nearly neutral effect on surface temperature, as warming from GHG emissions and cooling from biophysical effects are nearly offsetting each other when averaged at global levels (Hallgren et al. 2013). When the differences in GHG emissions are eliminated, the land use change associated with clearing land for bioenergy production can result in reductions in global mean temperature (Jones et al. 2013). The switch from annual crops to perennial bioenergy plantations like *Miscanthus* in the US are found to impart a significant local to regional cooling that is mainly related to local increases in transpiration and higher albedo (Georgescu et al. 2011; Harding et al. 2016). This cooling is estimated to be equivalent to a carbon emission reduction of 78 t C ha^{-1}, which is six times larger than what arises from offsetting fossil fuel use, and it is sufficiently large to partially offset the regional projected warming due to increasing GHG concentrations over the next few decades (Georgescu et al. 2011). Perennial bioenergy crop expansion over suitable abandoned and degraded farmlands to avoid competition with existing food cropping systems is found to cause near-surface cooling up to 5°C during the growing season in large portions of the central US (Wang et al. 2017). In general, there are significant differences in regional patterns of the responses to land use and management changes, and local biophysical climate effects following

2.7.1.8 Demand management (diet change, waste reduction)

There is uncertainty as to how the demand for agricultural and forestry goods will evolve in the future (Valin et al. 2014; Popp et al. 2017; Bodirsky et al. 2014) and how the land system dynamics will respond to an anticipated increase. However, demand side mitigation in the AFOLU sector can play an important role for both, reducing GHG emissions via lower levels of agricultural and forestry production and in consequence decreased competition for land and thereby improved sustainability of land and water ecosystems which are already strongly under pressure today (see chapter 6). Demand changes in food and fiber has the potential for climate change mitigation via on the one hand reducing emissions from production in general or switching to consumption to less emission intensive commodities, on the other hand by making land available for carbon dioxide removal. Major measures for demand side mitigation are dietary changes (especially reducing meat consumption) which are of great importance due to projected global population growth and incomes rise and reductions of agricultural and food losses and waste (Smith et al. 2013b). Reducing food losses and waste increases the overall efficiency of food value chains, therefore the negative trade-offs are limited and there are vast opportunities for savings (less land and inputs needed, increased yields) along the entire supply chain. Such demand-side measures have the potential to significantly mitigate emissions of 2.78-11.37 Gt $CO_2e\ yr^{-1}$ from reductions in food loss and waste (food wastage), changes in diets, and increases in wood for construction. Approximately 55% of the upper bound of this estimate comes from changes in diet and the other 40% comes from reductions in food wastage (Roe et al. 2018).

A recent study concluded that reducing beef consumption (decrease in the US by 50%, Brazil by 25% and stabilisation in China) could provide a 12% mitigation of livestock emissions by 2030 solely from avoided enteric fermentation and manure emissions (Haupt 2017). This is supported by Stevanović et al. (2017) who found a GHG reduction potential for agriculture of more than 40 % in 2100 with additional beneficial effects for food prices (see chapter 5 and 6). In addition to mitigation gains, decreasing meat consumption, primarily of ruminants, reduces water use, soil degradation, pressure on forests, land used for feed, and manure and pollution into water systems (Tilman and Clark 2014) (see chapter 6).

The production of beef produces the highest GHG, water, land, and energy footprint of all proteins – approximately 10 times higher in GHG emissions than any other animal protein (dairy cattle, pigs, chicken) (Dickie et al. 2014; Tilman and Clark 2014; Henders et al. 2015). Countries with the highest overall and projected beef consumption include predominantly developed and emerging countries: US, EU, China, Brazil, Argentina, Russia. A recent study concluded that reducing beef consumption (decrease in the US by 50%, Brazil by 25% and stabilisation in China) could provide a 12% mitigation of livestock emissions by 2030 solely from avoided enteric fermentation and manure emissions (Haupt et al. 2017). In addition to reduced emissions, shifting diets has the potential to deliver additional environmental, health and economic co-benefits. Decreasing meat consumption, primarily of ruminants, reduces water use, soil degradation, pressure on forests, and manure and pollution into water systems (Dickie et al. 2014). Reducing the amount of land and grains used for livestock could also increase food supply by 50% by freeing available resources (Foley et al. 2011). Given the established links between diet-related diseases and high levels of meat consumption, keeping global average per capita meat consumption at healthy levels will also have important health benefits (reduced risks of cardiovascular diseases, cancer, stoke and diabetes) (Johns Hopkins Center for a Livable Future, 2017). Shifting to healthier diets and away from emissions-intensive foods like beef delivers a significant mitigation potential of 2.15-6.4 Gt $CO_2e\ yr^{-1}$ (Stehfest et al. 2009; Bajželj and Richards 2014; Dickie et al. 2014; Tilman and Clark 2014; Herrero et al. 2016; Hawken 2017; Hedenus et al. 2014; Springmann et al. 2016).

Demand side measures are not only relevant for the agricultural but also for forestry systems are covered in 2.7.1.1.

2.7.1.9 Enhanced weathering

(note: text to add for the SOD)

2.7.2 Integrated transformation pathways for climate change mitigation

Land-based mitigation options have the potential to interact, resulting in positive additive effects or negative, and thus need to be assessed together, as well as with mitigation options in other sectors (such as energy or transport), under different climate mitigation targets and in combination with other sustainability goals (Popp et al. 2017; Obersteiner et al. 2016; Humpenöder et al. 2018).

Integrated Assessment Models (IAMs) with distinctive land use modules lie at the basis of the assessment of mitigation pathways as they combine insights from various disciplines in a single framework and cover the largest sources of anthropogenic GHG emissions from different sectors. Over time, IAMs have extended their system coverage (Krey 2014), however, the explicit modeling and analysis of integrated energy and land use systems is relatively new. Many of the IAMs assessing mitigation scenarios now include a process-based description of the land system in addition to the energy system (Popp et al. 2014; Leimbach et al. 2011). IAMs taking account for land are a diverse set of models ranging from loosely coupled partial equilibrium models of energy and land to computable general equilibrium models of the global economy, from myopic to perfect foresight models. They differ in their portfolio and representation of land-based mitigation options as well as the interplay with mitigation in other sectors. These structural differences have implications for the deployment of different mitigation options.

As a consequence of the relative novelty of land-based mitigation assessment in IAMs, the portfolio of land-based mitigation options does not cover the full option space as outlined in 2.7.1.1, at least not in all assessments. The inclusion and detail of a specific mitigation measure differs across models and is influenced by the availability of data for its techno-economic characteristics and future prospects as well as the computational challenge, e.g. in terms of spatial and process detail, to represent the measure. The land use modules of IAMs cover most of the supply-side mitigation options on the process level, while many demand-side options are treated as part of the underlying assumptions, which can be varied. CDR options are only partially included in IAM analyses, which mostly rely on afforestation and bioenergy with CCS (BECCS).

For example, the IAM scenarios based on the Shared Socio-economic Pathways (SSPs) (Serrano-Cinca et al. 2005b) provide five different stories of future socio-economic development and are the basis for the CMIP6 model intercomparison exercise leading up to the IPCC 6th Assessment Report (AR6). They include possible trends in agriculture and land use, but cover a limited set of land-based mitigation options: dietary changes, higher efficiency in food processing (especially in livestock production systems), reduction of food waste, increasing agricultural productivity, methane reductions in rice paddies, livestock and grazing management for reduced methane emissions from enteric fermentation, manure management, improvement of N-efficiency, 1st generation of biofuels, avoided deforestation, afforestation, bioenergy and BECCS (Popp et al. 2017). Mitigation options not included in integrated pathway modelling, include "nature based solutions" (Griscom et al. 2017) such as soil carbon management or wetland management which have the potential to alter the contribution of land-based mitigation in terms of timing, potential and sustainability consequences.

Mitigation pathways, based on IAMs, are typically designed to achieve a climate target, based on economic optimisation taking account of sustainability considerations depending on scenario setting (Serrano-Cinca et al. 2005b). Such cost-optimal mitigation pathways project GHG emissions to peak early in the 20th century, strict GHG emission reduction afterwards and, depending on the climate target net CDR from the atmosphere in the 2nd half of the century (see Chapter 2 of SR1.5, Tavoni et al. 2015; Riahi et al. 2017). In most of these pathways, land use is of great importance as it (i) turns from a source into a sink of atmospheric CO_2 due to large-scale afforestation and reforestation, (ii) provides high amounts of biomass for bioenergy or BECCS and (iii), even under improved agricultural management, still delivers residual non-CO_2 emissions from agricultural production(Popp et al. 2017; Rogelj et al. 2018a; van Vuuren et al. 2018) as shown exemplarily in Figure 2.7.3.

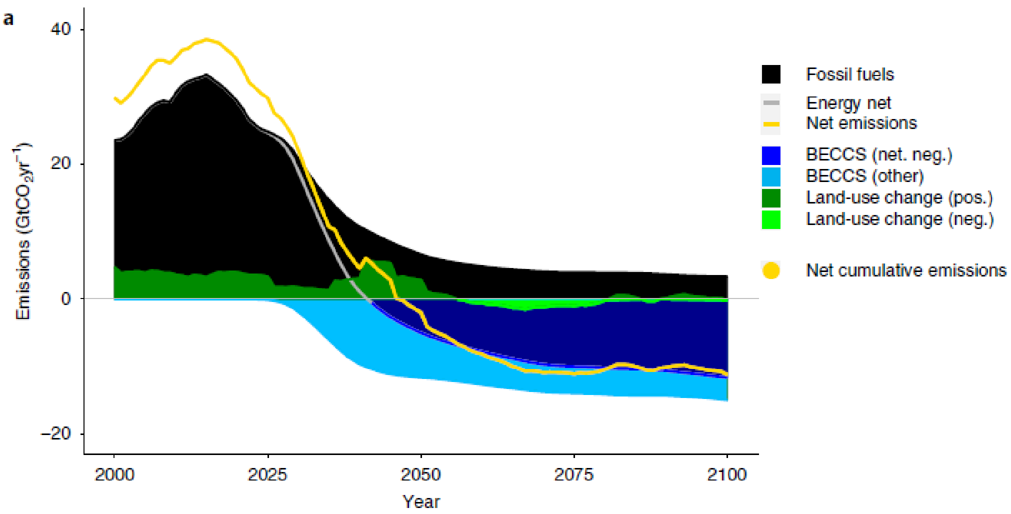

Figure. 2.7.3: CO_2 emissions for a typical 1P5 mitigation scenario (based on (van Vuuren et al. 2018) ***Figure. 2.7.3 is currently used as a placeholder for an updated figure based on the SRCCL database as soon as the database is available; this figure will then also cover non-CO_2 emissions but will have to be discussed and developed in detail for SOD of SRCCL*****)**

From the scenarios available to this assessment, a set of possible mitigation pathways have be identified which are illustrative of a range of possibilities in their GHG and land use consequences as well as their consequences for sustainable development (see chapter 6). They vary due to underlying socio-economic and policy assumptions, mitigation options considered, long-term climate goal, the level of inclusion of other sustainability goals (such as land and water restrictions for biodiversity conservation or food production), and models by which they are generated. Since AR5, the scenario literature has greatly expanded the exploration of these dimensions. This includes the Shared Socio-economic Pathways (SSPs) (O'Neill et al. 2017; Popp et al. 2017; Rogelj et al. 2018b) but also scenarios taking into account a larger set of sustainable development goals (e.g. (Iyer et al. 2018)), scenarios with restricted availability of CDR technologies (e.g. Bauer et al. submitted, (Strefler et al. 2018; van Vuuren et al. 2018) and scenarios with near-term action dominated by regulatory policies (e.g. Kriegler et al. 2018).

For example the IAM assessment based on the SSPs (Serrano-Cinca et al. 2005b; Popp et al. 2017; Rogelj et al. 2018b) clearly highlight the importance of socioeconomic baseline conditions, international cooperation, timing and sectoral participation for climate change mitigation as well as specifications of climate long-term goals (Figure 2.7.3). In the mitigation case RCP4.5, avoided deforestation strongly reduces CO_2 emissions in SSP5, SSP4 and SSP2 compared to the baseline scenarios. However, as a result of weak land use change regulation, CO_2 emissions from land use change still occur in SSP3 (307 Gt CO_2 cumulatively until 2100). In the RCP2.6 mitigation case, emissions are again higher than the baseline in SSP4 and SSP5, due to displacement effects into pasture land caused by high bioenergy production combined with forest protection only (Popp et al. 2014), and (for SSP4) due to additional land demand for bioenergy crop production in low income regions like MAF and ASIA without forest protection. Afforestation increases terrestrial C sequestration especially in SSP2 in LAM, MAF and ASIA and in the high-income regions (OECD, LAM and REF) of SSP4 where land use change is successfully regulated. CH_4 emissions in the mitigation cases are remarkably lower compared to the baseline cases in all SSPs due to improved agricultural management (such as improved water management in rice production, improved manure management by e.g. covering of storages or adoption of biogas plants, better herd management and better quality of livestock through breeding and improved feeding practices). Dietary shifts away from emissions-intensive livestock products (SSP2) also lead to decreased CH_4 emissions. N_2O emissions are significantly lower particularly in the RCP4.5 scenario due to improvement of N-efficiency and improved manure management. However, high levels of bioenergy production result in increased N_2O emissions in SSP5 due to N fertilisation of dedicated grassy bioenergy crops such as Miscanthus.

High levels of carbon dioxide removal through mitigation options that require land conversion (BECCS and afforestation) can shape the land system dramatically. In the different SSPs and across different RCPs, the global forest area can change from about -500 Mha up to+1000 Mha in 2100 compared to 2010, and demand for 2[nd] generation bioenergy crops can range from less than 5000 up to about 20,000 million ton per year by 2100, sourced from about 200–1500 million ha of land (Popp et al. 2017; Rogelj et al. 2018b) (Figure 2.7.4). Such a pace of projected land use change over the coming decades goes well beyond historical changes in some instances (Turner et al. 2018b), see also SR1P5). This raises issues for societal acceptance, and distinct policy and governance for avoiding negative consequences for other sustainability goals (Humpenöder et al. 2018; Obersteiner et al. 2016), see chapter 6 and 7). Land requirements for bioenergy for a 1.5 degrees scenario are much higher than a 2 degrees scenario.

(*This paragraph is currently based on Popp et al 2014, GEC. But after release of the SRCCL database this text and related figures will be updated also including RCP1.9*)

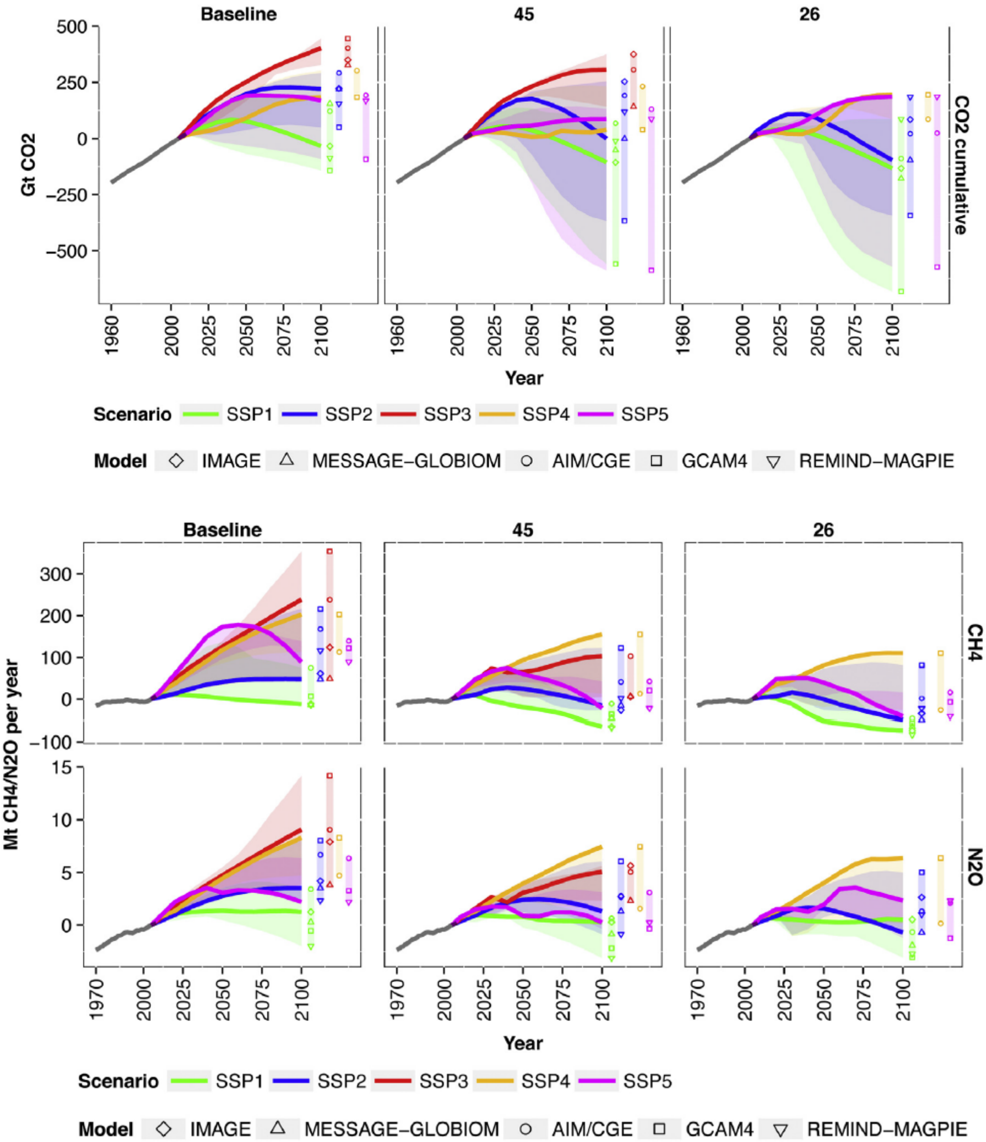

Figure 2.7.4: land-based GHG emissions across different SSPs & RCPs based on integrated pathways (based on (Popp et al. 2017)) (*Figure. 2.7.4 is currently used as a placeholder for an updated figure based on the SRCCL database as soon as the database is available; this figure will then also cover RCP1.9 scenarios but will have to be*

discussed and developed in detail for SOD of SRCCL)

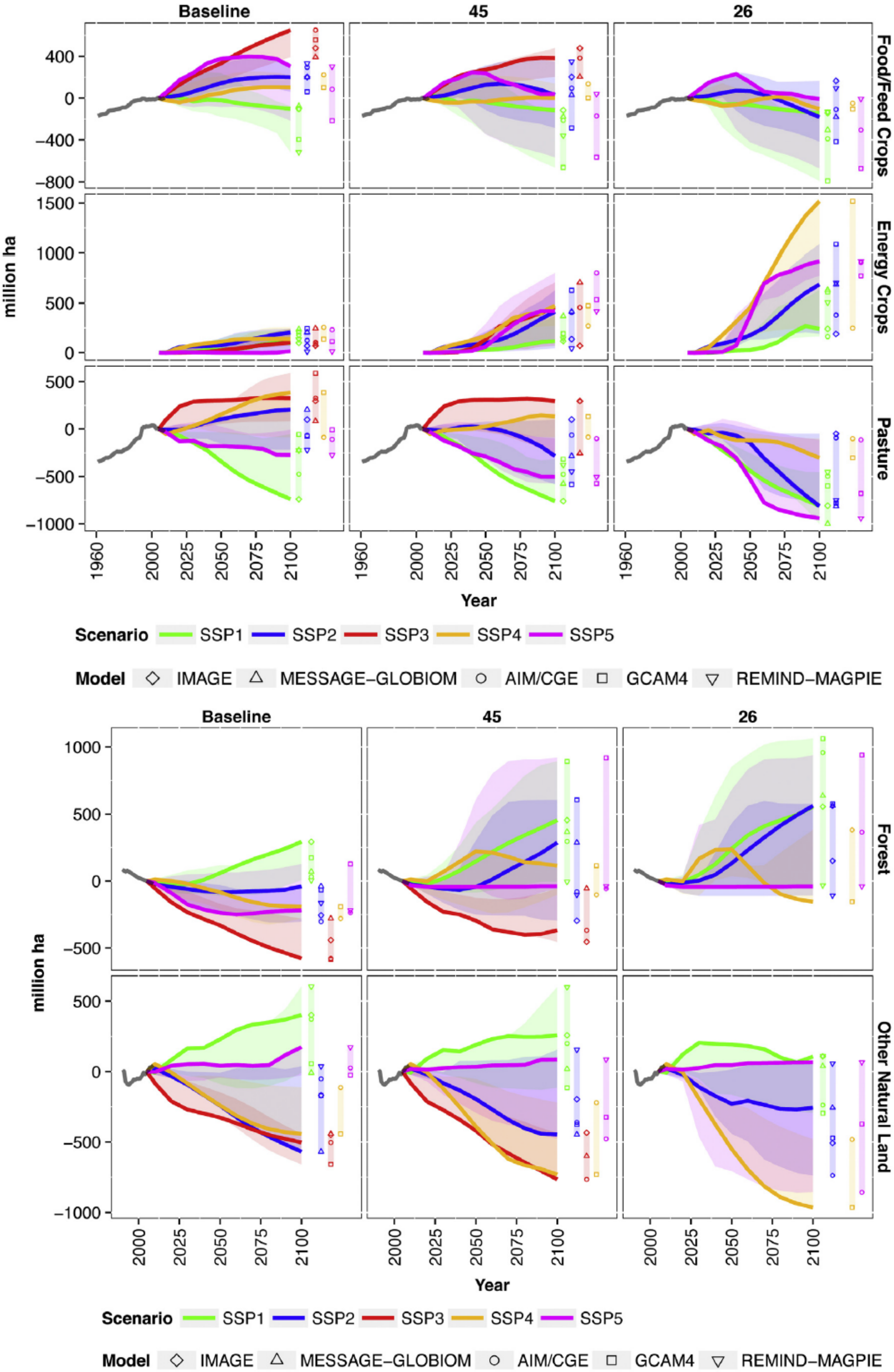

Figure 2.7.5: land dynamics across different SSPs & RCPs based on integrated pathways (based on (Popp et al. 2017)) (*Figure 2.7.5 is currently used as a placeholder for an updated figure based on the SRCCL database as soon as the database is available; this figure will then also cover RCP1.9 scenarios but will have to be discussed and developed in detail for SOD of SRCCL*)

Several additional IAM studies have become available since AR5, exploring alternative land-based mitigation pathways in more detail. Those assessed the importance and potentials on specific land-based mitigation technologies, as well as the interplay with other sector mitigation efforts, timing of mitigation action and sustainable development for the contribution of the AFOLU sector to climate change mitigation, related land dynamics and sustainability consequences (see chapter 6) (e.g. (Strefler et al. 2018; van Vuuren et al. 2018; McCollum et al. 2017)

Figure 2.7.5 shows several alternative pathways of achieving climate change targets which mitigate climate change in very different ways (1.5, 2.6) as well as baseline situations for cumulative GHG emissions. The deep reductions in non-CO_2 GHG in the low non-CO_2 scenario (and lifestyle change and agriculture intensification, in which reduced cattle stocks play an important role) allow for a higher amount of total cumulative CO_2 emissions and less need for CDR. A significant reduction in the energy-related CDR can also be achieved in scenarios reducing agricultural area, leading to an uptake of CO_2 through regrowth of natural vegetation, as illustrated for the lifestyle and low non-CO_2 scenarios. Reducing CO_2 emissions in other sectors rapidly can furthermore contribute to less CDR need (all other scenarios). The alternatives offer a means to diversify transition pathways to meet the Paris Agreement targets, while simultaneously benefiting other sustainability goals (see chapter 6).
(*This paragraph is currently based on* (van Vuuren et al. 2018), *After release of the SRCCL database this text and related figures will be updated for SOD based on multi-sectoral emission wedges (timeline; not cumulative) for CO_2 & non-CO_2 as well as land dynamics for baseline and selected land-mitigation pathways (e.g. baseline, default mitigation case, other NET options reducing pressure on land, high agricultural intensification, sustainable food demand, low food waste, no overshoot, explicit limitation of terrestrial CDR (regulation), different mitigation target (level of ambition))*)

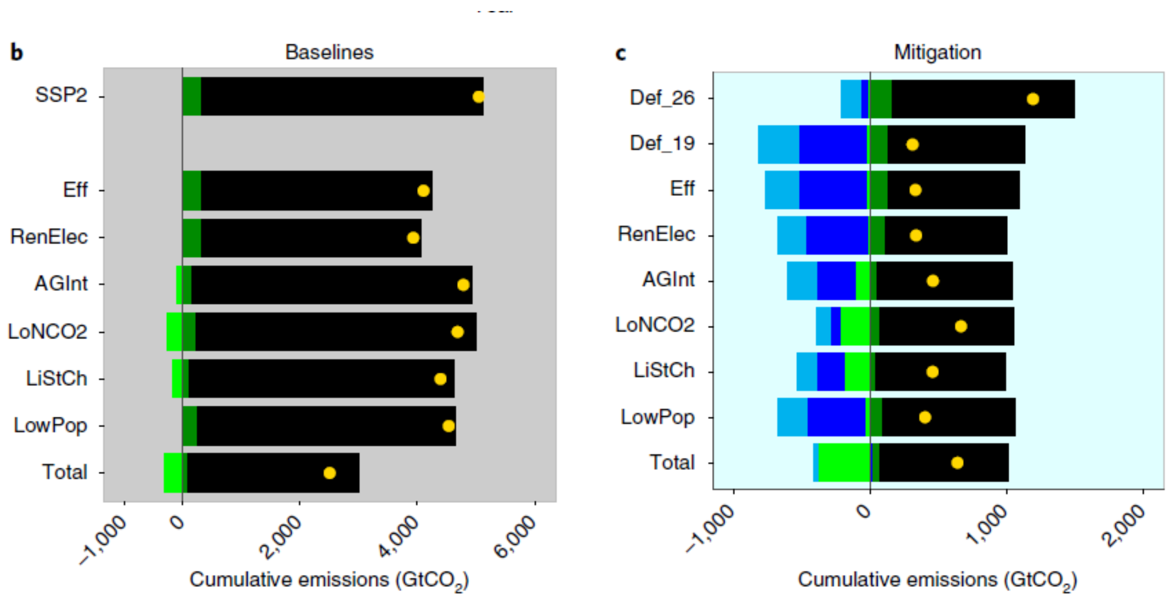

Figure 2.7.6: CO_2 emissions for alternative archetypes of integrated mitigation pathways (based on (van Vuuren et al. 2018). (*Fig 2.7.6 is currently used as a placeholder for an updated figure based on the SRCCL database as soon as the database is available; this figure will contain multi-sectoral emission wedges for CO_2 & non-CO_2 as well as land dynamics for baseline and selected land-mitigation pathways but will have to be discussed and developed in detail for SOD of SRCCL*)

In the efficiency scenario (Eff), current investment barriers to efficiency are assumed to be overcome and efficient technologies are adopted in transport, industrial production, buildings and use of materials. In the renewable electricity scenario (RenElec), rapid electrification takes place driven by technological breakthroughs in storage and load management. The agricultural intensification scenario (AGInt) assumes strategies to further intensify agriculture, leading to higher crop yields and more land-efficient livestock farming. In the low non-CO_2 scenario (LoNCO_2), mitigation is driven by stringent enforcement of measures to reduce end-of-pipe emissions and by introduction of in vitro (cultured) meat, produced on the basis of stem-cell technology, and input of energy and proteins (mostly based on soya). The lifestyle change scenario (LiStCh) assumes a radical value shift towards more environmentally friendly behavior, including a healthy, low-meat diet, changes in transport habits and a reduction of heating and cooling levels at homes. The low population scenario (LowPop), finally, assumes a decrease in fertility rates in most regions, which could be achieved by stronger education policies.

Besides their consequences of mitigation pathways and land consequences, those archetypes can also affect multiple other sustainable development goals that provide both challenges and opportunities for climate action (see Chapter 6). Taking this into account, there is growing literature to evaluate the effects of the various mitigation pathways on sustainable development, focusing in particular on aspects for which Integrated Assessment Models (IAMs) provide useful information (e.g. land use changes and biodiversity, food security, and air quality). Accounting for those sustainability interactions is affecting mitigation potentials, land consequences and mitigation costs and will be assessed in chapter 6.

(*In this section after SRCCL database is available terrestrial mitigation pathway consequences of other SDG prioritisation will be discussed*)

2.7.3 The contribution of land-based mitigation options to the Paris agreement

Land sector mitigation is central to the Paris Agreement (Serrano-Cinca et al. 2005a) To realise the long term temperature goal to hold *"the increase in the global average temperature to well below 2°C"* (Article 2) the Agreement recognises the need of achieving globally *"…a balance between anthropogenic emissions by sources and removals by sinks of greenhouse gases in the second half of this century …"* (Article 4)(Serrano-Cinca et al. 2005a). As the land sector is responsible for around a quarter of all anthropogenic GHG emissions, and the only current direct anthropogenic, sinks removing 22% of anthropogenic CO_2 (section 2.4), it has been a focus of both the Paris Agreement text and subsequent decisions.

Article 5 is explicit about the role of forests: "*Parties should take action to conserve and enhance, as appropriate, sinks and reservoirs of greenhouse gases … including forests. …. policy approaches and positive incentives for activities relating to reducing emissions from deforestation and forest degradation, and the role of conservation, sustainable management of forests and enhancement of forest carbon stocks in developing countries; and alternative policy approaches, such as joint mitigation and adaptation approaches for the integral and sustainable management of forests…*".

In addition the UNFCCC launched the Koronivia joint work program on agriculture at COP23 in 2017 (Decision -/CP.23[3]). While no including the term "*mitigation"*, the decision refers to *"adaptation co-benefits"*, and many of the measures mentioned (improved soil carbon, improved nutrient use and manure management, improved livestock management systems) would indeed have mitigation co-benefits.

According to Article 4 paragraph 2 of the Paris Agreement each Party shall prepare, communicate and maintain successive nationally determined contributions (NDCs) that it intends to achieve. At the time of adoption the Paris Agreement, 187 of the 195 signatory countries submitted Intended Nationally Determined Contributions (INDCS), upon ratification these become the formal NDCs and as of May 2018, 170 had been submitted and the vast majority include commitments in the land use sector (http://www4.unfccc.int/ndcregistry/Pages/Home.aspx).

[3] UNFCCC (Lee, D. and Sanz 2017b) Decision -/CP.23 Koronivia joint work on agriculture. http://unfccc.int/files/meetings/bonn_nov_2017/application/pdf/cp23_auv_agri.pdf

The Paris Agreement includes an Enhanced Transparency Framework, to track countries' progress towards achieving their individual targets (i.e., NDCs), and a Global Stocktake (every five years starting in 2023), to assess the countries' collective progress towards the long-term goals of the Paris Agreement . The Global Stocktake is potentially the real "engine" of the Paris Agreement , because any identified "gap" between "collective progress" and the "well-below 2°C trajectory" is expected to motivate increased mitigation ambition by countries in successive rounds of NDCs. This means issues around uncertainties in estimating land sector emissions (section 2.4) but equally mitigation, will be key to transparency and credibility. The details of the Transparency Framework and of the Global Stocktake will be included in the Paris Agreement's "rulebook" (decisions that will rule its implementation), currently being elaborated by the United Nations Framework Convention on Climate Change (UNFCCC).

Including land use in the UNFCCC process has been long and complex. This is in part due to the high uncertainties in estimating anthropogenic GHG flux (section 2.4) and issues such as additionality (i.e. showing that proposed mitigation efforts go beyond Business-as-Usual), leakage (displacement of land use activities to other areas or "indirect Land Use Change" see 2.7.1.5) and permanence (ensuring longevity of mitigation under climate change and future management (section 2.4.4) have often led to controversies and compromises_ENREF_11 (Schlamadinger et al. 2007). Addressing credibility and transparency in estimates of greenhouse gas fluxes is a further aspect of the Paris Agreement critical to the land sector.

2.7.3.1 Assessments of land sector in the INDCs

While most NDCs include the land sector, they vary with how much information is given and they type of target, with more ambitions targets for developing countries often being "conditional" on support and climate finance. Compared to land sector emissions 2010,

Under implementation of unconditional pledges, the net LULUCF flux in 2030 has been estimated to be a sink of -0.41 ± 0.68 $GtCO_2e\ yr^{-1}$, which rises to -1.14 ± 0.48 $GtCO_2e\ yr^{-1}$ in 2030 under additional "conditional" activities (Grassi et al. 2017). This compares to net LULUCF in 2010 calculated from the GHG Inventories GHGI) of 0.01 ± 0.86 $GtCO_2e\ yr^{-1}$ in 2010 (Grassi et al. 2017), see also figure 2.7.7). Forsell et al. 2016) similarly find a reduction in 2030 compared to 2010 of 0.5 $GtCO_2e\ yr^{-1}$ (range: 0.2-0.8) by 2020 and 0.9 Gt $CO_2e\ yr^{-1}$ (range: 0.5-1.3) by 2030 cod unconditional and conditional cases. **The approach to calculating the LULUCF towards the NDC target by countries can result in a threefold difference in estimated mitigation in 2030 (1.2 to 3.8 $GtCO_2e\ yr^{-1}$), with implications for transparency (Figure 2.7.7).**

- 1.2 to 1.9 $GtCO_2e\ yr^{-1}$ in 2030 compared to 2005 emissions
- 0.7 to 1.4 $GtCO_2e\ yr^{-1}$ compared to "current activity" or "pre-INDC" reference scenario
- 2.3 to 3.0 $GtCO_2e\ yr^{-1}$ compared to country stated "BAU" reference scenario
- 3.0 to 3.8 $GtCO_2e\ yr^{-1}$ based on the countries' approach to calculating LULUCF contribution

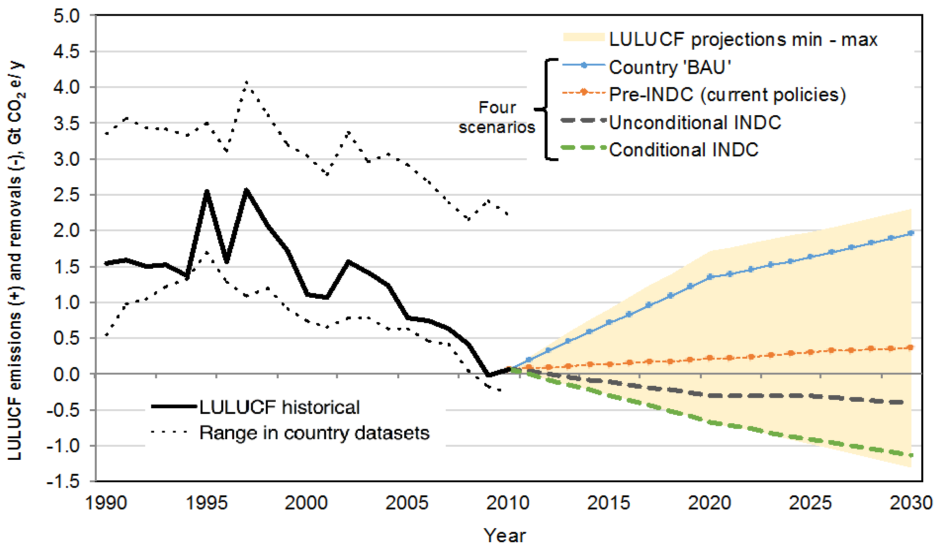

Figure 2.7.7 Global LULUCF net greenhouse gas flux for the historical period and future scenarios based on analyses of countries' documents and mitigation pledges ((I)NDCs).

The LULUCF historical data (black solid line) reflect the following countries' documents (in order of priority): data submitted to UNFCCC ((I)NDCs_ENREF_3[4], 2015 GHG Inventories[5], recent National Communications[6],[7]); other official countries' documents; FAO-based datasets, i.e. FAO-FRA for forest (Tian et al. 2015a) (as elaborated by ref (Achard et al. 2014) and FAOSTAT_ENREF_23 (FAO 2015) for non-forest land use emissions. The future four scenarios reflect official countries information (mostly (I)NDCs, complemented by Biennial Update Reports[8] and National Communications), and show: the BAU scenario as defined by the country (country BAU); the trend based on pre-(I)NDC levels of activity (current policies); the unconditional (I)NDC scenario assuming that all countries implement their unconditional targets in their (I)NDCs; the conditional (I)NDC scenario assuming that all countries implement the unconditional and conditional targets in their (I)NDCs. The shaded area indicates the full range of countries' available projections (min-max), expressing the available countries' information on uncertainties beyond the specific scenarios shown. The uncertainty of historical and future data may be analysed through two different perspectives. First, the range of historical country datasets (dotted lines) reflects differences between alternative selections of country sources, i.e. GHG inventories for developed countries complemented by FAO-based datasets (upper range) or by data in National Communications (lower range) for developing countries (see Methods for details). Similarly, the range of future scenarios gives an order of magnitude of the impact of different assumptions by countries. Secondly, based on available information from countries' reports to UNFCCC complemented by expert judgment, we estimated the uncertainties (at 95% CI) for LULUCF GHG emission levels over time and for the associated trends.

Overall, the land sector is expected to deliver between 20 and 25% of mitigation pledged in the (I) NDCs. The countries contributing most to LULUCF mitigation under this perspective are Brazil and Indonesia, followed by other countries focusing either on avoiding carbon emissions (e.g. Ethiopia, Gabon, Mexico,

[4] UNFCCC. INDCs as communicated by Parties, http://www4.unfccc.int/submissions/indc/Submission%20Pages/submissions.aspx. (UNFCCC, 2015).
[5] UNFCCC. Greenhouse Gas Inventories, http://unfccc.int/national_reports/annex_i_ghg_inventories/national_inventories_submissions/items/8812.php. (UNFCCC, 2015).
[6] UNFCCC. National Communications Non-Annex 1, http://unfccc.int/nationalreports/non-annexinatcom/submittednatcom/items/653.php (UNFCCC, 2015).
[7] UNFCCC. National Communications Annex 1, http://unfccc.int/nationalreports/annexinatcom/submittednatcom/items/7742.php; (UNFCCC, 2015).
[8] UNFCCC. Biennial Update Reports, http://unfccc.int/national_reports/non-annex_i_natcom/reporting_on_climate_change/items/8722.php (UNFCCC, 2015).

DRC, Guyana and Madagascar) or on promoting the sink through large afforestation programs (e.g. China, India). For example:

- **Brazil:** aim to "achieve, in the Brazilian Amazonia, zero illegal deforestation by 2030 and compensating for emissions from legal suppression of vegetation by 2030".
- **Indonesia**: *all sector emission target: -29% (unconditional) and -41% (conditional) relative to a 2030 BAU emission of 2.8* $GtCO_2$ yr^{-1}. including AFOLU emissions in 2005 (1.01 $GtCO_2e$ yr^{-1}, representing about 65% of total GHG emissions) and the expected AFOLU emissions in 2030 for the BAU (1.08 $GtCO_2e$ yr^{-1}), the unconditional (0.55 $GtCO_2e$ yr^{-1}) and the conditional (0.42 $GtCO_2e$ yr^{-1}) scenarios (data presented at the COP-21, (BAPPENAS 2015)),
- **Mexico**: 0% deforestation, afforestation for wetland protection
- **China**: increase forest stock volume by 4.5 billion m^3
- **India**: Green India Mission: enhance carbon sequestration annually by about 100 $MtCO_2e$
- **Russia**: forest management is one of the "most important elements of Russian policy to reduce GHG emissions".

Most NDCS focused on the role of forests in LULUCF, few included agricultural mitigation specifically, or bioenergy, BECCS, soils, agriculture, wetlands

2.7.3.2 Raising ambition in the land sector to close the emission gap:

(note this section will be based on an assessment of material in SR1.5 report and databased on expectations in the land sector in high mitigation pathways, compared to current activity and the mitigation potential presented in 2.7.1. This will be done for the SOD).

The submitted Nationally Determined Contributions (NDCs), currently fall short of the goal (Rogelj et al. 2016). Current commitments are more compatible with 2.5°C to 3°C of warming by 2100 (Schleussner et al. 2016; Rockström, J., Gaffney, O., Rogelj, J., Meinshausen, M., Nakicenovic, N., & Schellnhuber 2017). To limit warming to 1.5°C (and 2°C), countries must submit more ambitious NDCs in subsequent negotiations (starting in 2018), and plan for a more rapid transformation of their national energy, industry, transport, and land use sectors (Rogelj et al. 2016; Peters and Geden 2017; Millar et al. 2017). Sections 2.7.1 and 2.7.2 indicate many additional mitigation options that could go towards filling the Gap. A specific analysis of the pathway to filling this gap was developed by Roe et al. (2018) (See figure 2.7.8) (Note we will update this analysis and include other data in the assessment for the SOD)

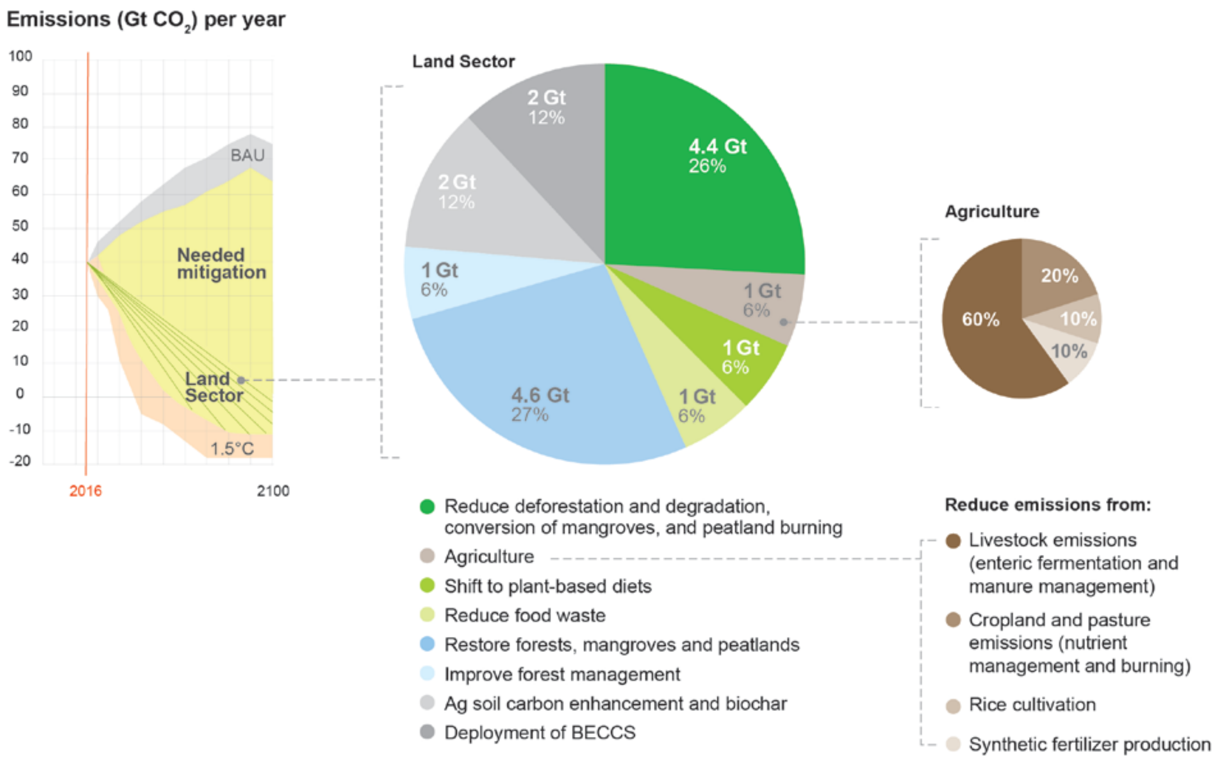

Figure 2.7.8. Land-based mitigation wedges and available strategies to deliver total mitigation of ~17 $GtCO_2e$ yr^{-1} in 2050.

The land sector makes up 33% of total needed mitigation (left panel), which is delivered by the eight wedges (land sector pie chart in middle panel). The green and brown wedges represent emissions reduction measures, and the blue and grey wedges represent carbon removal measures. The table details the priority regions and activity types for each wedge, and their estimated emissions and removals trajectories in percent change compared to 2018 levels. The wedges are measures which are individually accounted for with the intent of avoiding counting of emissions reductions. Demand-side measures only account for mitigation from overall reductions (of GHG-intensive foods and food loss and waste), and do not include efficiency or LUC mitigation.

Land sector mitigation is not a substitute for strong action in the energy and industrial sectors, as both will be needed. As it will be impossible to eliminate emissions in some sectors, including the substantial emissions associated with food production (Section 2.4) it will be necessary to have a contribution of carbon dioxide removal (negative emissions) from the land sector. The evidence suggests that land sector mitigation, both emissions reduction and net removals, are necessary and also have the technical potential to achieve reaching the Paris Agreement goal of a "balance in anthropogenic emissions and removals". However there is a need for more transparency and credibility in monitoring, reporting and verifying net fluxes (Section 2.4) and wider climate impacts (Section 2.6), along with other co-benefits and trade-offs (chapter 6).

Reference List

A., B. M., and Coauthors, 2008: Thermal adaptation of soil microbial respiration to elevated temperature. *Ecol. Lett.*, **11**, 1316–1327, doi:10.1111/j.1461-0248.2008.01251.x. https://doi.org/10.1111/j.1461-0248.2008.01251.x.

Abatzoglou, J. T., and A. P. Williams, 2016: Impact of anthropogenic climate change on wildfire across western US forests. *Proc. Natl. Acad. Sci.*, **113**, 11770–11775, doi:10.1073/pnas.1607171113. http://www.pnas.org/lookup/doi/10.1073/pnas.1607171113.

Abbott, B. W., and Coauthors, 2016: Biomass offsets little or none of permafrost carbon release from soils, streams, and wildfire: An expert assessment. *Environ. Res. Lett.*, **11**, 34014, doi:10.1088/1748-9326/11/3/034014. http://stacks.iop.org/1748-9326/11/i=3/a=034014.

Abdalla, M., A. Hastings, J. Truu, M. Espenberg, Ü. Mander, and P. Smith, 2016: Emissions of methane from northern peatlands: a review of management impacts and implications for future management options. *Ecol. Evol.*, **6**, 7080–7102, doi:10.1002/ece3.2469.

Abiodun, B. J., Z. D. Adeyewa, P. G. Oguntunde, A. T. Salami, and V. O. Ajayi, 2012: Modeling the impacts of reforestation on future climate in West Africa. *Theor. Appl. Climatol.*, **110**, 77–96, doi:10.1007/s00704-012-0614-1.

——, J. Adegoke, A. A. Abatan, C. A. Ibe, T. S. Egbebiyi, F. Engelbrecht, and I. Pinto, 2017: Potential impacts of climate change on extreme precipitation over four African coastal cities. *Clim. Change*, **143**, 399–413, doi:10.1007/s10584-017-2001-5. http://link.springer.com/10.1007/s10584-017-2001-5 (Accessed May 24, 2018).

Achard, F., and Coauthors, 2014: Determination of tropical deforestation rates and related carbon losses from 1990 to 2010. *Glob. Chang. Biol.*, **20**, 2540–2554, doi:10.1111/gcb.12605. https://doi.org/10.1111/gcb.12605.

Adachi, S. A., F. Kimura, H. Kusaka, T. Inoue, and H. Ueda, 2012: Comparison of the impact of global climate changes and urbanization on summertime future climate in the Tokyo metropolitan area. *J. Appl. Meteorol. Climatol.*, **51**, 1441–1454, doi:10.1175/JAMC-D-11-0137.1.

Agency, E. P., 2012: Global Mitigation of Non CO2 Greenhouse Gases - Landfills. *Environ. Prot.*, 4–6, doi:EPA-430-R-13-011.

Ainsworth, E. A., and A. Rogers, 2007: The response of photosynthesis and stomatal conductance to rising (CO2): Mechanisms and environmental interactions. *Plant, Cell Environ.*, **30**, 258–270, doi:10.1111/j.1365-3040.2007.01641.x.

Akagi, S. K., R. J. Yokelson, C. Wiedinmyer, M. J. Alvarado, J. S. Reid, T. Karl, J. D. Crounse, and P. O. Wennberg, 2011: Emission factors for open and domestic biomass burning for use in atmospheric models. *Atmos. Chem. Phys.*, **11**, 4039–4072, doi:10.5194/acp-11-4039-2011.

Alatalo, J. M., and A. Ferrarini, 2017: Braking effect of climate and topography on global change-induced upslope forest expansion. *Int. J. Biometeorol.*, **61**, 541–548, doi:10.1007/s00484-016-1231-y. http://link.springer.com/10.1007/s00484-016-1231-y (Accessed May 20, 2018).

Aldersley, A., S. J. Murray, and S. E. Corn, 2011: Scien ce of th e Total En viron m en t Global an d region al an alysis of clim ate an d h um an drivers of w ild fi re. *Sci. Total Environ.*, **409**, 3472–3481, doi:10.1016/j.scitoten.

Alizadeh-Choobari, O., P. Ghafarian, and P. Adibi, 2016: Inter-annual variations and trends of the urban warming in Tehran. *Atmos. Res.*, **170**, 176–185, doi:10.1016/j.atmosres.2015.12.001.

Alkama, R., and A. Cescatti, 2016: Biophysical climate impacts of recent changes in global forest cover. *Science (80-.).*, **351**, 600–604, doi:10.1126/science.aac8083. http://www.sciencemag.org/cgi/doi/10.1126/science.aac8083.

Allen, C. D., and Coauthors, 2010: A global overview of drought and heat-induced tree mortality reveals emerging climate change risks for forests. *For. Ecol. Manage.*, **259**, 660–684, doi:https://doi.org/10.1016/j.foreco.2009.09.001. http://www.sciencedirect.com/science/article/pii/S037811270900615X.

Allen, C. D., D. D. Breshears, and N. G. McDowell, 2015: On underestimation of global vulnerability to tree mortality and forest die-off from hotter drought in the Anthropocene. *Ecosphere*, **6**, 1–55, doi:10.1890/ES15-00203.1.

Allison, S. D., M. D. Wallenstein, and M. A. Bradford, 2010: Soil-carbon response to warming dependent on microbial physiology. *Nat. Geosci.*, **3**, 336. http://dx.doi.org/10.1038/ngeo846.

Alongi, D. M., 2014: Carbon Cycling and Storage in Mangrove Forests. *Ann. Rev. Mar. Sci.*, **6**, 195–219, doi:10.1146/annurev-marine-010213-135020. http://www.annualreviews.org/doi/10.1146/annurev-marine-010213-135020.

Alter, R. E., E. S. Im, and E. A. B. Eltahir, 2015: Rainfall consistently enhanced around the Gezira Scheme in East Africa due to irrigation. *Nat. Geosci.*, **8**, 763–767, doi:10.1038/ngeo2514.

Amundson, R., A. A. Berhe, J. W. Hopmans, C. Olson, A. E. Sztein, and D. L. Sparks, 2015: Soil and human security in the 21st century. *Science (80-.).*, **348**, doi:10.1126/science.1261071.

Andela, N., and G. R. Van Der Werf, 2014: Recent trends in African fires driven by cropland expansion and El Niño to la Niña transition. *Nat. Clim. Chang.*, **4**, 791–795, doi:10.1038/nclimate2313.

Andela, N., and Coauthors, 2017: A human-driven decline in global burned area. *Science (80-.).*, **356**, 1356–1362, doi:10.1126/science.aal4108. http://science.sciencemag.org/content/356/6345/1356.abstract.

Anderegg, W. R. L., J. M. Kane, and L. D. L. Anderegg, 2012: Consequences of widespread tree mortality triggered by drought and temperature stress. *Nat. Clim. Chang.*, **3**, 30. http://dx.doi.org/10.1038/nclimate1635.

——, T. Klein, M. Bartlett, L. Sack, A. F. A. Pellegrini, B. Choat, and S. Jansen, 2016: Meta-analysis reveals that hydraulic traits explain cross-species patterns of drought-induced tree mortality across the globe. *Proc. Natl. Acad. Sci.*, **113**, 5024 LP-5029. http://www.pnas.org/content/113/18/5024.abstract.

Anderson, K., and G. Peters, 2016: The trouble with negative emissions. *Science (80-.).*, **354**, 182–183, doi:10.1126/science.aah4567. http://science.sciencemag.org/content/354/6309/182.abstract.

Archibald, S., and Coauthors, 2017: Biological and geophysical feedbacks with fire in the Earth System. *Environ. Res. Lett.*, **13**, 033003, doi:10.1088/1748-9326/aa9ead. http://iopscience.iop.org/article/10.1088/1748-9326/aa9ead.

Argüeso, D., J. P. Evans, L. Fita, and K. J. Bormann, 2014: Temperature response to future urbanization and climate change. *Clim. Dyn.*, **42**, 2183–2199, doi:10.1007/s00382-013-1789-6.

Armenteras-Pascual, D., J. Retana-Alumbreros, R. Molowny-Horas, R. M. Roman-Cuesta, F. Gonzalez-Alonso, and M. Morales-Rivas, 2011: Characterising fire spatial pattern interactions with climate and vegetation in Colombia. *Agric. For. Meteorol.*, **151**, 279–289, doi:10.1016/j.agrformet.2010.11.002. https://www-sciencedirect-com.ezproxy.uct.ac.za/science/article/pii/S016819231000290X (Accessed May 5, 2018).

Arneth, A., G. Schurgers, J. Lathiere, T. Duhl, D. J. Beerling, C. N. Hewitt, M. Martin, and A. Guenther, 2011: Global terrestrial isoprene emission models: Sensitivity to variability in climate and vegetation. *Atmos. Chem. Phys.*, **11**, 8037–8052, doi:10.5194/acp-11-8037-2011. https://www.atmos-chem-phys.net/11/8037/2011/.

Arneth, A., and Coauthors, 2017a: Historical carbon dioxide emissions caused by land use changes are possibly larger than assumed. *Nat. Geosci.*, **10**, 79. http://dx.doi.org/10.1038/ngeo2882.

Arneth, A., and Coauthors, 2017b: Historical carbon dioxide emissions caused by land use changes are possibly larger than assumed. *Nat. Geosci.*, **10**, 79–84, doi:10.1038/ngeo2882.

Arora, V. K., and A. Montenegro, 2011: Small temperature benefits provided by realistic afforestation efforts. *Nat. Geosci.*, **4**, 514–518, doi:10.1038/ngeo1182.

Arsiso, B. K., G. Mengistu Tsidu, G. H. Stoffberg, and T. Tadesse, 2018: Influence of urbanization-driven land use/cover change on climate: The case of Addis Ababa, Ethiopia. *Phys. Chem. Earth*, doi:10.1016/j.pce.2018.02.009.

Ashpole, I., and R. Washington, 2013: A new high-resolution central and western Saharan summertime dust source map from automated satellite dust plume tracking. *J. Geophys. Res. Atmos.*, **118**, 6981–6995, doi:10.1002/jgrd.50554. http://dx.doi.org/10.1002/jgrd.50554.

Asseng, S., 2013: <P020130613413794449840.pdf>. *Nat. Clim. Chang.*, **3**, 627–632, doi:10.1038/ncliamte1916.

Asseng, S., and Coauthors, 2015a: Rising temperatures reduce global wheat production. *Nat. Clim. Chang.*, **5**, 143–147, doi:10.1038/nclimate2470.

——, and Coauthors, 2015b: Rising temperatures reduce global wheat production. *Nat. Clim. Chang.*, **5**, 143–147, doi:10.1038/nclimate2470. http://www.nature.com/articles/nclimate2470 (Accessed May 21, 2018).

Atkin, O. K., and Coauthors, 2015: Global variability in leaf respiration in relation to climate, plant functional types and leaf traits. *New Phytol.*, **206**, 614–636, doi:10.1111/nph.13253.

Attribution, C. C., S. Sitch, and S. Sitch, 2015: Supplement of Recent trends and drivers of regional sources and sinks of carbon dioxide. *Biogeosciences*, **12**, 653–679, doi:10.5194/bg-12-653-2015-supplement.

Atwood, T. B., and Coauthors, 2017: Author Correction: Global patterns in mangrove soil carbon stocks and losses. *Nat. Clim. Chang.*, **7**, 1, doi:10.1038/s41558-017-0019-3. http://dx.doi.org/10.1038/nclimate3326.

Auffret, M. D., and Coauthors, 2016: The Role of Microbial Community Composition in Controlling Soil Respiration Responses to Temperature. *PLoS One*, **11**, e0165448, doi:10.1371/journal.pone.0165448. http://dx.plos.org/10.1371/journal.pone.0165448.

Augustin, J., J. Couwenberg, and M. Minke, 2011: Peatlands and greenhouse gases. *Carbon credits from peatland rewetting: climate - biodiversity - land use*, T. Parish, F., Sirin, A., Charman, D., Joosten, H., Minayeva and L. Silvius, M. and Stringer, Eds., Global Environment Centre and Wetlands International, Kuala Lumpur and Wageningen, 13–19 http://www.imcg.net/media/download_gallery/books/assessment_peatland.pdf.

Averill, C., B. L. Turner, and A. C. Finzi, 2014: Mycorrhiza-mediated competition between plants and decomposers drives soil carbon storage. *Nature*, **505**, 543. http://dx.doi.org/10.1038/nature12901.

Baccini, A., and Coauthors, 2012: Estimated carbon dioxide emissions from tropical deforestation improved by carbon-density maps. *Nat. Clim. Chang.*, **2**, 182. http://dx.doi.org/10.1038/nclimate1354.

Baccini, A., W. Walker, L. Carvalho, M. Farina, D. Sulla-Menashe, and R. A. Houghton, 2017a: Tropical forests are a net carbon source based on aboveground measurements of gain and loss. *Science (80-.).*, **358**, 230–234, doi:10.1126/science.aam5962.

——, ——, ——, ——, ——, and ——, 2017b: Tropical forests are a net carbon source based on aboveground measurements of gain and loss. *Science (80-.).*, **358**, 230–234, doi:10.1126/science.aam5962.

Bader, D. A., N. York, R. Blake, N. York, and A. Grimm, 2016: Urban Climate Science. 1–41.

Bae, J., and Y. Ryu, 2015: Land use and land cover changes explain spatial and temporal variations of the soil organic carbon stocks in a constructed urban park. *Landsc. Urban Plan.*, **136**, 57–67, doi:https://doi.org/10.1016/j.landurbplan.2014.11.015.
http://www.sciencedirect.com/science/article/pii/S0169204614002758.

Bailis, R., R. Drigo, A. Ghilardi, and O. Masera, 2015: The carbon footprint of traditional woodfuels. *Nat. Clim. Chang.*, **5**, 266–272, doi:10.1038/nclimate2491.

Bajželj, B., and K. Richards, 2014: The Positive Feedback Loop between the Impacts of Climate Change and Agricultural Expansion and Relocation. *Land*, **3**, 898–916, doi:10.3390/land3030898. http://www.mdpi.com/2073-445X/3/3/898/.

Di Baldassarre, G., A. Viglione, G. Carr, L. Kuil, K. Yan, L. Brandimarte, and G. Blöschl, 2015: Debates - Perspectives on socio-hydrology: Capturing feedbacks between physical and social processes. *Water Resour. Res.*, **51**, 4770–4781, doi:10.1002/2014WR016416. http://doi.wiley.com/10.1002/2014WR016416 (Accessed May 25, 2018).

Ballantyne, A., and Coauthors, 2017: Accelerating net terrestrial carbon uptake during the warming hiatus due to reduced respiration. *Nat. Clim. Chang.*, **7**, 148–152, doi:10.1038/nclimate3204. http://dx.doi.org/10.1038/nclimate3204.

Ballantyne, A. P., C. B. Alden, J. B. Miller, P. P. Tans, and J. W. C. White, 2012: Increase in observed net carbon dioxide uptake by land and oceans during the last 50 years. *Nature*, **488**, 70–72,

doi:10.1038/nature11299. http://dx.doi.org/10.1038/nature11299.
Baltzer, J. L., T. Veness, L. E. Chasmer, A. E. Sniderhan, and W. L. Quinton, 2014: Forests on thawing permafrost: Fragmentation, edge effects, and net forest loss. *Glob. Chang. Biol.*, **20**, 824–834, doi:10.1111/gcb.12349.
BAPPENAS, 2015: *Lessons Learnt From Unilateral Process Of Reducing Emissions From Land-based Sector In Indonesia*.
Barnes, C. J., C. J. van der Gast, N. P. Mcnamara, R. Rowe, and G. D. Bending, 2018: Extreme rainfall affects assembly of the root-associated fungal community. *New Phytol.*, doi:10.1111/nph.14990. http://doi.wiley.com/10.1111/nph.14990 (Accessed May 25, 2018).
Barnes, E. A., J. Slingo, and T. Woollings, 2012: A methodology for the comparison of blocking climatologies across indices, models and climate scenarios. *Clim. Dyn.*, **38**, 2467–2481, doi:10.1007/s00382-011-1243-6. http://link.springer.com/10.1007/s00382-011-1243-6 (Accessed May 23, 2018).
——, E. Dunn-Sigouin, G. Masato, and T. Woollings, 2014: Exploring recent trends in Northern Hemisphere blocking. *Geophys. Res. Lett.*, **41**, 638–644, doi:10.1002/2013GL058745. http://doi.wiley.com/10.1002/2013GL058745 (Accessed May 23, 2018).
Baron, R. E., W. D. Montgomery, and S. D. Tuladhar, 2009: *An Analysis of Black Carbon Mitigation as a Response to Climate Change a Response to Climate Change*. 29pp pp.
Baskaran, P., R. Hyvï¿½nen, S. L. Berglund, K. E. Clemmensen, G. I. ï¿½gren, B. D. Lindahl, and S. Manzoni, 2017: Modelling the influence of ectomycorrhizal decomposition on plant nutrition and soil carbon sequestration in boreal forest ecosystems. *New Phytol.*, **213**, 1452–1465, doi:10.1111/nph.14213. https://doi.org/10.1111/nph.14213.
Bassett, R., X. Cai, L. Chapman, C. Heaviside, and J. E. Thornes, 2017: The Effects of Heat Advection on UK Weather and Climate Observations in the Vicinity of Small Urbanized Areas. *Boundary-Layer Meteorol.*, **165**, 181–196, doi:10.1007/s10546-017-0263-0.
Bassu, S., and Coauthors, 2014: How do various maize crop models vary in their responses to climate change factors? *Glob. Chang. Biol.*, **20**, 2301–2320, doi:10.1111/gcb.12520.
Battipaglia, G., M. Saurer, P. Cherubini, C. Calfapietra, H. R. Mccarthy, R. J. Norby, and M. Francesca Cotrufo, 2013: Elevated CO2increases tree-level intrinsic water use efficiency: Insights from carbon and oxygen isotope analyses in tree rings across three forest FACE sites. *New Phytol.*, **197**, 544–554, doi:10.1111/nph.12044.
Beare, M. H., S. J. McNeill, D. Curtin, R. L. Parfitt, H. S. Jones, M. B. Dodd, and J. Sharp, 2014: Estimating the organic carbon stabilisation capacity and saturation deficit of soils: A New Zealand case study. *Biogeochemistry*, **120**, 71–87, doi:10.1007/s10533-014-9982-1.
Beer, T., 2018: The Impact of Extreme Weather Events on Food Security. Springer, Cham, 121–133 http://link.springer.com/10.1007/978-3-319-56469-2_8 (Accessed May 25, 2018).
Berg, A., and Coauthors, 2016: Land-atmosphere feedbacks amplify aridity increase over land under global warming. *Nat. Clim. Chang.*, **6**, 869–874, doi:10.1038/nclimate3029.
——, B. R. Lintner, K. Findell, and A. Giannini, 2017: Uncertain soil moisture feedbacks in model projections of Sahel precipitation. *Geophys. Res. Lett.*, **44**, 6124–6133, doi:10.1002/2017GL073851.
Berg, P., C. Moseley, and J. O. Haerter, 2013: Strong increase in convective precipitation in response to higher temperatures. *Nat. Geosci.*, **6**, 181–185, doi:10.1038/ngeo1731. http://www.nature.com/articles/ngeo1731 (Accessed May 19, 2018).
Bergamaschi, P., and Coauthors, 2013: Atmospheric CH<inf>4</inf> in the first decade of the 21st century: Inverse modeling analysis using SCIAMACHY satellite retrievals and NOAA surface measurements. *J. Geophys. Res. Atmos.*, **118**, 7350–7369, doi:10.1002/jgrd.50480.
Berhe, A. A., J. Harte, J. W. Harden, and M. S. Torn, 2007: The Significance of the Erosion-induced Terrestrial Carbon Sink. *Bioscience*, **57**, 337–346. http://dx.doi.org/10.1641/B570408.
——, J. W. Harden, M. S. Torn, and J. Harte, 2008: Linking soil organic matter dynamics and erosion-induced terrestrial carbon sequestration at different landform positions. *J. Geophys. Res. Biogeosciences*, **113**, 1–12, doi:10.1029/2008JG000751.
Berry, J. A., D. J. Beerling, and P. J. Franks, 2010: Stomata: Key players in the earth system, past and

present. *Curr. Opin. Plant Biol.*, **13**, 233–240, doi:10.1016/j.pbi.2010.04.013. http://dx.doi.org/10.1016/j.pbi.2010.04.013.

Bertrand, G., C. Marta, C. Philippe, T. Marwa, M. Fabienne, S. J. L., and J. I. A., 2018: Impact of priming on global soil carbon stocks. *Glob. Chang. Biol.*, **24**, 1873–1883, doi:10.1111/gcb.14069. https://doi.org/10.1111/gcb.14069.

Betts, R. A., 2000: Offset of the potential carbon sink from boreal forestation by decreases in surface albedo. *Nature*, **408**, 187–190, doi:10.1038/35041545.

Blanco-Canqui, H., and R. Lal, 2004: Mechanisms of Carbon Sequestration in Soil Aggregates. *CRC. Crit. Rev. Plant Sci.*, **23**, 481–504, doi:10.1080/07352680490886842. https://doi.org/10.1080/07352680490886842.

Bodirsky, B. L., and Coauthors, 2014: Reactive nitrogen requirements to feed the world in 2050 and potential to mitigate nitrogen pollution. *Nat. Commun.*, **5**, 3858, doi:10.1038/ncomms4858. http://dx.doi.org/10.1038/ncomms4858.

Bohnenstengel, S. I., I. Hamilton, M. Davies, and S. E. Belcher, 2014: Impact of anthropogenic heat emissions on London's temperatures. *Q. J. R. Meteorol. Soc.*, **140**, 687–698, doi:10.1002/qj.2144.

Boisier, J. P., and Coauthors, 2012: Attributing the impacts of land-cover changes in temperate regions on surface temperature and heat fluxes to specific causes: Results from the first LUCID set of simulations. *J. Geophys. Res. Atmos.*, **117**, 1–16, doi:10.1029/2011JD017106.

Bonan, G. B., 2008: Forests and Climate Change: Forcings, Feedbacks, and the Climate Benefits of Forests. *Science (80-.).*, **320**, 1444 LP-1449. http://science.sciencemag.org/content/320/5882/1444.abstract.

Bond, T. C., E. Bhardwaj, R. Dong, R. Jogani, S. Jung, C. Roden, D. G. Streets, and N. M. Trautmann, 2007: Historical emissions of black and organic carbon aerosol from energy-related combustion, 1850-2000. *Global Biogeochem. Cycles*, **21**, doi:10.1029/2006GB002840.

Bond, T. C., and Coauthors, 2013: Bounding the role of black carbon in the climate system: A scientific assessment. *J. Geophys. Res. Atmos.*, **118**, 5380–5552, doi:10.1002/jgrd.50171. https://doi.org/10.1002/jgrd.50171.

Bond, W. J., F. I. Woodward, and G. F. Midgley, 2005: The global distribution of ecosystems in a world without fire. *New Phytol.*, **165**, 525–538, doi:10.1111/j.1469-8137.2004.01252.x. https://doi.org/10.1111/j.1469-8137.2004.01252.x.

Bonfils, C., and D. Lobell, 2007: Empirical evidence for a recent slowdown in irrigation-induced cooling. *Proc. Natl. Acad. Sci.*, **104**, 13582–13587, doi:10.1073/pnas.0700144104. http://www.pnas.org/cgi/doi/10.1073/pnas.0700144104.

Bonfils, C. J. W., T. J. Phillips, D. M. Lawrence, P. Cameron-Smith, W. J. Riley, and Z. M. Subin, 2012: On the influence of shrub height and expansion on northern high latitude climate. *Environ. Res. Lett.*, **7**, doi:10.1088/1748-9326/7/1/015503.

Borodina, A., E. M. Fischer, and R. Knutti, 2017: Models are likely to underestimate increase in heavy rainfall in the extratropical regions with high rainfall intensity. *Geophys. Res. Lett.*, **44**, 7401–7409, doi:10.1002/2017GL074530. http://doi.wiley.com/10.1002/2017GL074530 (Accessed May 16, 2018).

Borrelli, P., and Coauthors, 2017: An assessment of the global impact of 21st century land use change on soil erosion. *Nat. Commun.*, **8**, doi:10.1038/s41467-017-02142-7.

Bossio, D. A., and K. M. Scow, 1998: Impacts of carbon and flooding on soil microbial communities: Phospholipid fatty acid profiles and substrate utilization patterns. *Microb. Ecol.*, **35**, 265–278, doi:10.1007/s002489900082. http://link.springer.com/10.1007/s002489900082 (Accessed May 25, 2018).

Boucher, O., G. Myhre, and A. Myhre, 2004: Direct human influence of irrigation on atmospheric water vapour and climate. *Clim. Dyn.*, **22**, 597–603, doi:10.1007/s00382-004-0402-4.

Boucher, O., and Coauthors, 2013: Clouds and aerosols. *Climate Change 2013 the Physical Science Basis: Working Group I Contribution to the Fifth Assessment Report of the Intergovernmental Panel on Climate Change*, T.F. Stocker et al., Eds., Vol. 9781107057 of, Cambridge University Press, Cambridge, UK, 571–658.

Bousquet, P., and Coauthors, 2006: Contribution of anthropogenic and natural sources to atmospheric methane variability. *Nature*, **443**, 439–443, doi:10.1038/nature05132.

——, and Coauthors, 2011: Source attribution of the changes in atmospheric methane for 2006-2008. *Atmos. Chem. Phys.*, **11**, 3689–3700, doi:10.5194/acp-11-3689-2011.

Bouwer, L. M., 2011: Have disaster losses increased due to anthropgenic climate change? *Am. Meteorol. Soc.*, **BAMS**, 39–46, doi:10.1175/2010BAMS3092.1. http://journals.ametsoc.org/doi/abs/10.1175/2010BAMS3092.1 (Accessed May 25, 2018).

Bouwman, A. F., and Coauthors, 2013: Global trends and uncertainties in terrestrial denitrification and N2O emissions. *Philos. Trans. R. Soc. B Biol. Sci.*, **368**, 20130112–20130112, doi:10.1098/rstb.2013.0112. http://rstb.royalsocietypublishing.org/cgi/doi/10.1098/rstb.2013.0112.

Bowman, D. M. J. S., and Coauthors, 2011: The human dimension of fire regimes on Earth. *J. Biogeogr.*, **38**, 2223–2236, doi:10.1111/j.1365-2699.2011.02595.x. http://doi.wiley.com/10.1111/j.1365-2699.2011.02595.x.

Bowman, D. M. J. S., G. J. Williamson, J. T. Abatzoglou, C. A. Kolden, M. A. Cochrane, and A. M. S. Smith, 2017: Human exposure and sensitivity to globally extreme wildfire events. *Nat. Ecol. &Amp; Evol.*, **1**, 58. http://dx.doi.org/10.1038/s41559-016-0058.

Boysen, L. R., V. Brovkin, V. K. Arora, P. Cadule, N. de Noblet-Ducoudré, E. Kato, J. Pongratz, and V. Gayler, 2014: Global and regional effects of land use change on climate in 21st century simulations with interactive carbon cycle. *Earth Syst. Dyn. Discuss.*, **5**, 443–472, doi:10.5194/esdd-5-443-2014. http://www.earth-syst-dynam-discuss.net/5/443/2014/.

Boysen, L. R., W. Lucht, and D. Gerten, 2017: Trade-offs for food production, nature conservation and climate limit the terrestrial carbon dioxide removal potential. *Glob. Chang. Biol.*, **23**, 4303–4317, doi:10.1111/gcb.13745.

Brando, P. M., D. C. Nepstad, E. A. Davidson, S. E. Trumbore, D. Ray, and P. Camargo, 2008: Drought effects on litterfall, wood production and belowground carbon cycling in an Amazon forest: results of a throughfall reduction experiment. *Philos. Trans. R. Soc. B Biol. Sci.*, **363**, 1839–1848, doi:10.1098/rstb.2007.0031. http://rstb.royalsocietypublishing.org/cgi/doi/10.1098/rstb.2007.0031 (Accessed May 21, 2018).

Brando, P. M., and Coauthors, 2014: Abrupt increases in Amazonian tree mortality due to drought-fire interactions. *Proc. Natl. Acad. Sci.*, **111**, 6347–6352, doi:10.1073/pnas.1305499111. http://www.pnas.org/cgi/doi/10.1073/pnas.1305499111.

Bremer, D. J., and J. M. Ham, 1999: Effect of spring burning on the surface energy balance in a tallgrass prairie. *Agric. For. Meteorol.*, **97**, 43–54, doi:10.1016/S0168-1923(99)00034-9. http://www.sciencedirect.com/science/article/pii/S0168192399000349.

Breshears, D. D., and Coauthors, 2005: Regional vegetation die-off in response to global-change-type drought. *Proc. Natl. Acad. Sci.*, **102**, 15144–15148, doi:10.1073/pnas.0505734102. http://www.pnas.org/cgi/doi/10.1073/pnas.0505734102.

Brodribb, T. J., 2009: Xylem hydraulic physiology: The functional backbone of terrestrial plant productivity. *Plant Sci.*, **177**, 245–251, doi:https://doi.org/10.1016/j.plantsci.2009.06.001. http://www.sciencedirect.com/science/article/pii/S0168945209001599.

Brovkin, V., and Coauthors, 2013: Effect of anthropogenic land use and land-cover changes on climate and land carbon storage in CMIP5 projections for the twenty-first century. *J. Clim.*, **26**, 6859–6881, doi:10.1175/JCLI-D-12-00623.1.

Bruhwiler, L., and Coauthors, 2014: CarbonTracker-CH4: An assimilation system for estimating emissions of atmospheric methane. *Atmos. Chem. Phys.*, **14**, 8269–8293, doi:10.5194/acp-14-8269-2014.

Brutel-Vuilmet, C., M. Ménégoz, and G. Krinner, 2013: An analysis of present and future seasonal Northern Hemisphere land snow cover simulated by CMIP5 coupled climate models. *Cryosphere*, **7**, 67–80, doi:10.5194/tc-7-67-2013. https://www.the-cryosphere.net/7/67/2013/.

Buchkowski, R. W., M. A. Bradford, A. S. Grandy, O. J. Schmitz, and W. R. Wieder, 2017: Applying population and community ecology theory to advance understanding of belowground biogeochemistry. *Ecol. Lett.*, **20**, 231–245, doi:10.1111/ele.12712. https://doi.org/10.1111/ele.12712.

Buitenhuis, E. T., P. Suntharalingam, and C. Le Quéré, 2017: Constraints on global oceanic emissions of N₂O from observations and models. *Biogeosciences Discuss.*, 1–23, doi:10.5194/bg-2017-193. https://www.biogeosciences-discuss.net/bg-2017-193/.

Burakowski, E., A. Tawfik, A. Ouimette, L. Lepine, K. Novick, S. Ollinger, C. Zarzycki, and G. Bonan, 2018: The role of surface roughness, albedo, and Bowen ratio on ecosystem energy balance in the Eastern United States. *Agric. For. Meteorol.*, **249**, 367–376, doi:10.1016/j.agrformet.2017.11.030.

Burke, E. J., S. J. Brown, and N. Christidis, 2006: Modeling the Recent Evolution of Global Drought and Projections for the Twenty-First Century with the Hadley Centre Climate Model. *J. Hydrometeorol.*, **7**, 1113–1125, doi:10.1175/JHM544.1. http://journals.ametsoc.org/doi/abs/10.1175/JHM544.1 (Accessed May 8, 2018).

——, and Coauthors, 2017: Quantifying uncertainties of permafrost carbon-climate feedbacks. *Biogeosciences*, **14**, 3051–3066, doi:10.5194/bg-14-3051-2017.

Burkett, V. R., A. G. Suarez, M. Bindi, C. Conde, R. Mukerji, M. J. Prather, A. L. St. Clair, and G. W. Yohe, 2014: *Global and Sectoral Aspects. Contribution of Working Group II to the Fifth Assessment Report of the Intergovernmental Panel on Climate Change*. C.B. Field et al., Eds. Cambridge University Pres, Cambridge, United Kingdom and New York, NY, USA, 169-194 pp.

Busch, J., and J. Engelmann, 2015: *The future of forests: Emissions from tropical deforestation with and without a carbon price, 2016-2050. Working Paper 411. CGD Climate and Forest Paper Series #22*. 42 pp. https://papers.ssrn.com/sol3/papers.cfm?abstract_id=2671559.

Butt, N., P. A. De Oliveira, and M. H. Costa, 2011: Evidence that deforestation affects the onset of the rainy season in Rondonia, Brazil. *J. Geophys. Res. Atmos.*, **116**, 2–9, doi:10.1029/2010JD015174.

Cai, W., and Coauthors, 2014: Increasing frequency of extreme El Niño events due to greenhouse warming. *Nat. Clim. Chang.*, **4**, 111–116, doi:10.1038/nclimate2100. http://www.nature.com/articles/nclimate2100 (Accessed May 15, 2018).

——, and Coauthors, 2015: Increased frequency of extreme La Niï¿½a events under greenhouse warming. *Nat. Clim. Chang.*, **5**, 132–137, doi:10.1038/nclimate2492. http://www.nature.com/articles/nclimate2492 (Accessed May 17, 2018).

Calvo, A. I., C. Alves, A. Castro, V. Pont, A. M. Vicente, and R. Fraile, 2013: Research on aerosol sources and chemical composition: Past, current and emerging issues. *Atmos. Res.*, **120–121**, 1–28, doi:10.1016/j.atmosres.2012.09.021.

Camenzind, T., S. Hättenschwiler, K. K. Treseder, A. Lehmann, and M. C. Rillig, 2018: Nutrient limitation of soil microbial processes in tropical forests. *Ecol. Monogr.*, **88**, 4–21, doi:10.1002/ecm.1279.

Campbell, B. M., and Coauthors, 2017: Agriculture production as a major driver of the Earth system exceeding planetary boundaries. *Ecol. Soc.*, **22**, art8, doi:10.5751/ES-09595-220408.

Canadell, J. G., and Coauthors, 2007: Contributions to accelerating atmospheric CO2 growth from economic activity, carbon intensity, and efficiency of natural sinks. *Proc. Natl. Acad. Sci.*, **104**, 18866–18870, doi:10.1073/pnas.0702737104. http://www.pnas.org/cgi/doi/10.1073/pnas.0702737104.

Carey, J. C., and Coauthors, 2016: Temperature response of soil respiration largely unaltered with experimental warming. *Proc. Natl. Acad. Sci.*, **113**, 13797–13802, doi:10.1073/pnas.1605365113. http://www.pnas.org/content/113/48/13797.

Carissimo, B. C., A. H. Oort, and T. H. Vonder Haar, 1985: Estimating the Meridional Energy Transports in the Atmosphere and Ocean. *J. Phys. Oceanogr.*, **15**, 82–91, doi:10.1175/1520-0485(1985)015<0082:ETMETI>2.0.CO;2. http://journals.ametsoc.org/doi/abs/10.1175/1520-0485%281985%29015%3C0082%3AETMETI%3E2.0.CO%3B2 (Accessed May 7, 2018).

Carlson, K. M., and Coauthors, 2016: Greenhouse gas emissions intensity of global croplands. *Nat. Clim. Chang.*, **7**, 63–71, doi:10.1038/NCLIMATE3158.

Carter, S., M. Herold, M. C. Rufino, K. Neumann, L. Kooistra, and L. Verchot, 2015: Mitigation of agricultural emissions in the tropics: Comparing forest land-sparing options at the national level. *Biogeosciences*, **12**, 4809–4825, doi:10.5194/bg-12-4809-2015. https://www.biogeosciences.net/12/4809/2015/.

Ceccherini, G., S. Russo, I. Ameztoy, A. Francesco Marchese, and C. Carmona-Moreno, 2017: Heat waves in Africa 1981-2015, observations and reanalysis. *Nat. Hazards Earth Syst. Sci.*, **17**, 115–125, doi:10.5194/nhess-17-115-2017.

Ceschia, D. C. and G. P. and M. F. and X. C. and E., 2018: What is the potential of cropland albedo management in the fight against global warming? A case study based on the use of cover crops.

Environ. Res. Lett., **13**, 44030. http://stacks.iop.org/1748-9326/13/i=4/a=044030.
Chae, Y., S. M. Kang, S. J. Jeong, B. Kim, and D. M. W. Frierson, 2015: Arctic greening can cause earlier seasonality of Arctic amplification. *Geophys. Res. Lett.*, **42**, 536–541, doi:10.1002/2014GL061841.
Challinor, A. J., J. Watson, D. B. Lobell, S. M. Howden, D. R. Smith, and N. Chhetri, 2014: A meta-analysis of crop yield under climate change and adaptation. *Nat. Clim. Chang.*, **4**, 287–291, doi:10.1038/nclimate2153.
Change, C., 2015: Importance of food-demand management for climate mitigation policy. *Nat. Clim. Chang.*, **4**, 2–4. http://dx.doi.org/10.1038/nclimate2353.
Charles, A., P. Rochette, J. K. Whalen, D. A. Angers, M. H. Chantigny, and N. Bertrand, 2017: Global nitrous oxide emission factors from agricultural soils after addition of organic amendments: A meta-analysis. *Agric. Ecosyst. Environ.*, **236**, 88–98, doi:10.1016/j.agee.2016.11.021. http://dx.doi.org/10.1016/j.agee.2016.11.021.
Charney, J. G., 1975: Dynamics of deserts and drought in the Sahel. *Q. J. R. Meteorol. Soc.*, **101**, 193–202, doi:10.1002/qj.49710142802.
Cheesman, S., C. Thierfelder, N. S. Eash, G. T. Kassie, and E. Frossard, 2016: Soil carbon stocks in conservation agriculture systems of Southern Africa. *Soil Tillage Res.*, **156**, 99–109, doi:10.1016/j.still.2015.09.018.
Chen, B., L. Dong, X. Liu, G. Y. Shi, L. Chen, T. Nakajima, and A. Habib, 2016a: Exploring the possible effect of anthropogenic heat release due to global energy consumption upon global climate: a climate model study. *Int. J. Climatol.*, **36**, 4790–4796, doi:10.1002/joc.4669.
Chen, H., Y. Zhang, M. Yu, W. Hua, S. Sun, X. Li, and C. Gao, 2016b: Large-scale urbanization effects on eastern Asian summer monsoon circulation and climate. *Clim. Dyn.*, **47**, 117–136, doi:10.1007/s00382-015-2827-3.
Chen, L., P. A. Dirmeyer, Z. Guo, and N. M. Schultz, 2018: Pairing FLUXNET sites to validate model representations of land use/land-cover change. *Hydrol. Earth Syst. Sci.*, **22**, 111–125, doi:10.5194/hess-22-111-2018. https://www.hydrol-earth-syst-sci.net/22/111/2018/.
Chen, S., W. B. Li, Y. D. Du, C. Y. Mao, and L. Zhang, 2015: Urbanization effect on precipitation over the Pearl River Delta based on CMORPH data. *Adv. Clim. Chang. Res.*, **6**, 16–22, doi:10.1016/j.accre.2015.08.002. http://dx.doi.org/10.1016/j.accre.2015.08.002.
Chen, W., Y. Zhang, X. Mai, and Y. Shen, 2016c: Multiple mechanisms contributed to the reduced stability of Inner Mongolia grassland ecosystem following nitrogen enrichment. *Plant Soil*, **409**, 283–296, doi:10.1007/s11104-016-2967-1. http://dx.doi.org/10.1007/s11104-016-2967-1.
Chen, X., and S.-J. Jeong, 2018: Irrigation enhances local warming with greater nocturnal warming effects than daytime cooling effects. *Environ. Res. Lett.*, **13**, 024005, doi:10.1088/1748-9326/aa9dea. http://stacks.iop.org/1748-9326/13/i=2/a=024005?key=crossref.4a93ef61f758279985613f5e49fa2cd5.
Chen, Y., D. C. Morton, N. Andela, G. R. Van Der Werf, L. Giglio, and J. T. Randerson, 2017a: A pan-tropical cascade of fire driven by El Niño/Southern Oscillation. *Nat. Clim. Chang.*, **7**, 906–911, doi:10.1038/s41558-017-0014-8. http://dx.doi.org/10.1038/s41558-017-0014-8.
Cheng, W., W. J. Parton, M. A. Gonzalez-Meler, R. Phillips, S. Asao, G. G. Mcnickle, E. Brzostek, and J. D. Jastrow, 2014: Synthesis and modeling perspectives of rhizosphere priming. *New Phytol.*, **201**, 31–44, doi:10.1111/nph.12440.
Choat, B., and Coauthors, 2012: Global convergence in the vulnerability of forests to drought. *Nature*, **491**, 752. http://dx.doi.org/10.1038/nature11688.
Christensen, J. H., and O. B. Christensen, 2003: Severe summertime flooding in Europe. *Nature*, **421**, 805–806, doi:10.1038/421805a. http://www.nature.com/articles/421805a (Accessed May 17, 2018).
Christensen, J. H., and Coauthors, 2013: Climate phenomena and their relevance for future regional climate change. *Climate Change 2013 the Physical Science Basis: Working Group I Contribution to the Fifth Assessment Report of the Intergovernmental Panel on Climate Change*, T.F. Stocker et al., Eds., Vol. 9781107057 of, Cambridge University Press, Cambridge, United Kingdom and New York, NY, USA, 1217–1308.
Christidis, N., P. A. Stott, S. Brown, G. C. Hegerl, and J. Caesar, 2005: Detection of changes in temperature extremes during the second half of the 20th century. *Geophys. Res. Lett.*, **32**, 1–4,

doi:10.1029/2005GL023885. http://doi.wiley.com/10.1029/2005GL023885 (Accessed May 24, 2018).
Chrysanthou, A., G. Van Der Schrier, E. J. M. Van Den Besselaar, A. M. G. Klein Tank, and T. Brandsma, 2014: The effects of urbanization on the rise of the European temperature since 1960. *Geophys. Res. Lett.*, **41**, 7716–7722, doi:10.1002/2014GL061154.
Chum, H., A. Faaij, J. Moreira, B. G., P. Dhamija, H. Dong, and K. Pingoud, 2011: Bioenergy. *IPCC Special Report on Renewable Energy Sources and Climate Change Mitigation*, O. Edenhofer et al., Eds., Cambridge, United Kingdom and New York, NY, USA, 209–332.
Ciais, P., and Coauthors, 2013: Carbon and other biogeochemical cycles. *Climate Change 2013 the Physical Science Basis: Working Group I Contribution to the Fifth Assessment Report of the Intergovernmental Panel on Climate Change*, V.B. and P.M.M. (eds.). (Stocker, T.F., D. Qin, G.-K. Plattner, M. Tignor, S.K. Allen, J. Boschung, A. Nauels, Y. Xia, Ed., Vol. 9781107057 of, IPCC, New York, 465–570 http://www.ipcc.ch/report/ar5/wg1/docs/review/WG1AR5_SOD_Ch06_All_Final.pdf.
Claeys, M., W. Wang, A. C. Ion, I. Kourtchev, A. Gelencsér, and W. Maenhaut, 2004: Formation of secondary organic aerosols from isoprene and its gas-phase oxidation products through reaction with hydrogen peroxide. *Atmos. Environ.*, **38**, 4093–4098, doi:10.1016/j.atmosenv.2004.06.001. http://linkinghub.elsevier.com/retrieve/pii/S1352231004004996%5Cn%3CGo to ISI%3E://000222706000001%5Cnhttp://ac.els-cdn.com/S1352231004004996/1-s2.0-S1352231004004996-main.pdf?_tid=92b72d1c-7be1-11e5-be24-00000aacb35f&acdnat=1445864626_a476e4a5b538fa72632.
Clark, J. M., and Coauthors, 2010: Assessing the vulnerability of blanket peat to climate change using an ensemble of statistical bioclimatic envelope models. *Clim. Res.*, **45**, 131–150, doi:10.3354/cr00929. https://www.int-res.com/abstracts/cr/v45/p131-150/.
Clarke, L. E., and Coauthors, 2014: Assessing transformation pathways. *Climate Change 2014: Mitigation of Climate Change. Contribution of Working Group III to the Fifth Assessment Report of the Intergovernmental Panel on Climate Change*, O. Denhofer et al., Eds., Cambridge University Pres, Cambridge, United Kingdom and New York, NY, USA, 413–510 https://www.ipcc.ch/pdf/assessment-report/ar5/wg3/ipcc_wg3_ar5_chapter6.pdf.
Claussen, M., V. Brovkin, and A. Ganopolski, 2001: Biophysical versus biogeochemical feedbacks of large-scale land cover change. *Geophys. Res. Lett.*, **28**, 1011–1014, doi:10.1029/2000GL012471. http://onlinelibrary.wiley.com/doi/10.1029/2000GL012471/full.
Cleveland, C., K. Todd-brown, W. R. Wieder, C. C. Cleveland, W. K. Smith, and K. Todd-brown, 2015: Future productivity and carbon storage limited by terrestrial nutrient availability Future productivity and carbon storage limited by terrestrial nutrient availability. *Nat. Geosci.*, **8**, 441, doi:10.1038/NGEO2413. http://dx.doi.org/10.1038/ngeo2413.
Climate Focus, 2016: *Progress on the New York Declaration on Forests - Achieving Collective Forest Goals. Updates on Goals 1-10*. 54pp pp. http://www.climatefocus.com/sites/default/files/2016-Updates-on-Goals-1-10-Report.pdf.
Cohen, J. B., and C. Wang, 2014: Estimating global black carbon emissions using a top-down Kalman Filter approach. *J. Geophys. Res. Atmos.*, **119**, 307–323, doi:10.1002/2013JD019912. http://doi.wiley.com/10.1002/2013JD019912.
Collins, W. J., and Coauthors, 2018: Increased importance of methane reduction for a 1.5 degree target. *Environ. Res. Lett.*, **13**, 054003, doi:10.1088/1748-9326/aab89c. http://stacks.iop.org/1748-9326/13/i=5/a=054003?key=crossref.70d07fb114d80fc70bd1b8927f03ac6b.
Colwell, R. K., G. Brehm, C. L. Cardelús, A. C. Gilman, and J. T. Longino, 2008: Global warming, elevational range shifts, and lowland biotic attrition in the wet tropics. *Science (80-.).*, **322**, 258–261, doi:10.1126/science.1162547. http://science.sciencemag.org/content/344/6183/1247579.abstract.
Combal, B., and Coauthors, 2003: Retrieval of canopy biophysical variables from bidirectional reflectance using prior information to solve the ill-posed inverse problem. *Remote Sens. Environ.*, **84**, 1–15, doi:10.1016/S0034-4257(02)00035-4.
Conant, R. T., and Coauthors, 2011: Temperature and soil organic matter decomposition rates - synthesis of current knowledge and a way forward. *Glob. Chang. Biol.*, **17**, 3392–3404, doi:10.1111/j.1365-2486.2011.02496.x. https://doi.org/10.1111/j.1365-2486.2011.02496.x.

Conway, G., 2012a: How to create resilient agriculture. *Appropriate Technology*, O. Edenhofer et al., Eds., Vol. 39 of, Cambridge University Press, Cambridge, United Kingdom and New York, NY, USA, 12–14.
——, 2012b: How to create resilient agriculture. *Appropr. Technol.*, **39**, 12–14, doi:10.1146/annurev-environ-020411-130608. http://ccafs.cgiar.org/news/press-releases/agriculture-and-food-production-contribute-29-percent-global-greenhouse-gas.
Cook, B. I., S. P. Shukla, M. J. Puma, and L. S. Nazarenko, 2015: Irrigation as an historical climate forcing. *Clim. Dyn.*, **44**, 1715–1730, doi:10.1007/s00382-014-2204-7. https://doi.org/10.1007/s00382-014-2204-7.
Corbeels, M., R. Cardinael, K. Naudin, H. Guibert, and E. Torquebiau, 2018: The 4 per 1000 goal and soil carbon storage under agroforestry and conservation agriculture systems in sub-Saharan Africa. *Soil Tillage Res.*, doi:10.1016/j.still.2018.02.015.
da Costa, A. C. L., and Coauthors, 2010: Effect of 7 yr of experimental drought on vegetation dynamics and biomass storage of an eastern Amazonian rainforest. *New Phytol.*, **187**, 579–591, doi:10.1111/j.1469-8137.2010.03309.x. http://doi.wiley.com/10.1111/j.1469-8137.2010.03309.x (Accessed May 21, 2018).
Coumou, D., and S. Rahmstorf, 2012: A decade of weather extremes. *Nat. Clim. Chang.*, **2**, 491–496, doi:10.1038/nclimate1452. http://www.nature.com/doifinder/10.1038/nclimate1452 (Accessed May 19, 2018).
Couwenberg, J., R. Dommain, and H. Joosten, 2010: Greenhouse gas fluxes from tropical peatlands in south-east Asia. *Glob. Chang. Biol.*, **16**, 1715–1732, doi:10.1111/j.1365-2486.2009.02016.x. https://doi.org/10.1111/j.1365-2486.2009.02016.x.
Cowie, S. M., P. Knippertz, and J. H. Marsham, 2013: Are vegetation-related roughness changes the cause of the recent decrease in dust emission from the Sahel? *Geophys. Res. Lett.*, **40**, 1868–1872, doi:10.1002/grl.50273.
Cowling, S. A., C. D. Jones, and P. M. Cox, 2009: Greening the terrestrial biosphere: Simulated feedbacks on atmospheric heat and energy circulation. *Clim. Dyn.*, **32**, 287–299, doi:10.1007/s00382-008-0481-8.
Creutzig, F., and Coauthors, 2015: Bioenergy and climate change mitigation: An assessment. *GCB Bioenergy*, **7**, 916–944, doi:10.1111/gcbb.12205. https://doi.org/10.1111/gcbb.12205.
Crichton, K. A., N. Bouttes, D. M. Roche, J. Chappellaz, and G. Krinner, 2016: Permafrost carbon as a missing link to explain CO 2 changes during the last deglaciation. *Nat. Geosci.*, **9**, 683–686, doi:10.1038/ngeo2793.
Crook, J. A., and P. M. Forster, 2014: Comparison of surface albedo feedback in climate models and observations. *Geophys. Res. Lett.*, **41**, 1717–1723, doi:10.1002/2014GL059280.Received. http://onlinelibrary.wiley.com/doi/10.1002/2014GL059280/full.
Crooks, S., D. Herr, J. Tamelander, D. Laffoley, and J. Vandever, 2011: *Mitigating Climate Change through Restoration and Management of Coastal Wetlands and Near-shore Marine Ecosystems: Challenges and Opportunities*. 59 pp. http://www.cabi.org/environmentalimpact/default.aspx?site=138&page=179.
Crowther, T. W., S. M. Thomas, D. S. Maynard, P. Baldrian, K. Covey, S. D. Frey, L. T. A. van Diepen, and M. A. Bradford, 2015: Biotic interactions mediate soil microbial feedbacks to climate change. *Proc. Natl. Acad. Sci.*, **112**, 7033–7038, doi:10.1073/pnas.1502956112. http://www.pnas.org/content/112/22/7033.
Crowther, T. W., and Coauthors, 2016a: Quantifying global soil carbon losses in response to warming. *Nature*, **540**, 104–108, doi:10.1038/nature20150.
——, and Coauthors, 2016b: Quantifying global soil carbon losses in response to warming. *Nature*, **540**, 104–108, doi:10.1038/nature20150. http://dx.doi.org/10.1038/nature20150.
Curtis, S., and R. F. Adler, 2003: Evolution of El Niño-precipitation relationships from satellites and gauges. *J. Geophys. Res. - Atmos.*, **108**, 1–8, doi:10.1029/2002JD002690. http://doi.wiley.com/10.1029/2002JD002690 (Accessed May 5, 2018).
D'Odorico, P., A. Bhattachan, K. F. Davis, S. Ravi, and C. W. Runyan, 2013: Global desertification: Drivers and feedbacks. *Adv. Water Resour.*, **51**, 326–344, doi:10.1016/j.advwatres.2012.01.013. https://www-sciencedirect-com.ezproxy.uct.ac.za/science/article/pii/S0309170812000231 (Accessed May 8, 2018).
Dai, A., 2011: Drought under global warming: A review. *Wiley Interdiscip. Rev. Clim. Chang.*, **2**, 45–65,

doi:10.1002/wcc.81. http://doi.wiley.com/10.1002/wcc.81 (Accessed December 20, 2017).

——, 2013: Increasing drought under global warming in observations and models. *Nat. Clim. Chang.*, **3**, 52–58, doi:10.1038/nclimate1633. http://www.nature.com/doifinder/10.1038/nclimate1633 (Accessed December 20, 2017).

Daniels, E. E., G. Lenderink, R. W. A. Hutjes, and A. A. M. Holtslag, 2016: Observed urban effects on precipitation along the Dutch West coast. *Int. J. Climatol.*, **36**, 2111–2119, doi:10.1002/joc.4458.

Das, S. K., R. K. Avasthe, R. Singh, and S. Babu, 2014: Biochar as carbon negative in carbon credit under changing climate. *Curr. Sci.*, **107**, 1090–1091, doi:10.1038/ncomms1053.

Davidson, E. A., 2009: The contribution of manure and fertilizer nitrogen to atmospheric nitrous oxide since 1860. *Nat. Geosci.*, **2**, 659–662, doi:10.1038/ngeo608. http://dx.doi.org/10.1038/ngeo608.

——, and I. A. Janssens, 2006: Temperature sensitivity of soil carbon decomposition and feedbacks to climate change. *Nature*, **440**, 165–173, doi:10.1038/nature04514.

——, and D. Kanter, 2014: Inventories and scenarios of nitrous oxide emissions. *Environ. Res. Lett.*, **9**, 105012, doi:10.1088/1748-9326/9/10/105012. http://stacks.iop.org/1748-9326/9/i=10/a=105012?key=crossref.01a0f3325fa29b16abd7cf9b4bb98871.

——, and Coauthors, 2012a: The Amazon basin in transition. *Nature*, **481**, 321–328, doi:10.1038/nature10717.

——, and Coauthors, 2012b: The Amazon basin in transition. *Nature*, **481**, 321–328, doi:10.1038/nature10717.

Davies-Barnard, T., P. J. Valdes, J. S. Singarayer, A. J. Wiltshire, and C. D. Jones, 2015: Quantifying the relative importance of land cover change from climate and land use in the representative concentration pathways. *Global Biogeochem. Cycles*, **29**, 842–853, doi:10.1002/2014GB004949. https://doi.org/10.1002/2014GB004949.

Davin, E. L., and N. de Noblet-Ducoudre, 2010: Climatic impact of global-scale Deforestation: Radiative versus nonradiative processes. *J. Clim.*, **23**, 97–112, doi:10.1175/2009JCLI3102.1.

Davin, E. L., N. de Noblet-Ducoudré, and P. Friedlingstein, 2007: Impact of land cover change on surface climate: Relevance of the radiative forcing concept. *Geophys. Res. Lett.*, **34**, n/a-n/a, doi:10.1029/2007GL029678. http://doi.wiley.com/10.1029/2007GL029678.

Davin, E. L., S. I. Seneviratne, P. Ciais, A. Olioso, and T. Wang, 2014: Preferential cooling of hot extremes from cropland albedo management. *Proc. Natl. Acad. Sci.*, **111**, 9757–9761, doi:10.1073/pnas.1317323111. http://www.pnas.org/lookup/doi/10.1073/pnas.1317323111.

Delire, C., N. de Noblet-Ducoudré, A. Sima, and I. Gouirand, 2011: Vegetation dynamics enhancing long-term climate variability confirmed by two models. *J. Clim.*, **24**, 2238–2257, doi:10.1175/2010JCLI3664.1.

Derksen, C., and R. Brown, 2012: Spring snow cover extent reductions in the 2008-2012 period exceeding climate model projections. *Geophys. Res. Lett.*, **39**, doi:10.1029/2012GL053387. https://doi.org/10.1029/2012GL053387.

Derner, J. D., and Coauthors, 2003: Above- and below-ground responses of C3-C4 species mixtures to elevated CO2 and soil water availability. *Glob. Chang. Biol.*, **9**, 452–460, doi:10.1046/j.1365-2486.2003.00579.x. http://doi.wiley.com/10.1046/j.1365-2486.2003.00579.x.

Deryng, D., D. Conway, N. Ramankutty, J. Price, and R. Warren, 2014: Global crop yield response to extreme heat stress under multiple climate change futures. *Environ. Res. Lett.*, **9**, 034011, doi:10.1088/1748-9326/9/3/034011. http://stacks.iop.org/1748-9326/9/i=3/a=034011?key=crossref.dbe03166b591fb71af81975aae0cc1ee (Accessed May 11, 2018).

——, and Coauthors, 2016: Regional disparities in the beneficial effects of rising CO2 concentrations on crop water productivity. *Nat. Clim. Chang.*, doi:10.1038/nclimate2995.

Devaraju, N., E. Robertson, A. J. Wiltshire, and N. de Noblet-Ducoudré, Sensitivity of surface air temperature to biogeophysical and biogeochemical effects of land cover change. *To be Defin.*,.

Devaraju, N., G. Bala, and A. Modak, 2015: Effects of large-scale deforestation on precipitation in the monsoon regions: Remote versus local effects. *Proc. Natl. Acad. Sci.*, **112**, 3257–3262, doi:10.1073/pnas.1423439112. http://www.pnas.org/lookup/doi/10.1073/pnas.1423439112 (Accessed December 20, 2017).

——, N. de Noblet-Ducoudré, B. Quesada, and G. Bala, 2018: Quantifying the relative importance of direct and indirect biophysical effects of deforestation on surface temperature and teleconnections. *J. Clim.*, **in rev.**, JCLI-D-17-0563.1, doi:10.1175/JCLI-D-17-0563.1. http://journals.ametsoc.org/doi/10.1175/JCLI-D-17-0563.1.

Devries, T., 2014: The oceanic anthropogenic CO_2sink: Storage, air-sea fluxes, and transports over the industrial era. *Global Biogeochem. Cycles*, **28**, 631–647, doi:10.1002/2013GB004739. https://doi.org/10.1002/2013GB004739.

Diaz, D., B. Rashford, S. De Gryze, S. Zakreski, R. Dell, and M. Niles, 2012: *Evaluation of Avoided Grassland Conversion and Cropland Conversion to Grassland as Potential Carbon Offset Project Types*. 189 pp. http://climatetrust.org/documents/Grasslands-Issue-Paper_PUBLISHED_2012-12-28_small.pdf.

Dickie, A., C. Streck, S. Roe, M. Zurek, F. Haupt, and A. Dolginow, 2014: *Strategies for Mitigating Climate Change in Agriculture*. 87 pp. www.agriculturalmitigation.org.

Diffenbaugh, N. S., and Coauthors, 2017: Quantifying the influence of global warming on unprecedented extreme climate events. *Proc. Natl. Acad. Sci.*, **114**, 4881–4886, doi:10.1073/pnas.1618082114. http://www.pnas.org/lookup/doi/10.1073/pnas.1618082114 (Accessed May 15, 2018).

Van Dijk, A. I. J. M., H. E. Beck, R. S. Crosbie, R. A. M. De Jeu, Y. Y. Liu, G. M. Podger, B. Timbal, and N. R. Viney, 2013: The Millennium Drought in southeast Australia (2001-2009): Natural and human causes and implications for water resources, ecosystems, economy, and society. *Water Resour. Res.*, **49**, 1040–1057, doi:10.1002/wrcr.20123. http://doi.wiley.com/10.1002/wrcr.20123 (Accessed May 7, 2018).

Dirmeyer, P. A., Z. Wang, M. J. Mbuh, and H. E.Norton, 2014: Intensified land surface control on boundary layer growth in a changing climate. *Geophys. Res. Lett.*, **45**, 1290–1294, doi:10.1002/2013GL058826.Received.

Dlugokencky, E. J., 2003: *Atmospheric methane levels off: Temporary pause or a new steady-state?* 1992 pp. http://doi.wiley.com/10.1029/2003GL018126.

——, L. P. Steele, P. M. Lang, and K. a. Masarie, 1994: The growth rate and distribution of atmospheric methane. *J. Geophys. Res.*, **99**, 17021, doi:10.1029/94JD01245. https://doi.org/10.1029/94JD01245.

Doan, Q. Van, H. Kusaka, and Q. B. Ho, 2016: Impact of future urbanization on temperature and thermal comfort index in a developing tropical city: Ho Chi Minh City. *Urban Clim.*, **17**, 20–31, doi:10.1016/j.uclim.2016.04.003.

Doerr, S. H., and C. Santín, 2016: Global trends in wildfire and its impacts: perceptions versus realities in a changing world. *Philos. Trans. R. Soc. B Biol. Sci.*, **371**, 20150345, doi:10.1098/rstb.2015.0345. http://rstb.royalsocietypublishing.org/lookup/doi/10.1098/rstb.2015.0345.

Domine, F., M. Barrere, and S. Morin, 2016: The growth of shrubs on high Arctic tundra at Bylot Island: Impact on snow physical properties and permafrost thermal regime. *Biogeosciences*, **13**, 6471–6486, doi:10.5194/bg-13-6471-2016.

Don, A., J. Schumacher, and A. Freibauer, 2011: Impact of tropical land use change on soil organic carbon stocks - a meta-analysis. *Glob. Chang. Biol.*, **17**, 1658–1670, doi:10.1111/j.1365-2486.2010.02336.x.

Donohue, R. J., M. L. Roderick, T. R. McVicar, and G. D. Farquhar, 2013: Impact of CO_2 fertilization on maximum foliage cover across the globe's warm, arid environments. *Geophys. Res. Lett.*, **40**, 3031–3035, doi:10.1002/grl.50563.

Dosio, A., 2017: Projection of temperature and heat waves for Africa with an ensemble of CORDEX Regional Climate Models. *Clim. Dyn.*, **49**, 493–519, doi:10.1007/s00382-016-3355-5.

Dou, J., Y. Wang, R. Bornstein, and S. Miao, 2014: Observed Spatial Characteristics of Beijing Urban Climate Impacts on Summer Thunderstorms. *J. Appl. Meteorol. Climatol.*, **54**, 94–105, doi:10.1175/JAMC-D-13-0355.1. https://doi.org/10.1175/JAMC-D-13-0355.1.

Doughty, C. E., and Coauthors, 2015: Drought impact on forest carbon dynamics and fluxes in Amazonia. *Nature*, **519**, 78–82, doi:10.1038/nature14213. http://www.nature.com/articles/nature14213 (Accessed May 7, 2018).

Drake, J. E., and Coauthors, 2011: Increases in the flux of carbon belowground stimulate nitrogen uptake and sustain the long-term enhancement of forest productivity under elevated CO_2. *Ecol. Lett.*, **14**, 349–

357, doi:10.1111/j.1461-0248.2011.01593.x.

Drösler, M., L. V. Verchot, A. Freibauer, and G. Pan, 2013: Drained inland organic soils. *2013 Suppl. to 2006 IPCC Guidel. Natl. Greenh. Gas Invent. Wetl.*, 1–79. http://www.ipcc-nggip.iges.or.jp/public/wetlands/.

Duarte, C. M., 2017: Reviews and syntheses: Hidden forests, the role of vegetated coastal habitats in the ocean carbon budget. *Biogeosciences*, **14**, 301–310, doi:10.5194/bg-14-301-2017. https://www.biogeosciences.net/14/301/2017/.

Duarte, C. M., I. J. Losada, I. E. Hendriks, I. Mazarrasa, and N. Marba, 2013: The role of coastal plant communities for climate change mitigation and adaptation. *Nat. Clim. Chang.*, **3**, 961–968, doi:10.1038/nclimate1970\rhttp://www.nature.com/nclimate/journal/v3/n11/abs/nclimate1970.html#supplementary-information. http://dx.doi.org/10.1038/nclimate1970.

Duffy, P. A., J. E. Walsh, J. M. Graham, D. H. Mann, and T. S. Rupp, 2005: Impacts of large-scale atmospheric-ocean variability on Alaskan fire season severity. *Ecol. Appl.*, **15**, 1317–1330, doi:10.1890/04-0739. http://doi.wiley.com/10.1890/04-0739 (Accessed May 5, 2018).

Dungait, J. A. J., D. W. Hopkins, A. S. Gregory, and A. P. Whitmore, 2012: Soil organic matter turnover is governed by accessibility not recalcitrance. *Glob. Chang. Biol.*, **18**, 1781–1796, doi:10.1111/j.1365-2486.2012.02665.x. https://doi.org/10.1111/j.1365-2486.2012.02665.x.

Durigon, A., and Q. de Jong van Lier, 2013: Canopy temperature versus soil water pressure head for the prediction of crop water stress. *Agric. Water Manag.*, **127**, 1–6, doi:10.1016/j.agwat.2013.05.014. https://www-sciencedirect-com.ezproxy.uct.ac.za/science/article/pii/S0378377413001339 (Accessed May 21, 2018).

Dutaur, L., and L. V. Verchot, 2007: A global inventory of the soil CH4 sink. *Global Biogeochem. Cycles*, **21**, 1–9, doi:10.1029/2006GB002734.

Dutta, M. K., T. S. Bianchi, and S. K. Mukhopadhyay, 2017: Mangrove Methane Biogeochemistry in the Indian Sundarbans: A Proposed Budget. *Front. Mar. Sci.*, **4**, 187, doi:10.3389/fmars.2017.00187. http://journal.frontiersin.org/article/10.3389/fmars.2017.00187/full.

Duveiller, G., J. Hooker, and A. Cescatti, 2018a: A dataset mapping the potential biophysical effects of vegetation cover change. *Sci. Data*, doi:10.1038/sdata.2018.14.

——, ——, and ——, 2018b: The mark of vegetation change on Earth's surface energy balance. *Nat. Commun.*, **9**, 679, doi:10.1038/s41467-017-02810-8. https://doi.org/10.1038/s41467-017-02810-8.

Edelenbosch, O. Y., and Coauthors, 2017: Decomposing passenger transport futures: Comparing results of global integrated assessment models. *Transp. Res. Part D Transp. Environ.*, **55**, 281–293, doi:10.1016/j.trd.2016.07.003. http://linkinghub.elsevier.com/retrieve/pii/S1361920916301304.

Edwards, M. E., L. B. Brubaker, A. V Lozhkin, and M. Patricia, 2018: Structurally Novel Biomes : A Response to past Warming in Beringia Published by : Wiley on behalf of the Ecological Society of America Stable URL : http://www.jstor.org/stable/3450612 REFERENCES Linked references are available on JSTOR for this article : . **86**, 1696–1703.

Elagib, N. A., 2011: Evolution of urban heat island in Khartoum. *Int. J. Climatol.*, **31**, 1377–1388, doi:10.1002/joc.2159.

Elliott, J., and Coauthors, 2014: Constraints and potentials of future irrigation water availability on agricultural production under climate change. *Proc. Natl. Acad. Sci. U. S. A.*, **111**, 3239–3244, doi:10.1073/pnas.1222474110.

——, and Coauthors, 2017: Characterizing agricultural impacts of recent large-scale US droughts and changing technology and management. *Agric. Syst.*, **159**, 275–281, doi:10.1016/j.agsy.2017.07.012.

Ellison, D., and Coauthors, 2017: Trees, forests and water: Cool insights for a hot world. *Glob. Environ. Chang.*, **43**, 51–61, doi:10.1016/j.gloenvcha.2017.01.002. http://dx.doi.org/10.1016/j.gloenvcha.2017.01.002.

EPA, 2013: *Global Mitigation of Non-CO2 Greenhouse Gases: 2010-2030*. United States Environmental Protecti0n Agency, Washington DC, 410 pp. http://www.epa.gov/climatechange/Downloads/EPAactivities/MAC_Report_2013.pdf.

Erb, K. H., and Coauthors, 2018: Unexpectedly large impact of forest management and grazing on global vegetation biomass. *Nature*, **553**, 73–76, doi:10.1038/nature25138. https://mailattachment.googleusercontent.com/attachment/u/0/?ui=2&ik=03e7b0d8bd&attid=0.1&th=1607f69aea225672&view=att&disp=inline&sadnir=1&saddbat=ANGjdJ9CDan5p6BLIbdOTgzuhFb4s5ubaWK_I7GRvgjjx-1BFJdJqGIgYVkj5jtWcZMDxelV3jtvs77_dCNs0Go4vu6yTtRXDgLhlRvj82.

Espinoza, J. C., J. Ronchail, J. L. Guyot, C. Junquas, P. Vauchel, W. Lavado, G. Drapeau, and R. Pombosa, 2011: Climate variability and extreme drought in the upper Solim??es River (western Amazon Basin): Understanding the exceptional 2010 drought. *Geophys. Res. Lett.*, **38**, n/a-n/a, doi:10.1029/2011GL047862. http://doi.wiley.com/10.1029/2011GL047862 (Accessed May 8, 2018).

Estoque, R. C., and Y. Murayama, 2017: Monitoring surface urban heat island formation in a tropical mountain city using Landsat data (1987–2015). *ISPRS J. Photogramm. Remote Sens.*, **133**, 18–29, doi:https://doi.org/10.1016/j.isprsjprs.2017.09.008. http://www.sciencedirect.com/science/article/pii/S0924271617303064.

Evan, A. T., C. Flamant, S. Fiedler, and O. Doherty, 2014: An analysis of aeolian dust in climate models. *Geophys. Res. Lett.*, **41**, 5996–6001, doi:10.1002/2014GL060545. https://doi.org/10.1002/2014GL060545.

——, ——, M. Gaetani, and F. Guichard, 2016: The past, present and future of African dust. *Nature*, **531**, 493–495, doi:10.1038/nature17149. http://dx.doi.org/10.1038/nature17149.

Evans, S., P. Ginoux, S. Malyshev, and E. Shevliakova, 2016: Climate-vegetation interaction and amplification of Australian dust variability. *Geophys. Res. Lett.*, **43**, 11,823-11,830, doi:10.1002/2016GL071016. http://doi.wiley.com/10.1002/2016GL071016 (Accessed January 23, 2018).

Fahey, C., K. Winter, M. Slot, and K. Kitajima, 2016: Influence of arbuscular mycorrhizal colonization on whole-plant respiration and thermal acclimation of tropical tree seedlings. *Ecol. Evol.*, **6**, 859–870, doi:10.1002/ece3.1952.

Fan, C., and Coauthors, 2017: Understanding the Impact of Urbanization on Surface Urban Heat Islands—A Longitudinal Analysis of the Oasis Effect in Subtropical Desert Cities. *Remote Sens.*, **9**.

Fang, C., P. Smith, and J. U. Smith, 2006: Is resistant soil organic matter more sensitive to temperature than the labile organic matter? *Biogeosciences*, **3**, 65–68, doi:10.5194/bg-3-65-2006. http://www.nature.com/nature/journal/v433/n7023/abs/nature03226.html.

Fanin, T., and G. R. Van Der Werf, 2017: Precipitation-fire linkages in Indonesia (1997-2015). *Biogeosciences*, **14**, 3995–4008, doi:10.5194/bg-14-3995-2017.

FAO, 2015: FAOSTAT. Land use emissions database.

Farquhar, G. D., 1989: Models of Integrated Photosynthesis of Cells and Leaves. *Philos. Trans. R. Soc. B Biol. Sci.*, **323**, 357–367, doi:10.1098/rstb.1989.0016. http://rstb.royalsocietypublishing.org/cgi/doi/10.1098/rstb.1989.0016.

Farquhar, G. D., S. Von Caemmerer, and J. A. Berry, 1980: A Biochemical Model of Photosynthetic CO 2 Assimilation in Leaves of C 3 Species. *Planta*, **149**, 78–90, doi:10.1007/BF00386231.

Fay, P. A., D. M. Kaufman, J. B. Nippert, J. D. Carlisle, and C. W. Harper, 2008: Changes in grassland ecosystem function due to extreme rainfall events: Implications for responses to climate change. *Glob. Chang. Biol.*, **14**, 1600–1608, doi:10.1111/j.1365-2486.2008.01605.x. http://doi.wiley.com/10.1111/j.1365-2486.2008.01605.x (Accessed May 25, 2018).

Federici, S., F. N. Tubiello, M. Salvatore, H. Jacobs, and J. Schmidhuber, 2015: New estimates of CO2 forest emissions and removals: 1990-2015. *For. Ecol. Manage.*, **352**, 89–98, doi:10.1016/j.foreco.2015.04.022. http://dx.doi.org/10.1016/j.foreco.2015.04.022.

Feng, S., and Q. Fu, 2013: Expansion of global drylands under a warming climate. *Atmos. Chem. Phys.*, **13**, 10081–10094, doi:10.5194/acp-13-10081-2013. http://www.atmos-chem-phys.net/13/10081/2013/ (Accessed May 8, 2018).

Feng, W., A. F. Plante, and J. Six, 2013: Improving estimates of maximal organic carbon stabilization by fine soil particles. *Biogeochemistry*, **112**, 81–93, doi:10.1007/s10533-011-9679-7.

Fernandes, K., and Coauthors, 2011: North Tropical Atlantic influence on western Amazon fire season variability. *Geophys. Res. Lett.*, **38**, 1–6, doi:10.1029/2011GL047392.

Fernandes, K., L. Verchot, W. Baethgen, V. Gutierrez-Velez, M. Pinedo-Vasquez, and C. Martius, 2017: Heightened fire probability in Indonesia in non-drought conditions: The effect of increasing temperatures. *Environ. Res. Lett.*, **12**, doi:10.1088/1748-9326/aa6884.

Field, C. B., R. B. Jackson, and H. A. Mooney, 1995: Stomatal responses to increased CO2: implications from the plant to the global scale. *Plant. Cell Environ.*, **18**, 1214–1225, doi:10.1111/j.1365-3040.1995.tb00630.x.

Findell, K. L., A. Berg, P. Gentine, J. P. Krasting, B. R. Lintner, S. Malyshev, J. A. Santanello, and E. Shevliakova, 2017: The impact of anthropogenic land use and land cover change on regional climate extremes. *Nat. Commun.*, **8**, 989, doi:10.1038/s41467-017-01038-w. https://doi.org/10.1038/s41467-017-01038-w.

Finzi, A. C., R. Z. Abramoff, K. S. Spiller, E. R. Brzostek, B. A. Darby, M. A. Kramer, and R. P. Phillips, 2015: Rhizosphere processes are quantitatively important components of terrestrial carbon and nutrient cycles. *Glob. Chang. Biol.*, **21**, 2082–2094, doi:10.1111/gcb.12816. https://doi.org/10.1111/gcb.12816.

Fischer, E. M., and R. Knutti, 2014: Detection of spatially aggregated changes in temperature and precipitation extremes. *Geophys. Res. Lett.*, **41**, 547–554, doi:10.1002/2013GL058499. http://doi.wiley.com/10.1002/2013GL058499 (Accessed May 21, 2018).

——, U. Beyerle, and R. Knutti, 2013: Robust spatially aggregated projections of climate extremes. *Nat. Clim. Chang.*, **3**, 1033–1038, doi:10.1038/nclimate2051.

Flanner, M. G., K. M. Shell, M. Barlage, D. K. Perovich, and M. A. Tschudi, 2011: Radiative forcing and albedo feedback from the Northern Hemisphere cryosphere between 1979 and 2008. *Nat. Geosci.*, **4**, 151–155, doi:10.1038/ngeo1062. http://dx.doi.org/10.1038/ngeo1062.

Flannigan, M. D., M. A. Krawchuk, W. J. De Groot, B. M. Wotton, and L. M. Gowman, 2009: Implications of changing climate for global wildland fire. *Int. J. Wildl. Fire*, **18**, 483–507, doi:10.1071/WF08187. http://www.publish.csiro.au/?paper=WF08187 (Accessed May 23, 2018).

Flores Rojas, J. L., A. J. Pereira Filho, H. A. Karam, F. Vemado, and V. Masson, 2018: Effects of Explicit Urban-Canopy Representation on Local Circulations Above a Tropical Mega-City. *Boundary-Layer Meteorol.*, **166**, 83–111, doi:10.1007/s10546-017-0292-8.

Foley, J. a., and Coauthors, 2011: Solutions for a cultivated planet. *Nature*, **478**, 337–342, doi:10.1038/nature10452.

Fontaine, S., S. Barot, P. Barré, N. Bdioui, B. Mary, and C. Rumpel, 2007: Stability of organic carbon in deep soil layers controlled by fresh carbon supply. *Nature*, **450**, 277. http://dx.doi.org/10.1038/nature06275.

Forsell, N., O. Turkovska, M. Gusti, M. Obersteiner, M. Den Elzen, and P. Havlik, 2016: Assessing the INDCs' land use, land use change, and forest emission projections. *Carbon Balance Manag.*, **11**, doi:10.1186/s13021-016-0068-3.

Forzieri, G., R. Alkama, D. G. Miralles, and A. Cescatti, 2017a: Satellites reveal contrasting responses of regional climate to the widespread greening of Earth. *Science (80-.).*, **356**, 1180–1184, doi:10.1126/science.aal1727. http://www.sciencemag.org/lookup/doi/10.1126/science.aal1727.

——, ——, ——, and ——, 2017b: Satellites reveal contrasting responses of regional climate to the widespread greening of Earth. *Science (80-.).*, **356**, 1180–1184, doi:10.1126/science.aal1727. http://www.sciencemag.org/lookup/doi/10.1126/science.aal1727.

Founda, D., and M. Santamouris, 2017: Synergies between Urban Heat Island and Heat Waves in Athens (Greece), during an extremely hot summer (2012). *Sci. Rep.*, **7**, 1–11, doi:10.1038/s41598-017-11407-6. http://dx.doi.org/10.1038/s41598-017-11407-6.

Fowler, D., and Coauthors, 2015: Effects of global change during the 21st century onthe nitrogen cycle. *Atmos. Chem. Phys.*, **15**, 13849–13893, doi:10.5194/acp-15-13849-2015. https://www.atmos-chem-phys.net/15/13849/2015/.

Francesca, C. M., W. M. D., B. C. M., D. Karolien, and P. Eldor, 2012: The Microbial Efficiency-Matrix Stabilization (MEMS) framework integrates plant litter decomposition with soil organic matter stabilization: do labile plant inputs form stable soil organic matter? *Glob. Chang. Biol.*, **19**, 988–995, doi:10.1111/gcb.12113. https://doi.org/10.1111/gcb.12113.

Frank, D., and Coauthors, 2015: Effects of climate extremes on the terrestrial carbon cycle: Concepts, processes and potential future impacts. *Glob. Chang. Biol.*, **21**, 2861–2880, doi:10.1111/gcb.12916. http://doi.wiley.com/10.1111/gcb.12916 (Accessed May 16, 2018).

Frank, S., and Coauthors, 2017: Reducing greenhouse gas emissions in agriculture without compromising food security? *Environ. Res. Lett.*, **12**, 105004, doi:10.1088/1748-9326/aa8c83. http://stacks.iop.org/1748-9326/12/i=10/a=105004?key=crossref.000b6ab1748d1b0af07f66e0f496f0a3.

Frankenberg, C., and Coauthors, 2011: Global column-averaged methane mixing ratios from 2003 to 2009 as derived from SCIAMACHY: Trends and variability. *J. Geophys. Res. Atmos.*, **116**, doi:10.1029/2010JD014849.

Frey, S. D., J. Lee, J. M. Melillo, and J. Six, 2013: The temperature response of soil microbial efficiency and its feedback to climate. *Nat. Clim. Chang.*, **3**, 395. http://dx.doi.org/10.1038/nclimate1796.

Friedlingstein, P., and Coauthors, 2006: Climate-carbon cycle feedback analysis: Results from the C4MIP model intercomparison. *J. Clim.*, **19**, 3337–3353, doi:10.1175/JCLI3800.1. http://journals.ametsoc.org/doi/abs/10.1175/JCLI3800.1.

Frost, G. V., and H. E. Epstein, 2014: Tall shrub and tree expansion in Siberian tundra ecotones since the 1960s. *Glob. Chang. Biol.*, **20**, 1264–1277, doi:10.1111/gcb.12406.

Früh, B., and Coauthors, 2011: Estimation of Climate-Change Impacts on the Urban Heat Load Using an Urban Climate Model and Regional Climate Projections. *J. Appl. Meteorol. Climatol.*, **50**, 167–184, doi:10.1175/2010JAMC2377.1. http://journals.ametsoc.org/doi/abs/10.1175/2010JAMC2377.1.

Fuentes, J. D., and Coauthors, 2000: Biogenic Hydrocarbons in the Atmospheric Boundary Layer: A Review. *Bull. Am. Meteorol. Soc.*, **81**, 1537–1575, doi:10.1175/1520-0477(2000)081<1537:BHITAB>2.3.CO;2. https://doi.org/10.1175/1520-0477(2000)081%3C1537:BHITAB%3E2.3.CO.

Fuglestvedt, J., and Coauthors, 2018: Implications of possible interpretations of ‘greenhouse gas balance’ in the Paris Agreement. *Philos. Trans. R. Soc. A Math. Phys. Eng. Sci.*, **376**, 20160445, doi:10.1098/rsta.2016.0445. http://rsta.royalsocietypublishing.org/lookup/doi/10.1098/rsta.2016.0445.

Fujibe, F., 2009: Detection of urban warming in recent temperature trends in Japan. *Int. J. Climatol.*, **29**, 1811–1822, doi:10.1002/joc.1822. https://doi.org/10.1002/joc.1822.

Fuzzi, S., and Coauthors, 2015: Particulate matter, air quality and climate: Lessons learned and future needs. *Atmos. Chem. Phys.*, **15**, 8217–8299, doi:10.5194/acp-15-8217-2015. https://www.atmos-chem-phys.net/15/8217/2015/.

Galik, C. S., and R. C. Abt, 2016: Sustainability guidelines and forest market response: An assessment of European Union pellet demand in the southeastern United States. *GCB Bioenergy*, **8**, 658–669, doi:10.1111/gcbb.12273. https://doi.org/10.1111/gcbb.12273.

Gallego-Sala, A. V, and al et, 2010: Application of a global bioclimatic envelope model to assess the impact of climate change on the distribution of blanket peatlands in Great Britain. *Clim. Res.*,.

Gallo, N. D., D. G. Victor, and L. A. Levin, 2017: Ocean commitments under the Paris Agreement. *Nat. Clim. Chang.*, **7**, 833–838, doi:10.1038/nclimate3422. http://dx.doi.org/10.1038/nclimate3422.

Gálos, B., C. Mátyás, and D. Jacob, 2011: Regional characteristics of climate change altering effects of afforestation. *Environ. Res. Lett.*, **6**, 44010, doi:10.1088/1748-9326/6/4/044010.

——, S. Hagemann, A. Hänsler, G. Kindermann, D. Rechid, K. Sieck, C. Teichmann, and D. Jacob, 2013: Case study for the assessment of the biogeophysical effects of a potential afforestation in Europe. *Carbon Balance Manag.*, **8**, 1–13, doi:10.1186/1750-0680-8-3.

Ganeshan, M., and R. Murtugudde, 2015: Nocturnal propagating thunderstorms may favor urban “hot-spots”: A model-based study over Minneapolis. *Urban Clim.*, **14**, 606–621, doi:10.1016/j.uclim.2015.10.005. http://dx.doi.org/10.1016/j.uclim.2015.10.005.

García-Palacios, P., and Coauthors, 2015: Are there links between responses of soil microbes and ecosystem functioning to elevated CO_2, N deposition and warming? A global perspective. *Glob. Chang. Biol.*, **21**, 1590–1600, doi:10.1111/gcb.12788. http://doi.wiley.com/10.1111/gcb.12788 (Accessed February 4, 2018).

Garnaud, C., and L. Sushama, 2015: Journal of Geophysical Research : Atmospheres. 1–18, doi:10.1002/2014JD022055.Received.

Garnett, T., and Coauthors, 2013: Sustainable intensification in agriculture: Premises and policies. *Science (80-.).*, **341**, 33–34, doi:10.1126/science.1234485. http://science.sciencemag.org/content/341/6141/33.

Gasser, T., and P. Ciais, 2013: A theoretical framework for the net land-to-atmosphere CO2 flux and its

implications in the definition of "emissions from land use change." *Earth Syst. Dyn.*, **4**, 171–186, doi:10.5194/esd-4-171-2013. https://www.earth-syst-dynam.net/4/171/2013/.
Gattuso, J. P., and et al, 2018: Ocean solutions to address climate change and its effects on marine ecosystems. *Nature*,.
Gaveau, D. L. A., and Coauthors, 2014: Major atmospheric emissions from peat fires in Southeast Asia during non-drought years: Evidence from the 2013 Sumatran fires. *Sci. Rep.*, **4**, doi:10.1038/srep06112.
Gedalof, Z., and A. A. Berg, 2010: Tree ring evidence for limited direct CO $_2$ fertilization of forests over the 20th century. *Global Biogeochem. Cycles*, **24**, n/a-n/a, doi:10.1029/2009GB003699. http://doi.wiley.com/10.1029/2009GB003699.
GEO-6, 2017: *Global Environmental Outlook 6 Regional assessment*.
Georgescu, M., D. B. Lobell, and C. B. Field, 2011: Direct climate effects of perennial bioenergy crops in the United States. *Proc. Natl. Acad. Sci.*, **108**, 4307–4312, doi:10.1073/pnas.1008779108. http://www.pnas.org/cgi/doi/10.1073/pnas.1008779108.
——, ——, ——, and A. Mahalov, 2013a: Simulated hydroclimatic impacts of projected Brazilian sugarcane expansion. *Geophys. Res. Lett.*, **40**, 972–977, doi:10.1002/grl.50206.
——, M. Moustaoui, A. Mahalov, and J. Dudhia, 2013b: Summer-time climate impacts of projected megapolitan expansion in Arizona. *Nat. Clim. Chang.*, **3**, 37–41, doi:10.1038/nclimate1656. http://dx.doi.org/10.1038/nclimate1656.
van Gestel, N., and Coauthors, 2018: Predicting soil carbon loss with warming. *Nature*, **554**, E4. http://dx.doi.org/10.1038/nature25745.
Gharajehdaghipour, T., J. D. Roth, P. M. Fafard, and J. H. Markham, 2016: Arctic foxes as ecosystem engineers: Increased soil nutrients lead to increased plant productivity on fox dens. *Sci. Rep.*, **6**, 29987, doi:10.1038/srep24020. http://dx.doi.org/10.1038/srep24020.
Giglio, L., J. T. Randerson, and G. R. Van Der Werf, 2013: Analysis of daily, monthly, and annual burned area using the fourth-generation global fire emissions database (GFED4). *J. Geophys. Res. Biogeosciences*, **118**, 317–328, doi:10.1002/jgrg.20042.
Ginoux, P., M. Chin, I. Tegen, J. M. Prospero, B. Holben, O. Dubovik, and S.-J. Lin, 2001: Sources and distributions of dust aerosols simulated with the GOCART model. *J. Geophys. Res. Atmos.*, **106**, 20255–20273, doi:10.1029/2000JD000053. http://doi.wiley.com/10.1029/2000JD000053.
Giri, C., E. Ochieng, L. L. Tieszen, Z. Zhu, A. Singh, T. Loveland, J. Masek, and N. Duke, 2011: Status and distribution of mangrove forests of the world using earth observation satellite data. *Glob. Ecol. Biogeogr.*, **20**, 154–159, doi:10.1111/j.1466-8238.2010.00584.x. https://doi.org/10.1111/j.1466-8238.2010.00584.x.
Gleeson, T., Y. Wada, M. F. P. Bierkens, and L. P. H. van Beek, 2012: Water balance of global aquifers revealed by groundwater footprint. *Nature*, **488**, 197–200, doi:10.1038/nature11295.
Goetz, S. J., M. C. Hansen, R. A. Houghton, W. Walker, N. Laporte, and J. Busch, 2015: Measurement and monitoring needs , capabilities and potential for addressing reduced emissions from deforestation and forest degradation under Measurement and monitoring needs , capabilities and potential for addressing reduced emissions from deforestatio. *Environ. Res. Lett.*, **10**.
Goldstein, A. H., C. D. Koven, C. L. Heald, and I. Y. Fung, 2009: Biogenic carbon and anthropogenic pollutants combine to form a cooling haze over the southeastern United States. *Proc. Natl. Acad. Sci.*, **106**, 8835–8840, doi:10.1073/pnas.0904128106. http://www.pnas.org/cgi/doi/10.1073/pnas.0904128106.
Gonsamo, A., J. M. Chen, Y. W. Ooi, C. J. M., and O. Y. W., 2017: Peak season plant activity shift towards spring is reflected by increasing carbon uptake by extratropical ecosystems. *Glob. Chang. Biol.*, **24**, 2117–2128, doi:10.1111/gcb.14001. https://doi.org/10.1111/gcb.14001.
González-Jaramillo, V., A. Fries, R. Rollenbeck, J. Paladines, F. Oñate-Valdivieso, and J. Bendix, 2016: Assessment of deforestation during the last decades in Ecuador using NOAA-AVHRR satellite data. *Erdkunde*, **70**, 217–235, doi:10.3112/erdkunde.2016.03.02.
Goodrick, S. L., and D. E. Hanley, 2009: Florida wildfire activity and atmospheric teleconnections. *Int. J. Wildl. Fire*, **18**, 476, doi:10.1071/WF07034. http://www.publish.csiro.au/?paper=WF07034 (Accessed May 5, 2018).

Gordo, O., and J. J. Sanz, 2010: Impact of climate change on plant phenology in Mediterranean ecosystems. *Glob. Chang. Biol.*, **16**, 1082–1106, doi:10.1111/j.1365-2486.2009.02084.x.

Gourdji, S. M., A. M. Sibley, and D. B. Lobell, 2013: Global crop exposure to critical high temperatures in the reproductive period: Historical trends and future projections. *Environ. Res. Lett.*, **8**, 024041, doi:10.1088/1748-9326/8/2/024041. http://stacks.iop.org/1748-9326/8/i=2/a=024041?key=crossref.71d4bd7d0045166be569277634403f63.

Govaerts, B., N. Verhulst, A. Castellanos-Navarrete, K. D. Sayre, J. Dixon, and L. Dendooven, 2009: Conservation agriculture and soil carbon sequestration: Between myth and farmer reality. *CRC. Crit. Rev. Plant Sci.*, **28**, 97–122, doi:10.1080/07352680902776358.

Grace, J., F. Berninger, and L. Nagy, 2002: Impacts of climate change on the tree line. *Ann. Bot.*, **90**, 537–544, doi:10.1093/aob/mcf222. https://academic.oup.com/aob/article-lookup/doi/10.1093/aob/mcf222 (Accessed May 20, 2018).

Grassi, G., J. House, W. A. Kurz, A. Cescatti, and R. A. Houghton, Reconciling global model estimates and country reporting of anthropogenic forest CO 2 sinks. *Nat. Clim. Chang.*, 1–35.

——, M. G. J. den Elzen, A. F. Hof, R. Pilli, and S. Federici, 2012: The role of the land use, land use change and forestry sector in achieving Annex I reduction pledges. *Clim. Change*, **115**, 873–881, doi:10.1007/s10584-012-0584-4. https://doi.org/10.1007/s10584-012-0584-4.

——, J. House, F. Dentener, S. Federici, M. Den Elzen, and J. Penman, 2017: The key role of forests in meeting climate targets requires science for credible mitigation. *Nat. Clim. Chang.*, **7**, 220–226, doi:10.1038/nclimate3227. http://www.nature.com/doifinder/10.1038/nclimate3227.

Gray, S. B., and Coauthors, 2016: Intensifying drought eliminates the expected benefits of elevated carbon dioxide for soybean. *Nat. Plants*, **2**, 16132, doi:10.1038/nplants.2016.132. http://www.nature.com/articles/nplants2016132 (Accessed May 10, 2018).

Green, J. K., A. G. Konings, S. H. Alemohammad, J. Berry, D. Entekhabi, J. Kolassa, J.-E. Lee, and P. Gentine, 2017a: Regionally strong feedbacks between the atmosphere and terrestrial biosphere. *Nat. Geosci.*, **10**, 410–414, doi:10.1038/ngeo2957.

Greenville, A. C., C. R. Dickman, G. M. Wardle, and M. Letnic, 2009: The fire history of an arid grassland: The influence of antecedent rainfall and ENSO. *Int. J. Wildl. Fire*, **18**, 631–639, doi:10.1071/WF08093. http://www.publish.csiro.au/?paper=WF08093 (Accessed May 5, 2018).

Gregory, P. J., and B. Marshall, 2012: Attribution of climate change: A methodology to estimate the potential contribution to increases in potato yield in Scotland since 1960. *Glob. Chang. Biol.*, **18**, 1372–1388, doi:10.1111/j.1365-2486.2011.02601.x. http://doi.wiley.com/10.1111/j.1365-2486.2011.02601.x (Accessed May 10, 2018).

Griffis, T. J., Z. Chen, J. M. Baker, J. D. Wood, D. B. Millet, X. Lee, R. T. Venterea, and P. A. Turner, 2017: Nitrous oxide emissions are enhanced in a warmer and wetter world. *Proc. Natl. Acad. Sci.*, **114**, 12081–12085, doi:10.1073/pnas.1704552114. http://www.pnas.org/lookup/doi/10.1073/pnas.1704552114.

Griscom, B. W., and Coauthors, 2017: Natural climate solutions. *Proc. Natl. Acad. Sci.*, **114**, 11645–11650, doi:10.1073/pnas.1710465114. http://www.pnas.org/lookup/doi/10.1073/pnas.1710465114.

van Groenigen, K. J., X. Qi, C. W. Osenberg, Y. Luo, and B. A. Hungate, 2014: Faster Decomposition Under Increased Atmospheric CO₂ Limits Soil Carbon Storage. *Science (80-.).*, **344**, 508 LP-509. http://science.sciencemag.org/content/344/6183/508.abstract.

Groffman, P. M., and Coauthors, 2009: Challenges to incorporating spatially and temporally explicit phenomena (hotspots and hot moments) in denitrification models. *Biogeochemistry*, **93**, 49–77, doi:10.1007/s10533-008-9277-5.

Groß, S., V. Freudenthaler, K. Schepanski, C. Toledano, A. Schäfler, A. Ansmann, and B. Weinzierl, 2015: Optical properties of long-range transported Saharan dust over Barbados as measured by dual-wavelength depolarization Raman lidar measurements. *Atmos. Chem. Phys.*, **15**, 11067–11080, doi:10.5194/acp-15-11067-2015.

Grossman-Clarke, S., S. Schubert, and D. Fenner, 2017: Urban effects on summertime air temperature in Germany under climate change. *Int. J. Climatol.*, **37**, 905–917, doi:10.1002/joc.4748.

Del Grosso, S. J., S. M. Ogle, W. J. Parton, and F. J. Breidt, 2010: Estimating uncertainty in N_2O emissions from U.S. cropland soils. *Global Biogeochem. Cycles*, **24**, n/a-n/a, doi:10.1029/2009GB003544. http://doi.wiley.com/10.1029/2009GB003544.

Grotjahn, R., and Coauthors, 2016: North American extreme temperature events and related large scale meteorological patterns: a review of statistical methods, dynamics, modeling, and trends. *Clim. Dyn.*, **46**, 1151–1184, doi:10.1007/s00382-015-2638-6. http://link.springer.com/10.1007/s00382-015-2638-6 (Accessed May 23, 2018).

Guenther, A. B., X. Jiang, C. L. Heald, T. Sakulyanontvittaya, T. Duhl, L. K. Emmons, and X. Wang, 2012: The model of emissions of gases and aerosols from nature version 2.1 (MEGAN2.1): An extended and updated framework for modeling biogenic emissions. *Geosci. Model Dev.*, **5**, 1471–1492, doi:10.5194/gmd-5-1471-2012. https://www.geosci-model-dev.net/5/1471/2012/.

Guhathakurta, P., D. S. Pai, and M. N. Rajeevan, 2017: Variability and Trends of Extreme Rainfall and Rainstorms. Springer, Singapore, 37–49 http://link.springer.com/10.1007/978-981-10-2531-0_3 (Accessed May 24, 2018).

Guimberteau, M., K. Laval, A. Perrier, and J. Polcher, 2012: Global effect of irrigation and its impact on the onset of the Indian summer monsoon. *Clim. Dyn.*, **39**, 1329–1348, doi:10.1007/s00382-011-1252-5.

Guo, Z., and Coauthors, 2006: GLACE: The Global Land–Atmosphere Coupling Experiment. Part II: Analysis. *J. Hydrometeorol.*, **7**, 611–625, doi:10.1175/JHM511.1. http://journals.ametsoc.org/doi/abs/10.1175/JHM511.1.

Gutiérrez-Velez, V. H., M. Uriarte, R. Defries, M. Pinedo-Vasquez, K. Fernandes, P. Ceccato, W. Baethgen, and C. Padoch, 2014: Land cover change interacts with drought severity to change fire regimes in Western Amazonia. *Ecol. Appl.*, **24**, 1323–1340, doi:10.1890/13-2101.1.

Haberlie, A. M., W. S. Ashley, and T. J. Pingel, 2015: The effect of urbanisation on the climatology of thunderstorm initiation. *Q. J. R. Meteorol. Soc.*, **141**, 663–675, doi:10.1002/qj.2499.

Haddaway, N. R., K. Hedlund, L. E. Jackson, T. Kätterer, E. Lugato, I. K. Thomsen, H. B. Jørgensen, and P. E. Isberg, 2017: How does tillage intensity affect soil organic carbon? A systematic review. *Environ. Evid.*, **6**, 30, doi:10.1186/s13750-017-0108-9.

Hagos, S., L. R. Leung, Y. Xue, A. Boone, F. de Sales, N. Neupane, M. Huang, and J. H. Yoon, 2014: Assessment of uncertainties in the response of the African monsoon precipitation to land use change simulated by a regional model. *Clim. Dyn.*, **43**, 2765–2775, doi:10.1007/s00382-014-2092-x.

Hamdi, R., 2010: Estimating urban heat island effects on the temperature series of Uccle (Brussels, Belgium) using remote sensing data and a land surface scheme. *Remote Sens.*, **2**, 2773–2784, doi:10.3390/rs2122773.

——, P. Termonia, and P. Baguis, 2011: Effects of urbanization and climate change on surface runoff of the Brussels Capital Region: A case study using an urban soil-vegetation-atmosphere-transfer model. *Int. J. Climatol.*, **31**, 1959–1974, doi:10.1002/joc.2207.

Hamdi, R., D. Degrauwe, and P. Termonia, 2012: Coupling the Town Energy Balance (TEB) Scheme to an Operational Limited-Area NWP Model: Evaluation for a Highly Urbanized Area in Belgium. *Weather Forecast.*, **27**, 323–344, doi:10.1175/WAF-D-11-00064.1. http://journals.ametsoc.org/doi/abs/10.1175/WAF-D-11-00064.1.

——, H. Van de Vyver, R. De Troch, and P. Termonia, 2014: Assessment of three dynamical urban climate downscaling methods: Brussels's future urban heat island under an A1B emission scenario. *Int. J. Climatol.*, **34**, 978–999, doi:10.1002/joc.3734.

——, F. Duchêne, J. Berckmans, A. Delcloo, C. Vanpoucke, and P. Termonia, 2016: Evolution of urban heat wave intensity for the Brussels Capital Region in the ARPEGE-Climat A1B scenario. *Urban Clim.*, **17**, 176–195, doi:10.1016/j.uclim.2016.08.001. http://dx.doi.org/10.1016/j.uclim.2016.08.001.

Hamilton, S. E., and D. A. Friess, 2018: Global carbon stocks and potential emissions due to mangrove deforestation from 2000 to 2012. *Nat. Clim. Chang.*, **8**, 240–244, doi:10.1038/s41558-018-0090-4. https://doi.org/10.1038/s41558-018-0090-4.

Hammond, J., S. Shackley, S. Sohi, and P. Brownsort, 2009: Life Cycle Analysis for Pyrolysis Biochar Systems in the UK. *Carbon N. Y.*, **39**, 2030–2030, doi:https://doi.org/10.1016/j.enpol.2011.02.033. 10.1016/j.enpol.2011.02.033%5Cnhttp://search.ebscohost.com/login.aspx?direct=true&db=bth&AN=59776017&site=ehost-live.

Han, J.-Y., J.-J. Baik, and A. P. Khain, 2011: A Numerical Study of Urban Aerosol Impacts on Clouds and Precipitation. *J. Atmos. Sci.*, **69**, 504–520, doi:10.1175/JAS-D-11-071.1. https://doi.org/10.1175/JAS-D-11-071.1.

Han Weng, Z., and Coauthors, 2017: Biochar built soil carbon over a decade by stabilizing rhizodeposits. *Nat. Clim. Chang.*, **7**, 371–376, doi:10.1038/nclimate3276. http://dx.doi.org/10.1038/nclimate3276.

Hansis, E., S. J. Davis, and J. Pongratz, 2015: Relevance of methodological choices for accounting of land use change carbon fluxes. *Global Biogeochem. Cycles*, **29**, 1230–1246, doi:10.1002/2014GB004997. https://agupubs.onlinelibrary.wiley.com/doi/full/10.1002/2014GB004997.

Harris, R. M. B., T. A. Remenyi, G. J. Williamson, N. L. Bindoff, and D. M. J. S. Bowman, 2016: Climate–vegetation–fire interactions and feedbacks: trivial detail or major barrier to projecting the future of the Earth system? *Wiley Interdiscip. Rev. Clim. Chang.*, **7**, 910–931, doi:10.1002/wcc.428. https://doi.org/10.1002/wcc.428.

Harris, Z. M., R. Spake, and G. Taylor, 2015: Land use change to bioenergy: A meta-analysis of soil carbon and GHG emissions. *Biomass and Bioenergy*, **82**, 27–39, doi:10.1016/j.biombioe.2015.05.008. http://www.sciencedirect.com/science/article/pii/S0961953415001853.

Harrison, S. P., J. R. Marlon, and P. J. Bartlein, 2010: Fire in the Earth System. *Chang. Clim. Earth Syst. Soc.*, **324**, 21–48, doi:10.1007/978-90-481-8716-4_3. http://link.springer.com/10.1007/978-90-481-8716-4_3.

Harsch, M. A., P. E. Hulme, M. S. McGlone, and R. P. Duncan, 2009: Are treelines advancing? A global meta-analysis of treeline response to climate warming. *Ecol. Lett.*, **12**, 1040–1049, doi:10.1111/j.1461-0248.2009.01355.x. http://doi.wiley.com/10.1111/j.1461-0248.2009.01355.x (Accessed May 20, 2018).

Hartley, I. P., D. W. Hopkins, M. H. Garnett, M. Sommerkorn, and P. A. Wookey, 2008: Soil microbial respiration in arctic soil does not acclimate to temperature. *Ecol. Lett.*, **11**, 1092–1100, doi:10.1111/j.1461-0248.2008.01223.x.

Hartley, I. P., M. H. Garnett, M. Sommerkorn, D. W. Hopkins, B. J. Fletcher, V. L. Sloan, G. K. Phoenix, and P. A. Wookey, 2012: A potential loss of carbon associated with greater plant growth in the European Arctic. *Nat. Clim. Chang.*, **2**, 875. http://dx.doi.org/10.1038/nclimate1575.

Hartmann, D. L., and Coauthors, 2013: No Title. *Climate Change 2013: The Physical Science Basis. Contribution of Working Group I to the Fifth Assessment Report of the Intergovernmental Panel on Climate Change*, T.F. Stocker et al., Eds., Cambridge University Pres, Cambridge, United Kingdom and New York, NY, USA.

Hartmann, H., and Coauthors, 2018: Research frontiers for improving our understanding of drought-induced tree and forest mortality. *New Phytol.*, **218**, 15–28, doi:10.1111/nph.15048. https://doi.org/10.1111/nph.15048.

Hassink, J., and A. P. Whitmore, 1997: A Model of the Physical Protection of Organic Matter in Soils. *Soil Sci. Soc. Am. J.*, **61**, 131, doi:10.2136/sssaj1997.03615995006100010020x. https://www.soils.org/publications/sssaj/abstracts/61/1/SS0610010131.

Hatchett, B. J., D. Koračin, J. F. Mejía, and D. P. Boyle, 2016: Assimilating urban heat island effects into climate projections. *J. Arid Environ.*, **128**, 59–64, doi:10.1016/j.jaridenv.2016.01.007.

Haupt, M., 2017: Sulphur defficiency in southern Ontario soils; how fertilization will impact canola (Brassica napus L.) and Alfalfa (Medicago sativa L.) yield and quality. The University of Guelph, .

Hauser, M., R. Orth, and S. I. Seneviratne, 2017: Investigating soil moisture--climate interactions with prescribed soil moisture experiments: an assessment with the Community Earth System Model (version 1.2). *Geosci. Model Dev.*, **10**, 1665–1677, doi:10.5194/gmd-10-1665-2017. https://www.geosci-model-dev.net/10/1665/2017/.

Hausfather, Z., M. J. Menne, C. N. Williams, T. Masters, R. Broberg, and D. Jones, 2013: Quantifying the effect of urbanization on u.s. Historical climatology network temperature records. *J. Geophys. Res. Atmos.*, **118**, 481–494, doi:10.1029/2012JD018509.

Hawken, P., 2017: *Drawdown : the most comprehensive plan ever proposed to reverse global warming*. Penguin Books, 240 pp.

Hawkins, E., and Coauthors, 2014: Uncertainties in the timing of unprecedented climates. *Nature*, **511**, E3–E5, doi:10.1038/nature13523.

Hayden, B. P., 1998: Ecosystem feedbacks on climate at the landscape scale. *Philos. Trans. R. Soc. B Biol. Sci.*, **353**, 5–18, doi:10.1098/rstb.1998.0186. http://rstb.royalsocietypublishing.org/cgi/doi/10.1098/rstb.1998.0186.
Hayes, D. J., D. W. Kicklighter, A. D. McGuire, M. Chen, Q. Zhuang, F. Yuan, J. M. Melillo, and S. D. Wullschleger, 2014: The impacts of recent permafrost thaw on land-atmosphere greenhouse gas exchange. *Environ. Res. Lett.*, **9**, 045005, doi:10.1088/1748-9326/9/4/045005. http://stacks.iop.org/1748-9326/9/i=4/a=045005.
Hedenus, F., S. Wirsenius, and D. J. A. Johansson, 2014: The importance of reduced meat and dairy consumption for meeting stringent climate change targets. *Clim. Change*, **124**, 79–91, doi:10.1007/s10584-014-1104-5. https://doi.org/10.1007/s10584-014-1104-5.
Henders, S., U. M. Persson, and T. Kastner, 2015: Trading forests: Land use change and carbon emissions embodied in production and exports of forest-risk commodities. *Environ. Res. Lett.*, **10**, 125012, doi:10.1088/1748-9326/10/12/125012. http://stacks.iop.org/1748-9326/10/i=12/a=125012.
Henderson, B. B., P. J. Gerber, T. E. Hilinski, A. Falcucci, D. S. Ojima, M. Salvatore, and R. T. Conant, 2015: Greenhouse gas mitigation potential of the world's grazing lands: Modeling soil carbon and nitrogen fluxes of mitigation practices. *Agric. Ecosyst. Environ.*, **207**, 91–100, doi:10.1016/j.agee.2015.03.029. http://www.sciencedirect.com/science/article/pii/S0167880915001139.
Hergoualc'h, K. A., and L. V. Verchot, 2012: Changes in soil CH 4 fluxes from the conversion of tropical peat swamp forests: a meta-analysis. *J. Integr. Environ. Sci.*, **9**, 93–101, doi:10.1080/1943815X.2012.679282. http://www.scopus.com/inward/record.url?eid=2-s2.0-84863448205&partnerID=tZOtx3y1.
Herr, D., M. von Unger, D. Laffoley, and A. McGivern, 2017: Pathways for implementation of blue carbon initiatives. *Aquat. Conserv. Mar. Freshw. Ecosyst.*, **27**, 116–129, doi:10.1002/aqc.2793. https://doi.org/10.1002/aqc.2793.
Herrera-Estrada, J. E., and J. Sheffield, 2017: Uncertainties in future projections of summer droughts and heat waves over the contiguous United States. *J. Clim.*, **30**, 6225–6246, doi:10.1175/JCLI-D-16-0491.1. http://journals.ametsoc.org/doi/10.1175/JCLI-D-16-0491.1 (Accessed May 21, 2018).
Herrero, M., and Coauthors, 2013: Biomass use, production, feed efficiencies, and greenhouse gas emissions from global livestock systems. *Proc. Natl. Acad. Sci.*, **110**, 20888–20893, doi:10.1073/pnas.1308149110. http://www.pnas.org/cgi/doi/10.1073/pnas.1308149110.
Herrero, M., and Coauthors, 2016: Greenhouse gas mitigation potentials in the livestock sector. *Nat. Clim. Chang.*, **IN PRESS**, 452, doi:10.1038/nclimate2925. http://dx.doi.org/10.1038/nclimate2925.
Heskel, M. A., and Coauthors, 2016: Convergence in the temperature response of leaf respiration across biomes and plant functional types. *Proc. Natl. Acad. Sci.*, **113**, 3832–3837, doi:10.1073/pnas.1520282113. http://www.pnas.org/lookup/doi/10.1073/pnas.1520282113.
Hicks Pries, C. E., C. Castanha, R. C. Porras, and M. S. Torn, 2017: The whole-soil carbon flux in response to warming. *Science (80-.).*, **355**, 1420 LP-1423. http://science.sciencemag.org/content/355/6332/1420.abstract.
Hirsch, A. L., M. Wilhelm, E. L. Davin, W. Thiery, and S. I. Seneviratne, 2017: Can climate-effective land management reduce regional warming? *J. Geophys. Res.*, **122**, 2269–2288, doi:10.1002/2016JD026125.
Hodzic, A., P. S. Kasibhatla, D. S. Jo, C. D. Cappa, J. L. Jimenez, S. Madronich, and R. J. Park, 2016: Rethinking the global secondary organic aerosol (SOA) budget: Stronger production, faster removal, shorter lifetime. *Atmos. Chem. Phys.*, **16**, 7917–7941, doi:10.5194/acp-16-7917-2016. https://www.atmos-chem-phys.net/16/7917/2016/.
Hoerling, M., J. Eischeid, and J. Perlwitz, 2010: Regional precipitation trends: Distinguishing natural variability from anthropogenic forcing. *J. Clim.*, **23**, 2131–2145, doi:10.1175/2009JCLI3420.1. http://journals.ametsoc.org/doi/abs/10.1175/2009JCLI3420.1 (Accessed May 8, 2018).
Hoffman, F. M., and Coauthors, 2014: Causes and implications of persistent atmospheric carbon dioxide biases in Earth System Models. *J. Geophys. Res. Biogeosciences*, **119**, 141–162, doi:10.1002/2013JG002381.

Hoffmann, P., R. Schoetter, and K. H. Schlünzen, 2015: Statistical-dynamical downscaling of the urban heat island in Hamburg, Germany. *Meteorol. Zeitschrift*, 1–21, doi:10.1127/metz/2016/0773. http://www.schweizerbart.de/papers/metz/detail/prepub/87180/Statistical_dynamical_downscaling_of_the_urban_hea?af=crossref.

Hollinger, D. Y., and Coauthors, 2010: Albedo estimates for land surface models and support for a new paradigm based on foliage nitrogen concentration. *Glob. Chang. Biol.*, **16**, 696–710, doi:10.1111/j.1365-2486.2009.02028.x. http://doi.wiley.com/10.1111/j.1365-2486.2009.02028.x.

Holmes, C. D., M. J. Prather, O. A. Søvde, and G. Myhre, 2013: Future methane, hydroxyl, and their uncertainties: Key climate and emission parameters for future predictions. *Atmos. Chem. Phys.*, **13**, 285–302, doi:10.5194/acp-13-285-2013.

Hooijer, A., M. Silvius, H. Woesten, and S. Page, 2006: *Peat-CO2 Assessment of CO2 emissions from drained peatlands in SE Asia*. Netherlands,.

——, S. Page, J. G. Canadell, M. Silvius, J. Kwadijk, H. Wösten, and J. Jauhiainen, 2010: Current and future CO₂ emissions from drained peatlands in Southeast Asia. *Biogeosciences*, **7**, 1505–1514, doi:10.5194/bg-7-1505-2010. http://www.biogeosciences.net/7/1505/2010/.

Hopkins, F. M., T. R. Filley, G. Gleixner, M. Lange, S. M. Top, and S. E. Trumbore, 2014: Increased belowground carbon inputs and warming promote loss of soil organic carbon through complementary microbial responses. *Soil Biol. Biochem.*, **76**, 57–69, doi:https://doi.org/10.1016/j.soilbio.2014.04.028. http://www.sciencedirect.com/science/article/pii/S0038071714001485.

Houghton, R. A., 2013: The emissions of carbon from deforestation and degradation in the tropics: past trends and future potential. *Carbon Manag.*, **4**, 539–546, doi:10.4155/cmt.13.41. http://www.tandfonline.com/doi/abs/10.4155/cmt.13.41.

Houghton, R. A., and A. A. Nassikas, 2017: Global and regional fluxes of carbon from land use and land cover change 1850–2015. *Global Biogeochem. Cycles*, **31**, 456–472, doi:10.1002/2016GB005546.

Houghton, R. A., and A. A. Nassikas, 2018a: Negative emissions from stopping deforestation and forest degradation, globally. *Glob. Chang. Biol.*, **24**, 350–359, doi:10.1111/gcb.13876. https://doi.org/10.1111/gcb.13876.

——, and ——, 2018b: Negative emissions from stopping deforestation and forest degradation, globally. *Glob. Chang. Biol.*, **24**, 350–359, doi:10.1111/gcb.13876. http://dx.doi.org/10.1111/gcb.13876.

Houghton, R. A., J. I. House, J. Pongratz, G. R. Van Der Werf, R. S. Defries, M. C. Hansen, C. Le Quéré, and N. Ramankutty, 2012a: Carbon emissions from land use and land-cover change. *Biogeosciences*, **9**, 5125–5142, doi:10.5194/bg-9-5125-2012.

——, G. R. van der Werf, R. S. DeFries, M. C. Hansen, J. I. House, C. Le Quéré, J. Pongratz, and N. Ramankutty, 2012b: Chapter G2 Carbon emissions from land use and land-cover change. *Biogeosciences Discuss.*, **9**, 835–878, doi:10.5194/bgd-9-835-2012. http://www.biogeosciences-discuss.net/9/835/2012/.

Houlton, B. Z., S. L. Morford, and R. A. Dahlgren, 2018: Convergent evidence for widespread rock nitrogen sources in Earth’s surface environment. *Science (80-.).*, **360**, 58–62, doi:10.1126/science.aan4399. http://science.sciencemag.org/content/360/6384/58.abstract.

Houweling, S., and Coauthors, 2014: A multi-year methane inversion using SCIAMACHY, accounting for systematic errors using TCCON measurements. *Atmos. Chem. Phys.*, **14**, 3991–4012, doi:10.5194/acp-14-3991-2014.

Howard, J., A. Sutton-Grier, D. Herr, J. Kleypas, E. Landis, E. Mcleod, E. Pidgeon, and S. Simpson, 2017: Clarifying the role of coastal and marine systems in climate mitigation. *Front. Ecol. Environ.*, **15**, 42–50, doi:10.1002/fee.1451. https://doi.org/10.1002/fee.1451.

Howden, S. M., J.-F. Soussana, F. N. Tubiello, N. Chhetri, M. Dunlop, and H. Meinke, 2007: Adapting agriculture to climate change. *Proc. Natl. Acad. Sci.*, **104**, 19691–19696, doi:10.1073/pnas.0701890104. http://www.pnas.org/cgi/doi/10.1073/pnas.0701890104.

Hristov, A. N., and Coauthors, 2013: *FAO Animal Production and Health Paper No 177 BT - Mitigation of Greenhouse Gas Emissions in Livestock Production: A Review of Technical Options for Non-CO2 Emissions*. Rome, 226pp pp.

Huang, J., H. Yu, X. Guan, G. Wang, and R. Guo, 2016: Accelerated dryland expansion under climate change. *Nat. Clim. Chang.*, **6**, 166–171, doi:10.1038/nclimate2837. http://www.nature.com/articles/nclimate2837 (Accessed April 17, 2018).

Huang, J., and Coauthors, 2017a: Dryland climate change: Recent progress and challenges. *Rev. Geophys.*, **55**, 719–778, doi:10.1002/2016RG000550. http://doi.wiley.com/10.1002/2016RG000550 (Accessed May 24, 2018).

Huang, J., H. Yu, A. Dai, Y. Wei, and L. Kang, 2017b: Drylands face potential threat under 2 °c global warming target. *Nat. Clim. Chang.*, **7**, 417–422, doi:10.1038/nclimate3275.

Huang, Y., S. Wu, and J. O. Kaplan, 2014: Sensitivity of global wildfire occurrences to various factors in thecontext of global change. *Atmos. Environ.*, **121**, 86–92, doi:10.1016/j.atmosenv.2015.06.002. http://www.sciencedirect.com/science/article/pii/S1352231015301448.

Hugelius, G., C. Tarnocai, G. Broll, J. G. Canadell, P. Kuhry, and D. K. Swanson, 2013: The northern circumpolar soil carbon database: Spatially distributed datasets of soil coverage and soil carbon storage in the northern permafrost regions. *Earth Syst. Sci. Data*, **5**, 3–13, doi:10.5194/essd-5-3-2013. https://www.earth-syst-sci-data.net/5/3/2013/.

——, and Coauthors, 2014: Estimated stocks of circumpolar permafrost carbon with quantified uncertainty ranges and identified data gaps. *Biogeosciences*, **11**, 6573–6593, doi:10.5194/bg-11-6573-2014.

Hulme, M., 2001: Climatic perspectives on Sahelian desiccation: 1973-1998. *Glob. Environ. Chang.*, **11**, 19–29, doi:10.1016/S0959-3780(00)00042-X. https://www-sciencedirect-com.ezproxy.uct.ac.za/science/article/pii/S095937800000042X (Accessed May 7, 2018).

——, E. M. Barrow, N. W. Arnell, P. A. Harrison, T. C. Johns, and T. E. Downing, 1999: Relative impacts of human-induced climate change and natural climate variability. *Nature*, **397**, 688–691, doi:10.1038/17789. http://www.nature.com/articles/17789 (Accessed May 7, 2018).

Humpenöder, F., and Coauthors, 2018: Large-scale bioenergy production: how to resolve sustainability trade-offs? *Environ. Res. Lett.*, **13**, 024011, doi:10.1088/1748-9326/aa9e3b. http://stacks.iop.org/1748-9326/13/i=2/a=024011?key=crossref.ecb4dde273241bb18b2b44b439e5f874 (Accessed May 22, 2018).

Hungate, B. A., and Coauthors, 2013: Cumulative response of ecosystem carbon and nitrogen stocks to chronic CO2 exposure in a subtropical oak woodland. *New Phytol.*, **200**, 753–766, doi:10.1111/nph.12333. https://doi.org/10.1111/nph.12333.

Huntingford, C., and Coauthors, 2017: Implications of improved representations of plant respiration in a changing climate. *Nat. Commun.*, **8**, 1602, doi:10.1038/s41467-017-01774-z. http://www.nature.com/articles/s41467-017-01774-z.

Hurtt, G., L. Chini, R. Sahajpal, and S. Frolking, 2017: Harmonization of global land use change and management for the period 850-2100. *Geosci. Model Dev.*,. http://luh.umd.edu/.

Hurtt, G. C., and Coauthors, 2011: Harmonization of land use scenarios for the period 1500-2100: 600 years of global gridded annual land use transitions, wood harvest, and resulting secondary lands. *Clim. Change*, **109**, 117–161, doi:10.1007/s10584-011-0153-2.

Hutchison, J., A. Manica, R. Swetnam, A. Balmford, and M. Spalding, 2014: Predicting global patterns in mangrove forest biomass. *Conserv. Lett.*, **7**, 233–240, doi:10.1111/conl.12060. https://doi.org/10.1111/conl.12060.

Ian, A., and W. Richard, 2013: Intraseasonal variability and atmospheric controls on daily dust occurrence frequency over the central and western Sahara during the boreal summer. *J. Geophys. Res. Atmos.*, **118**, 12,912-915,926, doi:10.1002/2013JD020267. https://doi.org/10.1002/2013JD020267.

Ichinose, T., K. Shimodozono, and K. Hanaki, 1999: Impact of anthropogenic heat on urban climate in Tokyo. *Atmos. Environ.*, **33**, 3897–3909, doi:10.1016/S1352-2310(99)00132-6.

IFPRI, 2009: Climate change: Impact on agriculture and costs of adaptation. *Int. Food Policy*, 307–324, doi:10.2499/0896295354. http://ebrary.ifpri.org/cdm/ref/collection/p15738coll2/id/130648.

Iizumi, T., M. Yokozawa, and M. Nishimori, 2011: Probabilistic evaluation of climate change impacts on paddy rice productivity in Japan. *Clim. Change*, **107**, 391–415, doi:10.1007/s10584-010-9990-7. https://doi.org/10.1007/s10584-010-9990-7.

Im, E. S., M. P. Marcella, and E. A. B. Eltahir, 2014: Impact of potential large-scale irrigation on the West African monsoon and its dependence on location of irrigated area. *J. Clim.*, **27**, 994–1009, doi:10.1175/JCLI-D-13-00290.1.

Ingrid, K., G. Georg, K. Markus, K. Ellen, K. Karsten, S. Stefan, E. Karin, and L. Peter, 2008: Organo-mineral associations in temperate soils: Integrating biology, mineralogy, and organic matter chemistry. *J. Plant Nutr. Soil Sci.*, **171**, 61–82, doi:10.1002/jpln.200700048. https://doi.org/10.1002/jpln.200700048.

Intergovernmental Panel on Climate Change, I., 2006: *2006 IPCC guidelines for national greenhouse gas inventories*. S. Eggleston, L. Buendia, K. Miwa, T. Ngara, and K. Tanabe, Eds. Institute for Global Environmental Strategies (IGES), Hayama,.

Ipcc, 2003: Good practice guidance for land use, land use change and forestry. Institute for Global Environmental Strategies (IGES), Hayama, ISBN 4-88788-003-0 - Annex 3A.1 Biomass Default Tables for Section 3.2 Forest Land.

IPCC, 2006: 2006 IPCC Guidelines for National Greenhouse Gas Inventories. Institute for Global Environmental Strategies (IGES) for the Intergovernmental Panel on Climate Change.

——, 2010: Revisiting the use of managed land as a proxy for estimating national anthropogenic emissions and removals. *Metting Report, 5-7 May, 2009, INPE, Sao Jose dos Campos, Brazil.*, H.S. Eggleston, N. Srivastava, K. Tanabe, and J. Baasansuren, Eds., Institute for Global Environmental Strategies (IGES).

——, 2013: AR5 - Summary for Policymakers. *Clim. Chang. 2013 - Phys. Sci. Basis, Contrib. Work. Gr. I to Fifth Assess. Rep. Intergov. Panel Clim. Chang.*, 78, doi:10.1017/CBO9781107415324.Summary.

——, 2014: Climate Change 2013 - The Physical Science Basis. *Climate Change 2014: Synthesis Report. Contribution of Working Groups I, II and III to the Fifth Assessment Report of the Intergovernmental Panel on Climate Change*, V.R. Barros et al., Eds., Cambridge University Press, Cambridge, United Kingdom and New York, NY, USA, 117–130 http://ebooks.cambridge.org/ref/id/CBO9781107415324.

Isaacman-Vanwertz, G., and Coauthors, 2018: Chemical evolution of atmospheric organic carbon over multiple generations of oxidation. *Nat. Chem.*, **10**, 462–468, doi:10.1038/s41557-018-0002-2. https://doi.org/10.1038/s41557-018-0002-2.

Iyer, G., and Coauthors, 2018: Implications of sustainable development considerations for comparability across nationally determined contributions. *Nat. Clim. Chang.*, **8**, 124–129, doi:10.1038/s41558-017-0039-z. http://www.nature.com/articles/s41558-017-0039-z (Accessed May 22, 2018).

Jackson, R. B., K. Lajtha, S. E. Crow, G. Hugelius, M. G. Kramer, and G. Piñeiro, 2017: The Ecology of Soil Carbon: Pools, Vulnerabilities, and Biotic and Abiotic Controls. *Annu. Rev. Ecol. Evol. Syst.*, **48**, annurev-ecolsys-112414-054234, doi:10.1146/annurev-ecolsys-112414-054234. http://www.annualreviews.org/doi/10.1146/annurev-ecolsys-112414-054234.

Jacobson, M. Z., 2012: Investigating cloud absorption effects: Global absorption properties of black carbon, tar balls, and soil dust in clouds and aerosols. *J. Geophys. Res. Atmos.*, **117**, doi:10.1029/2011JD017218.

Jagadish, S. V. K., M. V. R. Murty, and W. P. Quick, 2015: Rice responses to rising temperatures - challenges, perspectives and future directions. *Plant, Cell Environ.*, **38**, 1686–1698, doi:10.1111/pce.12430. http://doi.wiley.com/10.1111/pce.12430 (Accessed May 21, 2018).

Janssens-Maenhout, G., M. Crippa, D. Guizzardi, M. Muntean, E. Schaaf, J. G. J. Olivier, J. A. H. W. Peters, and K. M. Schure, 2017: *Fossil CO 2 & GHG emissions of all world countries*. 239 pp. http://edgar.jrc.ec.europa.eu.

Jennerjahn, T. C., E. Gilman, K. W. Krauss, L. D. Lacerda, I. Nordhaus, and E. Wolanski, 2017: Mangrove Ecosystems under Climate Change. *Mangrove Ecosystems: A Global Biogeographic Perspective*, V.H. Rivera-Monroy, S.Y. Lee, E. Kristensen, and R.R. Twilley, Eds., Springer International Publishing, Cham, 211–244 http://link.springer.com/10.1007/978-3-319-62206-4_7.

Jeong, S. J., C. H. Ho, S. Piao, J. Kim, P. Ciais, Y. B. Lee, J. G. Jhun, and S. K. Park, 2014: Effects of double cropping on summer climate of the North China Plain and neighbouring regions. *Nat. Clim. Chang.*, **4**, 615–619, doi:10.1038/nclimate2266.

Jetz, W., D. S. Wilcove, and A. P. Dobson, 2007: Projected impacts of climate and land use change on the global diversity of birds. *PLoS Biol.*, **5**, 1211–1219, doi:10.1371/journal.pbio.0050157. http://dx.plos.org/10.1371/journal.pbio.0050157 (Accessed January 8, 2018).

Jiang, Z., F. Huo, H. Ma, J. Song, and A. Dai, 2017: Impact of Chinese urbanization and aerosol emissions on the East Asian summer monsoon. *J. Clim.*, **30**, 1019–1039, doi:10.1175/JCLI-D-15-0593.1.

Jolly, W. M., M. A. Cochrane, P. H. Freeborn, Z. A. Holden, T. J. Brown, G. J. Williamson, and D. M. J. S. Bowman, 2015: Climate-induced variations in global wildfire danger from 1979 to 2013. *Nat. Commun.*, **6**, 7537, doi:10.1038/ncomms8537. http://www.nature.com/doifinder/10.1038/ncomms8537.

Jones, A. D., and Coauthors, 2013: Greenhouse gas policy influences climate via direct effects of land use change. *J. Clim.*, **26**, 3657–3670, doi:10.1175/JCLI-D-12-00377.1.

Jones, P. D., and D. H. Lister, 2009: The urban heat island in central London and urban-related warming trends in central London since 1900. *Weather*, **64**, 323–327, doi:10.1002/wea.432.

Jongman, B., H. C. Winsemius, J. C. J. H. Aerts, E. Coughlan de Perez, M. K. van Aalst, W. Kron, and P. J. Ward, 2015: Declining vulnerability to river floods and the global benefits of adaptation. *Proc. Natl. Acad. Sci.*, **112**, E2271–E2280, doi:10.1073/pnas.1414439112. http://www.pnas.org/lookup/doi/10.1073/pnas.1414439112 (Accessed May 25, 2018).

Joosten, H., and J. Couwenberg, 2008: Peatlands and Carbon. *Assessment on Peatlands, Biodiversity and Climate Change*, F. Parish, A. Sirin, D. Charman, H. Joosten, T. Minayeva, M. Silvius, and L. Stringer, Eds., Vol. 1 of, Wageningen, 99–111.

Journet, E., Y. Balkanski, and S. P. Harrison, 2014: A new data set of soil mineralogy for dust-cycle modeling. *Atmos. Chem. Phys.*, **14**, 3801–3816, doi:10.5194/acp-14-3801-2014.

Kageyama, M., S. Charbit, C. Ritz, M. Khodri, and G. Ramstein, 2004: Quantifying ice-sheet feedbacks during the last glacial inception. *Geophys. Res. Lett.*, **31**, 1–4, doi:10.1029/2004GL021339.

Kallenbach, C. M., S. D. Frey, and A. S. Grandy, 2016: Direct evidence for microbial-derived soil organic matter formation and its ecophysiological controls. *Nat. Commun.*, **7**, 13630. http://dx.doi.org/10.1038/ncomms13630.

Kaplan, S., M. Georgescu, N. Alfasi, and I. Kloog, 2017: Impact of future urbanization on a hot summer: a case study of Israel. *Theor. Appl. Climatol.*, **128**, 325–341, doi:10.1007/s00704-015-1708-3.

Karhu, K., and Coauthors, 2014: Temperature sensitivity of soil respiration rates enhanced by microbial community response. *Nature*, **513**, 81–84, doi:10.1038/nature13604.

Kattge, J., and W. Knorr, 2007: Temperature acclimation in a biochemical model of photosynthesis: A reanalysis of data from 36 species. *Plant, Cell Environ.*, **30**, 1176–1190, doi:10.1111/j.1365-3040.2007.01690.x.

Kauffman, J. B., D. C. Donato, J. B. Kauffman, D. Murdiyarso, S. Kurnianto, and M. Stidham, 2011: Mangroves among the most carbon-rich forests in the tropics . Nature Geoscience 4 : 293-297 Mangroves among the most carbon-rich forests in the tropics. *Nat. Geosci.*, **4**, 293–297, doi:10.1038/ngeo1123. http://dx.doi.org/10.1038/ngeo1123.

Kauppi, P., and Coauthors, 2001: Technological and economic potential of options to enhance, maintain, and manage biological carbon reservoirs and geo-engineering. *IPCC 3rd assessment report Ch.4*, B. Metz, O. Davidson, R. Swart, and J.H. Pan, Eds., Academic Press, New York, 301–344.

Kayo, C., C. Watanabe, T. Sasaki, S. Kumagai, R. Noda, and S. Hashimoto, 2015: Life cycle greenhouse gas emissions of woodchip-paved walkways using tsunami salt-damaged wood: examination in Otsuchi, Iwate Prefecture. *J. Wood Sci.*, **61**, 620–629, doi:10.1007/s10086-015-1502-y. https://doi.org/10.1007/s10086-015-1502-y.

Keenan, T. F., D. Y. Hollinger, G. Bohrer, D. Dragoni, J. W. Munger, H. P. Schmid, and A. D. Richardson, 2013: Increase in forest water-use efficiency as atmospheric carbon dioxide concentrations rise. *Nature*, **499**, 324–327, doi:10.1038/nature12291.

Keiluweit, M., J. J. Bougoure, P. S. Nico, J. Pett-Ridge, P. K. Weber, and M. Kleber, 2015: Mineral protection of soil carbon counteracted by root exudates. *Nat. Clim. Chang.*, **5**, 588. http://dx.doi.org/10.1038/nclimate2580.

——, P. S. Nico, M. Kleber, and S. Fendorf, 2016: Are oxygen limitations under recognized regulators of organic carbon turnover in upland soils? *Biogeochemistry*, **127**, 157–171, doi:10.1007/s10533-015-0180-6. https://doi.org/10.1007/s10533-015-0180-6.

Kelleway, J. J., K. Cavanaugh, K. Rogers, I. C. Feller, E. Ens, C. Doughty, and N. Saintilan, 2017: Review of the ecosystem service implications of mangrove encroachment into salt marshes. *Glob. Chang. Biol.*, **23**, 3967–3983, doi:10.1111/gcb.13727. https://doi.org/10.1111/gcb.13727.

Kellner, O., and D. Niyogi, 2014: Land surface heterogeneity signature in tornadoclimatology? An

illustrative analysis over Indiana, 1950-2012. *Earth Interact.*, **18**, 1–32, doi:10.1175/2013EI000548.1.
Kemena, T. P., K. Matthes, T. Martin, S. Wahl, and A. Oschlies, 2017: Atmospheric feedbacks in North Africa from an irrigated, afforested Sahara. *Clim. Dyn.*, **0**, 1–21, doi:10.1007/s00382-017-3890-8.
Khanna, J., D. Medvigy, S. Fueglistaler, and R. Walko, 2017: Regional dry-season climate changes due to three decades of Amazonian deforestation. *Nat. Clim. Chang.*, **7**, 200–204, doi:10.1038/nclimate3226.
Khatiwala, S., and Coauthors, 2013: Global ocean storage of anthropogenic carbon. *Biogeosciences*, **10**, 2169–2191, doi:10.5194/bg-10-2169-2013. https://www.biogeosciences.net/10/2169/2013/.
Kim, H., Y. K. Kim, S. K. Song, and H. W. Lee, 2016: Impact of future urban growth on regional climate changes in the Seoul Metropolitan Area, Korea. *Sci. Total Environ.*, **571**, 355–363, doi:10.1016/j.scitotenv.2016.05.046.
Kimball, B. A., J. W. White, M. J. Ottman, G. W. Wall, C. J. Bernacchi, J. Morgan, and D. P. Smith, 2015: Predicting canopy temperatures and infrared heater energy requirements for warming field plots. *Agron. J.*, **107**, 121–141, doi:10.2134/agronj14.0109. https://dl.sciencesocieties.org/publications/aj/abstracts/107/1/129 (Accessed May 21, 2018).
Kirschke, S., and Coauthors, 2013: Three decades of global methane sources and sinks. *Nat. Geosci.*, **6**, 813–823, doi:10.1038/ngeo1955. http://www.nature.com/doifinder/10.1038/ngeo1955.
Klein, C., J. Bliefernicht, D. Heinzeller, U. Gessner, I. Klein, and H. Kunstmann, 2017: Feedback of observed interannual vegetation change: a regional climate model analysis for the West African monsoon. *Clim. Dyn.*, **48**, 2837–2858, doi:10.1007/s00382-016-3237-x.
de Klein, C. A. M., M. A. Shepherd, and T. J. van der Weerden, 2014: Nitrous oxide emissions from grazed grasslands: Interactions between the N cycle and climate change - a New Zealand case study. *Curr. Opin. Environ. Sustain.*, **9**–**10**, 131–139, doi:10.1016/j.cosust.2014.09.016.
Klein Goldewijk, K., and P. H. Verburg, 2013: Uncertainties in global-scale reconstructions of historical land use: an illustration using the HYDE data set. *Landsc. Ecol.*, **28**, 861–877, doi:10.1007/s10980-013-9877-x. https://doi.org/10.1007/s10980-013-9877-x.
Knauf, M., 2015: An Analysis of Wood Market Balance Modeling in Germany. *For. Policy Econ.*, **50**, 319–326, doi:10.1016/j.forpol.2014.09.013. http://www.sciencedirect.com/science/article/pii/S1389934114001683.
Knorr, W., A. Arneth, and L. Jiang, 2016a: Demographic controls of future global fire risk. *Nat. Clim. Chang.*, **6**, 781–785, doi:10.1038/nclimate2999. http://www.nature.com/articles/nclimate2999.
——, L. Jiang, and A. Arneth, 2016b: Climate, CO2 and human population impacts on global wildfire emissions. *Biogeosciences*, **13**, 267–282, doi:10.5194/bg-13-267-2016. https://www.biogeosciences.net/13/267/2016/.
Kocha, C., P. Tulet, J. P. Lafore, and C. Flamant, 2013: The importance of the diurnal cycle of Aerosol Optical Depth in West Africa. *Geophys. Res. Lett.*, **40**, 785–790, doi:10.1002/grl.50143. http://doi.wiley.com/10.1002/grl.50143.
Koehler, A. K., A. J. Challinor, E. Hawkins, and S. Asseng, 2013: Influences of increasing temperature on Indian wheat: Quantifying limits to predictability. *Environ. Res. Lett.*, **8**, 34016, doi:10.1088/1748-9326/8/3/034016. http://stacks.iop.org/1748-9326/8/i=3/a=034016.
Kok, J. F., S. Albani, N. M. Mahowald, and D. S. Ward, 2014: An improved dust emission model - Part 2: Evaluation in the Community Earth System Model, with implications for the use of dust source functions. *Atmos. Chem. Phys.*, **14**, 13043–13061, doi:10.5194/acp-14-13043-2014.
Kok, J. F., D. S. Ward, N. M. Mahowald, and A. T. Evan, 2018: Global and regional importance of the direct dust-climate feedback. *Nat. Commun.*, **9**, 241, doi:10.1038/s41467-017-02620-y. https://doi.org/10.1038/s41467-017-02620-y.
Körner, C., 2006: Plant CO2responses: An issue of definition, time and resource supply. *New Phytol.*, **172**, 393–411, doi:10.1111/j.1469-8137.2006.01886.x.
——, 2015: Paradigm shift in plant growth control. *Curr. Opin. Plant Biol.*, **25**, 107–114, doi:10.1016/j.pbi.2015.05.003.
Kottek, M., J. Grieser, C. Beck, B. Rudolf, and F. Rubel, 2006: World map of the Köppen-Geiger climate classification updated. *Meteorol. Zeitschrift*, **15**, 259–263, doi:10.1127/0941-2948/2006/0130. http://www.schweizerbart.de/papers/metz/detail/15/55034/World_Map_of_the_Koppen_Geiger_climat

e_classificat?af=crossref (Accessed May 7, 2018).
Koven, C. D., and Coauthors, 2015: A simplified, data-constrained approach to estimate the permafrost carbon–climate feedback. *Philos. Trans. R. Soc. A Math. Phys. Eng. Sci.*, **373**, 20140423, doi:10.1098/rsta.2014.0423. http://rsta.royalsocietypublishing.org/lookup/doi/10.1098/rsta.2014.0423.
Krawchuk, M. A., and M. A. Moritz, 2011: Constraints on global fire activity vary across a resource gradient. *Ecology*, **92**, 121–132, doi:10.1890/09-1843.1. https://doi.org/10.1890/09-1843.1.
Kreibich, H., and Coauthors, 2017: Adaptation to flood risk: Results of international paired flood event studies. *Earth's Futur.*, **5**, 953–965, doi:10.1002/2017EF000606. http://doi.wiley.com/10.1002/2017EF000606 (Accessed May 25, 2018).
Kreidenweis, U., F. Humpenöder, M. Stevanovic, B. L. Bodirsky, E. Kriegler, H. Lotze-Campen, and A. Popp, 2016: Afforestation to Mitigate Climate Change: Impacts on Food Prices under Consideration of Albedo Effects. *Environ. Res. Lett.*, **11**, 85001, doi:doi:10.1088/1748-9326/11/8/085001. http://stacks.iop.org/1748-9326/11/i=8/a=085001.
Kreuzwieser, J., C. Cojocariu, V. Jüssen, and H. Rennenberg, 2002: Elevated atmospheric CO2 causes seasonal changes in carbonyl emissions from Quercus ilex. *New Phytol.*, **154**, 327–333, doi:10.1046/j.1469-8137.2002.00394.x. https://doi.org/10.1046/j.1469-8137.2002.00394.x.
Krey, V., 2014: Global energy-climate scenarios and models: A review. *Wiley Interdiscip. Rev. Energy Environ.*, **3**, 363–383, doi:10.1002/wene.98. http://doi.wiley.com/10.1002/wene.98 (Accessed May 22, 2018).
Kriegler, E., and Coauthors, 2018: Short term policies to keep the door open for Paris climate goals. *Nat. Clim. Chang.*, **submitted**, doi:10.1088/1748-9326/aac4f1. http://iopscience.iop.org/10.1088/1748-9326/aac4f1.
Kundzewicz, Z. W., and P. Germany, 2012: Changes in Impacts of Climate Extremes : Human Systems and Ecosystems Coordinating Lead Authors : Lead Authors : Review Editors : Contributing Authors : *Managing the Risks of Extreme Events and Disasters to Advance Climate Change Adaptation - A Special Report of Working Groups I and II of the Intergovernmental Panel on Climate Change (IPCC)*, C.B. Field et al., Eds., Cambridge University Press, Cambridge, United Kingdom and New York, NY, USA, 231–290.
Kunkel, K. E., and Coauthors, 2013: Monitoring and understanding trends in extreme storms: State of knowledge. *Bull. Am. Meteorol. Soc.*, **94**, 499–514, doi:10.1175/BAMS-D-11-00262.1. http://journals.ametsoc.org/doi/abs/10.1175/BAMS-D-11-00262.1 (Accessed May 16, 2018).
Kurz, W. A., C. C. Dymond, G. Stinson, G. J. Rampley, E. T. Neilson, A. L. Carroll, T. Ebata, and L. Safranyik, 2008: Mountain pine beetle and forest carbon feedback to climate change. *Nature*, **452**, 987–990, doi:10.1038/nature06777. http://www.ncbi.nlm.nih.gov/pubmed/18432244.
Kusaka, H., K. Nawata, A. Suzuki-Parker, Y. Takane, and N. Furuhashi, 2013: Mechanism of Precipitation Increase with Urbanization in Tokyo as Revealed by Ensemble Climate Simulations. *J. Appl. Meteorol. Climatol.*, **53**, 824–839, doi:10.1175/JAMC-D-13-065.1. https://doi.org/10.1175/JAMC-D-13-065.1.
——, A. Suzuki-Parker, T. Aoyagi, S. A. Adachi, and Y. Yamagata, 2016: Assessment of RCM and urban scenarios uncertainties in the climate projections for August in the 2050s in Tokyo. *Clim. Change*, **137**, 427–438, doi:10.1007/s10584-016-1693-2. http://dx.doi.org/10.1007/s10584-016-1693-2.
KUSAKA, H., F. CHEN, M. TEWARI, J. DUDHIA, D. O. GILL, M. G. DUDA, W. WANG, and Y. MIYA, 2012a: Numerical Simulation of Urban Heat Island Effect by the WRF Model with 4-km Grid Increment: An Inter-Comparison Study between the Urban Canopy Model and Slab Model. *J. Meteorol. Soc. Japan. Ser. II*, **90B**, 33–45, doi:10.2151/jmsj.2012-B03. http://jlc.jst.go.jp/DN/JST.JSTAGE/jmsj/2012-B03?lang=en&from=CrossRef&type=abstract.
——, M. HARA, and Y. TAKANE, 2012b: Urban Climate Projection by the WRF Model at 3-km Horizontal Grid Increment: Dynamical Downscaling and Predicting Heat Stress in the 2070^|^rsquo;s August for Tokyo, Osaka, and Nagoya Metropolises. *J. Meteorol. Soc. Japan. Ser. II*, **90B**, 47–63, doi:10.2151/jmsj.2012-B04. http://jlc.jst.go.jp/DN/JST.JSTAGE/jmsj/2012-B04?lang=en&from=CrossRef&type=abstract.
Kuzyakov, Y., 2010: Priming effects: Interactions between living and dead organic matter. *Soil Biol. Biochem.*, **42**, 1363–1371, doi:https://doi.org/10.1016/j.soilbio.2010.04.003.

http://www.sciencedirect.com/science/article/pii/S0038071710001355.
——, and E. Blagodatskaya, 2015: Microbial hotspots and hot moments in soil: Concept & review. *Soil Biol. Biochem.*, **83**, 184–199, doi:https://doi.org/10.1016/j.soilbio.2015.01.025. http://www.sciencedirect.com/science/article/pii/S0038071715000449.
——, I. Bogomolova, and B. Glaser, 2014: Biochar stability in soil: Decomposition during eight years and transformation as assessed by compound-specific 14C analysis. *Soil Biol. Biochem.*, **70**, 229–236, doi:https://doi.org/10.1016/j.soilbio.2013.12.021. http://www.sciencedirect.com/science/article/pii/S0038071713004653.
Laanbroek, H. J., 2010: Methane emission from natural wetlands: Interplay between emergent macrophytes and soil microbial processes. A mini-review. *Ann. Bot.*, **105**, 141–153, doi:10.1093/aob/mcp201.
Laguë, M. M., and A. L. S. Swann, 2016: Progressive Midlatitude Afforestation: Impacts on Clouds, Global Energy Transport, and Precipitation. *J. Clim.*, **29**, 5561–5573, doi:10.1175/JCLI-D-15-0748.1. http://journals.ametsoc.org/doi/10.1175/JCLI-D-15-0748.1.
Lajtha, K., K. L. Townsend, M. G. Kramer, C. Swanston, R. D. Bowden, and K. Nadelhoffer, 2014a: Changes to particulate versus mineral-associated soil carbon after 50 years of litter manipulation in forest and prairie experimental ecosystems. *Biogeochemistry*, **119**, 341–360, doi:10.1007/s10533-014-9970-5. https://doi.org/10.1007/s10533-014-9970-5.
——, K. L. Townsend, M. G. Kramer, C. Swanston, R. D. Bowden, and K. Nadelhoffer, 2014b: Changes to particulate versus mineral-associated soil carbon after 50 years of litter manipulation in forest and prairie experimental ecosystems. *Biogeochemistry*, **119**, 341–360, doi:10.1007/s10533-014-9970-5. https://doi.org/10.1007/s10533-014-9970-5.
Lal, R., 2011a: Sequestering carbon in soils of agro-ecosystems. *Food Policy*, **36**, S33--S39, doi:10.1016/j.foodpol.2010.12.001.
Lal, R., 2011b: Sequestering carbon in soils of agro-ecosystems. *Food Policy*, **36**, S33--S39, doi:10.1016/j.foodpol.2010.12.001.
Lal, R., 2013: Soil carbon management and climate change. *Carbon Manag.*, **4**, 439–462, doi:10.4155/cmt.13.31. http://www.tandfonline.com/doi/abs/10.4155/cmt.13.31.
Lamarque, J. F., and Coauthors, 2010: Historical (1850-2000) gridded anthropogenic and biomass burning emissions of reactive gases and aerosols: Methodology and application. *Atmos. Chem. Phys.*, **10**, 7017–7039, doi:10.5194/acp-10-7017-2010.
Lambin, E. F., and P. Meyfroidt, 2011: Global land use change, economic globalization, and the looming land scarcity. *Proc. Natl. Acad. Sci.*, **108**, 3465–3472, doi:10.1073/pnas.1100480108. http://www.pnas.org/cgi/doi/10.1073/pnas.1100480108.
Landhäusser, S. M., D. Deshaies, and V. J. Lieffers, 2010: Disturbance facilitates rapid range expansion of aspen into higher elevations of the Rocky Mountains under a warming climate. *J. Biogeogr.*, **37**, 68–76, doi:10.1111/j.1365-2699.2009.02182.x. http://doi.wiley.com/10.1111/j.1365-2699.2009.02182.x (Accessed May 20, 2018).
Lauwaet, D., H. Hooyberghs, B. Maiheu, W. Lefebvre, G. Driesen, S. Van Looy, and K. De Ridder, 2015: Detailed Urban Heat Island Projections for Cities Worldwide: Dynamical Downscaling CMIP5 Global Climate Models. *Climate*, **3**, 391–415, doi:10.3390/cli3020391. http://www.mdpi.com/2225-1154/3/2/391.
Lavell, A., and Coauthors, 2012: Climate Change: New Dimensions in Disaster Risk, Exposure, Vulnerability, and Resilience. *Manag. Risks Extrem. Events Disasters to Adv. Clim. Chang. Adapt.*, 25–64, doi:10.1017/CBO9781139177245.004. http://ebooks.cambridge.org/ref/id/CBO9781139177245A014.
Lawrence, D., and K. Vandecar, 2015a: Effects of tropical deforestation on climate and agriculture. *Nat. Clim. Chang.*, **5**, 27–36, doi:10.1038/nclimate2430.
——, and ——, 2015b: Effects of tropical deforestation on climate and agriculture. *Nat. Clim. Chang.*, **5**, 27–36, doi:10.1038/nclimate2430.
Lawrence, D. M., and Coauthors, 2016: The Land Use Model Intercomparison Project (LUMIP) contribution to CMIP6: Rationale and experimental design. *Geosci. Model Dev.*, **9**, 2973–2998, doi:10.5194/gmd-9-2973-2016.

Layton, K., and D. Ellison, 2016: Induced precipitation recycling (IPR): A proposed concept for increasing precipitation through natural vegetation feedback mechanisms. *Ecol. Eng.*, **91**, 553–565, doi:10.1016/j.ecoleng.2016.02.031.

Leakey, A. D. B., K. A. Bishop, and E. A. Ainsworth, 2012: A multi-biome gap in understanding of crop and ecosystem responses to elevated CO2. *Curr. Opin. Plant Biol.*, **15**, 228–236, doi:10.1016/j.pbi.2012.01.009. http://www.sciencedirect.com/science/article/pii/S1369526612000106.

Lean, J., and D. A. Warrilow, 1989: Simulation of the regional climatic impact of Amazon deforestation. *Nature*, **342**, 411–413, doi:10.1038/342411a0.

Lee, D. and Sanz, M. J., 2017a: UNFCCC Accounting for Forests: What's in and what's out of NDCs and REDD+ - Climate and Land Use Alliance.

——, 2017b: *UNFCCC Accounting for Forests: What's in and what's out of NDCs and REDD+ - Climate and Land Use Alliance*.

Lee, X., and Coauthors, 2011: Observed increase in local cooling effect of deforestation at higher latitudes. *Nature*, doi:10.1038/nature10588.

Lehmann, J., D. Coumou, and K. Frieler, 2015: Increased record-breaking precipitation events under global warming. *Clim. Change*, **132**, 501–515, doi:10.1007/s10584-015-1434-y. https://doi.org/10.1007/s10584-015-1434-y.

Lehner, F., and T. F. Stocker, 2015: From local perception to global perspective. *Nat. Clim. Chang.*, **5**, 731–734, doi:10.1038/nclimate2660. http://www.nature.com/doifinder/10.1038/nclimate2660.

——, S. Coats, T. F. Stocker, A. G. Pendergrass, B. M. Sanderson, C. C. Raible, and J. E. Smerdon, 2017: Projected drought risk in 1.5°C and 2°C warmer climates. *Geophys. Res. Lett.*, **44**, 7419–7428, doi:10.1002/2017GL074117.

Leimbach, M., A. Popp, H. Lotze-Campen, N. Bauer, J. P. Dietrich, and D. Klein, 2011: 10 Integrated assessment models–the interplay of climate change, agriculture and land use in a policy tool. *Handbook on Climate Change and Agriculture*, p. 204 https://www.elgaronline.com/view/9781849801164.00018.xml (Accessed May 22, 2018).

Lejeune, Q., S. I. Seneviratne, and E. L. Davin, 2017: Historical land-cover change impacts on climate: Comparative assessment of LUCID and CMIP5 multimodel experiments. *J. Clim.*, **30**, 1439–1459, doi:10.1175/JCLI-D-16-0213.1.

——, E. L. Davin, L. Gudmundsson, and S. I. Seneviratne, 2018: Historical deforestation increased the risk of heat extremes in northern mid-latitudes 2. *Nat. Clim. Chang.*, **8**, 1–16, doi:10.1038/s41558-018-0131-z. https://doi.org/10.1038/s41558-018-0131-z.

Lemonsu, A., R. Kounkou-Arnaud, J. Desplat, J. L. Salagnac, and V. Masson, 2013: Evolution of the Parisian urban climate under a global changing climate. *Clim. Change*, **116**, 679–692, doi:10.1007/s10584-012-0521-6.

Lenton, T. M., 2014: CHAPTER 3. The Global Potential for Carbon Dioxide Removal. *Geoengineering of the Climate System*, R.M. Harrison and R.E. Hester, Eds., Royal Society of Chemistry, 52–79 http://ebook.rsc.org/?DOI=10.1039/9781782621225-00052.

Leonard, M., and Coauthors, 2014: A compound event framework for understanding extreme impacts. *Wiley Interdiscip. Rev. Clim. Chang.*, **5**, 113–128, doi:10.1002/wcc.252. http://doi.wiley.com/10.1002/wcc.252 (Accessed May 17, 2018).

Lesk, C., P. Rowhani, and N. Ramankutty, 2016: Influence of extreme weather disasters on global crop production. *Nature*, **529**, 84. http://dx.doi.org/10.1038/nature16467.

Li, C., S. Frolking, and K. Butterbach-Bahl, 2005: Carbon sequestration in arable soils is likely to increase nitrous oxide emissions, offsetting reductions in climate radiative forcing. *Clim. Change*, **72**, 321–338, doi:10.1007/s10584-005-6791-5.

Li, D., and E. Bou-Zeid, 2013: Synergistic interactions between urban heat islands and heat waves: The impact in cities is larger than the sum of its parts. *J. Appl. Meteorol. Climatol.*, **52**, 2051–2064, doi:10.1175/JAMC-D-13-02.1.

——, T. Sun, M. Liu, L. Yang, L. Wang, and Z. Gao, 2015a: Contrasting responses of urban and rural surface energy budgets to heat waves explain synergies between urban heat islands and heat waves. *Environ. Res. Lett.*, **10**, 54009, doi:10.1088/1748-9326/10/5/054009. http://stacks.iop.org/1748-

9326/10/i=5/a=054009.

Li, H., X. Cui, and D. L. Zhang, 2017a: Sensitivity of the initiation of an isolated thunderstorm over the Beijing metropolitan region to urbanization, terrain morphology and cold outflows. *Q. J. R. Meteorol. Soc.*, **143**, 3153–3164, doi:10.1002/qj.3169.

Li, H., Y. Zhou, X. Li, L. Meng, X. Wang, S. Wu, and S. Sodoudi, 2018a: A new method to quantify surface urban heat island intensity. *Sci. Total Environ.*, **624**, 262–272, doi:https://doi.org/10.1016/j.scitotenv.2017.11.360. http://www.sciencedirect.com/science/article/pii/S0048969717334186.

Li, M., Z. Mao, Y. Song, M. Liu, and X. Huang, 2015b: Impacts of the decadal urbanization on thermally induced circulations in eastern China. *J. Appl. Meteorol. Climatol.*, **54**, 259–282, doi:10.1175/JAMC-D-14-0176.1.

Li, T., and Coauthors, 2015c: Uncertainties in predicting rice yield by current crop models under a wide range of climatic conditions. *Glob. Chang. Biol.*, **21**, 1328–1341, doi:10.1111/gcb.12758.

Li, W., and Coauthors, 2018b: Recent Changes in Global Photosynthesis and Terrestrial Ecosystem Respiration Constrained From Multiple Observations. *Geophys. Res. Lett.*, **45**, 1058–1068, doi:10.1002/2017GL076622.

Li, X., Y. Zhou, G. R. Asrar, J. Mao, X. Li, and W. Li, 2017b: Response of vegetation phenology to urbanization in the conterminous United States. *Glob. Chang. Biol.*, **23**, 2818–2830, doi:10.1111/gcb.13562.

Li, X., C. Mitra, L. Dong, and Q. Yang, 2018c: Understanding land use change impacts on microclimate using Weather Research and Forecasting (WRF) model. *Phys. Chem. Earth*, **103**, 115–126, doi:10.1016/j.pce.2017.01.017. https://doi.org/10.1016/j.pce.2017.01.017.

Li, Y., M. Zhao, S. Motesharrei, Q. Mu, E. Kalnay, and S. Li, 2015d: Local cooling and warming effects of forests based on Satellite Observations. *Nat. Commun.*, **6**, 1–8, doi:10.1038/ncomms7603. http://dx.doi.org/10.1038/ncomms7603.

Liang, P., and Y. Ding, 2017: The long-term variation of extreme heavy precipitation and its link to urbanization effects in Shanghai during 1916–2014. *Adv. Atmos. Sci.*, **34**, 321–334, doi:10.1007/s00376-016-6120-0.

Liao, W., D. Wang, X. Liu, G. Wang, and J. Zhang, 2017: Estimated influence of urbanization on surface warming in Eastern China using time-varying land use data. *Int. J. Climatol.*, **37**, 3197–3208, doi:10.1002/joc.4908.

Liu, B., and Coauthors, 2016a: Similar estimates of temperature impacts on global wheat yield by three independent methods. *Nat. Clim. Chang.*, **6**, 1130–1136, doi:10.1038/nclimate3115.

Liu, C., C. E. Chung, F. Zhang, and Y. Yin, 2016b: The colors of biomass burning aerosols in the atmosphere. *Sci. Rep.*, **6**, doi:10.1038/srep28267.

Liu, L., and T. L. Greaver, 2009: A review of nitrogen enrichment effects on three biogenic GHGs: The CO 2 sink may be largely offset by stimulated N2O and CH 4 emission. *Ecol. Lett.*, **12**, 1103–1117, doi:10.1111/j.1461-0248.2009.01351.x.

——, J. S. King, F. L. Booker, C. P. Giardina, H. Lee Allen, and S. Hu, 2009: Enhanced litter input rather than changes in litter chemistry drive soil carbon and nitrogen cycles under elevated CO2: A microcosm study. *Glob. Chang. Biol.*, **15**, 441–453, doi:10.1111/j.1365-2486.2008.01747.x. https://doi.org/10.1111/j.1365-2486.2008.01747.x.

Liu, R., M. Wang, and W. Chen, 2018: The influence of urbanization on organic carbon sequestration and cycling in soils of Beijing. *Landsc. Urban Plan.*, **169**, 241–249, doi:https://doi.org/10.1016/j.landurbplan.2017.09.002. http://www.sciencedirect.com/science/article/pii/S0169204617302037.

Liu, Y., J. Stanturf, and S. Goodrick, 2010: Trends in global wildfire potential in a changing climate. *For. Ecol. Manage.*, **259**, 685–697, doi:10.1016/j.foreco.2009.09.002.

——, S. L. Goodrick, and J. A. Stanturf, 2013: Future U.S. wildfire potential trends projected using a dynamically downscaled climate change scenario. *For. Ecol. Manage.*, **294**, 120–135, doi:10.1016/j.foreco.2012.06.049. http://linkinghub.elsevier.com/retrieve/pii/S037811271200388X (Accessed May 3, 2014).

Liu, Y., Y. Li, S. Li, and S. Motesharrei, 2015a: Spatial and Temporal Patterns of Global NDVI Trends: Correlations with Climate and Human Factors. *Remote Sens.*, **7**, 13233–13250, doi:10.3390/rs71013233.

Liu, Y. Y., A. I. J. M. Van Dijk, R. A. M. De Jeu, J. G. Canadell, M. F. McCabe, J. P. Evans, and G. Wang, 2015b: Recent reversal in loss of global terrestrial biomass. *Nat. Clim. Chang.*, **5**, 470–474, doi:10.1038/nclimate2581.

Loarie, S. R., D. B. Lobell, G. P. Asner, Q. Mu, and C. B. Field, 2011: Direct impacts on local climate of sugar-cane expansion in Brazil. *Nat. Clim. Chang.*, **1**, 105–109, doi:10.1038/nclimate1067. http://dx.doi.org/10.1038/nclimate1067.

Lobell, D. B., and C. Tebaldi, 2014: Getting caught with our plants down: The risks of a global crop yield slowdown from climate trends in the next two decades. *Environ. Res. Lett.*, **9**, 074003, doi:10.1088/1748-9326/9/7/074003.

——, W. Schlenker, and J. Costa-Roberts, 2011: Climate trends and global crop production since 1980. *Science (80-.).*, **333**, 616–620, doi:10.1126/science.1204531. http://www.ncbi.nlm.nih.gov/pubmed/21551030 (Accessed December 20, 2017).

Lohberger, S., M. Stängel, E. C. Atwood, and F. Siegert, 2018: Spatial evaluation of Indonesia's 2015 fire-affected area and estimated carbon emissions using Sentinel-1. *Glob. Chang. Biol.*, **24**, 644–654, doi:10.1111/gcb.13841. http://doi.wiley.com/10.1111/gcb.13841 (Accessed April 16, 2018).

Lokoshchenko, M. A., 2017: Urban heat island and urban dry island in Moscow and their centennial changes. *J. Appl. Meteorol. Climatol.*, **56**, 2729–2745, doi:10.1175/JAMC-D-16-0383.1.

Van Loon, A. F., and G. Laaha, 2015: Hydrological drought severity explained by climate and catchment characteristics. *J. Hydrol.*, **526**, 3–14, doi:10.1016/j.jhydrol.2014.10.059. https://www.sciencedirect.com/science/article/pii/S0022169414008543 (Accessed May 24, 2018).

Loranty, M. M., L. T. Berner, S. J. Goetz, Y. Jin, and J. T. Randerson, 2014: Vegetation controls on northern high latitude snow-albedo feedback: Observations and CMIP5 model simulations. *Glob. Chang. Biol.*, **20**, 594–606, doi:10.1111/gcb.12391.

Lorenz, R., and Coauthors, 2016a: Influence of land-atmosphere feedbacks on temperature and precipitation extremes in the GLACE-CMIP5 ensemble. *J. Geophys. Res.*, **121**, 607–623, doi:10.1002/2015JD024053.

Lorenz, R., A. J. Pitman, and S. A. Sisson, 2016b: Does Amazonian deforestation cause global effects; Can we be sure? *J. Geophys. Res.*, **121**, 5567–5584, doi:10.1002/2015JD024357.

Los, S. O., 2013: Analysis of trends in fused AVHRR and MODIS NDVI data for 1982-2006: Indication for a CO2fertilization effect in global vegetation. *Global Biogeochem. Cycles*, **27**, 318–330, doi:10.1002/gbc.20027.

Lovelock, C. E., I. C. Feller, R. Reef, S. Hickey, and M. C. Ball, 2017: Mangrove dieback during fluctuating sea levels. *Sci. Rep.*, **7**, 1680, doi:10.1038/s41598-017-01927-6. https://doi.org/10.1038/s41598-017-01927-6.

Luo, Y., S. Wan, D. Hui, and L. L. Wallace, 2001: Acclimatization of soil respiration to warming in a tall grass prairie. *Nature*, **413**, 622. http://dx.doi.org/10.1038/35098065.

Luo, Z., E. Wang, and O. J. Sun, 2010: Can no-tillage stimulate carbon sequestration in agricultural soils? A meta-analysis of paired experiments. *Agric. Ecosyst. Environ.*, **139**, 224–231, doi:10.1016/j.agee.2010.08.006.

Lützow, M. V., I. Kögel-Knabner, K. Ekschmitt, E. Matzner, G. Guggenberger, B. Marschner, and H. Flessa, 2006: Stabilization of organic matter in temperate soils: Mechanisms and their relevance under different soil conditions - A review. *Eur. J. Soil Sci.*, **57**, 426–445, doi:10.1111/j.1365-2389.2006.00809.x. https://doi.org/10.1111/j.1365-2389.2006.00809.x.

Luyssaert, S., and Coauthors, 2014a: Land management and land-cover change have impacts of similar magnitude on surface temperature. *Nat. Clim. Chang.*, **4**, 389–393, doi:10.1038/nclimate2196. http://www.nature.com/doifinder/10.1038/nclimate2196 (Accessed December 20, 2017).

——, and Coauthors, 2014b: Land management and land-cover change have impacts of similar magnitude on surface temperature. *Nat. Clim. Chang.*, **4**, 389–393, doi:10.1038/nclimate2196.

M., H. A., A. W. S., and P. T. J., 2014: The effect of urbanisation on the climatology of thunderstorm initiation. *Q. J. R. Meteorol. Soc.*, **141**, 663–675, doi:10.1002/qj.2499. https://doi.org/10.1002/qj.2499.

Ma, E., A. Liu, X. Li, F. Wu, and J. Zhan, 2013: Impacts of vegetation change on the regional surface climate: A scenario-based analysis of afforestation in Jiangxi Province, China. *Adv. Meteorol.*, **2013**, doi:10.1155/2013/796163.

Ma, S., A. Pitman, M. Hart, J. P. Evans, N. Haghdadi, and I. MacGill, 2017a: The impact of an urban canopy and anthropogenic heat fluxes on Sydney's climate. *Int. J. Climatol.*, **37**, 255–270, doi:10.1002/joc.5001.

Ma, W., G. Jia, and A. Zhang, 2017b: Multiple satellite-based analysis reveals complex climate effects of temperate forests and related energy budget. *J. Geophys. Res. Atmos.*, **122**, 3806–3820, doi:10.1002/2016JD026278. http://doi.wiley.com/10.1002/2016JD026278.

Maeda, E. E., N. Utsumi, and T. Oki, 2012: Decreasing precipitation extremes at higher temperatures in tropical regions. *Nat. Hazards*, **64**, 935–941, doi:10.1007/s11069-012-0222-5. http://link.springer.com/10.1007/s11069-012-0222-5 (Accessed May 24, 2018).

Mahmood, R., K. G. Hubbard, R. D. Leeper, and S. A. Foster, 2008: Increase in Near-Surface Atmospheric Moisture Content due to Land Use Changes: Evidence from the Observed Dewpoint Temperature Data. *Mon. Weather Rev.*, **136**, 1554–1561, doi:10.1175/2007MWR2040.1. http://journals.ametsoc.org/doi/abs/10.1175/2007MWR2040.1.

——, and Coauthors, 2014: Land cover changes and their biogeophysical effects on climate. *Int. J. Climatol.*, **34**, 929–953, doi:10.1002/joc.3736. http://doi.wiley.com/10.1002/joc.3736 (Accessed December 18, 2017).

Makkonen, R., A. Asmi, V. M. Kerminen, M. Boy, A. Arneth, A. Guenther, and M. Kulmala, 2012: BVOC-aerosol-climate interactions in the global aerosol-climate model ECHAM5.5-HAM2. *Atmos. Chem. Phys.*, **12**, 10077–10096, doi:10.5194/acp-12-10077-2012.

Malhi, Y., C. Doughty, and D. Galbraith, 2011: The allocation of ecosystem net primary productivity in tropical forests. *Philos. Trans. R. Soc. B Biol. Sci.*, **366**, 3225–3245, doi:10.1098/rstb.2011.0062. http://rstb.royalsocietypublishing.org/cgi/doi/10.1098/rstb.2011.0062.

Manish, S., and Coauthors, 2017: Recent advances in understanding secondary organic aerosol: Implications for global climate forcing. *Rev. Geophys.*, **55**, 509–559, doi:10.1002/2016RG000540. https://doi.org/10.1002/2016RG000540.

Mao, J., and Coauthors, 2016: Human-induced greening of the northern extratropical land surface. *Nat. Clim. Chang.*, **6**, 959–963, doi:10.1038/nclimate3056. http://dx.doi.org/10.1038/nclimate3056.

Maraun, D., and Coauthors, 2017: Towards process-informed bias correction of climate change simulations. *Nature Climate Change,* Vol. 7 of, Nature Publishing Group, 764–773 http://www.nature.com/doifinder/10.1038/nclimate3418 (Accessed May 25, 2018).

MARKUS, K., N. P. S., P. ALAIN, F. TIMOTHY, K. MARC, S. CHRISTOPHER, and S. PHILLIP, 2011: Old and stable soil organic matter is not necessarily chemically recalcitrant: implications for modeling concepts and temperature sensitivity. *Glob. Chang. Biol.*, **17**, 1097–1107, doi:10.1111/j.1365-2486.2010.02278.x. https://doi.org/10.1111/j.1365-2486.2010.02278.x.

Marland, G., T. A. Boden, and R. J. Andres, *Global, Regional, and National Fossil-Fuel CO2 Emissions*. Oak Ridge, http://cdiac.ornl.gov/trends/emis/overview_%0D2014.html%0D.

Van Marle, M. J. E., and Coauthors, 2017: Historic global biomass burning emissions for CMIP6 (BB4CMIP) based on merging satellite observations with proxies and fire models (1750-2015). *Geosci. Model Dev.*, **10**, 3329–3357, doi:10.5194/gmd-10-3329-2017.

Marlon, J. R., P. J. Bartlein, A. L. Daniau, S. P. Harrison, S. Y. Maezumi, M. J. Power, W. Tinner, and B. Vanniére, 2013: Global biomass burning: A synthesis and review of Holocene paleofire records and their controls. *Quat. Sci. Rev.*, **65**, 5–25, doi:10.1016/j.quascirev.2012.11.029.

Marschner, B., and Coauthors, 2008: How relevant is recalcitrance for the stabilization of organic matter in soils? *J. Plant Nutr. Soil Sci.*, **171**, 91–110, doi:10.1002/jpln.200700049. https://doi.org/10.1002/jpln.200700049.

Mason, S. J., and L. Goddard, 2001: Probabilistic precipitation anomalies associated with ENSO. *Bull. Am. Meteorol. Soc.*, **82**, 619–638, doi:10.1175/1520-0477(2001)082<0619:PPAAWE>2.3.CO;2.

Matthews, H. D., A. J. Weaver, K. J. Meissner, N. P. Gillett, and M. Eby, 2004: Natural and anthropogenic climate change: incorporating historical land cover change, vegetation dynamics and the global carbon cycle. *Clim. Dyn.*, **22**, 461–479, doi:10.1007/s00382-004-0392-2. http://link.springer.com/10.1007/s00382-004-0392-2.

Maule, C. F., T. Mendlik, and O. B. Christensen, 2017: The effect of the pathway to a two degrees warmer world on the regional temperature change of Europe. *Clim. Serv.*, **7**, 3–11, doi:10.1016/j.cliser.2016.07.002.

Mauritz, M., and Coauthors, 2017: Nonlinear CO2flux response to 7 years of experimentally induced permafrost thaw. *Glob. Chang. Biol.*, **23**, 3646–3666, doi:10.1111/gcb.13661. https://doi.org/10.1111/gcb.13661.

Mazzoncini, M., T. B. Sapkota, P. Bàrberi, D. Antichi, and R. Risaliti, 2011: Long-term effect of tillage, nitrogen fertilization and cover crops on soil organic carbon and total nitrogen content. *Soil Tillage Res.*, **114**, 165–174, doi:10.1016/j.still.2011.05.001.

Mccarthy, M. P., C. Harpham, C. M. Goodess, and P. D. Jones, 2012: Simulating climate change in UK cities using a regional climate model, HadRM3. *Int. J. Climatol.*, **32**, 1875–1888, doi:10.1002/joc.2402.

McCarthy, M. P., M. J. Best, and R. A. Betts, 2010: Climate change in cities due to global warming and urban effects. *Geophys. Res. Lett.*, **37**, 1–5, doi:10.1029/2010GL042845.

McCollum, D. L., and Coauthors, 2017: Improving the behavioral realism of global integrated assessment models: An application to consumers' vehicle choices. *Transp. Res. Part D Transp. Environ.*, **55**, 322–342, doi:10.1016/j.trd.2016.04.003. http://www.sciencedirect.com/science/article/pii/S1361920915300900.

McDowell, N. G., D. J. Beerling, D. D. Breshears, R. A. Fisher, K. F. Raffa, and M. Stitt, 2011: The interdependence of mechanisms underlying climate-driven vegetation mortality. *Trends Ecol. Evol.*, **26**, 523–532, doi:https://doi.org/10.1016/j.tree.2011.06.003. http://www.sciencedirect.com/science/article/pii/S0169534711001698.

McGuire, A. D., and Coauthors, 2016: Variability in the sensitivity among model simulations of permafrost and carbon dynamics in the permafrost region between 1960 and 2009. *Global Biogeochem. Cycles*, **30**, 1015–1037, doi:10.1002/2016GB005405. https://doi.org/10.1002/2016GB005405.

——, and Coauthors, 2018: Dependence of the evolution of carbon dynamics in the northern permafrost region on the trajectory of climate change. *Proc. Natl. Acad. Sci.*, **115**, 201719903, doi:10.1073/pnas.1719903115. http://www.pnas.org/lookup/doi/10.1073/pnas.1719903115.

Mckee, K. L., D. R. Cahoon, and I. C. Feller, 2007: Caribbean mangroves adjust to rising sea level through biotic controls on change in soil elevation. *Glob. Ecol. Biogeogr.*, **16**, 545–556, doi:10.1111/j.1466-8238.2007.00317.x.

Mckeever, D. B., 2009: *stimated annual timber products consumption in major end uses in the United States,1950-2006*. 49 pp.

McLeod, E., and Coauthors, 2011: A blueprint for blue carbon: Toward an improved understanding of the role of vegetated coastal habitats in sequestering CO2. *Front. Ecol. Environ.*, **9**, 552–560, doi:10.1890/110004. https://doi.org/10.1890/110004.

McLeod, J., M. Shepherd, and C. E. Konrad, 2017: Spatio-temporal rainfall patterns around Atlanta, Georgia and possible relationships to urban land cover. *Urban Clim.*, **21**, 27–42, doi:10.1016/j.uclim.2017.03.004. http://dx.doi.org/10.1016/j.uclim.2017.03.004.

Mcnorton, J., and Coauthors, 2016: Role of OH variability in the stalling of the global atmospheric CH4 growth rate from 1999 to 2006. *Atmos. Chem. Phys.*, **16**, 7943–7956, doi:10.5194/acp-16-7943-2016.

McPhaden, M. J., S. E. Zebiak, and M. H. Glantz, 2006: ENSO as an integrating concept in earth science. *Science (80-.).*, **314**, 1740–1745, doi:10.1126/science.1132588. http://www.ncbi.nlm.nih.gov/pubmed/17170296 (Accessed May 5, 2018).

Mechler, R., and L. M. Bouwer, 2015: Understanding trends and projections of disaster losses and climate change: is vulnerability the missing link? *Clim. Change*, **133**, 23–35, doi:10.1007/s10584-014-1141-0. http://link.springer.com/10.1007/s10584-014-1141-0 (Accessed May 25, 2018).

Meinshausen, M., S. C. B. Raper, and T. M. L. Wigley, 2011: Emulating coupled atmosphere-ocean and carbon cycle models with a simpler model, MAGICC6 - Part 1: Model description and calibration. *Atmos. Chem. Phys.*, **11**, 1417–1456, doi:10.5194/acp-11-1417-2011.

Melillo, J. M., and Coauthors, 2017: Long-term pattern and magnitude of soil carbon feedback to the climate system in a warming world. *Science (80-.).*, **358**, 101–105, doi:10.1126/science.aan2874. http://science.sciencemag.org/content/358/6359/101.

Melton, J. R., and Coauthors, 2013: Geoscientific Instrumentation Methods and Data Systems Present state of global wetland extent and wetland methane modelling: conclusions from a model inter-comparison project (WETCHIMP). *Biogeosciences*, **10**, 753–788, doi:10.5194/bg-10-753-2013. www.biogeosciences.net/10/753/2013/.

Mercado, L. M., and Coauthors, 2018: Large sensitivity in land carbon storage due to geographical and temporal variation in the thermal response of photosynthetic capacity. *New Phytol.*, doi:10.1111/nph.15100.

Mercedes, B., and Coauthors, 2014: Co‐benefits, trade‐offs, barriers and policies for greenhouse gas mitigation in the agriculture, forestry and other land use (AFOLU) sector. *Glob. Chang. Biol.*, **20**, 3270–3290, doi:doi:10.1111/gcb.12591. https://doi.org/10.1111/gcb.12591.

Miettinen, J., C. Shi, and S. C. Liew, 2016: Land cover distribution in the peatlands of Peninsular Malaysia, Sumatera and Borneo in 2015.pdf. *Glob. Ecol. Conserv.*, **6**, 67–78, doi:https://doi.org/10.1016/j.gecco.2016.02.004. http://www.sciencedirect.com/science/article/pii/S2351989415300470.

Millar, R. J., and Coauthors, 2017: Emission budgets and pathways consistent with limiting warming to 1.5 °c. *Nat. Geosci.*, **10**, 741–747, doi:10.1038/NGEO3031. http://dx.doi.org/10.1038/ngeo3031.

Min, S. K., X. Zhang, F. W. Zwiers, and G. C. Hegerl, 2011: Human contribution to more-intense precipitation extremes. *Nature*, **470**, 378–381, doi:10.1038/nature09763. http://www.nature.com/articles/nature09763 (Accessed May 25, 2018).

Minasny, B., and A. B. McBratney, 2018a: Limited effect of organic matter on soil available water capacity. *Eur. J. Soil Sci.*, **69**, 39–47, doi:10.1111/ejss.12475. https://doi.org/10.1111/ejss.12475.

——, and ——, 2018b: Limited effect of organic matter on soil available water capacity. *Eur. J. Soil Sci.*, **69**, 39–47, doi:10.1111/ejss.12475. https://doi.org/10.1111/ejss.12475.

Minasny, B., and Coauthors, 2017: Soil carbon 4 per mille. *Geoderma*, **292**, 59–86, doi:10.1016/J.GEODERMA.2017.01.002.

Miner, R., 2010: *Impact of the global forest industry on atmospheric greenhouse gases*. Rome, 71 pp. http://library.wur.nl/WebQuery/clc/1941440.

Mishra, V., A. R. Ganguly, B. Nijssen, and D. P. Lettenmaier, 2015: Changes in observed climate extremes in global urban areas. *Environ. Res. Lett.*, **10**, 024005, doi:10.1088/1748-9326/10/2/024005. http://stacks.iop.org/1748-9326/10/i=2/a=024005?key=crossref.66eab66a177894abf6a0f8b554f971af (Accessed May 17, 2018).

Mistry, M. N., I. Sue Wing, and E. De Cian, 2017: Simulated vs. empirical weather responsiveness of crop yields: US evidence and implications for the agricultural impacts of climate change. *Environ. Res. Lett.*, **12**, 075007, doi:10.1088/1748-9326/aa788c.

Miteva, D. A., 2016: Social and Environmental Impacts of Forest Management Certification in Indonesia. *PLoS One*, **10**, 13–15, doi:10.1371/journal.pone.0129675. https://doi.org/10.1371/journal.pone.0129675.

Mohajerani, A., J. Bakaric, and T. Jeffrey-Bailey, 2017: The urban heat island effect, its causes, and mitigation, with reference to the thermal properties of asphalt concrete. *J. Environ. Manage.*, **197**, 522–538, doi:https://doi.org/10.1016/j.jenvman.2017.03.095. http://www.sciencedirect.com/science/article/pii/S0301479717303201.

Mohan, T. S., and M. Rajeevan, 2017: Past and future trends of hydroclimatic intensity over the Indian monsoon region. *J. Geophys. Res. Atmos.*, **122**, 896–909, doi:10.1002/2016JD025301. http://doi.wiley.com/10.1002/2016JD025301 (Accessed May 24, 2018).

Mondal, N., and R. Sukumar, 2016: Fires in Seasonally Dry Tropical Forest: Testing the Varying Constraints Hypothesis across a Regional Rainfall Gradient. *PLoS One*, **11**, e0159691. https://doi.org/10.1371/journal.pone.0159691.

Montzka, S. A., E. J. Dlugokencky, and J. H. Butler, 2011: Non-CO 2 greenhouse gases and climate change. *Nature*, **476**, 43–50, doi:10.1038/nature10322. http://www.nature.com/doifinder/10.1038/nature10322.

Moore, K. E., D. R. Fitzjarrald, R. K. Sakai, M. L. Goulden, J. W. Munger, and S. C. Wofsy, 1996: Seasonal Variation in Radiative and Turbulent Exchange at a Deciduous Forest in Central Massachusetts. *J. Appl. Meterology*, **35**, 122–134, doi:10.1175/1520-0450(1996)035<0122:SVIRAT>2.0.CO;2. http://journals.ametsoc.org/doi/abs/10.1175/1520-0450%281996%29035%3C0122%3ASVIRAT%3E2.0.CO%3B2.

Mora, C., and Coauthors, 2013: The projected timing of climate departure from recent variability. *Nature*, **502**, 183–187, doi:10.1038/nature12540.

——, and Coauthors, 2014: Mora et al. reply. *Nature*, **511**, E5–E6, doi:10.1038/nature13524.

Morgan, J. A., and Coauthors, 2011: C4grasses prosper as carbon dioxide eliminates desiccation in warmed semi-arid grassland. *Nature*, **476**, 202–205, doi:10.1038/nature10274. http://dx.doi.org/10.1038/nature10274.

Mosley, L. M., 2015: Drought impacts on the water quality of freshwater systems; review and integration. *Earth-Science Rev.*, **140**, 203–214, doi:10.1016/j.earscirev.2014.11.010. https://www.sciencedirect.com/science/article/pii/S0012825214002086 (Accessed May 24, 2018).

Mosquera, O., P. Buurman, B. L. Ramirez, and M. C. Amezquita, 2012: Carbon stocks and dynamics under improved tropical pasture and silvopastoral systems in Colombian Amazonia. *Geoderma*, **189–190**, 81–86, doi:10.1016/j.geoderma.2012.04.022.

Mouillot, F., and C. B. Field, 2005: Fire history and the global carbon budget: A 1° × 1° fire history reconstruction for the 20th century. *Glob. Chang. Biol.*, **11**, 398–420, doi:10.1111/j.1365-2486.2005.00920.x. https://doi.org/10.1111/j.1365-2486.2005.00920.x.

Mudryk, L. R., P. J. Kushner, C. Derksen, and C. Thackeray, 2017: Snow cover response to temperature in observational and climate model ensembles. *Geophys. Res. Lett.*, **44**, 919–926, doi:10.1002/2016GL071789.

Mueller, B., and S. I. Seneviratne, 2012: Hot days induced by precipitation deficits at the global scale. *Proc. Natl. Acad. Sci.*, **109**, 12398–12403, doi:10.1073/pnas.1204330109. http://www.pnas.org/cgi/doi/10.1073/pnas.1204330109.

Mueller, N. D., E. E. Butler, K. A. McKinnon, A. Rhines, M. Tingley, N. M. Holbrook, and P. Huybers, 2015: Cooling of US Midwest summer temperature extremes from cropland intensification. *Nat. Clim. Chang.*, **6**, 317–322, doi:10.1038/nclimate2825. http://dx.doi.org/10.1038/nclimate2825.

Mueller, T., and Coauthors, 2014: Human Land use Practices Lead to Global Long-Term Increases in Photosynthetic Capacity. *Remote Sens.*, **6**, 5717–5731, doi:10.3390/rs6065717.

Mulholland, P. J., and Coauthors, 2008: Stream denitrification across biomes and its response to anthropogenic nitrate loading. *Nature*, **452**, 202–205, doi:10.1038/nature06686.

Müller, C., J. Elliott, A. C. Ruane, C. Rosenzweig, S. Asseng, K. J. Boote, and J. Elliott, 2017: An AgMIP framework for improved agricultural representation in integrated assessment models OPEN ACCESS An AgMIP framework for improved agricultural representation in integrated assessment models. *Environ. Res. Lett.*, **12**, 125003. http://stacks.iop.org/1748-9326/12/i=12/a=125003.

Murdiyarso, D., and Coauthors, 2015: The potential of Indonesian mangrove forests for global climate change mitigation. *Nat. Clim. Chang.*, **5**, 1089–1092, doi:10.1038/nclimate2734.

Myers-Smith, I. H., and D. S. Hik, 2018: Climate warming as a driver of tundra shrubline advance. *J. Ecol.*, **106**, 547–560, doi:10.1111/1365-2745.12817.

——, and Coauthors, 2015: Climate sensitivity of shrub growth across the tundra biome. *Nat. Clim. Chang.*, **5**, 887–891, doi:10.1038/nclimate2697.

Myhre, G., and Coauthors, 2013: Anthropogenic and Natural Radiative Forcing. *Climate Change 2013: The Physical Science Basis. Contribution of Working Group 1 to the Fifth Assessment Report of the Intergovernmental Panel on Climate Change*, T.F. Stocker et al., Eds., Cambridge University Pres, Cambridge, United Kingdom and New York, NY, USA, p. 714.

Nabuurs, G. J., and Coauthors, 2007: Forestry. *Climate Change 2007: Working Group III: Mitigation of Climate Change*, B. Metz, O.R. Davidson, P.R. Bosch, R. Dave, and L.A. Meyer, Eds., Cambridge University Press, Cambridge, United Kingdom and New York, NY, USA.

——, E. J. M. M. Arets, and M. J. Schelhaas, 2017: European forests show no carbon debt, only a long parity effect. *For. Policy Econ.*, **75**, 120–125, doi:10.1016/j.forpol.2016.10.009.

Nazemi, A., and H. S. Wheater, 2015: On inclusion of water resource management in Earth system models – Part 1: Problem definition and representation of water demand. *Hydrol. Earth Syst. Sci.*, **19**, 33–61, doi:10.5194/hess-19-33-2015. https://www.hydrol-earth-syst-sci.net/19/33/2015/.

Nelson, G. C., and Coauthors, 2014: Climate change effects on agriculture: Economic responses to biophysical shocks. *Proc. Natl. Acad. Sci.*, **111**, 3274–3279, doi:10.1073/pnas.1222465110. http://www.pnas.org/lookup/doi/10.1073/pnas.1222465110.

Nicholson, S. E., 2011: *Dryland climatology*. Cambridge University Press, New York, 1-516 pp.

Niu, S., Y. Luo, D. Li, S. Cao, J. Xia, J. Li, and M. D. Smith, 2014: Plant growth and mortality under climatic extremes: An overview. *Environ. Exp. Bot.*, **98**, 13–19, doi:10.1016/j.envexpbot.2013.10.004. https://www-sciencedirect-com.ezproxy.uct.ac.za/science/article/pii/S0098847213001482 (Accessed May 25, 2018).

Niyogi, D., 2004: Direct observations of the effects of aerosol loading on net ecosystem CO $_2$ exchanges over different landscapes. *Geophys. Res. Lett.*, **31**, L20506, doi:10.1029/2004GL020915. http://doi.wiley.com/10.1029/2004GL020915.

——, C. Kishtawal, S. Tripathi, and R. S. Govindaraju, 2010: Observational evidence that agricultural intensification and land use change may be reducing the Indian summer monsoon rainfall. *Water Resour. Res.*, **46**, 1–17, doi:10.1029/2008WR007082.

——, M. Lei, C. Kishtawal, P. Schmid, and M. Shepherd, 2017: Urbanization impacts on the summer heavy rainfall climatology over the eastern United States. *Earth Interact.*, **21**, 1–17, doi:10.1175/EI-D-15-0045.1. https://doi.org/10.1175/EI-D-15-0045.1.

De Noblet-Ducoudré, N., M. Claussen, and C. Prentice, 2000: Mid-Holocene greening of the Sahara: First results of the GAIM 6000 year BP experiment with two asynchronously coupled atmosphere/biome models. *Clim. Dyn.*, **16**, 643–659, doi:10.1007/s003820000074.

De Noblet-Ducoudré, N., and Coauthors, 2012: Determining robust impacts of land use-induced land cover changes on surface climate over North America and Eurasia: Results from the first set of LUCID experiments. *J. Clim.*, **25**, 3261–3281, doi:10.1175/JCLI-D-11-00338.1.

Nobre, P., M. Malagutti, D. F. Urbano, R. A. F. De Almeida, and E. Giarolla, 2009: Amazon deforestation and climate change in a coupled model simulation. *J. Clim.*, **22**, 5686–5697, doi:10.1175/2009JCLI2757.1.

Nogherotto, R., E. Coppola, F. Giorgi, and L. Mariotti, 2013: Impact of Congo Basin deforestation on the African monsoon. *Atmos. Sci. Lett.*, **14**, 45–51, doi:10.1002/asl2.416.

Norby, R. J., J. M. Warren, C. M. Iversen, B. E. Medlyn, and R. E. McMurtrie, 2010: CO2 enhancement of forest productivity constrained by limited nitrogen availability. *Proc. Natl. Acad. Sci.*, **107**, 19368–19373, doi:10.1073/pnas.1006463107. http://www.pnas.org/cgi/doi/10.1073/pnas.1006463107.

O'Gorman, P. A., 2014: Contrasting responses of mean and extreme snowfall to climate change. *Nature*, **512**, 416–418, doi:10.1038/nature13625. http://www.nature.com/articles/nature13625 (Accessed May 16, 2018).

O'ishi, R., A. Abe-Ouchi, I. C. Prentice, and S. Sitch, 2009: Vegetation dynamics and plant CO2responses as positive feedbacks in a greenhouse world. *Geophys. Res. Lett.*, **36**, 0–4, doi:10.1029/2009GL038217.

O'Neill, B. C., and Coauthors, 2017: The roads ahead: Narratives for shared socioeconomic pathways describing world futures in the 21st century. *Glob. Environ. Chang.*, **42**, 169–180, doi:10.1016/j.gloenvcha.2015.01.004.
https://www.sciencedirect.com/science/article/pii/S0959378015000060 (Accessed May 22, 2018).

Obersteiner, M., and Coauthors, 2016: Assessing the land resource–food price nexus of the Sustainable Development Goals. *Sci. Adv.*, **2**, e1501499–e1501499, doi:10.1126/sciadv.1501499. http://advances.sciencemag.org/cgi/doi/10.1126/sciadv.1501499 (Accessed May 22, 2018).

Obersteiner, S. F. and P. H. and J.-F. S. and A. L. and H. V. and E. W. and U. K. and O. F. and M. G. and M. H. and P. S. and T. H. and F. K. and M., 2017: Reducing greenhouse gas emissions in agriculture without compromising food security? *Environ. Res. Lett.*, **12**, 105004. http://stacks.iop.org/1748-9326/12/i=10/a=105004.

Oenema, O., and Coauthors, 2014: Reducing nitrous oxide emissions from the global food system. *Curr. Opin. Environ. Sustain.*, **9–10**, 55–64, doi:10.1016/j.cosust.2014.08.003.

http://dx.doi.org/10.1016/j.cosust.2014.08.003.
Olefeldt, D., and Coauthors, 2016: Circumpolar distribution and carbon storage of thermokarst landscapes. *Nat. Commun.*, **7**, 1–11, doi:10.1038/ncomms13043.
Oleson, K., 2012: Contrasts between Urban and rural climate in CCSM4 CMIP5 climate change scenarios. *J. Clim.*, **25**, 1390–1412, doi:10.1175/JCLI-D-11-00098.1.
Oleson, K. W., G. B. Bonan, J. Feddema, and T. Jackson, 2011: An examination of urban heat island characteristics in a global climate model. *Int. J. Climatol.*, **31**, 1848–1865, doi:10.1002/joc.2201.
Ooi, M. C. G., A. Chan, M. J. Ashfold, K. I. Morris, M. Y. Oozeer, and S. A. Salleh, 2017: Numerical study on effect of urban heating on local climate during calm inter-monsoon period in greater Kuala Lumpur, Malaysia. *Urban Clim.*, **20**, 228–250, doi:10.1016/j.uclim.2017.04.010. http://dx.doi.org/10.1016/j.uclim.2017.04.010.
Oort, A. H., and J. P. Peixóto, 1983: Global angular momentum and energy balance requirements from observations. *Adv. Geophys.*, **25**, 355–490, doi:10.1016/S0065-2687(08)60177-6. https://www.sciencedirect.com/science/article/pii/S0065268708601776 (Accessed May 7, 2018).
Orlowsky, B., and S. I. Seneviratne, 2012: Global changes in extreme events: Regional and seasonal dimension. *Clim. Change*, **110**, 669–696, doi:10.1007/s10584-011-0122-9. https://doi.org/10.1007/s10584-011-0122-9.
Ornstein, L., I. Aleinov, and D. Rind, 2009: Irrigated afforestation of the Sahara and Australian Outback to end global warming. *Clim. Change*, **97**, 409–437, doi:10.1007/s10584-009-9626-y.
Orwin, K. H., M. U. F. Kirschbaum, M. G. St John, and I. A. Dickie, 2011: Organic nutrient uptake by mycorrhizal fungi enhances ecosystem carbon storage: A model-based assessment. *Ecol. Lett.*, **14**, 493–502, doi:10.1111/j.1461-0248.2011.01611.x. https://doi.org/10.1111/j.1461-0248.2011.01611.x.
Page, S. E., J. O. Rieley, and C. J. Banks, 2011: Global and regional importance of the tropical peatland carbon pool. *Glob. Chang. Biol.*, **17**, 798–818, doi:10.1111/j.1365-2486.2010.02279.x. https://doi.org/10.1111/j.1365-2486.2010.02279.x.
Pall, P., M. R. Allen, and D. A. Stone, 2007: Testing the Clausius-Clapeyron constraint on changes in extreme precipitation under CO2 warming. *Clim. Dyn.*, **28**, 351–363, doi:10.1007/s00382-006-0180-2. http://link.springer.com/10.1007/s00382-006-0180-2 (Accessed May 19, 2018).
Pall, P., T. Aina, D. A. Stone, P. A. Stott, T. Nozawa, A. G. J. Hilberts, D. Lohmann, and M. R. Allen, 2011: Anthropogenic greenhouse gas contribution to flood risk in England and Wales in autumn 2000. *Nature*, **470**, 382–385, doi:10.1038/nature09762. http://www.nature.com/articles/nature09762 (Accessed May 25, 2018).
Palm, C., H. Blanco-Canqui, F. DeClerck, L. Gatere, and P. Grace, 2014: Conservation agriculture and ecosystem services: An overview. *Agric. Ecosyst. Environ.*, **187**, 87–105, doi:10.1016/j.agee.2013.10.010.
Pan, Y., and Coauthors, 2011: A large and persistent carbon sink in the world's forests. *Science (80-.).*, **333**, 988–993, doi:10.1126/science.1201609.
Park, J. H., A. H. Goldstein, J. Timkovsky, S. Fares, R. Weber, J. Karlik, and R. Holzinger, 2013: Active atmosphere-ecosystem exchange of the vast majority of detected volatile organic compounds. *Science (80-.).*, **341**, 643–647, doi:10.1126/science.1235053. http://science.sciencemag.org/content/341/6146/643.
Park, S., and Coauthors, 2012: Trends and seasonal cycles in the isotopic composition of nitrous oxide since 1940. *Nat. Geosci.*, **5**, 261–265, doi:10.1038/ngeo1421. http://dx.doi.org/10.1038/ngeo1421.
Park, T., and Coauthors, 2016: Changes in growing season duration and productivity of northern vegetation inferred from long-term remote sensing data. *Environ. Res. Lett.*, **11**, doi:10.1088/1748-9326/11/8/084001.
Parmesan, C., and G. Yohe, 2003: A globally coherent fingerprint of climate change impacts across natural systems. *Nature*, **421**, 37–42, doi:10.1038/nature01286. http://www.nature.com/articles/nature01286 (Accessed May 7, 2018).
Parry, M., C. Rosenzweig, and M. Livermore, 2005: Climate change, global food supply and risk of hunger. *Philos. Trans. R. Soc. B Biol. Sci.*, **360**, 2125–2138, doi:10.1098/rstb.2005.1751. http://rstb.royalsocietypublishing.org/cgi/doi/10.1098/rstb.2005.1751.

Parry, M. L., C. Rosenzweig, A. Iglesias, M. Livermore, and G. Fischer, 2004: Effects of climate change on global food production under SRES emissions and socio-economic scenarios. *Glob. Environ. Chang.*, **14**, 53–67, doi:10.1016/j.gloenvcha.2003.10.008.

Paschalis, A., G. G. Katul, S. Fatichi, S. Palmroth, and D. Way, 2017: On the variability of the ecosystem response to elevated atmospheric CO2across spatial and temporal scales at the Duke Forest FACE experiment. *Agric. For. Meteorol.*, **232**, 367–383, doi:10.1016/j.agrformet.2016.09.003. http://dx.doi.org/10.1016/j.agrformet.2016.09.003.

Pathirana, A., H. B. Denekew, W. Veerbeek, C. Zevenbergen, and A. T. Banda, 2014: Impact of urban growth-driven landuse change on microclimate and extreme precipitation - A sensitivity study. *Atmos. Res.*, **138**, 59–72, doi:10.1016/j.atmosres.2013.10.005. http://dx.doi.org/10.1016/j.atmosres.2013.10.005.

Pau, S., D. K. Okamoto, O. Calderón, and S. J. Wright, 2018: Long-term increases in tropical flowering activity across growth forms in response to rising CO2and climate change. *Glob. Chang. Biol.*, **24**, 2105–2116, doi:10.1111/gcb.14004. http://doi.wiley.com/10.1111/gcb.14004 (Accessed January 8, 2018).

Pausas, J. G., and S. Paula, 2012: Fuel shapes the fire-climate relationship: Evidence from Mediterranean ecosystems. *Glob. Ecol. Biogeogr.*, **21**, 1074–1082, doi:10.1111/j.1466-8238.2012.00769.x. https://doi.org/10.1111/j.1466-8238.2012.00769.x.

Paustian, K., J. Lehmann, S. Ogle, D. Reay, G. P. Robertson, and P. Smith, 2016a: Climate-smart soils. *Nature*, **532**, 49–57, doi:10.1038/nature17174.

Pearson, R. G., S. J. Phillips, M. M. Loranty, P. S. A. Beck, T. Damoulas, S. J. Knight, and S. J. Goetz, 2013: Shifts in Arctic vegetation and associated feedbacks under climate change. *Nat. Clim. Chang.*, **3**, 673–677, doi:10.1038/nclimate1858. http://www.nature.com/articles/nclimate1858.

Pearson, T. R. H., S. Brown, L. Murray, and G. Sidman, 2017: Greenhouse gas emissions from tropical forest degradation: An underestimated source. *Carbon Balance Manag.*, **12**, 3, doi:10.1186/s13021-017-0072-2. https://doi.org/10.1186/s13021-017-0072-2.

Pechony, O., and D. T. Shindell, 2010: Driving forces of global wildfires over the past millennium and the forthcoming century. *Proc. Natl. Acad. Sci.*, **107**, 19167–19170, doi:10.1073/pnas.1003669107. http://www.pnas.org/cgi/doi/10.1073/pnas.1003669107.

Pellitier, P. T., and D. R. Zak, 2018: Ectomycorrhizal fungi and the enzymatic liberation of nitrogen from soil organic matter: why evolutionary history matters. *New Phytol.*, **217**, 68–73, doi:10.1111/nph.14598. https://doi.org/10.1111/nph.14598.

Pendleton, L., and Coauthors, 2012: Estimating global "blue carbon" emissions from conversion and degradation of vegetated coastal ecosystems. *PLoS One*, **7**, e43542, doi:10.1371/journal.pone.0043542. http://www.ncbi.nlm.nih.gov/pubmed/22962585%5Cnhttp://www.pubmedcentral.nih.gov/articlerender.fcgi?artid=PMC3433453.

Peng, S.-S., and Coauthors, 2014: Afforestation in China cools local land surface temperature. *Proc. Natl. Acad. Sci.*, **111**, 2915–2919, doi:10.1073/pnas.1315126111. http://www.pnas.org/cgi/doi/10.1073/pnas.1315126111.

Peng, S., and Coauthors, 2004: Rice yields decline with higher night temperature from global warming. *Proc. Natl. Acad. Sci.*, **101**, 9971–9975, doi:10.1073/pnas.0403720101. http://www.pnas.org/cgi/doi/10.1073/pnas.0403720101.

Peñuelas, J., 2009: Phenology feedbacks on climate change. *Science (80-.).*, **324**, 887–888, doi:10.1126/science.1173004. isi:000266048800020%5Cnhttp://www.sciencemag.org/cgi/reprint/324/5929/887.pdf%5Cnhttp://www.sciencemag.org/content/324/5929/887.full.pdf.

——, and J. Llusià, 2003: BVOCs: Plant defense against climate warming? *Trends Plant Sci.*, **8**, 105–109, doi:10.1016/S1360-1385(03)00008-6.

——, and M. Staudt, 2010: BVOCs and global change. *Trends Plant Sci.*, **15**, 133–144, doi:10.1016/j.tplants.2009.12.005.

——, and Coauthors, 2013: Human-induced nitrogen-phosphorus imbalances alter natural and managed

ecosystems across the globe. *Nat. Commun.*, **4**, doi:10.1038/ncomms3934.
——, and Coauthors, 2017: Shifting from a fertilization-dominated to a warming-dominated period. *Nat. Ecol. Evol.*, **1**, 1438–1445, doi:10.1038/s41559-017-0274-8. http://dx.doi.org/10.1038/s41559-017-0274-8.
Perket, J., M. G. Flanner, and J. E. Kay, 2014: Diagnosing shortwave cryosphere radiative effect and its 21st century evolution in CESM. *J. Geophys. Res.*, **119**, 1356–1362, doi:10.1002/2013JD021139. https://doi.org/10.1002/2013JD021139.
Perlwitz, J. P., C. Pérez García-Pando, and R. L. Miller, 2015: Predicting the mineral composition of dust aerosols - Part 2: Model evaluation and identification of key processes with observations. *Atmos. Chem. Phys.*, **15**, 11629–11652, doi:10.5194/acp-15-11629-2015.
Perugini, L., L. Caporaso, S. Marconi, A. Cescatti, B. Quesada, N. De Noblet-Ducoudré, J. I. House, and A. Arneth, 2017: Biophysical effects on temperature and precipitation due to land cover change. *Environ. Res. Lett.*, **12**, doi:10.1088/1748-9326/aa6b3f.
Pete, S., and Coauthors, 2015: Global change pressures on soils from land use and management. *Glob. Chang. Biol.*, **22**, 1008–1028, doi:10.1111/gcb.13068. https://doi.org/10.1111/gcb.13068.
Peters, G. P., and O. Geden, 2017: Catalysing a political shift from low to negative carbon. *Nat. Clim. Chang.*, **7**, 619–621, doi:10.1038/nclimate3369. http://dx.doi.org/10.1038/nclimate3369.
Pfahl, S., P. A. O'Gorman, and E. M. Fischer, 2017: Understanding the regional pattern of projected future changes in extreme precipitation. *Nat. Clim. Chang.*, **7**, 423–427, doi:10.1038/nclimate3287. http://www.nature.com/doifinder/10.1038/nclimate3287 (Accessed May 21, 2018).
Phelan, P. E., K. Kaloush, M. Miner, J. Golden, B. Phelan, H. Silva, and R. A. Taylor, 2015: Urban Heat Island: Mechanisms, Implications, and Possible Remedies. *Annu. Rev. Environ. Resour.*, **40**, 285–307, doi:10.1146/annurev-environ-102014-021155. https://doi.org/10.1146/annurev-environ-102014-021155.
Phillips, R. P., A. C. Finzi, and E. S. Bernhardt, 2011: Enhanced root exudation induces microbial feedbacks to N cycling in a pine forest under long-term CO2fumigation. *Ecol. Lett.*, **14**, 187–194, doi:10.1111/j.1461-0248.2010.01570.x.
Phoenix, G. K., and J. W. Bjerke, 2016: Arctic browning: extreme events and trends reversing arctic greening. *Glob. Chang. Biol.*, **22**, 2960–2962, doi:10.1111/gcb.13261. http://dx.doi.org/10.1111/gcb.13261.
Photiadou, C., M. R. Jones, D. Keellings, and C. F. Dewes, 2014: Modeling European hot spells using extreme value analysis. *Clim. Res.*, **58**, 193–207, doi:10.3354/cr01191. https://dspace.library.uu.nl/handle/1874/296265#.WwVQSO8zkS8.mendeley (Accessed May 23, 2018).
Pielke, R. A., J. Adegoke, A. Beltrán-Przekurat, C. A. Hiemstra, J. Lin, U. S. Nair, D. Niyogi, and T. E. Nobis, 2007: An overview of regional land use and land-cover impacts on rainfall. *Tellus, Series B: Chemical and Physical Meteorology*, Vol. 59 of, 587–601.
Pielke, R. A., and Coauthors, 2011: Land use/land cover changes and climate: Modeling analysis and observational evidence. *Wiley Interdiscip. Rev. Clim. Chang.*, **2**, 828–850, doi:10.1002/wcc.144. http://doi.wiley.com/10.1002/wcc.144 (Accessed December 18, 2017).
——, R. Mahmood, and C. McAlpine, 2016: Land's complex role in climate change. *Phys. Today*, **69**, 40–46, doi:10.1063/PT.3.3364.
Pilli, R., G. Fiorese, and G. Grassi, 2015: EU mitigation potential of harvested wood products. *Carbon Balance Manag.*, **10**, 6, doi:10.1186/s13021-015-0016-7. https://doi.org/10.1186/s13021-015-0016-7.
Pingali, P. L., 2012: Green Revolution: Impacts, limits, and the path ahead. *Proc. Natl. Acad. Sci.*, **109**, 12302–12308, doi:10.1073/pnas.0912953109.
Pison, I., B. Ringeval, P. Bousquet, C. Prigent, and F. Papa, 2013: Stable atmospheric methane in the 2000s: Key-role of emissions from natural wetlands. *Atmos. Chem. Phys.*, **13**, 11609–11623, doi:10.5194/acp-13-11609-2013.
Pithan, F., and T. Mauritsen, 2014: Arctic amplification dominated by temperature feedbacks in contemporary climate models. *Nat. Geosci.*, **7**, 181–184, doi:10.1038/ngeo2071.
Pitman, A. J., and R. Lorenz, 2016: Scale dependence of the simulated impact of Amazonian deforestation

on regional climate. *Environ. Res. Lett.*, **11**, 1–10, doi:10.1088/1748-9326/11/9/094025. http://dx.doi.org/10.1088/1748-9326/11/9/094025.
——, and Coauthors, 2009: Uncertainties in climate responses to past land cover change: First results from the LUCID intercomparison study. *Geophys. Res. Lett.*, **36**, 1–6, doi:10.1029/2009GL039076.
——, F. B. Avila, G. Abramowitz, Y. P. Wang, S. J. Phipps, and N. De Noblet-Ducoudré, 2011a: Importance of background climate in determining impact of land-cover change on regional climate. *Nat. Clim. Chang.*, **1**, 472–475, doi:10.1038/nclimate1294.
——, ——, ——, ——, ——, and ——, 2011b: Importance of background climate in determining impact of land-cover change on regional climate. *Nat. Clim. Chang.*, **1**, 472–475, doi:10.1038/nclimate1294. http://dx.doi.org/10.1038/nclimate1294.
Pitman, A. J., and Coauthors, 2012: Effects of land cover change on temperature and rainfall extremes in multi-model ensemble simulations. *Earth Syst. Dyn.*, **3**, 213–231, doi:10.5194/esd-3-213-2012. https://www.earth-syst-dynam.net/3/213/2012/.
Poeplau, C., and A. Don, 2013: Sensitivity of soil organic carbon stocks and fractions to different land use changes across Europe. *Geoderma*, **192**, 189–201, doi:10.1016/j.geoderma.2012.08.003.
——, and ——, 2015: Carbon sequestration in agricultural soils via cultivation of cover crops - A meta-analysis. *Agric. Ecosyst. Environ.*, **200**, 33–41, doi:10.1016/j.agee.2014.10.024.
——, ——, L. Vesterdal, J. Leifeld, B. Van Wesemael, J. Schumacher, and A. Gensior, 2011: Temporal dynamics of soil organic carbon after land use change in the temperate zone - carbon response functions as a model approach. *Glob. Chang. Biol.*, **17**, 2415–2427, doi:10.1111/j.1365-2486.2011.02408.x.
Pöhlker, M. L., and Coauthors, 2016: Long-term observations of cloud condensation nuclei in the Amazon rain forest - Part 1: Aerosol size distribution, hygroscopicity, and new model parametrizations for CCN prediction. *Atmos. Chem. Phys.*, **16**, 15709–15740, doi:10.5194/acp-16-15709-2016. https://www.atmos-chem-phys.net/16/15709/2016/.
Pokhrel, Y. N., N. Hanasaki, Y. Wada, and H. Kim, 2016: Recent progresses in incorporating human land-water management into global land surface models toward their integration into Earth system models. *Wiley Interdiscip. Rev. Water*, **3**, 548–574, doi:10.1002/wat2.1150. http://doi.wiley.com/10.1002/wat2.1150.
Polydoros, A., T. Mavrakou, and C. Cartalis, 2018: Quantifying the Trends in Land Surface Temperature and Surface Urban Heat Island Intensity in Mediterranean Cities in View of Smart Urbanization. *Urban Sci.*, **2**.
Pongratz, J., C. H. Reick, T. Raddatz, and M. Claussen, 2010: Biogeophysical versus biogeochemical climate response to historical anthropogenic land cover change. *Geophys. Res. Lett.*, **37**, 1–5, doi:10.1029/2010GL043010.
——, ——, R. A. Houghton, and J. I. House, 2014: Terminology as a key uncertainty in net land use and land cover change carbon flux estimates. *Earth Syst. Dyn.*, **5**, 177–195, doi:10.5194/esd-5-177-2014.
Popp, A., and Coauthors, 2014: Land use transition for bioenergy and climate stabilization: Model comparison of drivers, impacts and interactions with other land use based mitigation options. *Clim. Change*, **123**, 495–509, doi:10.1007/s10584-013-0926-x. http://link.springer.com/10.1007/s10584-013-0926-x (Accessed May 22, 2018).
——, and Coauthors, 2017: Land use futures in the shared socio-economic pathways. *Glob. Environ. Chang.*, **42**, 331–345, doi:10.1016/J.GLOENVCHA.2016.10.002. http://www.sciencedirect.com/science/article/pii/S0959378016303399 (Accessed May 22, 2018).
Port, U., V. Brovkin, and M. Claussen, 2012: The influence of vegetation dynamics on anthropogenic climate change. *Earth Syst. Dyn.*, **3**, 233–243, doi:10.5194/esd-3-233-2012.
Porter, J. R., and M. Gawith, 1999: Temperatures and the growth and development of wheat: A review. *Eur. J. Agron.*, **10**, 23–36, doi:10.1016/S1161-0301(98)00047-1. https://www-sciencedirect-com.ezproxy.uct.ac.za/science/article/pii/S1161030198000471 (Accessed May 24, 2018).
——, L. Xie, A. J. Challinor, K. Cochrane, S. M. Howden, M. M. Iqbal, D. B. Lobell, and M. I. Travasso, 2014: Food Security and Food Production Systems. *Climate Change 2014: Impacts, Adaptation, and Vulnerability. Part A: Global and Sectoral Aspects. Contribution of Working Group II to the Fifth*

Assessment Report of the Intergovernmental Panel of Climate Change, C.B. Field et al., Eds., Cambridge University Press, Cambridge, United Kingdom and New York, NY, USA, 1–82.
Poveda, G., and L. F. Salazar, 2004: Annual and interannual (ENSO) variability of spatial scaling properties of a vegetation index (NDVI) in Amazonia. *Remote Sens. Environ.*, **93**, 391–401, doi:10.1029/2001JD000717.
Powell, T. L., and Coauthors, 2013: Confronting model predictions of carbon fluxes with measurements of Amazon forests subjected to experimental drought. *New Phytol.*, **200**, 350–365, doi:10.1111/nph.12390. https://doi.org/10.1111/nph.12390.
Powlson, D. S., A. P. Whitmore, and K. W. T. Goulding, 2011: Soil carbon sequestration to mitigate climate change: A critical re-examination to identify the true and the false. *Eur. J. Soil Sci.*, **62**, 42–55, doi:10.1111/j.1365-2389.2010.01342.x.
Powlson, D. S., C. M. Stirling, M. L. Jat, B. G. Gerard, C. a. Palm, P. a. Sanchez, and K. G. Cassman, 2014: Limited potential of no-till agriculture for climate change mitigation. *Nat. Clim. Chang.*, **4**, 678–683, doi:10.1038/nclimate2292.
——, ——, C. Thierfelder, R. P. White, and M. L. Jat, 2016: Does conservation agriculture deliver climate change mitigation through soil carbon sequestration in tropical agro-ecosystems? *Agric. Ecosyst. Environ.*, **220**, 164–174, doi:10.1016/j.agee.2016.01.005.
Prather, M. J., and Coauthors, 2017: Global atmospheric chemistry - Which air matters. *Atmos. Chem. Phys.*, **17**, 9081–9102, doi:10.5194/acp-17-9081-2017.
Prein, A. F., R. M. Rasmussen, K. Ikeda, C. Liu, M. P. Clark, and G. J. Holland, 2017: The future intensification of hourly precipitation extremes. *Nat. Clim. Chang.*, **7**, 48–52, doi:10.1038/nclimate3168. http://www.nature.com/articles/nclimate3168 (Accessed May 24, 2018).
Price, H. C., and Coauthors, 2018: Atmospheric Ice-Nucleating Particles in the Dusty Tropical Atlantic. *J. Geophys. Res. Atmos.*, **123**, 2175–2193, doi:10.1002/2017JD027560. https://doi.org/10.1002/2017JD027560.
Prudhomme, C., and Coauthors, 2014: Hydrological droughts in the 21st century, hotspots and uncertainties from a global multimodel ensemble experiment. *Proc. Natl. Acad. Sci.*, **111**, 3262–3267, doi:10.1073/pnas.1222473110. http://www.pnas.org/lookup/doi/10.1073/pnas.1222473110 (Accessed May 24, 2018).
Pugh, T. A. M., and Coauthors, 2015: Simulated carbon emissions from land use change are substantially enhanced by accounting for agricultural management. *Environ. Res. Lett.*, **10**, 124008, doi:10.1088/1748-9326/10/12/124008.
Pugh, T. A. M., C. Müller, J. Elliott, D. Deryng, C. Folberth, S. Olin, E. Schmid, and A. Arneth, 2016: Climate analogues suggest limited potential for intensification of production on current croplands under climate change. *Nat. Commun.*, **7**, 1–8, doi:10.1038/ncomms12608.
Pulliainen, J., and Coauthors, 2017: Early snowmelt significantly enhances boreal springtime carbon uptake. *Proc. Natl. Acad. Sci.*, **114**, 201707889, doi:10.1073/pnas.1707889114. http://www.pnas.org/lookup/doi/10.1073/pnas.1707889114 (Accessed October 20, 2017).
Puma, M. J., S. Bose, S. Y. Chon, and B. I. Cook, 2015: Assessing the evolving fragility of the global food system. *Environ. Res. Lett.*, **10**, 024007, doi:10.1088/1748-9326/10/2/024007.
Qin, D., M. Tignor, S. K. Allen, J. Boschung, A. Nauels, Y. Xia, V. Bex, and U. Kingdom, 2013: Annex III: Glossary. *Change 2013: The Physical Science Basis. Contribution of Working Group I to the Fifth Assessment Report of the Intergovernmental Panel on Climate Change*, T.F. Stocker et al., Eds., Cambridge University Press, Cambridge, United Kingdom and New York, NY, USA, 1447–1466.
Qu, X., and A. Hall, 2014: On the persistent spread in snow-albedo feedback. *Clim. Dyn.*, **42**, 69–81, doi:10.1007/s00382-013-1774-0.
Le Quéré, C., and Coauthors, 2009: Trends in the sources and sinks of carbon dioxide. *Nat. Geosci.*, **2**, 831–836, doi:10.1038/ngeo689. http://www.nature.com/articles/ngeo689 (Accessed May 23, 2018).
——, and Coauthors, 2016a: Global Carbon Budget 2016. *Earth Syst. Sci. Data*, **8**, 605–649, doi:10.5194/essd-8-605-2016.
——, and Coauthors, 2016b: Global Carbon Budget 2016. *Earth Syst. Sci. Data*, **8**, 605–649, doi:10.5194/essd-8-605-2016.

——, and Coauthors, 2017: Global Carbon Budget 2017. *Earth Syst. Sci. Data Discuss.*, 1–79, doi:10.5194/essd-2017-123. https://www.earth-syst-sci-data-discuss.net/essd-2017-123/.

Quesada, B., A. Arneth, and N. De Noblet-Ducoudré, 2017a: Atmospheric, radiative, and hydrologic effects of future land use and land cover changes: A global and multimodel climate picture. *J. Geophys. Res.*, **122**, 5113–5131, doi:10.1002/2016JD025448.

——, N. Devaraju, N. de Noblet-Ducoudrï¿½, and A. Arneth, 2017b: Reduction of monsoon rainfall in response to past and future land use and land cover changes. *Geophys. Res. Lett.*, **44**, 1041–1050, doi:10.1002/2016GL070663.

Rachmayani, R., M. Prange, and M. Schulz, 2015: North African vegetation-precipitation feedback in early and mid-Holocene climate simulations with CCSM3-DGVM. *Clim. Past*, **11**, 175–185, doi:10.5194/cp-11-175-2015.

Rafael, S., H. Martins, M. Marta-Almeida, E. Sï¿½, S. Coelho, A. Rocha, C. Borrego, and M. Lopes, 2017: Quantification and mapping of urban fluxes under climate change: Application of WRF-SUEWS model to Greater Porto area (Portugal). *Environ. Res.*, **155**, 321–334, doi:10.1016/j.envres.2017.02.033.

Ramankutty, N., A. T. Evan, C. Monfreda, and J. A. Foley, 2008: Farming the planet: 1. Geographic distribution of global agricultural lands in the year 2000. *Global Biogeochem. Cycles*, **22**, doi:10.1029/2007GB002952.

Rasul, A., H. Balzter, and C. Smith, 2015: Spatial variation of the daytime Surface Urban Cool Island during the dry season in Erbil, Iraqi Kurdistan, from Landsat 8. *Urban Clim.*, **14**, 176–186, doi:https://doi.org/10.1016/j.uclim.2015.09.001. http://www.sciencedirect.com/science/article/pii/S2212095515300237.

Recha, J. W., J. Lehmann, M. T. Walter, A. Pell, L. Verchot, and M. Johnson, 2013: Stream water nutrient and organic carbon exports from tropical headwater catchments at a soil degradation gradient. *Nutr. Cycl. Agroecosystems*, **95**, 145–158, doi:10.1007/s10705-013-9554-0.

Reddington, C. L., D. V. Spracklen, P. Artaxo, D. A. Ridley, L. V. Rizzo, and A. Arana, 2016: Analysis of particulate emissions from tropical biomass burning using a global aerosol model and long-term surface observations. *Atmos. Chem. Phys.*, **16**, 11083–11106, doi:10.5194/acp-16-11083-2016. https://www.atmos-chem-phys.net/16/11083/2016/.

Reed, S. C., X. Yang, and P. E. Thornton, 2015: Incorporating phosphorus cycling into global modeling efforts: A worthwhile, tractable endeavor. *New Phytol.*, **208**, 324–329, doi:10.1111/nph.13521.

Reich, P. B., and S. E. Hobbie, 2013: Decade-long soil nitrogen constraint on the CO2 fertilization of plant biomass. *Nat. Clim. Chang.*, **3**, 278–282, doi:10.1038/nclimate1694. http://dx.doi.org/10.1038/nclimate1694.

——, ——, and T. D. Lee, 2014: Plant growth enhancement by elevated CO<inf>2</inf> eliminated by joint water and nitrogen limitation. *Nat. Geosci.*, **7**, 920–924, doi:10.1038/ngeo2284.

——, ——, ——, and M. A. Pastore, 2018: Unexpected reversal of C3 versus C4 grass response to elevated CO2 during a 20-year field experiment. *Science (80-.).*, **360**, 317–320, doi:10.1126/SCIENCE.AAS9313. http://science.sciencemag.org/content/360/6386/317.

Remer, L. A., and Coauthors, 2005: The MODIS Aerosol Algorithm, Products, and Validation. *J. Atmos. Sci.*, **62**, 947–973, doi:10.1175/JAS3385.1. http://journals.ametsoc.org/doi/abs/10.1175/JAS3385.1.

Renaud, V., and M. Rebetez, 2008: Comparison between open site and below canopy climatic conditions in {Switzerland} during the exceptionally hot summer of 2003. *Agric. For. Meteorol.*, **149**, 873–880, doi:https://doi.org/10.1016/j.agrformet.2008.11.006. http://www.sciencedirect.com/science/article/pii/S0168192308003171.

Renaud, V., J. L. Innes, M. Dobbertin, and M. Rebetez, 2011: Comparison between open-site and below-canopy climatic conditions in Switzerland for different types of forests over 10 years (1998-2007). *Theor. Appl. Climatol.*, **105**, 119–127, doi:10.1007/s00704-010-0361-0. https://doi.org/10.1007/s00704-010-0361-0.

Review, T. S., 2011: Climate change mitigation. *Soil carbon: science, management and policy for multiple benefits*, S.A. Banwart, E. Moellemeyer, and E. Milne, Eds., CAB International, 119–131.

Rice, A. L., C. L. Butenhoff, D. G. Teama, F. H. Röger, M. A. K. Khalil, and R. A. Rasmussen, 2016: Atmospheric methane isotopic record favors fossil sources flat in 1980s and 1990s with recent increase.

Proc. Natl. Acad. Sci., **113**, 10791–10796, doi:10.1073/pnas.1522923113. http://www.pnas.org/lookup/doi/10.1073/pnas.1522923113.

Richardson, A. ., T. . Keenana, M. Migliavaccab, Y. Ryua, O. Sonnentaga, and M. Toomeya, 2013: Climate change, phenology, and phenological controlof vegetatif feedbacks to the climate system. *Agric. For, Meteorol*, **169**, 156–157, doi:https://doi.org/10.1016/j.agrformet.2012.09.012. http://www.sciencedirect.com/science/article/pii/S0168192312002869.

Ridge, O., 2017: Comment on " Mycorrhizal association as a primary control of the CO 2 fertilization effect ." *Science (80-.).*, **355**, 27–29. http://science.sciencemag.org/content/355/6323/358.2.abstract.

Rigby, M., and Coauthors, 2017: Role of atmospheric oxidation in recent methane growth. *Proc. Natl. Acad. Sci.*, **114**, 5373–5377, doi:10.1073/pnas.1616426114. http://www.pnas.org/lookup/doi/10.1073/pnas.1616426114.

Robaa, S. M., 2013: Some aspects of the urban climates of Greater Cairo Region, Egypt. *Int. J. Climatol.*, **33**, 3206–3216, doi:10.1002/joc.3661.

Robinson, A. L., and Coauthors, 2007: Rethinking organic aerosols: Semivolatile emissions and photochemical aging. *Science (80-.).*, **315**, 1259–1262, doi:10.1126/science.1133061. http://science.sciencemag.org/content/315/5816/1259.abstract.

Rocha-Lima, A., and Coauthors, 2018: A detailed characterization of the Saharan dust collected during the Fennec campaign in 2011: In situ ground-based and laboratory measurements. *Atmos. Chem. Phys.*, **18**, 1023–1043, doi:10.5194/acp-18-1023-2018. https://www.atmos-chem-phys.net/18/1023/2018/.

Rockström, J., Gaffney, O., Rogelj, J., Meinshausen, M., Nakicenovic, N., & Schellnhuber, H. J., 2017: A Roadmap for Rapid Decarbonization. *Science (80-.).*, **355**, 1269–1271, doi:10.1126/science.aah3443. http://science.sciencemag.org/content/355/6331/1269.abstract.

Rodell, M., I. Velicogna, and J. S. Famiglietti, 2009: Satellite-based estimates of groundwater depletion in India. *Nature*, **460**, 999–1002, doi:10.1038/nature08238.

Roe, S., and Coauthors, 2018: Contribution of the land sector to a 1.5°C World. *Nat. Clim. Chang.*,.

Roebroeks, W., and P. Villa, 2011: On the earliest evidence for habitual use of fire in Europe. *Proc. Natl. Acad. Sci.*, **108**, 5209 LP-5214. http://www.pnas.org/content/108/13/5209.abstract.

Rogelj, J., and Coauthors, 2014: Disentangling the effects of CO_2 and short-lived climate forcer mitigation. *Proc. Natl. Acad. Sci.*, **111**, 16325–16330, doi:10.1073/pnas.1415631111. http://www.pnas.org/lookup/doi/10.1073/pnas.1415631111.

Rogelj, J., and Coauthors, 2016: Paris agreement climate proposal need a boost to keep warming weel below 2 C. *Nature*, **534(7609)**, 631–639, doi:10.1038/nature18307. http://dx.doi.org/10.1038/nature18307.

Rogelj, J., and Coauthors, 2018a: Scenarios towards limiting global mean temperature increase below 1.5 °c. *Nat. Clim. Chang.*, **8**, 325–332, doi:10.1038/s41558-018-0091-3. https://doi.org/10.1038/s41558-018-0091-3.

——, and Coauthors, 2018b: Scenarios towards limiting global mean temperature increase below 1.5 °c. *Nat. Clim. Chang.*, **8**, 325–332, doi:10.1038/s41558-018-0091-3. http://www.nature.com/articles/s41558-018-0091-3 (Accessed May 22, 2018).

Roman-Cuesta, R. M., and Coauthors, 2016: Multi-gas and multi-source comparisons of six land use emission datasets and AFOLU estimates in the Fifth Assessment Report, for the tropics for 2000-2005. *Biogeosciences*, **13**, 5799–5819, doi:10.5194/bg-13-5799-2016.

Rosenzweig, C., and F. N. Tubiello, 2007: Adaptation and mitigation strategies in agriculture: An analysis of potential synergies. *Mitig. Adapt. Strateg. Glob. Chang.*, **12**, 855–873, doi:10.1007/s11027-007-9103-8. https://doi.org/10.1007/s11027-007-9103-8.

Rosenzweig, C., and Coauthors, 2013: The Agricultural Model Intercomparison and Improvement Project (AgMIP): Protocols and pilot studies. *Agric. For. Meteorol.*, **170**, 166–182, doi:10.1016/j.agrformet.2012.09.011.

Roy, J., and Coauthors, 2016: Elevated CO_2 maintains grassland net carbon uptake under a future heat and drought extreme. *Proc. Natl. Acad. Sci.*, **113**, 6224–6229, doi:10.1073/pnas.1524527113. http://www.pnas.org/lookup/doi/10.1073/pnas.1524527113.

Roy, P., and G. Dias, 2017: Prospects for pyrolysis technologies in the bioenergy sector: A review. *Renew. Sustain. Energy Rev.*, **77**, 59–69, doi:10.1016/j.rser.2017.03.136.

http://www.sciencedirect.com/science/article/pii/S1364032117304719.
Rumpel, C., and I. Kögel-Knabner, 2011: Deep soil organic matter—a key but poorly understood component of terrestrial C cycle. *Plant Soil*, **338**, 143–158, doi:10.1007/s11104-010-0391-5. https://doi.org/10.1007/s11104-010-0391-5.
Russo, S., A. F. Marchese, J. Sillmann, and G. Immï¿½, 2016: When will unusual heat waves become normal in a warming Africa? *Environ. Res. Lett.*, **11**, 054016, doi:10.1088/1748-9326/11/5/054016.
Saatchi, S. S., and Coauthors, 2011: Benchmark map of forest carbon stocks in tropical regions across three continents. *Proc. Natl. Acad. Sci.*, **108**, 9899–9904, doi:10.1073/pnas.1019576108. http://www.pnas.org/content/108/24/9899.
Sachindra, D. A., A. W. M. Ng, S. Muthukumaran, and B. J. C. Perera, 2016: Impact of climate change on urban heat island effect and extreme temperatures: a case-study. *Q. J. R. Meteorol. Soc.*, **142**, 172–186, doi:10.1002/qj.2642. http://doi.wiley.com/10.1002/qj.2642.
Saeki, T., and P. K. Patra, 2017: Implications of overestimated anthropogenic CO2 emissions on East Asian and global land CO2 flux inversion. *Geosci. Lett.*, **4**, 9, doi:10.1186/s40562-017-0074-7. http://geoscienceletters.springeropen.com/articles/10.1186/s40562-017-0074-7.
Safriel, U. N., 2007: The assessment of global trends in land degradation. *Clim. L. Degrad.*, 1–38, doi:10.1007/978-3-540-72438-4_1.
Sagayama, H., K. Taniguchi, N. Abe, T. H. Arima, M. Soda, M. Matsuura, and K. Hirota, 2008: Correlation between ferroelectric polarization and sense of helical spin order in multiferroic MnWO4. *Physical Review B - Condensed Matter and Materials Physics*, S. Solomon, D. Qin, M. Manning, Z. Chen, M. Marquis, K.B. Averyt, M. Tignor, and H.L. Miller, Eds., Vol. 77 of, Cambridge University Pres, Cambridge, United Kingdom and New York, NY, USA, 129–234 http://en.scientificcommons.org/23467316.
Saikawa, E., and Coauthors, 2014: Global and regional emissions estimates for N2O. *Atmos. Chem. Phys.*, **14**, 4617–4641, doi:10.5194/acp-14-4617-2014.
Sánchez-Rodríguez, A. R., P. W. Hill, D. R. Chadwick, and D. L. Jones, 2017: Crop residues exacerbate the negative effects of extreme flooding on soil quality. *Biol. Fertil. Soils*, **53**, 751–765, doi:10.1007/s00374-017-1214-0. http://link.springer.com/10.1007/s00374-017-1214-0 (Accessed May 25, 2018).
Sanderman, J., T. Hengl, and G. J. Fiske, 2017: Soil carbon debt of 12,000 years of human land use. *Proc. Natl. Acad. Sci.*, **114**, 9575–9580, doi:10.1073/pnas.1706103114. http://www.pnas.org/lookup/doi/10.1073/pnas.1706103114.
Santamouris, M., C. Cartalis, A. Synnefa, and D. Kolokotsa, 2015: On the impact of urban heat island and global warming on the power demand and electricity consumption of buildings—A review. *Energy Build.*, **98**, 119–124, doi:https://doi.org/10.1016/j.enbuild.2014.09.052. http://www.sciencedirect.com/science/article/pii/S0378778814007907.
Santos, F., M. S. Torn, and J. A. Bird, 2012: Biological degradation of pyrogenic organic matter in temperate forest soils. *Soil Biol. Biochem.*, **51**, 115–124, doi:https://doi.org/10.1016/j.soilbio.2012.04.005. http://www.sciencedirect.com/science/article/pii/S0038071712001411.
Sardans, J., and J. Peñuelas, 2015: Potassium: A neglected nutrient in global change. *Glob. Ecol. Biogeogr.*, **24**, 261–275, doi:10.1111/geb.12259.
Sardans, J., A. Rivas-Ubach, and J. Peñuelas, 2012: The C:N:P stoichiometry of organisms and ecosystems in a changing world: A review and perspectives. *Perspect. Plant Ecol. Evol. Syst.*, **14**, 33–47, doi:10.1016/j.ppees.2011.08.002.
Sasaki, N., and Coauthors, 2016: Sustainable Management of Tropical Forests Can Reduce Carbon Emissions and Stabilize Timber Production. *Front. Environ. Sci.*, **4**, 50, doi:10.3389/fenvs.2016.00050. http://journal.frontiersin.org/Article/10.3389/fenvs.2016.00050/abstract.
Sathre, R., and J. O'Connor, 2010: Meta-analysis of greenhouse gas displacement factors of wood product substitution. *Environ. Sci. Policy*, **13**, 104–114, doi:10.1016/j.envsci.2009.12.005. http://www.sciencedirect.com/science/article/pii/S1462901109001804.
Satria, 2017: Environmental Research Letters Substantial N 2 O emissions from peat decomposition and N fertilization in an oil palm plantation exacerbated by hotspots. *Environ. Res. Lett*, **12**,

doi:https://doi.org/10.1088/1748-9326/aa80f1.
Saunois, M., and Coauthors, 2016: The global methane budget 2000-2012. *Earth Syst. Sci. Data*, **8**, 697–751, doi:10.5194/essd-8-697-2016.
Savo, V., D. Lepofsky, J. P. Benner, K. E. Kohfeld, J. Bailey, and K. Lertzman, 2016: Observations of climate change among subsistence-oriented communities around the world. *Nat. Clim. Chang.*, **6**, 462–473, doi:10.1038/nclimate2958. http://www.nature.com/articles/nclimate2958 (Accessed May 7, 2018).
Sayer, E. J., M. S. Heard, H. K. Grant, T. R. Marthews, and E. V. J. Tanner, 2011: Soil carbon release enhanced by increased tropical forest litterfall. *Nat. Clim. Chang.*, **1**, 304. http://dx.doi.org/10.1038/nclimate1190.
Schaefer, H., and Coauthors, 2016: A 21st-century shift from fossil-fuel to biogenic methane emissions indicated by13CH4. *Science (80-.).*, **352**, 80–84, doi:10.1126/science.aad2705.
Schauberger, B., and Coauthors, 2017: Consistent negative response of US crops to high temperatures in observations and crop models. *Nat. Commun.*, **8**, 13931, doi:10.1038/ncomms13931. http://www.nature.com/doifinder/10.1038/ncomms13931 (Accessed May 21, 2018).
Schimel, D., B. B. Stephens, and J. B. Fisher, 2015: Effect of increasing CO_2 on the terrestrial carbon cycle. *Proc. Natl. Acad. Sci.*, **112**, 436–441, doi:10.1073/pnas.1407302112. http://www.pnas.org/lookup/doi/10.1073/pnas.1407302112.
Schindlbacher, A., J. Schnecker, M. Takriti, W. Borken, and W. Wanek, 2015: Microbial physiology and soil CO2efflux after 9 years of soil warming in a temperate forest - no indications for thermal adaptations. *Glob. Chang. Biol.*, **21**, 4265–4277, doi:10.1111/gcb.12996.
Schlaepfer, D. R., and Coauthors, 2017: Climate change reduces extent of temperate drylands and intensifies drought in deep soils. *Nat. Commun.*, **8**, 14196, doi:10.1038/ncomms14196. http://dx.doi.org/10.1038/ncomms14196.
Schlamadinger, B., and Coauthors, 2007: Options for including land use in a climate agreement post-2012: improving the Kyoto Protocol approach. *Environ. Sci. Policy*, **10**, 295–305, doi:10.1016/j.envsci.2006.12.004.
Schlenker, W., and M. J. Roberts, 2009: Nonlinear temperature effects indicate severe damages to U.S. crop yields under climate change. *Proc. Natl. Acad. Sci.*, **106**, 15594–15598, doi:10.1073/pnas.0906865106. http://www.pnas.org/cgi/doi/10.1073/pnas.0906865106 (Accessed May 24, 2018).
Schlenker, W., and D. B. Lobell, 2010: Robust negative impacts of climate change on African agriculture. *Environ. Res. Lett.*, **5**, 014010, doi:10.1088/1748-9326/5/1/014010.
Schlesinger, W. H., M. C. Dietze, R. B. Jackson, R. P. Phillips, C. C. Rhoades, L. E. Rustad, and J. M. Vose, 2016: Forest biogeochemistry in response to drought. *Glob. Chang. Biol.*, **22**, 2318–2328, doi:10.1111/gcb.13105. http://doi.wiley.com/10.1111/gcb.13105 (Accessed May 7, 2018).
Schleussner, C. F., and Coauthors, 2016: Science and policy characteristics of the Paris Agreement temperature goal. *Nat. Clim. Chang.*, **6**, 827–835, doi:10.1038/nclimate3096. http://dx.doi.org/10.1038/nclimate3096.
Schlünzen, K. H., P. Hoffmann, G. Rosenhagen, and W. Riecke, 2010: Long-term changes and regional differences in temperature and precipitation in the metropolitan area of Hamburg. *Int. J. Climatol.*, **30**, 1121–1136, doi:10.1002/joc.1968.
Schmid, P. E., and D. Niyogi, 2014: Modeling urban precipitation modification by spatially heterogeneous aerosols. *J. Appl. Meteorol. Climatol.*, **56**, 2141–2153, doi:10.1175/JAMC-D-16-0320.1.
Schmidt, M., 2011: Persistance of soil organic matter as an ecosystem property. *Nature*, **478**, 49. http://www.nature.com/nature/journal/v478/n7367/pdf/nature10386.pdf.
Schmidt, M. W. I., and A. G. Noack, 2000: Black carbon in soils and sediments: Analysis, distribution, implications, and current challenges. *Global Biogeochem. Cycles*, **14**, 777–793, doi:10.1029/1999GB001208. https://doi.org/10.1029/1999GB001208.
Schneck, R., C. H. Reick, J. Pongratz, and V. Gayler, 2015: The mutual importance of anthropogenically and climate-induced changes in global vegetation cover for future land carbon emissions in the MPI-ESM CMIP5 simulations. *Global Biogeochem. Cycles*, **29**, 1816–1829, doi:10.1002/2014GB004959. https://doi.org/10.1002/2014GB004959.
Schulte-Uebbing, L., and W. de Vries, 2018: Global-scale impacts of nitrogen deposition on tree carbon

sequestration in tropical, temperate, and boreal forests: A meta-analysis. *Glob. Chang. Biol.*, **24**, e416–e431, doi:10.1111/gcb.13862.

Schuur, E. A. G., and Coauthors, 2015: Climate change and the permafrost carbon feedback. *Nature*, **520**, 171–179, doi:10.1038/nature14338. http://dx.doi.org/10.1038/nature14338.

Schwartz, M. D., T. R. Karl, M. D. Schwartz, and T. R. Karl, 1990: Spring Phenology: Nature's Experiment to Detect the Effect of "Green-Up" on Surface Maximum Temperatures. *Mon. Weather Rev.*, **118**, 883–890, doi:10.1175/1520-0493(1990)118<0883:SPNETD>2.0.CO;2. http://journals.ametsoc.org/doi/abs/10.1175/1520-0493%281990%29118%3C0883%3ASPNETD%3E2.0.CO%3B2.

Schwietzke, S., and Coauthors, 2016: Upward revision of global fossil fuel methane emissions based on isotope database. *Nature*, **538**, 88–91, doi:10.1038/nature19797. http://dx.doi.org/10.1038/nature19797.

Scott, A. ., 2000: The Pre-Quaternary history of fire. *Palaeogeogr. Palaeoclimatol. Palaeoecol.*, **164**, 281–329, doi:10.1016/S0031-0182(00)00192-9. https://www.sciencedirect.com/science/article/pii/S0031018200001929 (Accessed May 7, 2018).

Seddon, A. W. R., M. Macias-Fauria, P. R. Long, D. Benz, and K. J. Willis, 2016: Sensitivity of global terrestrial ecosystems to climate variability. *Nature*, **531**, 229–232, doi:10.1038/nature16986. http://www.nature.com/doifinder/10.1038/nature16986.

Seino, N., T. Aoyagi, and H. Tsuguti, 2018: Numerical simulation of urban impact on precipitation in Tokyo: How does urban temperature rise affect precipitation? *Urban Clim.*, **23**, 8–35, doi:10.1016/j.uclim.2016.11.007. https://doi.org/10.1016/j.uclim.2016.11.007.

Sellers, P. J., and Coauthors, 1996: Comparison of Radiative and Physiological Effects of Doubled Atmospheric CO2 on Climate. *Science (80-.).*, **271**, 1402–1406, doi:10.1126/science.271.5254.1402. http://www.sciencemag.org/cgi/doi/10.1126/science.271.5254.1402.

Seneviratne, S. I., and Coauthors, 2012a: Changes in climate extremes and their impacts on the natural physical environment. *Managing the Risks of Extreme Events and Disasters to Advance Climate Change Adaptation. A Special Report of Working Groups I and II of the Intergovernmental Panel on Climate Change (IPCC).*, C.B. Field et al., Eds., Cambridge University Press, Cambridge, United Kingdom and New York, NY, USA, 109–230 http://ipcc-wg2.gov/SREX/images/uploads/SREX-Chap3_FINAL.pdf.

Seneviratne, S. I., and Coauthors, 2012b: Changes in climate extremes and their impacts on the natural physical environment. *Managing the Risks of Extreme Events and Disasters to Advance Climate Change Adaptation. A Special Report of Working Groups I and II of the Intergovernmental Panel on Climate Change (IPCC).*, C.B. Field et al., Eds., Cambridge University Press, Cambridge, United Kingdom and New York, NY, USA, 109–230 http://ipcc-wg2.gov/SREX/images/uploads/SREX-Chap3_FINAL.pdf.

Seneviratne, S. I., and Coauthors, 2013: Impact of soil moisture-climate feedbacks on CMIP5 projections: First results from the GLACE-CMIP5 experiment. *Geophys. Res. Lett.*, **40**, 5212–5217, doi:10.1002/grl.50956.

——, M. G. Donat, A. J. Pitman, R. Knutti, and R. L. Wilby, 2016: Allowable CO2emissions based on regional and impact-related climate targets. *Nature*, **529**, 477–483, doi:10.1038/nature16542.

——, and Coauthors, 2018: Land radiative management as contributor to regional-scale climate adaptation and mitigation. *Nat. Geosci.*, **11**, 88–96, doi:10.1038/s41561-017-0057-5.

Serrano-Cinca, C., Y. Fuertes-Callén, and C. Mar-Molinero, 2005a: *Measuring DEA efficiency in Internet companies*. 557-573 pp. http://unfccc.int/resource/docs/2015/cop21/eng/l09r01.pdf.

——, ——, and ——, 2005b: Measuring DEA efficiency in Internet companies. *Decis. Support Syst.*, **38**, 557–573, doi:10.1016/j.dss.2003.08.004. https://www.sciencedirect.com/science/article/pii/S0959378016300681 (Accessed May 22, 2018).

Serrano-Silva, N., Y. Sarria-Guzmán, L. Dendooven, and M. Luna-Guido, 2014: Methanogenesis and Methanotrophy in Soil: A Review. *Pedosphere*, **24**, 291–307, doi:10.1016/S1002-0160(14)60016-3.

Settele, J., and Coauthors, 2015: Terrestrial and Inland water systems. *Climate Change 2014 Impacts, Adaptation and Vulnerability: Part A: Global and Sectoral Aspects*, C.B. Field et al., Eds., Cambridge University Press, Cambridge, United Kingdom and New York, NY, USA, 271–360

http://ebooks.cambridge.org/ref/id/CBO9781107415379A025.
Shabbar, A., W. Skinner, and M. D. Flannigan, 2011: Prediction of seasonal forest fire severity in Canada from large-scale climate patterns. *J. Appl. Meteorol. Climatol.*, **50**, 785–799, doi:10.1175/2010JAMC2547.1. http://journals.ametsoc.org/doi/abs/10.1175/2010JAMC2547.1 (Accessed May 5, 2018).
Shao, P., X. Zeng, D. J. P. Moore, and X. Zeng, 2013: Soil microbial respiration from observations and Earth System Models. *Environ. Res. Lett.*, **8**, doi:10.1088/1748-9326/8/3/034034.
Shastri, H., Paul, S., Ghosh, S., Paul, S., Ghosh, S., Karmakar, S., 2015: Impacts of urbanization on Indian summer monsoon rainfall extremes. *J. Geophys. Res. Atmos.*, **120**, 495–516, doi:10.1002/2014JD022061.Received.
Shcherbak, I., N. Millar, and G. P. Robertson, 2014: Global metaanalysis of the nonlinear response of soil nitrous oxide (N2O) emissions to fertilizer nitrogen. *Proc. Natl. Acad. Sci.*, **111**, 9199–9204, doi:10.1073/pnas.1322434111. http://www.pnas.org/cgi/doi/10.1073/pnas.1322434111.
Sheffield, J., E. F. Wood, and M. L. Roderick, 2012: Little change in global drought over the past 60 years. *Nature*, **491**, 435–438, doi:10.1038/nature11575. http://www.nature.com/articles/nature11575 (Accessed May 7, 2018).
Shen, M., and Coauthors, 2015a: Evaporative cooling over the Tibetan Plateau induced by vegetation growth. *Proc. Natl. Acad. Sci.*, **112**, 9299–9304, doi:10.1073/pnas.1504418112. http://www.pnas.org/lookup/doi/10.1073/pnas.1504418112 (Accessed February 4, 2018).
——, and Coauthors, 2015b: Evaporative cooling over the Tibetan Plateau induced by vegetation growth. *Proc. Natl. Acad. Sci. U. S. A.*, **112**, 9299–9304, doi:10.1073/pnas.1504418112. http://www.ncbi.nlm.nih.gov/pubmed/26170316 (Accessed February 4, 2018).
Shimadera, H., A. Kondo, K. L. Shrestha, K. Kitaoka, and Y. Inoue, 2015: Numerical Evaluation of the Impact of Urbanization on Summertime Precipitation in Osaka, Japan. *Adv. Meteorol.*, **2015**, 1–11, doi:10.1155/2015/379361. http://www.hindawi.com/journals/amete/aa/379361/.
Siebert, S., F. Ewert, E. Eyshi Rezaei, H. Kage, and R. Graß, 2014: Impact of heat stress on crop yield **-** On the importance of considering canopy temperature. *Environ. Res. Lett.*, **9**, 044012, doi:10.1088/1748-9326/9/4/044012. http://stacks.iop.org/1748-9326/9/i=4/a=044012?key=crossref.f519a45727609a14b26d2e2525f05877 (Accessed May 21, 2018).
——, H. Webber, G. Zhao, and F. Ewert, 2017: Heat stress is overestimated in climate impact studies for irrigated agriculture. *Environ. Res. Lett.*, **12**, 054023, doi:10.1088/1748-9326/aa702f. http://stacks.iop.org/1748-9326/12/i=5/a=054023?key=crossref.a46b95ee7233b45a96fada3a99ce956a (Accessed May 21, 2018).
Silva, L. C. R., and M. Anand, 2013: Probing for the influence of atmospheric CO2and climate change on forest ecosystems across biomes. *Glob. Ecol. Biogeogr.*, **22**, 83–92, doi:10.1111/j.1466-8238.2012.00783.x.
Sims, R., and Coauthors, 2014: Transport. *Climate Change 2014: Mitigation of Climate Change. Contribution of Working Group III to the Fifth Assessment Report of the Intergovernmental Panel on Climate Change*, O. Edenhofer et al., Eds., Cambridge University Press, Cambridge, United Kingdom and New York, NY, USA.
Singh, B. K., R. D. Bardgett, P. Smith, and D. S. Reay, 2010: Microorganisms and climate change: Terrestrial feedbacks and mitigation options. *Nat. Rev. Microbiol.*, **8**, 779–790, doi:10.1038/nrmicro2439. http://dx.doi.org/10.1038/nrmicro2439.
Singh, D., M. G. Flanner, and J. Perket, 2015: The global land shortwave cryosphere radiative effect during the MODIS era. *Cryosphere*, **9**, 2057–2070, doi:10.5194/tc-9-2057-2015.
Sinha, E., A. Michalak, and V. Balaji, 2017: Eutrophication will increase during the 21st century as a reult of precipitation changes. *Science (80-.).*, **357**, 405–408.
Sippel, S., and F. E. L. Otto, 2014: Beyond climatological extremes - assessing how the odds of hydrometeorological extreme events in South-East Europe change in a warming climate. *Clim. Change*, **125**, 381–398, doi:10.1007/s10584-014-1153-9. http://link.springer.com/10.1007/s10584-014-1153-9 (Accessed May 25, 2018).
Sirin, A.A., Suvorov, G.G., Chistotin, M.V., Glagolev, M. V., 2012: About Meaning of Methane Emission

From Drainage Channels. *Doosigik*, **2**, 1–10.
Sitch, S., V. Brovkin, W. von Bloh, D. van Vuuren, B. Eickhout, and A. Ganopolski, 2005: Impacts of future land cover changes on atmospheric CO2 and climate. *Global Biogeochem. Cycles*, **19**, 1–15, doi:10.1029/2004GB002311.
Sitch, S., and Coauthors, 2015: Recent trends and drivers of regional sources and sinks of carbon dioxide. *Biogeosciences*, **12**, 653–679, doi:10.5194/bg-12-653-2015. https://www.biogeosciences.net/12/653/2015/.
Six, J., R. T. Conant, E. A. Paul, and K. Paustian, 2002: Stabilization mechanisms of soil organic matter: Implications for C-saturation of soils. *Plant Soil*, **241**, 155–176, doi:10.1023/A:1016125726789.
Six, J., H. Bossuyt, S. Degryze, and K. Denef, 2004: A history of research on the link between (micro)aggregates, soil biota, and soil organic matter dynamics. *Soil Tillage Res.*, **79**, 7–31, doi:https://doi.org/10.1016/j.still.2004.03.008. http://www.sciencedirect.com/science/article/pii/S0167198704000881.
Slade, R., A. Bauen, and R. Gross, 2014: Global bioenergy resources. *Nat. Clim. Chang.*, **4**, 99–105, doi:10.1038/nclimate2097. http://dx.doi.org/10.1038/nclimate2097.
van der Sleen, P., and Coauthors, 2014: No growth stimulation of tropical trees by 150 years of CO2 fertilization but water-use efficiency increased. *Nat. Geosci.*, **8**, 24–28, doi:10.1038/ngeo2313. http://www.nature.com/doifinder/10.1038/ngeo2313.
Slot, M., and K. Kitajima, 2015: General patterns of acclimation of leaf respiration to elevated temperatures across biomes and plant types. *Oecologia*, **177**, 885–900, doi:10.1007/s00442-014-3159-4.
——, and K. Winter, 2017: Photosynthetic acclimation to warming in tropical forest tree Seedlings. *J. Exp. Bot.*, **68**, 2275–2284, doi:10.1093/jxb/erx071.
——, C. Rey-Sánchez, S. Gerber, J. W. Lichstein, K. Winter, and K. Kitajima, 2014: Thermal acclimation of leaf respiration of tropical trees and lianas: Response to experimental canopy warming, and consequences for tropical forest carbon balance. *Glob. Chang. Biol.*, **20**, 2915–2926, doi:10.1111/gcb.12563.
Smith, N. G., and J. S. Dukes, 2013: Plant respiration and photosynthesis in global-scale models: Incorporating acclimation to temperature and CO2. *Glob. Chang. Biol.*, **19**, 45–63, doi:10.1111/j.1365-2486.2012.02797.x.
——, S. L. Malyshev, E. Shevliakova, J. Kattge, and J. S. Dukes, 2016a: Foliar temperature acclimation reduces simulated carbon sensitivity to climate. *Nat. Clim. Chang.*, **6**, 407–411, doi:10.1038/nclimate2878.
——, D. Lombardozzi, A. Tawfik, G. Bonan, and J. S. Dukes, 2017: Biophysical consequences of photosynthetic temperature acclimation for climate. *J. Adv. Model. Earth Syst.*, **9**, 536–547, doi:10.1002/2016MS000732. http://doi.wiley.com/10.1002/2016MS000732 (Accessed December 17, 2017).
Smith, P., and Coauthors, 2008a: Greenhouse gas mitigation in agriculture. *Philos. Trans. R. Soc. London. Biol. Sci.*, **363**, 789–813, doi:10.1098/rstb.2007.2184.
Smith, P., and Coauthors, 2008b: Greenhouse gas mitigation in agriculture. *Philos. Trans. R. Soc. B Biol. Sci.*, **363**, 789–813, doi:10.1098/rstb.2007.2184. http://rstb.royalsocietypublishing.org/cgi/doi/10.1098/rstb.2007.2184.
Smith, P., and Coauthors, 2013a: How much land-based greenhouse gas mitigation can be achieved without compromising food security and environmental goals? *Glob. Chang. Biol.*, **19**, 2285–2302, doi:10.1111/gcb.12160. https://doi.org/10.1111/gcb.12160.
——, and Coauthors, 2016b: Biophysical and economic limits to negative CO2emissions. *Nat. Clim. Chang.*, **6**, 42–50, doi:10.1038/nclimate2870. http://dx.doi.org/10.1038/nclimate2870.
——, and Coauthors, 2016c: Global change pressures on soils from land use and management. *Glob. Chang. Biol.*, **22**, 1008–1028, doi:10.1111/gcb.13068. https://doi.org/10.1111/gcb.13068 (Accessed May 25, 2018).
Smith, T. T., B. F. Zaitchik, and J. M. Gohlke, 2013b: Heat waves in the United States: Definitions, patterns and trends. *Clim. Change*, **118**, 811–825, doi:10.1007/s10584-012-0659-2. http://link.springer.com/10.1007/s10584-012-0659-2 (Accessed May 16, 2018).

Smyth, C., G. Rampley, T. C. Lemprière, O. Schwab, and W. A. Kurz, 2017: Estimating product and energy substitution benefits in national-scale mitigation analyses for Canada. *GCB Bioenergy*, **9**, 1071–1084, doi:10.1111/gcbb.12389. https://doi.org/10.1111/gcbb.12389.

Snyder, P. K., and S. Liess, 2014: The simulated atmospheric response to expansion of the Arctic boreal forest biome. *Clim. Dyn.*, **42**, 487–503, doi:10.1007/s00382-013-1746-4.

Solmon, F., V. S. Nair, and M. Mallet, 2015: Increasing Arabian dust activity and the Indian summer monsoon. *Atmos. Chem. Phys.*, **15**, 8051–8064, doi:10.5194/acp-15-8051-2015.

Song, Y., H. Liu, X. Wang, N. Zhang, and J. Sun, 2016: Numerical Simulation of the Impact of Urban Non-uniformity on Precipitation. **33**, 783–793.

Sonntag, S., J. Pongratz, C. H. Reick, and H. Schmidt, 2016: Reforestation in a high-CO2world—Higher mitigation potential than expected, lower adaptation potential than hoped for. *Geophys. Res. Lett.*, **43**, 6546–6553, doi:10.1002/2016GL068824.

Sonntag, S., and Coauthors, 2018: Quantifying and Comparing Effects of Climate Engineering Methods on the Earth System. *Earth's Futur.*, doi:10.1002/eft2.285.

Soussana, J. F., T. Tallec, and V. Blanfort, 2010: Mitigating the greenhouse gas balance of ruminant production systems through carbon sequestration in grasslands. *Animal*, **4**, 334–350, doi:10.1017/S1751731109990784.

Spencer, T., and Coauthors, 2016: Global coastal wetland change under sea-level rise and related stresses: The DIVA Wetland Change Model. *Glob. Planet. Change*, **139**, 15–30, doi:10.1016/j.gloplacha.2015.12.018. http://www.sciencedirect.com/science/article/pii/S0921818115301879.

Sperry, J. S., and D. M. Love, 2015: What plant hydraulics can tell us about responses to climate-change droughts. *New Phytol.*, **207**, 14–27, doi:10.1111/nph.13354.

——, M. D. Venturas, W. R. L. Anderegg, M. Mencuccini, D. S. Mackay, Y. Wang, and D. M. Love, 2017: Predicting stomatal responses to the environment from the optimization of photosynthetic gain and hydraulic cost. *Plant Cell Environ.*, **40**, 816–830, doi:10.1111/pce.12852. https://doi.org/10.1111/pce.12852.

Springmann, M., H. C. J. Godfray, M. Rayner, and P. Scarborough, 2016: Analysis and valuation of the health and climate change cobenefits of dietary change. *Proc. Natl. Acad. Sci.*, **113**, 4146–4151, doi:10.1073/pnas.1523119113. http://www.pnas.org/lookup/doi/10.1073/pnas.1523119113.

Stahl, C., and Coauthors, 2017: Continuous soil carbon storage of old permanent pastures in Amazonia. *Glob. Chang. Biol.*, **23**, 3382–3392, doi:10.1111/gcb.13573.

Stanelle, T., I. Bey, T. Raddatz, C. Reick, and I. Tegen, 2014: Anthropogenically induced changes in twentieth century mineral dust burden and the associated impact on radiative forcing. *J. Geophys. Res.*, **119**, 13,526-13,546, doi:10.1002/2014JD022062.

Stanne, T. M., L. L. E. Sjögren, S. Koussevitzky, and A. K. Clarke, 2009: Identification of new protein substrates for the chloroplast ATP-dependent Clp protease supports its constitutive role in *Arabidopsis*. *Biochem. J.*, **417**, 257–269, doi:10.1042/BJ20081146. http://biochemj.org/lookup/doi/10.1042/BJ20081146.

Stéfanon, M., P. Drobinski, F. D'Andrea, C. Lebeaupin-Brossier, and S. Bastin, 2014: Soil moisture-temperature feedbacks at meso-scale during summer heat waves over Western Europe. *Clim. Dyn.*, **42**, 1309–1324, doi:10.1007/s00382-013-1794-9. http://link.springer.com/10.1007/s00382-013-1794-9 (Accessed May 22, 2018).

Stehfest, E., L. Bouwman, D. P. Van Vuuren, M. G. J. Den Elzen, B. Eickhout, and P. Kabat, 2009: Climate benefits of changing diet. *Clim. Change*, **95**, 83–102, doi:10.1007/s10584-008-9534-6. https://doi.org/10.1007/s10584-008-9534-6.

Stevanović, M., and Coauthors, 2017: Mitigation Strategies for Greenhouse Gas Emissions from Agriculture and Land use Change: Consequences for Food Prices. *Environ. Sci. Technol.*, **51**, 365–374, doi:10.1021/acs.est.6b04291. http://pubs.acs.org/doi/10.1021/acs.est.6b04291 (Accessed May 25, 2018).

Stott, P., 2016: How climate change affects extreme weather events: Research can increasingly determine the contribution of climate change to extreme events such as droughts. *Science (80-.).*, **352**, 1517–1518, doi:10.1126/science.aaf7271. http://www.ncbi.nlm.nih.gov/pubmed/27339968 (Accessed May 24, 2018).

Stowe, L. L., H. Jacobowitz, G. Ohring, K. Knapp, and N. Nalli, 2002: The Advanced Very High Resolution Pathfinder Atmosphere (PATMOS) climate dataset: Initial analysis and evaluations. *Climate*, **15**, 1243–1260.

Strack, M., and J. M. Waddington, 2008: Spatiotemporal variability in peatland subsurface methane dynamics. *J. Geophys. Res. Biogeosciences*, **113**, doi:10.1029/2007JG000472. https://doi.org/10.1029/2007JG000472.

Strefler, J., N. Bauer, E. Kriegler, A. Popp, and A. Giannousakis, 2018: Between Scylla and Charybdis : Delayed mitigation narrows the passage between large-scale CDR and high costs. *Environ. Res. Lett.*, **13**, 044015, doi:10.1088/1748-9326/aab2ba. http://stacks.iop.org/1748-9326/13/i=4/a=044015?key=crossref.10c0d39604d7db99c097f4342437109f (Accessed May 22, 2018).

Strengers, B. J., and Coauthors, 2010: Assessing 20th century climate-vegetation feedbacks of land use change and natural vegetation dynamics in a fully coupled vegetation-climate model. *Int. J. Climatol.*, **30**, 2055–2065, doi:10.1002/joc.2132.

Sulman, B. N., R. P. Phillips, A. C. Oishi, E. Shevliakova, and S. W. Pacala, 2014: Microbe-driven turnover offsets mineral-mediated storage of soil carbon under elevated CO2. *Nat. Clim. Chang.*, **4**, 1099. http://dx.doi.org/10.1038/nclimate2436.

Sulman, B. N., E. R. Brzostek, C. Medici, E. Shevliakova, D. N. L. Menge, and R. P. Phillips, 2017: Feedbacks between plant N demand and rhizosphere priming depend on type of mycorrhizal association. *Ecol. Lett.*, **20**, 1043–1053, doi:10.1111/ele.12802. https://doi.org/10.1111/ele.12802.

Sun, Y., X. Zhang, G. Ren, F. W. Zwiers, and T. Hu, 2016: Contribution of urbanization to warming in China. *Nat. Clim. Chang.*, **6**, 706–709, doi:10.1038/nclimate2956.

Suntharalingam, P., E. Buitenhuis, C. Le Quéré, F. Dentener, C. Nevison, J. H. Butler, H. W. Bange, and G. Forster, 2012: Quantifying the impact of anthropogenic nitrogen deposition on oceanic nitrous oxide. *Geophys. Res. Lett.*, **39**, 1–7, doi:10.1029/2011GL050778.

Swann, A. L. S., F. M. Hoffman, C. D. Koven, and J. T. Randerson, 2016: Plant responses to increasing CO $_2$ reduce estimates of climate impacts on drought severity. *Proc. Natl. Acad. Sci.*, **113**, 10019–10024, doi:10.1073/pnas.1604581113. http://www.pnas.org/lookup/doi/10.1073/pnas.1604581113 (Accessed May 8, 2018).

Talhelm, A. F., and Coauthors, 2014: Elevated carbon dioxide and ozone alter productivity and ecosystem carbon content in northern temperate forests. *Glob. Chang. Biol.*, **20**, 2492–2504, doi:10.1111/gcb.12564. https://doi.org/10.1111/gcb.12564.

Tan, Z. H., and Coauthors, 2017: Optimum air temperature for tropical forest photosynthesis: Mechanisms involved and implications for climate warming. *Environ. Res. Lett.*, **12**, doi:10.1088/1748-9326/aa6f97.

Tang, J., and W. J. Riley, 2014: Weaker soil carbon–climate feedbacks resulting from microbial and abiotic interactions. *Nat. Clim. Chang.*, **5**, 56. http://dx.doi.org/10.1038/nclimate2438.

Tao, Y., F. Li, X. Liu, D. Zhao, X. Sun, and L. Xu, 2015: Variation in ecosystem services across an urbanization gradient: A study of terrestrial carbon stocks from Changzhou, China. *Ecol. Modell.*, **318**, 210–216, doi:https://doi.org/10.1016/j.ecolmodel.2015.04.027. http://www.sciencedirect.com/science/article/pii/S0304380015001994.

Taraborrelli, D., M. G. Lawrence, J. N. Crowley, T. J. Dillon, S. Gromov, C. B. M. Groß, L. Vereecken, and J. Lelieveld, 2012: Hydroxyl radical buffered by isoprene oxidation over tropical forests. *Nat. Geosci.*, **5**, 190–193, doi:10.1038/ngeo1405.

Tate, K. R., 2015: Soil methane oxidation and land use change - from process to mitigation. *Soil Biol. Biochem.*, **80**, 260–272, doi:10.1016/j.soilbio.2014.10.010. http://dx.doi.org/10.1016/j.soilbio.2014.10.010.

Tavoni, M., and Coauthors, 2015: Post-2020 climate agreements in the major economies assessed in the light of global models. *Nat. Clim. Chang.*, **5**, 119–126, doi:10.1038/nclimate2475. http://www.nature.com/articles/nclimate2475 (Accessed May 22, 2018).

Taylor, C. M., and Coauthors, 2017: Frequency of extreme Sahelian storms tripled since 1982 in satellite observations. *Nature*, **544**, 475–478, doi:10.1038/nature22069.

http://www.nature.com/doifinder/10.1038/nature22069 (Accessed May 24, 2018).

Terrer, C., S. Vicca, B. A. Hungate, R. P. Phillips, and I. C. Prentice, 2016: Mycorrhizal association as a primary control of the CO₂ fertilization effect. *Science (80-.).*, **353**, 72 LP-74, doi:10.1126/science.aaf4610. http://science.sciencemag.org/content/353/6294/72.abstract.

——, ——, B. D. Stocker, B. A. Hungate, R. P. Phillips, P. B. Reich, A. C. Finzi, and I. C. Prentice, 2017: Ecosystem responses to elevated CO_2 governed by plant-soil interactions and the cost of nitrogen acquisition. *New Phytol.*, **2**, 507–522, doi:10.1111/nph.14872. http://doi.wiley.com/10.1111/nph.14872.

Teskey, R., T. Wertin, I. Bauweraerts, M. Ameye, M. A. McGuire, and K. Steppe, 2015: Responses of tree species to heat waves and extreme heat events. *Plant Cell Environ.*, **38**, 1699–1712, doi:10.1111/pce.12417. http://doi.wiley.com/10.1111/pce.12417 (Accessed May 25, 2018).

Thackeray, C. W., and C. G. Fletcher, 2015: Snow albedo feedback: Current knowledge, importance, outstanding issues and future directions. *Prog. Phys. Geogr.*, **40**, 392–408, doi:10.1177/0309133315620999.

Thalman, R., and Coauthors, 2017: CCN activity and organic hygroscopicity of aerosols downwind of an urban region in central Amazonia: Seasonal and diel variations and impact of anthropogenic emissions. *Atmos. Chem. Phys.*, **17**, 11779–11801, doi:10.5194/acp-17-11779-2017.

Thompson, V., N. J. Dunstone, A. A. Scaife, D. M. Smith, J. M. Slingo, S. Brown, and S. E. Belcher, 2017: High risk of unprecedented UK rainfall in the current climate. *Nat. Commun.*, **8**, 107, doi:10.1038/s41467-017-00275-3. http://www.nature.com/articles/s41467-017-00275-3 (Accessed May 24, 2018).

Thorstensson, L., 2001: This Business of Internationalization: The Academic Experiences of 6 Asian MBA International Students at the University of Minnesota's Carlson School of Management. *J. Stud. Int. Educ.*, **5**, 317–340, doi:10.1177/102831530154004. https://academic.oup.com/bioscience/article/54/9/817/252974 (Accessed May 8, 2018).

Tian, H., and Coauthors, 2015a: *Global patterns and controls of soil organic carbon dynamics as simulated by multiple terrestrial biosphere models: Current status and future directions*. 775-792 pp. http://www.fao.org/forest-resources-assessment/current-assessment/en/.

——, and Coauthors, 2015b: *Global patterns and controls of soil organic carbon dynamics as simulated by multiple terrestrial biosphere models: Current status and future directions*. 775-792 pp. http://www.fao.org/forest-resources-assessment/current-assessment/en/.

——, and Coauthors, 2016a: The terrestrial biosphere as a net source of greenhouse gases to the atmosphere. *Nature*, **531**, 225–228, doi:10.1038/nature16946. http://www.nature.com/doifinder/10.1038/nature16946.

——, and Coauthors, 2016b: The terrestrial biosphere as a net source of greenhouse gases to the atmosphere. *Nature*, **531**, 225–228, doi:10.1038/nature16946.

Tietjen, B., and Coauthors, 2017: Climate change-induced vegetation shifts lead to more ecological droughts despite projected rainfall increases in many global temperate drylands. *Glob. Chang. Biol.*, **23**, 2743–2754, doi:10.1111/gcb.13598. http://doi.wiley.com/10.1111/1365-2664.12742 (Accessed May 15, 2018).

Tifafi, M., B. Guenet, and C. Hatté, 2018: Large Differences in Global and Regional Total Soil Carbon Stock Estimates Based on SoilGrids, HWSD, and NCSCD: Intercomparison and Evaluation Based on Field Data From USA, England, Wales, and France. *Global Biogeochem. Cycles*, **32**, 42–56, doi:10.1002/2017GB005678.

Tilman, D., and M. Clark, 2014: Global diets link environmental sustainability and human health. *Nature*, **515**, 518–522, doi:10.1038/nature13959. http://dx.doi.org/10.1038/nature13959.

Tjoelker, M. G., 2018: The role of thermal acclimation of plant respiration under climate warming: Putting the brakes on a runaway train? *Plant Cell Environ.*, **41**, 501–503, doi:10.1111/pce.13126. http://doi.wiley.com/10.1111/pce.13126.

Todd-Brown, K. E. O., J. T. Randerson, W. M. Post, F. M. Hoffman, C. Tarnocai, E. A. G. Schuur, and S. D. Allison, 2013: Causes of variation in soil carbon simulations from CMIP5 Earth system models and comparison with observations. *Biogeosciences*, **10**, 1717–1736, doi:10.5194/bg-10-1717-2013. http://www.biogeosciences.net/10/1717/2013/.

——, and Coauthors, 2014: Changes in soil organic carbon storage predicted by Earth system models during the 21st century. *Biogeosciences*, **11**, 2341–2356, doi:10.5194/bg-11-2341-2014. http://www.biogeosciences.net/11/2341/2014/.

Todd, M. C., and C. Cavazos-Guerra, 2016: Dust aerosol emission over the Sahara during summertime from Cloud-Aerosol Lidar with Orthogonal Polarization (CALIOP) observations. *Atmos. Environ.*, **128**, 147–157, doi:10.1016/j.atmosenv.2015.12.037.

Torres-Valcárcel, Á. R., J. Harbor, A. L. Torres-Valcárcel, and C. J. González-Avilés, 2015: Historical differences in temperature between urban and non-urban areas in Puerto Rico. *Int. J. Climatol.*, **35**, 1648–1661, doi:10.1002/joc.4083.

Trenberth, K. E., 2012: Framing the way to relate climate extremes to climate change. *Clim. Change*, **115**, 283–290, doi:10.1007/s10584-012-0441-5.

——, A. Dai, G. Van Der Schrier, P. D. Jones, J. Barichivich, K. R. Briffa, and J. Sheffield, 2014: Global warming and changes in drought. *Nat. Clim. Chang.*, **4**, 17–22, doi:10.1038/nclimate2067. http://www.nature.com/articles/nclimate2067 (Accessed May 7, 2018).

——, J. T. Fasullo, and T. G. Shepherd, 2015: Attribution of climate extreme events. *Nat. Clim. Chang.*, **5**, 725–730, doi:10.1038/nclimate2657. http://www.nature.com/articles/nclimate2657 (Accessed May 16, 2018).

Trnka, M., R. P. Rötter, M. Ruiz-Ramos, K. C. Kersebaum, J. E. Olesen, Z. Žalud, and M. A. Semenov, 2014: Adverse weather conditions for European wheat production will become more frequent with climate change. *Nat. Clim. Chang.*, **4**, 637–643, doi:10.1038/nclimate2242. http://www.nature.com/articles/nclimate2242 (Accessed May 21, 2018).

Trost, B., A. Prochnow, K. Drastig, A. Meyer-Aurich, F. Ellmer, and M. Baumecker, 2013: Irrigation, soil organic carbon and N2O emissions. A review. *Agron. Sustain. Dev.*, **33**, 733–749, doi:10.1007/s13593-013-0134-0.

Trusilova, K., M. Jung, G. Churkina, U. Karsten, M. Heimann, and M. Claussen, 2008: Urbanization impacts on the climate in Europe: Numerical experiments by the PSU-NCAR mesoscale model (MM5). *J. Appl. Meteorol. Climatol.*, **47**, 1442–1455, doi:10.1175/2007JAMC1624.1.

Tsigaridis, K., and Coauthors, 2014: The AeroCom evaluation and intercomparison of organic aerosol in global models. *Atmos. Chem. Phys.*, **14**, 10845–10895, doi:10.5194/acp-14-10845-2014. https://www.atmos-chem-phys.net/14/10845/2014/.

Tubiello, F. N., J.-F. Soussana, and S. M. Howden, 2007: Crop and pasture response to climate change. *Proc. Natl. Acad. Sci.*, **104**, 19686–19690, doi:10.1073/pnas.0701728104. http://www.pnas.org/cgi/doi/10.1073/pnas.0701728104.

Tubiello, F. N., and Coauthors, 2014: Agriculture , Forestry and Other Land Use Emissions by Sources and Removals by Sinks. *ESS Work. Pap. No.2*, **2**, 4–89, doi:10.13140/2.1.4143.4245. http://www.fao.org/docrep/019/i3671e/i3671e.pdf.

Tubiello, F. N., and Coauthors, 2015: The Contribution of Agriculture, Forestry and other Land Use activities to Global Warming, 1990-2012. *Glob. Chang. Biol.*, **21**, 2655–2660, doi:10.1111/gcb.12865.

Turner, A. J., C. Frankenberg, P. O. Wennberg, and D. J. Jacob, 2017: Ambiguity in the causes for decadal trends in atmospheric methane and hydroxyl. *Proc. Natl. Acad. Sci.*, **114**, 5367–5372, doi:10.1073/pnas.1616020114. http://www.pnas.org/lookup/doi/10.1073/pnas.1616020114.

Turner, B. L., T. Brenes-Arguedas, and R. Condit, 2018a: Pervasive phosphorus limitation of tree species but not communities in tropical forests. *Nature*, **555**, 367–370, doi:10.1038/nature25789. http://dx.doi.org/10.1038/nature25789.

Turner, P. A., T. J. Griffis, X. Lee, J. M. Baker, R. T. Venterea, and J. D. Wood, 2015: Indirect nitrous oxide emissions from streams within the US Corn Belt scale with stream order. *Proc. Natl. Acad. Sci.*, **112**, 9839–9843, doi:10.1073/pnas.1503598112. http://www.pnas.org/lookup/doi/10.1073/pnas.1503598112.

Turner, P. A., C. B. Field, D. B. Lobell, D. L. Sanchez, and K. J. Mach, 2018b: Unprecedented rates of land use transformation in modelled climate change mitigation pathways. *Nat. Sustain.*, **1**, 240–245, doi:10.1038/s41893-018-0063-7. http://www.nature.com/articles/s41893-018-0063-7 (Accessed May 22, 2018).

Tuttle, S., and G. Salvucci, 2016: Atmospheric science: Empirical evidence of contrasting soil moisture-precipitation feedbacks across the United States. *Science (80-.).*, **352**, 825–828, doi:10.1126/science.aaa7185. http://science.sciencemag.org/content/352/6287/825.

Tyukavina, A., and Coauthors, 2015: Aboveground carbon loss in natural and managed tropical forests from 2000 to 2012. *Environ. Res. Lett.*, **10**, 74002–74002, doi:10.1088/1748-9326/10/7/074002. http://iopscience.iop.org/1748-9326/10/7/074002.

Tyukavina, A., M. C. Hansen, P. V. Potapov, S. V. Stehman, K. Smith-Rodriguez, C. Okpa, and R. Aguilar, 2017a: Types and rates of forest disturbance in Brazilian Legal Amazon, 2000–2013. *Sci. Adv.*, **3**, doi:10.1126/sciadv.1601047.

——, ——, ——, ——, ——, ——, and ——, 2017b: Types and rates of forest disturbance in Brazilian Legal Amazon, 2000–2013. *Sci. Adv.*, **3**, e1601047, doi:10.1126/sciadv.1601047. http://advances.sciencemag.org/lookup/doi/10.1126/sciadv.1601047.

Ummenhofer, C. C., and G. A. Meehl, 2017: Extreme weather and climate events with ecological relevance: a review. *Philos. Trans. R. Soc. B Biol. Sci.*, **372**, 20160135, doi:10.1098/rstb.2016.0135. http://rstb.royalsocietypublishing.org/lookup/doi/10.1098/rstb.2016.0135 (Accessed May 16, 2018).

United Nations University, 2015: *The global potential of indigenous fire management: findings of the regional feasibility assessments*. 178 pp. https://collections.unu.edu/eserv/UNU:5605/indigenous_fire_management.pdf.

Urbanski, S. P., 2014: Wildland fire emissions, carbon, and climate: Emission factors. *For. Ecol. Manage.*, **317**, 51–60, doi:https://doi.org/10.1016/j.foreco.2013.05.045. http://www.sciencedirect.com/science/article/pii/S0378112713003447.

Valin, H., and Coauthors, 2014: The future of food demand: understanding differences in global economic models. *Agric. Econ.*, **45**, 51–67, doi:10.1111/agec.12089. http://doi.wiley.com/10.1111/agec.12089.

Vanderwel, M. C., and Coauthors, 2015: Global convergence in leaf respiration from estimates of thermal acclimation across time and space. *New Phytol.*, **207**, 1026–1037, doi:10.1111/nph.13417.

Veraverbeke, S., I. Gitas, T. Katagis, A. Polychronaki, B. Somers, and R. Goossens, 2012: Assessing post-fire vegetation recovery using red-near infrared vegetation indices: Accounting for background and vegetation variability. *ISPRS J. Photogramm. Remote Sens.*, **68**, 28–39, doi:10.1016/j.isprsjprs.2011.12.007. http://www.sciencedirect.com/science/article/pii/S0924271611001614.

Veselovskii, I., and Coauthors, 2016: Retrieval of optical and physical properties of African dust from multiwavelength Raman lidar measurements during the SHADOW campaign in Senegal. *Atmos. Chem. Phys.*, **16**, 7013–7028, doi:10.5194/acp-16-7013-2016.

Vicente-Serrano, S. M., J. I. López-Moreno, L. Gimeno, R. Nieto, E. Morán-Tejeda, J. Lorenzo-Lacruz, S. Beguería, and C. Azorin-Molina, 2011: A multiscalar global evaluation of the impact of ENSO on droughts. *J. Geophys. Res. Atmos.*, **116**, D20109, doi:10.1029/2011JD016039. http://doi.wiley.com/10.1029/2011JD016039 (Accessed May 7, 2018).

Vogel, E., and R. Meyer, 2018: Climate Change, Climate Extremes, and Global Food Production—Adaptation in the Agricultural Sector. *Resilience*, 31–49, doi:10.1016/B978-0-12-811891-7.00003-7. http://linkinghub.elsevier.com/retrieve/pii/B9780128118917000037 (Accessed May 25, 2018).

Voulgarakis, A., and Coauthors, 2013: Analysis of present day and future OH and methane lifetime in the ACCMIP simulations. *Atmos. Chem. Phys.*, **13**, 2563–2587, doi:10.5194/acp-13-2563-2013.

De Vrese, P., S. Hagemann, and M. Claussen, 2016: Asian irrigation, African rain: Remote impacts of irrigation. *Geophys. Res. Lett.*, **43**, 3737–3745, doi:10.1002/2016GL068146.

van Vuuren, D. P., S. J. Smith, and K. Riahi, 2010: Downscaling socioeconomic and emissions scenarios for global environmental change research: A review. *Wiley Interdiscip. Rev. Clim. Chang.*, **1**, 393–404, doi:10.1002/wcc.50. https://doi.org/10.1002/wcc.50.

——, and Coauthors, 2011: RCP2.6: Exploring the possibility to keep global mean temperature increase below 2°C. *Clim. Change*, **109**, 95–116, doi:10.1007/s10584-011-0152-3. https://doi.org/10.1007/s10584-011-0152-3.

——, and Coauthors, 2018: Alternative pathways to the 1.5 °C target reduce the need for negative emission technologies. *Nat. Clim. Chang.*, **8**, 1–7, doi:10.1038/s41558-018-0119-8.

http://www.nature.com/articles/s41558-018-0119-8 (Accessed May 22, 2018).
Van Vuuren, D. P., P. L. Lucas, T. Häyhä, S. E. Cornell, and M. Stafford-Smith, 2016: Horses for courses: Analytical tools to explore planetary boundaries. *Earth Syst. Dyn.*, **7**, 267–279, doi:10.5194/esd-7-267-2016. https://www.earth-syst-dynam.net/7/267/2016/.
Wada, Y., D. Wisser, and M. F. P. Bierkens, 2014: Global modeling of withdrawal, allocation and consumptive use of surface water and groundwater resources. *Earth Syst. Dyn.*, **5**, 15–40, doi:10.5194/esd-5-15-2014.
Wagner-Riddle, C., K. A. Congreves, D. Abalos, A. A. Berg, S. E. Brown, J. T. Ambadan, X. Gao, and M. Tenuta, 2017: Globally important nitrous oxide emissions from croplands induced by freeze-thaw cycles. *Nat. Geosci.*, **10**, 279–283, doi:10.1038/ngeo2907.
Wang, G., E. A. B. Eltahir, J. A. Foley, D. Pollard, and S. Levis, 2004: Decadal variability of rainfall in the Sahel: Results from the coupled GENESIS-IBIS atmosphere-biosphere model. *Clim. Dyn.*, **22**, 625–637, doi:10.1007/s00382-004-0411-3.
Wang, G., D. Wang, K. E. Trenberth, A. Erfanian, M. Yu, M. G. Bosilovich, and D. T. Parr, 2017a: The peak structure and future changes of the relationships between extreme precipitation and temperature. *Nat. Clim. Chang.*, **7**, 268–274, doi:10.1038/nclimate3239. http://www.nature.com/articles/nclimate3239 (Accessed May 24, 2018).
Wang, G. S., W. M. Post, and M. A. Mayes, 2013: Development of microbial-enzyme-mediated decomposition model parameters through steady-state and dynamic analyses. *Ecol. Appl.*, **23**, 255–272.
Wang, J., B. Huang, D. Fu, P. M. Atkinson, and X. Zhang, 2016a: Response of urban heat island to future urban expansion over the Beijing–Tianjin–Hebei metropolitan area. *Appl. Geogr.*, **70**, 26–36, doi:https://doi.org/10.1016/j.apgeog.2016.02.010. http://www.sciencedirect.com/science/article/pii/S014362281630011X.
Wang, J., Z. Yan, X. W. Quan, and J. Feng, 2017b: Urban warming in the 2013 summer heat wave in eastern China. *Clim. Dyn.*, **48**, 3015–3033, doi:10.1007/s00382-016-3248-7.
Wang, L., J. N. S. Cole, P. Bartlett, D. Verseghy, C. Derksen, R. Brown, and K. Salzen, 2016b: Journal of Geophysical Research : Atmospheres for snow-covered forests in CMIP5 models. 1104–1119, doi:10.1002/2015JD023824.Received.
Wang, R., and Coauthors, 2014a: Trend in global black carbon emissions from 1960 to 2007. *Environ. Sci. Technol.*, **48**, 6780–6787, doi:10.1021/es5021422.
——, and Coauthors, 2017c: Global forest carbon uptake due to nitrogen and phosphorus deposition from 1850 to 2100. *Glob. Chang. Biol.*, **23**, 4854–4872, doi:10.1111/gcb.13766.
Wang, S., A. Wilkes, Z. Zhang, X. Chang, R. Lang, Y. Wang, and H. Niu, 2011: Management and land use change effects on soil carbon in northern China's grasslands: A synthesis. *Agric. Ecosyst. Environ.*, **142**, 329–340, doi:10.1016/j.agee.2011.06.002.
Wang, W., A. T. Evan, C. Flamant, and C. Lavaysse, 2015: On the decadal scale correlation between African dust and Sahel rainfall: The role of Saharan heat low-forced winds. *Sci. Adv.*, **1**, p.e1500646, doi:10.1126/sciadv.1500646.
Wang, Y., X. Yan, and Z. Wang, 2014b: The biogeophysical effects of extreme afforestation in modeling future climate. *Theor. Appl. Climatol.*, **118**, 511–521, doi:10.1007/s00704-013-1085-8.
Wang, Z., T. Hoffmann, J. Six, J. O. Kaplan, G. Govers, S. Doetterl, and K. Van Oost, 2017d: Human-induced erosion has offset one-third of carbon emissions from land cover change. *Nat. Clim. Chang.*, **7**, 345. http://dx.doi.org/10.1038/nclimate3263.
Ward, D. S., S. Kloster, N. M. Mahowald, B. M. Rogers, J. T. Randerson, and P. G. Hess, 2012: The changing radiative forcing of fires: Global model estimates for past, present and future. *Atmos. Chem. Phys.*, **12**, 10857–10886, doi:10.5194/acp-12-10857-2012. http://www.atmos-chem-phys.net/12/10857/2012/ (Accessed May 23, 2018).
——, N. M. Mahowald, and S. Kloster, 2014: Potential climate forcing of land use and land cover change. *Atmos. Chem. Phys.*, **14**, 12701–12724, doi:10.5194/acp-14-12701-2014.
Ward, K., S. Lauf, B. Kleinschmit, and W. Endlicher, 2016: Heat waves and urban heat islands in Europe: A review of relevant drivers. *Sci. Total Environ.*, **569–570**, 527–539, doi:10.1016/j.scitotenv.2016.06.119. http://dx.doi.org/10.1016/j.scitotenv.2016.06.119.

Warszawski, L., and Coauthors, 2013: A multi-model analysis of risk of ecosystem shifts under climate change. *Environ. Res. Lett.*, **8**, 044018, doi:10.1088/1748-9326/8/4/044018. http://stacks.iop.org/1748-9326/8/i=4/a=044018?key=crossref.2d722efbaf6d3e455e38f2c68888d873 (Accessed May 7, 2018).

Wassmann, R., and Coauthors, 2009: Chapter 3 Regional Vulnerability of Climate Change Impacts on Asian Rice Production and Scope for Adaptation. *Adv. Agron.*, **102**, 91–133, doi:10.1016/S0065-2113(09)01003-7. https://www-sciencedirect-com.ezproxy.uct.ac.za/science/article/pii/S0065211309010037 (Accessed May 24, 2018).

Wells, K. C., and Coauthors, 2018: Top-down constraints on global N2O emissions at optimal resolution: Application of a new dimension reduction technique. *Atmos. Chem. Phys.*, **18**, 735–756, doi:10.5194/acp-18-735-2018.

Wendt, J. W., and S. Hauser, 2013: An equivalent soil mass procedure for monitoring soil organic carbon in multiple soil layers. *Eur. J. Soil Sci.*, **64**, 58–65, doi:10.1111/ejss.12002.

van der Werf, G. R., and Coauthors, 2008: Climate regulation of fire emissions and deforestation in equatorial Asia. *Proc. Natl. Acad. Sci.*, **105**, 20350–20355, doi:10.1073/pnas.0803375105. http://www.pnas.org/cgi/doi/10.1073/pnas.0803375105 (Accessed May 5, 2018).

——, C. P. Meyer, and A. P., 2013: *Reducing N2O emissions from biomass burning in landscape fires and household stoves Drawing Down N2O to Protect Climate and the Ozone Layer*.

van der Werf, G. R., and Coauthors, 2017: Global fire emissions estimates during 1997–2015. *Earth Syst. Sci. Data Discuss.*, 1–43, doi:10.5194/essd-2016-62. http://www.earth-syst-sci-data-discuss.net/essd-2016-62/.

Van Der Werf, G. R., and Coauthors, 2010a: Global fire emissions and the contribution of deforestation, savanna, forest, agricultural, and peat fires (1997-2009). *Atmos. Chem. Phys.*, **10**, 11707–11735, doi:10.5194/acp-10-11707-2010.

——, and Coauthors, 2010b: Global fire emissions and the contribution of deforestation, savanna, forest, agricultural, and peat fires (1997-2009). *Atmos. Chem. Phys.*, **10**, 11707–11735, doi:10.5194/acp-10-11707-2010. http://www.atmos-chem-phys-discuss.net/6/3175/2006/.

Werth, D., and R. Avissar, 2005: The local and global effects of Southeast Asian deforestation. *Geophys. Res. Lett.*, **32**, 1–4, doi:10.1029/2005GL022970.

West, T. O., G. Marland, A. W. King, W. M. Post, A. K. Jain, and K. Andrasko, 2004: Carbon management response curves: Estimates of temporal soil carbon dynamics. *Environ. Manage.*, **33**, 507–518, doi:10.1007/s00267-003-9108-3. http://link.springer.com/10.1007/s00267-003-9108-3 (Accessed May 25, 2018).

Westra, S., L. V. Alexander, and F. W. Zwiers, 2013: Global increasing trends in annual maximum daily precipitation. *J. Clim.*, **26**, 3904–3918, doi:10.1175/JCLI-D-12-00502.1. http://journals.ametsoc.org/doi/abs/10.1175/JCLI-D-12-00502.1 (Accessed May 21, 2018).

Westra, S., and Coauthors, 2014: Future changes to the intensity and frequency of short-duration extreme rainfall. *Rev. Geophys.*, **52**, 522–555, doi:10.1002/2014RG000464. http://doi.wiley.com/10.1002/2014RG000464 (Accessed May 19, 2018).

Wheeler, T., and J. Von Braun, 2013: Climate change impacts on global food security. *Science (80-.).*, **341**, 508–513, doi:10.1126/science.1239402.

Wiebe, K., and Coauthors, 2015: Climate change impacts on agriculture in 2050 under a range of plausible socioeconomic and emissions scenarios. *Environ. Res. Lett.*, **10**, 85010, doi:10.1088/1748-9326/10/8/085010. http://stacks.iop.org/1748-9326/10/i=8/a=085010.

Wieder, W. R., G. B. Bonan, and S. D. Allison, 2013: Global soil carbon projections are improved by modelling microbial processes. *Nat. Clim. Chang.*, **3**, 909–912, doi:10.1038/nclimate1951.

Wiesen, P., T. J. Wallington, and W. Winiwarter, 2013: *Reducing N2O emissions from industry and fossil fuel combustion A UNEP Synthesis Report:Drawing Down N2O to Protect Climate and the Ozone Layer*.

Wilfert, L., G. Long, H. C. Leggett, P. Schmid-Hempel, R. Butlin, S. J. M. Martin, and M. Boots, 2016: Honeybee disease: Deformed wing virus is a recent global epidemic in honeybees driven by Varroa mites. *Science (80-.).*, **351**, 594–597, doi:10.1126/science.aac9976.

Williams, A. P., and J. T. Abatzoglou, 2016: Recent Advances and Remaining Uncertainties in Resolving

Past and Future Climate Effects on Global Fire Activity. *Curr. Clim. Chang. Reports*, **2**, 1–14, doi:10.1007/s40641-016-0031-0. https://doi.org/10.1007/s40641-016-0031-0.
Williams, J., and P. J. Crutzen, 2010: Nitrous oxide from aquaculture. *Nat. Geosci.*, **3**, 143, doi:10.1038/ngeo804. http://dx.doi.org/10.1038/ngeo804.
Wilson, D., C. A. Farrell, D. Fallon, G. Moser, C. Müller, and F. Renou-Wilson, 2016: Multiyear greenhouse gas balances at a rewetted temperate peatland. *Glob. Chang. Biol.*, **22**, 4080–4095, doi:10.1111/gcb.13325.
Wim, T., D. E. L., L. D. M., H. A. L., H. Mathias, and S. S. I., 2017: Present-day irrigation mitigates heat extremes. *J. Geophys. Res. Atmos.*, **122**, 1403–1422, doi:doi:10.1002/2016JD025740. https://doi.org/10.1002/2016JD025740.
Wise, M., E. L. Hodson, B. K. Mignone, L. Clarke, S. Waldhoff, and P. Luckow, 2015: An approach to computing marginal land use change carbon intensities for bioenergy in policy applications. *Energy Econ.*, **50**, 337–347, doi:10.1016/j.eneco.2015.05.009.
Wisser, D., S. Frolking, E. M. Douglas, B. M. Fekete, C. J. Vörösmarty, and A. H. Schumann, 2008: Global irrigation water demand: Variability and uncertainties arising from agricultural and climate data sets. *Geophys. Res. Lett.*, **35**, 1–5, doi:10.1029/2008GL035296.
Wolf, A., W. R. L. Anderegg, and S. W. Pacala, 2016: Optimal stomatal behavior with competition for water and risk of hydraulic impairment. *Proc. Natl. Acad. Sci.*, **113**, E7222 LP-E7230. http://www.pnas.org/content/113/46/E7222.abstract.
Wong, S. C., I. R. Cowan, and G. D. Farquhar, 1979: Stomatal conductance correlates with photosynthetic capacity. *Nature*, **282**, 424. http://dx.doi.org/10.1038/282424a0.
Wu, J., J. Zha, and D. Zhao, 2017a: Evaluating the effects of land use and cover change on the decrease of surface wind speed over China in recent 30 years using a statistical downscaling method. *Clim. Dyn.*, **48**, 131–149, doi:10.1007/s00382-016-3065-z.
Wu, M., G. Schurgers, M. Rummukainen, B. Smith, P. Samuelsson, C. Jansson, J. Siltberg, and W. May, 2016: Vegetation-climate feedbacks modulate rainfall patterns in Africa under future climate change. *Earth Syst. Dyn.*, **7**, 627–647, doi:10.5194/esd-7-627-2016.
Wu, M., G. Schurgers, A. Ahlström, M. Rummukainen, P. A. Miller, B. Smith, and W. May, 2017b: Impacts of land use on climate and ecosystem productivity over the Amazon and the South American continent Impacts of land use on climate and ecosystem productivity over the Amazon and the South American continent. *Environ. Res. Lett.*, **12**.
Wu, P., N. Christidis, and P. Stott, 2013: Anthropogenic impact on Earth's hydrological cycle. *Nat. Clim. Chang.*, **3**, 807–810, doi:10.1038/nclimate1932. http://www.nature.com/doifinder/10.1038/nclimate1932 (Accessed May 16, 2018).
Wuebbles, D., and K. Hayhoe, 2002: Atmospheric methane and global change. *Earth-Science Rev.*, **57**, 177–210, doi:10.1016/S0012-8252(01)00062-9. http://linkinghub.elsevier.com/retrieve/pii/S0012825201000629.
Xu, C., H. Liu, A. P. Williams, Y. Yin, and X. Wu, 2016a: Trends toward an earlier peak of the growing season in Northern Hemisphere mid-latitudes. *Glob. Chang. Biol.*, **22**, 2852–2860, doi:10.1111/gcb.13224. http://doi.wiley.com/10.1111/gcb.13224 (Accessed January 23, 2018).
Xu, L., A. Samanta, M. H. Costa, S. Ganguly, R. R. Nemani, and R. B. Myneni, 2011: Widespread decline in greenness of Amazonian vegetation due to the 2010 drought. *Geophys. Res. Lett.*, **38**, n/a-n/a, doi:10.1029/2011GL046824. http://doi.wiley.com/10.1029/2011GL046824 (Accessed May 7, 2018).
Xu, Q., R. Yang, Y.-X. Dong, Y.-X. Liu, and L.-R. Qiu, 2016b: The influence of rapid urbanization and land use changes on terrestrial carbon sources/sinks in Guangzhou, China. *Ecol. Indic.*, **70**, 304–316, doi:https://doi.org/10.1016/j.ecolind.2016.05.052. http://www.sciencedirect.com/science/article/pii/S1470160X16303120.
Yamato, H., T. Mikami, and H. Takahashi, 2017: Impact of sea breeze penetration over urban areas on midsummer temperature distributions in the Tokyo Metropolitan area. *Int. J. Climatol.*, **37**, 5154–5169, doi:10.1002/joc.5152.
Yamori, W., K. Hikosaka, and D. A. Way, 2014: Temperature response of photosynthesis in C3, C4, and CAM plants: Temperature acclimation and temperature adaptation. *Photosynth. Res.*, **119**, 101–117,

doi:10.1007/s11120-013-9874-6.
Yang, H., Q. Li, K. Wang, Y. Sun, and D. Sun, 2015a: Decomposing the meridional heat transport in the climate system. *Clim. Dyn.*, **44**, 2751–2768, doi:10.1007/s00382-014-2380-5. http://link.springer.com/10.1007/s00382-014-2380-5 (Accessed May 7, 2018).
Yang, H., and Coauthors, 2017: Regional patterns of future runoff changes from Earth system models constrained by observation. *Geophys. Res. Lett.*, **44**, 5540–5549, doi:10.1002/2017GL073454.
Yang, L., J. A. Smith, M. L. Baeck, E. Bou-Zeid, S. M. Jessup, F. Tian, and H. Hu, 2013: Impact of Urbanization on Heavy Convective Precipitation under Strong Large-Scale Forcing: A Case Study over the Milwaukee–Lake Michigan Region. *J. Hydrometeorol.*, **15**, 261–278, doi:10.1175/JHM-D-13-020.1. https://doi.org/10.1175/JHM-D-13-020.1.
Yang, L., G. Sun, L. Zhi, and J. Zhao, 2018: Negative soil moisture-precipitation feedback in dry and wet regions. *Sci. Rep.*, **8**, 4026, doi:10.1038/s41598-018-22394-7. https://doi.org/10.1038/s41598-018-22394-7.
Yang, X., and Coauthors, 2015b: Potential benefits of climate change for crop productivity in China. *Agric. For. Meteorol.*, **208**, 76–84, doi:10.1016/j.agrformet.2015.04.024. https://www-sciencedirect-com.ezproxy.uct.ac.za/science/article/pii/S0168192315001288 (Accessed May 10, 2018).
Ye, J. S., Y. H. Gong, F. Zhang, J. Ren, X. K. Bai, and Y. Zheng, 2018: Which temperature and precipitation extremes best explain the variation of warm versus cold years and wet versus dry years? *J. Clim.*, **31**, 45–59, doi:10.1175/JCLI-D-17-0377.1. http://journals.ametsoc.org/doi/10.1175/JCLI-D-17-0377.1 (Accessed May 17, 2018).
Yellen, B., J. D. Woodruff, L. N. Kratz, S. B. Mabee, J. Morrison, and A. M. Martini, 2014: Source, conveyance and fate of suspended sediments following Hurricane Irene. New England, USA. *Geomorphology*, **226**, 124–134, doi:10.1016/j.geomorph.2014.07.028. https://www-sciencedirect-com.ezproxy.uct.ac.za/science/article/pii/S0169555X14003936 (Accessed May 25, 2018).
Yu, L., Y. Huang, W. Zhang, T. Li, and W. Sun, 2017: Methane uptake in global forest and grassland soils from 1981 to 2010. *Sci. Total Environ.*, **607**–**608**, 1163–1172, doi:10.1016/j.scitotenv.2017.07.082. http://dx.doi.org/10.1016/j.scitotenv.2017.07.082.
Yu, M., G. Wang, and J. S. Pal, 2016: Effects of vegetation feedback on future climate change over West Africa. *Clim. Dyn.*, **46**, 3669–3688, doi:10.1007/s00382-015-2795-7.
Zaehle, S., C. D. Jones, B. Houlton, J. F. Lamarque, and E. Robertson, 2015: Nitrogen availability reduces CMIP5 projections of twenty-first-century land carbon uptake. *J. Clim.*, **28**, 2494–2511, doi:10.1175/JCLI-D-13-00776.1. http://journals.ametsoc.org/doi/abs/10.1175/JCLI-D-13-00776.1.
Zaitchik, B. F., A. K. Macalady, L. R. Bonneau, and R. B. Smith, 2006: Europe's 2003 heat wave: A satellite view of impacts and land - Atmosphere feedbacks. *Int. J. Climatol.*, **26**, 743–769, doi:10.1002/joc.1280.
Zak, D. R., K. S. Pregitzer, M. E. Kubiske, and A. J. Burton, 2011: Forest productivity under elevated CO2 and O3: Positive feedbacks to soil N cycling sustain decade-long net primary productivity enhancement by CO2. *Ecol. Lett.*, **14**, 1220–1226, doi:10.1111/j.1461-0248.2011.01692.x. https://doi.org/10.1111/j.1461-0248.2011.01692.x.
Zampieri, M., A. Ceglar, F. Dentener, and A. Toreti, 2017: Wheat yield loss attributable to heat waves, drought and water excess at the global, national and subnational scales. *Environ. Res. Lett.*, **12**, 064008, doi:10.1088/1748-9326/aa723b. http://stacks.iop.org/1748-9326/12/i=6/a=064008?key=crossref.e0e6a706a9eb5e129e871d54e2e59ba0 (Accessed May 21, 2018).
Zarin, D. J., and Coauthors, 2016a: Can carbon emissions from tropical deforestation drop by 50% in 5 years? *Glob. Chang. Biol.*, **22**, 1336–1347, doi:10.1111/gcb.13153. https://doi.org/10.1111/gcb.13153.
——, and Coauthors, 2016b: Can carbon emissions from tropical deforestation drop by 50% in 5 years? *Glob. Chang. Biol.*, **22**, 1336–1347, doi:10.1111/gcb.13153. https://doi.org/10.1111/gcb.13153.
Zedler, J. B., and S. Kercher, 2005: WETLAND RESOURCES: Status, Trends, Ecosystem Services, and Restorability. *Annu. Rev. Environ. Resour.*, **30**, 39–74, doi:10.1146/annurev.energy.30.050504.144248. http://www.annualreviews.org/doi/10.1146/annurev.energy.30.050504.144248.
Zemp, D. C., C. F. Schleussner, H. M. J. Barbosa, and A. Rammig, 2017: Deforestation effects on Amazon

forest resilience. *Geophys. Res. Lett.*, **44**, 6182–6190, doi:10.1002/2017GL072955.

Zeng, N., J. D. Neelin, K. M. Lau, and C. J. Tucker, 1999: Enhancement of interdecadal climate variability in the Sahel by vegetation interaction. *Science (80-.).*, **286**, 1537–1540, doi:10.1126/science.286.5444.1537.

Zeng, Z., and Coauthors, 2017: Climate mitigation from vegetation biophysical feedbacks during the past three decades. *Nat. Clim. Chang.*, **7**, 432–436, doi:10.1038/nclimate3299.

——, and Coauthors, 2018: Impact of Earth greening on the terrestrial water cycle. *J. Clim.*, JCLI-D-17-0236.1, doi:10.1175/JCLI-D-17-0236.1. http://journals.ametsoc.org/doi/10.1175/JCLI-D-17-0236.1.

Zhai, C., W. Wang, X. He, W. Zhou, L. Xiao, and B. Zhang, 2017: Urbanization Drives SOC Accumulation, Its Temperature Stability and Turnover in Forests, Northeastern China. *Forests*, **8**.

Zhang, A., G. Jia, H. E. Epstein, and J. Xia, 2017a: ENSO elicits opposing responses of semi-arid vegetation between Hemispheres. *Sci. Rep.*, **7**, 42281, doi:10.1038/srep42281. http://www.nature.com/articles/srep42281 (Accessed May 16, 2018).

——, ——, ——, and ——, 2017b: ENSO elicits opposing responses of semi-arid vegetation between Hemispheres. *Sci. Rep.*, **7**, 42281, doi:10.1038/srep42281. http://dx.doi.org/10.1038/srep42281.

Zhang, D., H. Zheng, Z. Ren, C. Zhai, G. Shen, Z. Mao, P. Wang, and X. He, 2015: Effects of forest type and urbanization on carbon storage of urban forests in Changchun, Northeast China. *Chinese Geogr. Sci.*, **25**, 147–158, doi:10.1007/s11769-015-0743-4. https://doi.org/10.1007/s11769-015-0743-4.

Zhang, D. L., Y. X. Shou, and R. R. Dickerson, 2009: Upstream urbanization exacerbates urban heat island effects. *Geophys. Res. Lett.*, **36**, 1–5, doi:10.1029/2009GL041082.

Zhang, G., and Coauthors, 2017c: Extensive and drastically different alpine lake changes on Asia's high plateaus during the past four decades. *Geophys. Res. Lett.*, **44**, 252–260, doi:10.1002/2016GL072033.

Zhang, G. J., M. Cai, and A. Hu, 2013a: Energy consumption and the unexplained winter warming over northern Asia and North America. *Nat. Clim. Chang.*, **3**, 466–470, doi:10.1038/nclimate1803.

Zhang, H. L., R. Lal, X. Zhao, J. F. Xue, and F. Chen, 2014: Opportunities and challenges of soil carbon sequestration by conservation agriculture in China. *Advances in Agronomy*, Vol. 124 of, 1–36.

Zhang, N., and Y. Chen, 2014: A case study of the upwind urbanization influence on the urban heat Island effects along the Suzhou-Wuxi corridor. *J. Appl. Meteorol. Climatol.*, **53**, 333–345, doi:10.1175/JAMC-D-12-0219.1.

Zhang, W. -f., and Coauthors, 2013b: New technologies reduce greenhouse gas emissions from nitrogenous fertilizer in China. *Proc. Natl. Acad. Sci.*, **110**, 8375–8380, doi:10.1073/pnas.1210447110. http://www.pnas.org/cgi/doi/10.1073/pnas.1210447110.

Zhang, X., H. Wan, F. W. Zwiers, G. C. Hegerl, and S. K. Min, 2013c: Attributing intensification of precipitation extremes to human influence. *Geophys. Res. Lett.*, **40**, 5252–5257, doi:10.1002/grl.51010. http://doi.wiley.com/10.1002/grl.51010 (Accessed May 25, 2018).

——, F. W. Zwiers, G. Li, H. Wan, and A. J. Cannon, 2017d: Complexity in estimating past and future extreme short-duration rainfall. *Nat. Geosci.*, **10**, 255–259, doi:10.1038/ngeo2911. http://www.nature.com/articles/ngeo2911 (Accessed May 24, 2018).

Zhang, Z., Y. Chen, C. Wang, P. Wang, and F. Tao, 2017e: Future extreme temperature and its impact on rice yield in China. *Int. J. Climatol.*, **37**, 4814–4827, doi:10.1002/joc.5125. http://doi.wiley.com/10.1002/joc.5125 (Accessed May 21, 2018).

Zhao, C., and Coauthors, 2017: Temperature increase reduces global yields of major crops in four independent estimates. *Proc. Natl. Acad. Sci.*, 201701762, doi:10.1073/pnas.1701762114. http://www.pnas.org/lookup/doi/10.1073/pnas.1701762114.

Zhao, L., X. Lee, R. B. Smith, and K. Oleson, 2014: Strong contributions of local background climate to urban heat islands. *Nature*, **511**, 216–219, doi:10.1038/nature13462. http://www.nature.com/articles/nature13462 (Accessed May 5, 2018).

Zhao, L., A. Dai, and B. Dong, 2018a: Changes in global vegetation activity and its driving factors during 1982–2013. *Agric. For. Meteorol.*, **249**, 198–209, doi:10.1016/j.agrformet.2017.11.013. https://www.sciencedirect.com/science/article/pii/S0168192317303866 (Accessed February 4, 2018).

Zhao, L., M. Oppenheimer, Q. Zhu, J. W. Baldwin, K. L. Ebi, E. Bou-Zeid, K. Guan, and X. Liu, 2018b: Interactions between urban heat islands and heat waves. *Environ. Res. Lett.*, **13**, 034003, doi:10.1088/1748-9326/aa9f73. http://stacks.iop.org/1748-9326/13/i=3/a=034003?key=crossref.11cceae00694f6275f6a1d9cb94fc02d.

Zhong, S., and X. Q. Yang, 2015: Mechanism of urbanization impact on a summer cold-frontal rainfall process in the greater Beijing metropolitan area. *J. Appl. Meteorol. Climatol.*, **54**, 1234–1247, doi:10.1175/JAMC-D-14-0264.1.

——, Y. Qian, C. Zhao, R. Leung, and X. Q. Yang, 2015: A case study of urbanization impact on summer precipitation in the greater Beijing metropolitan area: Urban heat island versus aerosol effects. *J. Geophys. Res.*, **120**, 10,903-10,914, doi:10.1002/2015JD023753. https://doi.org/10.1002/2015JD023753.

——, and Coauthors, 2017: Urbanization-induced urban heat island and aerosol effects on climate extremes in the Yangtze River Delta region of China. *Atmos. Chem. Phys.*, **17**, 5439–5457, doi:10.5194/acp-17-5439-2017. https://www.atmos-chem-phys.net/17/5439/2017/.

Zhou, B., D. Rybski, and J. P. Kropp, 2017: The role of city size and urban form in the surface urban heat island. *Sci. Rep.*, **7**, 4791, doi:10.1038/s41598-017-04242-2. https://doi.org/10.1038/s41598-017-04242-2.

Zhou, D., L. Zhang, L. Hao, G. Sun, Y. Liu, and C. Zhu, 2016: Spatiotemporal trends of urban heat island effect along the urban development intensity gradient in China. *Sci. Total Environ.*, **544**, 617–626, doi:10.1016/j.scitotenv.2015.11.168. http://dx.doi.org/10.1016/j.scitotenv.2015.11.168.

Zhou, J., and Coauthors, 2011: Microbial mediation of carbon-cycle feedbacks to climate warming. *Nat. Clim. Chang.*, **2**, 106. http://dx.doi.org/10.1038/nclimate1331.

Zhou, L., and Coauthors, 2014: Widespread decline of Congo rainforest greenness in the past decade. *Nature*, **508**, 86–90, doi:10.1038/nature13265. http://www.nature.com/articles/nature13265 (Accessed May 7, 2018).

Zhu, P., Q. Zhuang, P. Ciais, L. Welp, W. Li, and Q. Xin, 2017a: Elevated atmospheric CO2 negatively impacts photosynthesis through radiative forcing and physiology-mediated climate feedback. *Geophys. Res. Lett.*, **44**, 1956–1963, doi:10.1002/2016GL071733.

——, ——, J. Eva, and C. Bernacchi, 2017b: Importance of biophysical effects on climate warming mitigation potential of biofuel crops over the conterminous United States. *GCB Bioenergy*, **9**, 577–590, doi:10.1111/gcbb.12370.

Zhu, X., D. Li, W. Zhou, G. Ni, Z. Cong, and T. Sun, 2017c: An idealized LES study of urban modification of moist convection. *Q. J. R. Meteorol. Soc.*, **143**, 3228–3243, doi:10.1002/qj.3176.

Zhu, Z., and Coauthors, 2016: Greening of the Earth and its drivers. *Nat. Clim. Chang.*, doi:10.1038/nclimate3004.

Zhuang, Q., and Coauthors, 2006: CO<inf>2</inf> and CH<inf>4</inf> exchanges between land ecosystems and the atmosphere in northern high latitudes over the 21st century. *Geophys. Res. Lett.*, **33**, 2–6, doi:10.1029/2006GL026972.

——, and Coauthors, 2013: Response of global soil consumption of atmospheric methane to changes in atmospheric climate and nitrogen deposition. *Global Biogeochem. Cycles*, **27**, 650–663, doi:10.1002/gbc.20057.

Zilli, M. T., L. M. V. Carvalho, B. Liebmann, and M. A. Silva Dias, 2017: A comprehensive analysis of trends in extreme precipitation over southeastern coast of Brazil. *Int. J. Climatol.*, **37**, 2269–2279, doi:10.1002/joc.4840. http://doi.wiley.com/10.1002/joc.4840 (Accessed May 24, 2018).

Zipper, S. C., J. Schatz, C. J. Kucharik, and S. P. Loheide, 2017: Urban heat island-induced increases in evapotranspirative demand. *Geophys. Res. Lett.*, **44**, 873–881, doi:10.1002/2016GL072190.

Ziska, L. H., and G. B. Runion, 2006: Fugure weed, pest and disease problems for plants. *Agroecosystems in a Changing Climate2*, P.A.N. Paul C.D. Newton, R. Andrew Carran, Grant R. Edwards, Ed., CRC Press, Taylor & Francis Group, New York, 262–287.

Zscheischler, J., and Coauthors, 2018: Future climate risk from compound events. *Nat. Clim. Chang.*, 1, doi:10.1038/s41558-018-0156-3. http://www.nature.com/articles/s41558-018-0156-3 (Accessed May 17, 2018).

Zwiers, F. W., X. Zhang, and Y. Feng, 2011: Anthropogenic influence on long return period daily temperature extremes at regional scales. *J. Clim.*, **24**, 881–892, doi:10.1175/2010JCLI3908.1.

http://journals.ametsoc.org/doi/abs/10.1175/2010JCLI3908.1 (Accessed May 24, 2018).

APPENDIX

Land component	Land function/type	Observed change	Projected change	Climate driver(s)	Citations	Certainty statement	Confidence statement
VEGETATION							
	Greening						
	Browning						
	Growing season length						
	Dates of onset and senescence						
	Range shifts						
	Number of species (biodiversity)						
HYDROLOGY							
	Soil moisture (yearly amplitude, lowest seasonal amount, ...)						
	Permafrost						
	Surface Run-off						
	Sub Surface Run-off						
	Snow extent						
	Snow depth						
	Length of snow season						
THERMAL							
	dates of last / 1st frost						

Agriculture	
	Sowing dates for crops Harvesting dates Livestock (NEED CLARIFY) Growing degree days
Fires	
Greenhouse gasses	